RICE UNIVERSITY

Regional Characterization of the Knee Meniscus and Tissue Engineering with Dermal Stem Cells

by

Johannah Sanchez-Adams

A THESIS SUBMITTED
IN PARTIAL FULFILLMENT OF THE
REQUIREMENTS FOR THE DEGREE

Doctor of Philosophy

APPROVED, THESIS COMMITTEE:

Kyriacos A. Athanasiou, Thesis Director, Distinguished Professor, Biomedical Engineering, UC Davis

Antonios G. Mikos, Committee Chair, Professor, Bioengineering

K. Jane Grande-Allen, Associate Professor, Bioengineering

Jeffrey D. Hartgerink, Associate Professor, Chemistry

Jerry C. Hu, Development Engineer, Biomedical Engineering, UC Davis

HOUSTON, TEXAS
AUGUST, 2011

Abstract

Regional Characterization of the Knee Meniscus and Tissue Engineering with Dermal Stem Cells

By

Johannah Sanchez-Adams

The knee meniscus plays an integral role in providing lubrication, load distribution, and shock absorption, yet is frequently compromised through traumatic injury or disease. Unfortunately, many of the injuries sustained by the meniscus are unable to heal, and current clinical therapies lack the ability to restore full tissue functionality. Tissue engineering efforts provide a possible solution to this problem. To engineer functional meniscal cartilage, however, researchers need specific design criteria from native tissue as well as an abundant cell source for tissue generation. Tissue engineering efforts must also take into account the complex geometry of the meniscus, as well as regional variations in biochemical and biomechanical properties. In this thesis, meniscus cells and tissue are characterized regionally to identify key parameters for tissue engineering, and an alternate cell source is evaluated for *in vitro* engineering of fibrocartilage.

Towards understanding regional meniscus characteristics important for tissue engineering efforts, meniscus cells were characterized biomechanically and an effective method for isolating these cells for tissue engineering was determined. It was found that the meniscus contains cells that are biomechanically distinct, with outer meniscus cells showing higher stiffness than

inner cells. It was also determined that meniscus cells as a whole were more biomechanically similar to ligament cells than to articular chondrocytes, indicating that tissue properties may correlate with cellular mechanics. In addition to showing regionally distinct biomechanical properties, enzymatic isolation of meniscus cells was found to cause varying phenotypic changes in cells from the inner, middle, and outer regions. A comparison of isolation techniques also indicated that sequential digestion of meniscus tissue with pronase and collagenase was able to yield more cells with higher viability than other techniques tested, and those isolated cells created stiffer and more glycosaminoglycan (GAG) rich constructs when used in a tissue engineering modality than cells isolated using only collagenase. The identification of an effective mode of isolating meniscus cells is of great use to tissue engineering efforts, as they often require a large cell numbers. These findings illustrate that known regional variations in meniscus cell phenotype and biochemical composition are also evident in cellular mechanics, and phenotypic responses of these cells to isolation are varied and distinct.

To be successful tissue replacements, tissue engineered meniscus constructs must not elicit an immune response and must have sufficient mechanical properties to survive when implanted. To determine if allogeneic or xenogeneic implantation of scaffold-free meniscus constructs could be feasible, the immunogenicity of bovine and leporine meniscus cells and articular chondrocytes were determined in an *in vitro* model system. It was found that neither bovine nor leporine meniscus cells or articular chondrocytes caused

activation of leporine immune cells, suggesting that they may serve as allogeneic or xenogeneic cell sources for meniscus engineering. Additional analysis of the mechanical role of meniscus GAGs indicated that they are mechanically important in all regions of the meniscus, but especially in the inner region where the relatively high GAG content affects both compressive and tensile properties. Therefore, tissue engineering efforts should try to recapitulate GAG content and distribution to enhance the functionality of meniscus replacements.

As a major obstacle for meniscus engineering is the identification of an abundant cell source, this thesis also investigated the use of skin cells as an alternative to primary cells for tissue engineering. Previously identified chondroinducible dermis cells were found to have multilineage differentiation capacity, and were subsequently termed dermis isolated adult stem cells (DIAS). DIAS cells were also able to be expanded in monolayer without losing chondroinductive capacity, and were able to create constructs with cartilaginous properties which could be varied with growth factor application. Given the ease of expansion and ability of DIAS cells to form fibrocartilaginous tissue, these cells present an abundant cell source for meniscus tissue engineering.

Together, the studies performed in this thesis 1) offer valuable design parameters for meniscus cells and tissue from different regions, 2) provide indications for the immunogenicity of possible cell sources for meniscus engineering, and 3) enhance the understanding and utility of DIAS cells for engineering the cartilage spectrum.

Acknowledgements

The work presented in this thesis represents the culmination of a rewarding and challenging five year journey, during which I benefitted immensely from the wisdom, care, and experience of numerous individuals and organizations. I would most certainly like to thank the members of my thesis committee, Dr. Kyriacos Athanasiou, Dr. Antonios Mikos, Dr. Jane Grande-Allen, Dr. Jeffrey Hartgerink, and Dr. Jerry Hu for their support and encouragement throughout my graduate school career. Additionally, I would like to acknowledge Dr. Michael Gustin for his service on my thesis committee and for providing valuable feedback to improve my research.

I am thankful for the excellent work of graduate students and post docs that preceded me in the Athanasiou Lab and for the camaraderie and advice of my fellow labmates, past and present. Particularly, I would like to thank Dr. Vincent Willard; your friendship, loyalty, and support are irreplaceable. I am also very grateful to Drs. Daisy Deng, Deirdre Anderson, Eugene Koay, Gwen Hoben, and Jerry Hu for helping me become proficient in the lab, and to Drs. Dan Huey and Kerem Kalpacki for sharing their immense knowledge and expertise with me. I would also like to thank Sriram Eleswarapu and Donald Responte for adventurously moving with the lab to California, and for always surprising me with their creativity. I was also fortunate to receive the help and support of members from several other labs at Rice and UC Davis, and I would like to thank the Grande-Allen, West, Mikos, Reddi, and Griffiths labs for their advice over the past few years.

The completion of this work was dependent on funding and support from a variety of organizations. I am very grateful to the National Science Foundation Alliance for Graduate Education and the Professoriate program for their financial and moral support of my research, and in particular Ms. Teresa Chatman for her wonderfully joyous faith in me throughout my graduate career. Also integral to the completion of this thesis were several grants from the National Institutes of Health (R01AR047839 and R01DE019666) and an Innovative Research Grant from the Arthritis Foundation.

This work would not have been possible without the love and support of my family, especially my mom, Teresa, my dad, Russel, my brother, Josh, and my sister-in-law, Suzanne. Thank you for always believing in me and being the best cheerleaders of my life. I would also like to thank my friends and teammates Kim Breese, Austine Lin, Katey Forth, Julie Schellberg and AJ Beard; your camaraderie, humor, and support was essential to my success. Finally, I am deeply indebted to my mentor and friend Dr. Athanasiou for fiercely encouraging me to surpass my goals and for always serving as a model of confidence and understanding.

Table of Contents

Table of Figures

Chapter 10: Current Therapies for Meniscus Injuries

Chapter 11: Dermis Isolated Adult Stem Cells for Cartilage Tissue Engineering

Table of Tables

Introduction

The knee meniscus plays an integral role in the knee joint, providing stability, shock absorption, and redistributing load during normal activities such as standing or walking. However, despite its important function in the knee, the meniscus is prone to injury and has limited regenerative capacity. Tissue engineering efforts seek to address this problem by creating functional replacement tissue. For this goal to be achieved, a better understanding of the regional differences in meniscus cells and tissue is needed to provide design criteria for engineered constructs, and an abundant cell source for engineering the tissue should be identified. In an effort to meet these needs, this thesis has two global objectives: 1) to characterize regional variations in meniscus cells and tissue, and 2) to use a dermis-derived cell population for *in vitro* tissue engineering of the cartilage spectrum. These objectives are conducted under the following hypotheses. First, *the knee meniscus will show regional variations at the cell and tissue level.* Second, *a sub-population of dermis cells can be used to engineer fibrocartilaginous tissue.* These global objectives are achieved through the following three specific aims:

1. To understand regional meniscus cell phenotype and mechanical properties. The first study of this aim measures the mechanical properties of single cells from the inner and outer meniscus regions and compares them to other musculoskeletal cells. *It is hypothesized that cells from different meniscus regions will show regional variations in biomechanical properties.* In the second study in this aim, changes

in meniscus cell phenotype is measured as a function of isolation technique and meniscus region. *It is hypothesized that 1) cells from different meniscus regions will show distinct phenotypic responses to enzymatic isolation, and 2) the isolation technique yielding the highest number of cells can be used in a tissue engineering modality.* Together, the studies in this aim will allow for better understanding of regional mechanical and phenotypic differences in meniscus cells, and identify an effective mode of isolating these cells for tissue engineering.

2. To determine the immunogenicity of meniscus cells and the contribution of sulfated glycosaminoglycans (GAGs) to meniscus mechanics. This aim is concerned with the translatability of engineered constructs formed from meniscus cells and provides design criteria for the functional generation of these constructs. The first study in this aim characterizes the *in vitro* response of leporine immune cells to leporine and bovine meniscus cells and articular chondrocytes to gain an understanding of the immunogenicity of these cells in a rabbit model. *It is hypothesized that neither leporine nor bovine articular chondrocytes or meniscus cells will cause activation of leporine immune cells.* The second study characterizes the contribution of sulfated GAGs to regional meniscus mechanics to understand the mechanical role of this matrix component to compressive and tensile meniscus mechanics. *It*

is hypothesized that GAGs will show regional variation in their contribution to meniscus tissue mechanics.

3. To use dermis-derived cells as an alternate cell source for cartilage tissue engineering. This aim uses a phased approach to first evaluate methods of expansion, chondroinduction, and tissue engineering of a subpopulation of chondroinducible dermis cells. *In this phase, it is hypothesized that expansion of chondroinducible dermis cells will not diminish their chondroinductive capacity.* In the second phase, the most promising cell population from the first phase will be tested for multilineage differentiation capacity. *It is hypothesized that these cells will show multilineage differentiation capacity.* These cells will also be used for cartilage tissue engineering and growth factors will be used to modulate their cartilage-specific biochemical and biomechanical properties. *It is hypothesized that different growth factors will cause varying biochemical and biomechanical effects on tissue engineered constructs.* Identifying a method to expand and tissue engineer chondroinducible dermis cells may provide an abundant and potentially autologous cell source for meniscus engineering.

The following chapters provide background of this work and explain the results related to each specific aim. Chapter 1 provides general background on the knee meniscus and what is currently known regarding its structure and function, and its biochemical and biomechanical attributes. Chapters 2 and 3 detail methods of measuring single cell mechanics and discuss known

differences in regional meniscus cell morphology and phenotype. These chapters set the stage for the detailed analysis of meniscus cell mechanics and phenotype performed in aim 1.

All work related to the completion of specific aim 1 is presented in chapters 4 and 5. Chapter 4 addresses the mechanical characterization of meniscus cells from different regions, and compares the mechanical properties of meniscus cells to those of articular chondrocytes and ligament cells. Chapter 5 investigates the effects of isolation on meniscus cells from different regions and identifies an enzymatic digestion protocol to use for meniscus tissue engineering with primary cells. These studies enhance the understanding of the regional differences in meniscus cells which can inform further models or experimental designs for meniscus engineering.

Background on pathophysiology of the meniscus is represented in chapter 6 as an introduction to the work related to specific aim 2 (chapters 7 and 8). Chapter 7 investigates the potential immunogenicity of meniscus cells in an *in vitro* model system, indicating whether allogeneic or xenogeneic transplantation of meniscus cells could be a feasible process. Chapter 8 studies the mechanical contribution of GAGs in the knee meniscus with the goal of providing design parameters for engineered meniscus constructs.

Chapters 9 and 10 provide an introduction to the studies performed in specific aim 3, reviewing previous work related to meniscus tissue engineering, and underscoring the importance of design criteria for the creation of functional tissue. Chapter 11 details the work related to the completion of specific aim 3. In

this chapter, methods to enhance the utility of chondroinducible dermis cells are identified, and the effects of growth factors on tissue engineered constructs formed from these cells are determined.

The cumulative knowledge obtained through the completion of these specific aims is discussed in the Conclusions chapter. The significance of the work is presented, and future directions are proposed.

Chapter 1: Structure-Function Relationships of the Knee Meniscus

Section 1.1: Anatomy and Development

Anatomy of the knee meniscus

Integrating vasculature, cells, and extracellular matrix molecules, the knee meniscus comprises two semicircular, wedge-shaped pieces fixed in place via a network of ligaments. The meniscus is a glossy white fibrocartilaginous tissue that is an important component in the normal joint, as shown in Figure 1. The human knee contains a medial meniscus and a lateral meniscus which are located between the femoral condyle and tibial plateau (see Figure 2). The main functions of the meniscus are to increase congruency of shape between the curved condyle and flat plateau, maintain stability, and bear and transfer load within the joint. Because it functions in a joint articulation it exhibits a smooth surface macroscopically and microscopically.[1] Both the medial and lateral menisci are wedge-shaped and semilunar, but the medial meniscus is generally more circular in shape than the lateral meniscus.

There is an array of ligaments that aid in stabilizing the meniscus within the knee joint during loading conditions, as shown in Figure 3. The ligaments of

---

Chapter published as: Athanasiou, K. A., and Sanchez-Adams, J. "Part 1: Structure-Function Relationships of the Knee Meniscus." *Engineering the Knee Meniscus*. Morgan and Claypool Publishers. 2009.

Humphrey and Wrisberg connect the posterior horn of the lateral meniscus to a lateral insertion site on the medial femoral condyle. The Humphrey's and Wrisberg ligaments are located anteriorly and posteriorly to the posterior cruciate ligament (PCL), respectively. Studies on human cadaveric knees have shown that an estimated 50% of people have both of these ligaments, while 93% have either one or the other. The medial meniscus is connected on its periphery to the medial collateral ligament which connects the femoral condyle to the tibia.[2]

The anterior portions of the meniscus are joined together by the transverse ligament, and each meniscus is anchored to the tibial plateau via anterior and posterior meniscal horns. The insertion sites of these horns are highly innervated and display four different zones that connect the meniscus to the underlying bone, thereby maintaining their position within the joint. They are the ligamentous zone, uncalcified fibrocartilage, calcified fibrocartilage, and bone. Coronary ligaments run along the periphery of each meniscus, providing an additional attachment to the tibial plateau.[3] It is here in the periphery of each meniscus that the rest of the innervation is found, with no innervation present in the inner one-third of the tissue. Large nerve fibers run circumferentially along the tissue, while smaller fibers are positioned radially. The outer periphery of each meniscus is also covered by the synovial membrane, which imparts vasculature, and contains a highly fibrous matrix while the inner portion displays characteristics like those of hyaline articular cartilage, devoid of vasculature and innervation.

Development of the knee meniscus

When first formed in the body, both the medial and lateral menisci are completely vascular. This widespread vascularity diminishes rapidly from gestation to birth and then more gradually to adulthood, when it is estimated that 10-25% of the lateral meniscus and 10-30% of the medial meniscus contains blood vessels. This vascularity is confined to the outer periphery of the meniscus.[4]

Understanding meniscus development can greatly enhance tissue engineering efforts by providing a basis for evaluating engineered construct maturation *in vitro* and *in vivo.* A 1983 study on the developing meniscus revealed that from early in gestation to 11 years after birth vasculature as well as cellularity changes dramatically, but contact area between the tissue and bones remains constant.[5] Specifically, at 3.5 months gestation, the meniscus has little extracellular matrix but high cellularity and vascularity. The cells at this stage are similar to each other in that they have a high nucleus to cytoplasmic ratio, but are more compacted on the periphery of the tissue. By around 6 months' gestation, the cruciate ligaments are more defined and the collagen network is fairly well organized circumferentially, including some radial tie fibers. At this stage the meniscus is still completely vascularized. At 7.5 months gestation, the synovial membrane covering the meniscus is around three to four cell layers thick, the collagen organization is more pronounced, and the nuclear to cytoplasmic ratio of the cells has diminished. As the fetus grows larger and approaches 9 months gestation, the meniscus within the joint maintains a relatively constant ratio of

contact area with the tibial plateau, correlating with an increase in extracellular matrix around the meniscal cells.[5] Therefore, even before birth, the meniscus undergoes drastic changes in terms of its cellularity, vascularity, and size, which may be useful to mimic in tissue engineered constructs.

After birth, the meniscus continues to grow along with the joint, and the collagen organization changes to accommodate biomechanical loading. At 3 months after birth, vasculature can be identified throughout the meniscus but is more concentrated at the periphery. Vasculature in the inner one-third of the meniscus continues to diminish, and is almost completely gone by 9 months. As the tibia and femur develop, the meniscus continues to increase in collagen organization and size in concert with the increasing femoral and tibial surfaces. From 3 to 11 years, the synovial membrane decreases in thickness to one to two cell layers, and the collagen organization within the meniscus develops to contain not only circumferentially and radially oriented fibers but also vertically oriented fibers. The vasculature during this period continues to recede to the periphery of the tissue (see Figure 4).[5]

Through adulthood, the meniscus decreases in vascularity and cellularity, eventually becoming avascular in the inner one-third of the tissue. This change in vascularity is directly related to a 20 kDa portion of the C-terminal region of collagen type XVIII called endostatin, which acts as an inhibitor of vascular in-growth through inactivation of vascular endothelial growth factor.[6, 7] Early in development collagen type XVIII is homogeneously distributed throughout the meniscus, but as the aging process continues levels increase in the inner two-

thirds of the tissue and decrease in the outer one-third, creating a favorable environment for vascularization in the peripheral meniscus.[6] During early maturation (less than 20 years of age), the rate of proteoglycan production in the meniscus is 1-5 mM sulfate per hour per milligram of DNA and then gradually decreases with aging to around 1/20 of its initial rate.[8] The adult meniscus has a high degree of collagen organization allowing for specialized load transmission from the curved femoral condyles to the flat tibial plateau (see Section 1.3).

As the body moves through adulthood and begins to age, the meniscus undergoes degenerative changes. Collagen concentration increases from birth to 30 years and allows for the creation of a highly organized matrix. It then reaches a plateau from 30 to 80 years of age, and finally begins to decline.[9, 10] Around this time of decline there is an observed increase in ratio of chondroitin-6-sulfate to chondroitin-4-sulfate, and an increase in keratin sulfate to chondroitin sulfate, characteristics also seen in hyaline cartilage aging.[11] These degenerative changes may increase the risk of the meniscus to become injured (more discussion in Chapter 6).

Concepts

The knee meniscus is comprised of two semi-lunar, wedge-shaped tissues that act to stabilize, absorb shock, bear load, and transfer stresses within the joint. During articulation of the bones, these tissues are held in place by a network of ligaments. Direct ligamentous attachments that integrate the meniscus to the tibial plateau are made by the horns of the meniscus, which

contain both cartilaginous and calcified regions. During the initial stages of meniscal development, the tissue is completely vascularized, but with maturation blood vessels are restricted to the outer periphery. Marked differences in cell density and collagen organization can be seen as the tissue matures, as the meniscus contains condensed cells with little extracellular matrix early on, and fewer cells surrounded by abundant organized matrix in adulthood. Meniscal aging is apparent through a decline in collagen and an increase in chondroitin-6-sulfate and keratin sulfate relative abundances.

Section 1.2: Biochemical composition, structure, and function

Regional variation

While the meniscus contains blood vessels and nerves, these are only found peripherally in the tissue, and therefore the meniscus is generally considered in terms of two regions. The vascularized and innervated (red) region is located exclusively in the outer periphery, and the non-vascularized (white) region makes up the inner portion of the tissue (see Figure 5).[9, 12, 13] These two regions are joined together by a transitional region called the red-white region, which exhibits both red and white properties. The capacity for a region to self-repair correlates directly with the amount of vasculature present, giving the red region the highest regenerative potential. The red and white regions also differ greatly in terms of biochemical content, mechanical properties, and cell type.

Biochemical content

Overall, the meniscus is composed of approximately 70% water and 30% organic matter.[3] Of the organic matter, 75% is collagen. Although collagen is present throughout the meniscus, different types are prevalent in different regions. In the red region of the meniscus, collagen type I is the main collagen present while in the white region, both collagens type I and II are in abundance.[3, 12] Other collagens present in the meniscus are types III, IV, V, VI, and XVIII but to a much smaller degree than types I and II.[6, 12] The outer portion of the meniscus is 80% collagen by dry weight and is almost exclusively type I, with less than 1% of other collagen types.[14] In contrast, the inner portion of the meniscus is 70% collagen by dry weight. Of this collagen, 60% is type II and 40% is type I.[14] Therefore, the outer portion of the meniscus is more fibrous and the inner portion of the meniscus, containing collagen type II, has some hyaline cartilage-like properties.

As the largest fraction of the extracellular matrix, collagen has an important role in the functionality of the meniscus. Being a fibrillar protein, collagen type I is able to confer various types of mechanical integrity based on its structural organization. The alignment of collagen fibers in the meniscus varies from being mostly random within the superficial and lamellar layers, to oriented circumferentially in the deep layer and with radially oriented "tie" fibers present throughout (Figure 6).[12] This alignment allows for the meniscus to withstand hoop stresses generated by normal loading of the tissue.

While the overwhelming majority of fibers in the meniscus are collagens, elastin has also been found in the matrix, though it comprises 1% or less of the dry weight (Figure 7). The presence of even such a small degree of elastin is thought to provide resiliency to the tissue, as it is known for being able to recover its original shape after withstanding large strains. It has been proposed that elastin interacts directly with the collagen network during loading to impart resiliency to the matrix.[15]

The remaining 25% of the organic matter in the human meniscus is made up of proteoglycans (~15%), cellular DNA (~2%), and adhesion glycoproteins (<1%) (Figure 7).[12, 16] This breakdown can vary regionally within the meniscus. Proteoglycans are molecules consisting of a core protein that is decorated with glycosaminoglycans (GAGs), and are commonly classified based on the GAGs present. Of the GAGs that are found in the meniscus, 40% are chondroitin-6-sulfate, 10-20% are chondroitin-4-sulfate, 20-30% are dermatan sulfate, and 15% are keratin sulfate.[16] GAGs are negatively charged and therefore play a central role in attracting water into the tissue, imparting both hydration and compressive stiffness. Due to the need for compressive integrity, cells from the inner two-thirds of the meniscus produce more proteoglycans than the outer one-third.[17, 18] Biglycan, which is theorized to protect cells during loading, is at its highest concentration in the inner one-third of the meniscus.[17] In addition, decorin, which helps collagen fibril organization, is found mostly in the outer one-third of the tissue where collagen organization is highest.[17] Due to its wedge shape, the highest compressive loading on the meniscus is borne by the inner portion, while

the outer portion experiences a tensile hoop stress (more discussion ensues in Section 1.3). The spatial organization of proteoglycans within the meniscus therefore allows the tissue and the cells within it to withstand compressive loading and to organize collagen fibrils to bear tensile loads.

Adhesion glycoproteins are a specialized class of molecules that aid in binding matrix molecules to one another and to cells. Within the meniscus type VI collagen, fibronectin, and thrombospondin have been identified.[9] All of these molecules contain the Arginine-Glycine-Aspartic acid (RGD) amino acid sequence which aids in cell attachment and which allows for cellular and extracellular matrix connections.

Concepts

Water is the main component of the knee meniscus, comprising 70% of the total wet weight of the tissue. The dry weight contains 75% collagen, mainly types I and II, and 25% proteoglycans, cells, and adhesion glycoproteins. The main GAG present in the meniscus is chondroitin sulfate (50-60%), followed by dermatan sulfate (20-30%), and keratin sulfate (15%). Collagen is preferentially organized in the circumferential direction, with radial fibers dispersed throughout in order to bear tensile loads generated from joint movement. Given this general collagen organization, clear differences can be seen in the biochemical makeup of the outer and inner portions of the meniscus. In the outer portion of the meniscus collagen type I is dominant, but in the inner portion type II collagen is slightly more prevalent than type I. Proteoglycans are also more abundant in the

inner portion of the meniscus, allowing for high compressive loads to be borne. Resiliency of the knee meniscus is imparted to the tissue through the slight presence of elastin (<1% of dry weight). Cells are dispersed throughout the matrix and are anchored to it via adhesion glycoproteins which contain RGD peptides. Biochemical composition of the knee meniscus varies regionally, and allows for the specialized function of the tissue.

Section 1.3: Biomechanical properties and evaluation techniques

Geometrical considerations

Because the main functions of the knee meniscus are load transmission and stability, this tissue must withstand many different forces including shear, tension, and compression. The structure and composition of each semicircular meniscus is well-suited to this task, as evidenced by its unique biomechanical properties.

On a macroscopic level, the geometry of the meniscus gives the first indication of its function. The meniscus is both semilunar and wedge-shaped. In terms of its semilunar geometry (as shown in Figure 8), the medial and lateral menisci can be measured anteroposteriorly (lengthwise), and mediolaterally (widthwise). Typical dimensions for the medial meniscus are 40.5-45.5 mm in length, and 27 mm in width.[19, 20] For the lateral meniscus, length and width dimensions are typically 32.4-35.7 mm and 26.6-29.3 mm, respectively.[19, 20] The

circumferential dimension for the medial meniscus is approximately 90-110 mm, while for the lateral meniscus it is slightly shorter (approximately 80-100 mm).[19]

As the tissue is wedge-shaped, thick on the outer periphery and thin toward the middle of the joint, it is ideally suited to stabilize the femoral head as it articulates with the tibial plateau by increasing congruency between the two surfaces. Additionally, as load is applied from the femur to the tibia, the meniscus draws upon its unique shape to deform radially, thereby bearing some of the load that would otherwise be transmitted to the tibial cartilage. The radial displacement, opposed by posterior and anterior attachments on the tibial plate, results in a hoop stress in the tissue.

Normal loading conditions

During normal activities such as walking or ascending stairs, the knee joint experiences loads of 2.7-4.9 times body weight.[21] Overall, it is estimated that the knee meniscus bears anywhere from 45% to 75% of this total joint load, varying with degree of joint flexion, animal model, as well as health of the tissue.[22] As the knee flexes, the contact area between the bones in the joint decreases by 4% for every 30°, accounting for some of the variability in load-bearing capacity of the meniscus.[23] It has been shown that at full extension, the lateral meniscus bears almost all of the load on the lateral side, while the medial meniscus bears about 50% of the medial load.[24] The meniscus not only acts to increase congruence in the joint, it also acts as a spacer creating 1 mm of space between most of the articulating femoral and tibial surfaces and allowing only 10% of these surfaces

to contact.[24] Without the meniscus tissue, the support of the femoral condyles is dramatically reduced and the joint force is concentrated on the hyaline cartilages, increasing the stress on the tissue to 2 to 3 times higher than normal.[25] It is therefore evident that the load-bearing capacity of this structure and its role in protecting the hyaline cartilage surfaces of the femur and tibia act to prevent joint injury. Both geometry and anatomical anchors play an important role in the stabilizing, load-bearing, and protective functions of the meniscus.

Shock absorption

The meniscus also plays a distinct role in absorbing shock within the joint. Studies on the bovine meniscus have shown that this tissue has 1/2 the stiffness and 1/10 the permeability of hyaline cartilage.[26, 27] Additionally, as the collagen fibers within the meniscus have varying diameters, they are suited to absorb a variety of different frequencies.[28] These features make it easier for the meniscus to absorb shock and deform in response to joint movement.

Collagen organization

On a microscopic level an even more refined architecture can be distinguished that allows these specialized functions to be realized. As discussed previously, throughout the developmental process the collagen matrix in the meniscus becomes increasingly organized. This organization varies with depth in the tissue, imparting both tensile stiffness and resistance to splitting.[29, 30] Collagen orientation can be considered in three layers: superficial, lamellar, and

deep, which describe the tissue from surface to core. As shown in Figure 9, collagen fibers are amorphous in the superior superficial layer, but are more radially oriented in the inferior superficial layer, closest to the tibial plateau.[31] Amorphous collagen organization persists through the lamellar layer, but is distinguished from the superficial layer in that it contains short, radially oriented fibers only at the posterior and anterior horns.[30] In the deep layer, collagen is predominantly oriented circumferentially, with a few radially oriented fibers.[9, 28, 31, 32]

As described previously, during normal loading conditions the femur presses down on the meniscus, creating radial displacement that is opposed by anterior and posterior anchors. This displacement is translated within the tissue to hoop stresses, radial tension, shear, and compression which are borne by the special organization of collagen fibers and proteoglycans, as shown in Figure 10. In the superficial and lamellar layers, amorphous and radial collagen fibers act to resist mediolateral splitting of the meniscus and in the deep zone circumferentially oriented fibers work in tension as a result of hoop stresses.[10] Shear forces generated by the femur deforming the tissue are opposed by matrix molecule interactions, and negatively charged proteoglycans in the meniscus impart compressive integrity by resisting fluid loss.[12]

Biphasic behavior

Due to its makeup, the meniscus is considered biomechanically as a biphasic tissue. The first phase consists of the porous and permeable collagen

and proteoglycan solid matrix, while the second phase is made up of water and salts that are present throughout the matrix.[26, 33] While the solid matrix makes up only about 30% of the total tissue, it is the interplay between the solid and fluid phases that imparts viscoelastic properties to the meniscus (see Figure 11).[34] As a viscoelastic tissue, the mechanical behavior of the meniscus depends on both the magnitude and rate of loading. Frictional drag is produced by fluid being forced from the tissue during load application, producing creep and stress-relaxation responses.[26] When subjected to a constant force or stress applied suddenly as a step, the meniscus displays elastic-like properties immediately after loading. This initial behavior is controlled by the hydrostatic pressure developed in the interstitial fluid portion of the tissue. After this initial phase, still under constant stress, the tissue continues to deform, but at a slower rate as the fluid phase is expelled from the matrix, with the solid matrix resisting more of the load. This deformational behavior under a constant, step load is called the creep response.[33]

A similar behavior can be observed when a step strain or displacement is placed on meniscal tissue. Initially, the solid matrix responds elastically by creating a reaction force that is linearly related to the applied displacement. Over time, this reaction force diminishes exponentially as the fluid is expelled from the matrix and the load is shared by both fluid and solid, until eventually only the solid matrix supports the applied load. This behavior is called stress-relaxation.[33] Following load removal within the joint, the fluid that was expelled during loading is able to rehydrate the tissue, initiated by the negatively charged proteoglycans

in the matrix, resulting in recovery behavior. This fluid flow also functions to transport nutrition throughout the tissue and surrounding hyaline cartilage, remove waste, and provide lubrication.[32] Therefore, the mechanical behavior of the meniscus is not only vital to ensure proper load distribution, but is also instrumental in the overall health and lubrication of the joint.

Biomechanical evaluation

A number of mechanical tests are used to quantify just how mechanically robust this tissue is when subjected to tensile, compressive, and shear loading. Due to the variation in collagen alignment and the asymmetrical shape of the meniscus, a complete picture of the mechanical properties of the meniscus must consider specimens that vary spatially within the tissue and are oriented along and perpendicular to the preferred collagen alignment. Figure 12 details the various directions and regions that are important in meniscus characterization. The most common methods used to characterize the mechanical properties of meniscal tissue are tensile and compressive tests. It is important to note that as the availability of human tissue is limited, some mechanical characterization data are only available for other animals such as the cow, pig, or sheep.

Tension

For tensile testing, tissue can be harvested from the meniscus at a prescribed depth perpendicular to or parallel with the circumference of the meniscus. It is crucial to maintain consistency amongst samples with regard to

position and orientation because the meniscus is known to have anisotropic properties.[29, 32] Tensile tests are usually performed using a constant strain rate of 0.005 sec^{-1}, and the samples may or may not be preconditioned.[30, 32] This small strain rate is used to minimize the effects of frictional drag from interstitial fluid flow out of the solid matrix, and to neglect the viscoelastic properties of the collagen and proteoglycan matrix.[30]

When considering specimens from the anterior, central, and posterior meniscus it can be seen that the circumferential Young's modulus varies spatially, and that the lateral meniscus has a higher average tensile circumferential modulus than the medial meniscus (see Table 1).[32] When testing the bovine meniscus in the radial direction, its modulus is highest closest to the posterior region of the meniscus, and decreases moving toward the anterior horn.[30] There is evidence that the tie fibers in the posterior region of the bovine meniscus are closely packed and form sheets, which may explain the higher modulus found there.[30] In tension, the properties of the meniscus vary from being isotropic on its surface, to anisotropic in deeper layers due to the variation in collagen fiber alignment. These collagen fibers provide the tissue a robust tensile stiffness of up to 300 MPa.[32] In the superficial layer, the tissue fails at high stresses and low strains with no preferred direction. In the deeper zones, the tensile modulus in the circumferential direction can be 3 to 10 fold higher than in the radial direction, owing to the abundance of circumferential collagen fibers relative to radial fibers.[30, 32] Comparing tensile properties of the superior medial bovine meniscus, the layer 0.6-1 mm from the surface has the highest stiffness

circumferentially and is about 4-fold stiffer than the layer 0-0.2 mm from the surface.[27] This 0-0.2 mm layer of the bovine meniscus is about 3-fold stiffer than the layer 1.4-1.8 mm from the surface.[27]

Compression

Methods for compressive testing of meniscal tissue include confined or unconfined compression and creep indentation.[27, 35-37] The creep indentation apparatus is depicted in Figure 13.

Both compressive testing and creep indentation can yield the aggregate modulus and permeability, but creep indentation can additionally allow for the calculation of the Poisson's ratio, and thus, shear modulus of the tissue. This type of testing has shown that different regions in the meniscus have varying compressive properties, which is a result of their biochemical makeup and organization (see Table 2). Using the creep indentation apparatus, it has been shown that the aggregate modulus of the human meniscus is greatest in the anterior region of the meniscus (around 150 kPa), as compared to the central and posterior regions (around 100 kPa).[37] Also notable is that the permeability and shear modulus measured within the meniscus are relatively constant amongst all regions.[37] In unconfined compression at 20% strain, the meniscus again displays anisotropic behavior with the highest compressive Young's modulus in the vertical direction being twice as high as in the circumferential and radial directions.[36] This high stiffness in the vertical direction may be attributed to proteoglycans in the matrix of the tissue resisting fluid loss, thereby opposing the

vertical force.[35, 36] The compressive integrity of the meniscus allows for axial loading from the femur to be resisted, and because of the geometry of the tissue, some of this vertical loading is translated into circumferential, radial, and shear stresses.

Shear

For specifically testing the meniscus in shear, dynamic oscillatory or constant shear strain is applied to the specimen which can measure the dynamic shear modulus as well as the transient shear modulus relaxation function.[34] As mentioned previously, creep indentation can also be used to yield the shear modulus of a meniscus sample, though it is an indirect method of doing so. It has been shown that the dynamic shear modulus of the meniscus is frequency dependent and anisotropic (see Table 3). The frequency dependence again points to the viscoelastic nature of the tissue, while the anisotropy of the modulus indicates that collagen organization and interactions between collagen and proteoglycans are central to shear resistance.[34] The normal human meniscus has a shear modulus on the order of 120 kPa at 1.5 Hz and 10% strain.[32] The orientation of collagen fibers within the meniscus has a profound impact on shear modulus at low compressive strains. The shear modulus of a bovine meniscus sample that undergoes a dynamic shear test in the circumferential direction is 20-36% higher than a sample sheared in the radial direction, and depends on the amount of strain applied (up to 10%).[34] With compressive strains higher than 10%, these differences diminish.[34]

Concepts

Because of its geometrical shape and anchoring, the meniscus experiences tension, compression, and shear while bearing load or stabilizing the joint. Collagen and proteoglycans play an important role in imparting robust tensile, compressive, and shear properties to the meniscus and their anisotropic organization is vital to this function. The meniscus is modeled as a biphasic material, displaying viscoelastic behaviors when subjected to step stresses or strains. Biomechanical testing of the tissue reveals that the tissue has a tensile modulus on the order of 100-300 MPa in the circumferential direction, which is 10-fold higher than in the radial direction. It is also well-suited to resist compression axially, given an aggregate modulus of 100-150 kPa. In shear, the tissue exhibits a shear modulus on the order of 120 kPa.

Section 1.4: Cell types

Cell classification

Development of the meniscus begins with the condensation of a vast number of cells that are largely indistinguishable from one another. After the tissue has matured, however, the cells in the different meniscal layers are morphologically distinct. In the superficial layers of the meniscus, cells appear oval and fusiform, similar to fibroblasts.[38-40] In the deeper zones, however, cells are found to be more rounded in nature which is more similar to chondrocyte

morphology.[1, 38-40] These variations have made the classification of these cells difficult. Researchers have used various terms to describe them including fibroblasts, fibrocytes, chondrocytes, fibrochondrocytes, and meniscus cells.[1, 38, 39, 41-43] While the meniscus is made up of predominantly collagen type I, it is natural to expect fibroblast-like cells to inhabit it, and indeed the morphology and gene expression patterns of cells in the meniscus exhibit some fibroblastic characteristics; they also exhibit chondrocyte-like characteristics. These cells cannot be strictly classified as chondrocytes either because instead of exclusively producing collagen type II they are known to produce collagen type I as well. The term meniscal fibrochondrocytes has been used to collectively describe these heterogeneous cells, encompassing both their fibroblastic and chondrocytic natures, and studies have been performed to further characterize them.[40] In this book, we use the terms meniscal fibrochondrocytes and meniscus cells interchangeably.

Diversity of meniscus cells

In the rabbit meniscus, as many as four distinct cell types have been identified in various locations in the tissue based on morphology and the presence of gap junctions (Figure 14).[38] In the inner one-third of the tissue, cells with a rounded shape closely resembling chondrocytes have been found, while in the outer portion of the meniscus two cell types that display many cell processes are present.[38] Another cell type is found in the superficial zone of the meniscus and has a spindle-shaped morphology.[38] The cell types in the outer portion

contain gap junctions, while cells from the inner portion and superficial zone of the meniscus do not contain these processes.[38] In addition to fibrochondrocytes, endothelial cells are present to maintain the microvasculature of the outer meniscus.[44] These cells are distinct from fibrochondrocytes as they are found only in the lumen of meniscal vasculature.

Cell synthetic properties

Meniscus cells from all regions work in concert to produce the appropriate proteins needed to maintain healthy tissue. Total collagen synthesis does not vary amongst the regions of the meniscus, but the main types of collagens produced are types I and II. A lower degree of synthetic activity can be detected for collagen types III, IV, V, and VI by these cells.[18, 45] The GAGs produced by meniscal cells are predominantly chondroitin sulfate and, to a lesser degree, keratin sulfate.[46] Comprehensive gene expression profiles for meniscal fibrocartilage as a whole have been compared to hyaline cartilage, identifying common genes and genes specific to each cartilage type.[47] While there are numerous genes that hyaline and meniscal cartilages have in common, there are some genes that are more highly expressed in one cartilage type than the other. When compared to human mesenchymal stem cells (which are considered precursors to cartilage cells), certain genes are more highly expressed in chondrocytes than fibrochondrocytes, and vice versa, as shown in Table 4. This type of analysis allows for a better characterization of the tissue and highlights the differences between these two distinct cartilages at a molecular level.

Regional variation in synthetic profiles

Fibrochondrocytes from the inner and outer meniscus have distinct protein synthetic profiles and gene expression patterns, giving rise to the heterogeneous makeup of the meniscus (see Table 5). In the inner meniscus, cells display a mostly rounded morphology similar to chondrocytes and stain positively for α-smooth muscle actin which imparts contractile behavior to the cells.[42, 48, 49] These cells also tend to produce more proteoglycans than the polygonal and fusiform cells of the outer region.[18] Inner region cells can be characterized by higher gene expression and production of collagen type II and aggrecan, as well as negative staining for the cell surface marker CD34, which functions in cell to cell adhesion.[45, 50-53] Cells in this region also have high gene expression for nitric oxide synthase (NOS2), which is implemented in nitric oxide production and has been shown to regulate meniscus cell biosynthesis.[53, 54]

In contrast, cells of the outer region of the meniscus are characterized by high gene and protein expression of collagen type I, proteases MMP2 and MMP3, and stain positively for the cell surface marker CD34.[38, 45, 51, 53] The gene profile of these cells is more reminiscent of fibrous tissue due to the high degree of collagen I expression and the expression of proteases which can aid in cellular migration and remodeling of the tissue following injury.

Mechanosensitivity of meniscus cells

Gene expression and protein synthesis of meniscal cells can vary with age and region in the tissue, but are also sensitive to mechanical cues (see Table 6). Cells from the inner and outer meniscus are exposed to different cytomechanical environments.[55] Using finite element modeling of the meniscus, it has been predicted that the round, inner meniscus cells experience tensile strains on the order of 7% under normal loading conditions.[55] More elongated, outer meniscus cells, however, are predicted to experience strains ranging from 2– 4%.[55] These differences highlight that elongation of a spherical cell will result in a more pronounced shape change than the same deformation of an already elongated cell. When subjected to biaxial strains of 5% *in vitro*, all cells regardless of region increase their total protein synthesis.[56] There is also a marked increase in nitric oxide levels, but this is not accompanied by an upregulation of the NOS2 gene.[56] Therefore, cells from all regions of the meniscus respond similarly to biaxial strain *in vitro*, but may differ *in vivo* due to cues from various matrix molecules present.[56]

Cells from the meniscus change their gene expression profiles in response to different regimens of compressive loading.[57] Under static compressive loading of meniscal tissue, gene expression of decorin and collagen types I and II decrease 3- to 4- fold, while mRNA levels increase 2- to 3- fold for MMP-1.[57] Under dynamic compressive loading (~1 MPa, 0.5 Hz), decorin expression decreases 2-fold, collagen type II expression decreases 4-fold, and nitric oxide (NO) levels increase.[57, 58]

In vivo, joint immobilization at 90° flexion results in a 2- to 5-fold decrease in gene expression for aggrecan, the major proteoglycan of the meniscus, indicating that meniscal cells are dependent upon mechanical cues for normal function.[59] These observations suggest that mechanical stimuli, whether in the form of static or dynamic tensile or compressive stresses, can alter cellular processes to either increase or decrease protein synthesis. Additionally, mechanical cues may be another way for cells to assess the need to create or destroy their surrounding matrix, resulting in macroscopic changes in the tissue.

Concepts

Having both chondrocytic and fibroblastic characteristics, cells of the meniscus have been historically difficult to classify. The term meniscal fibrochondrocytes has been used to highlight the complex nature of the cells. As many as four distinct cell morphologies have been identified in the rabbit meniscus with rounded cells in the inner region, cells with increasing numbers of processes toward the outer region, and spindle-shaped, flattened cells in the superficial region.

Different cell synthetic profiles have been detected based on region within the tissue. Cells of the inner meniscus synthesize both collagen types I and II, while the outer meniscus cells synthesize collagen type I, as well as MMPs 2 and 3 for matrix remodeling.[38, 45, 51, 53] Normal meniscus cell functions are also dependent on mechanical stimulation, as joint immobilization has proved to decrease gene expression for aggrecan 2- to 5-fold.[59] Cells in the meniscus are

subject to varying loading conditions, with the outer meniscus cells experiencing tensile strains of 2–4%, and inner meniscus cells experiencing 7%. In response to static compression, meniscus cells decrease gene expression for matrix molecules and increase expression for MMPs, and dynamic compression also decreases collagen and decorin expression but increases nitric oxide levels.[57]

Tables

Table 1: Tensile properties of the native meniscus

Region	Direction	Animal	Stiffness (± SD; MPa)	Reference
Meniscus	Circumferential	Cow		32
Superior			59.8	
Deep			198.4	
Inferior			138	
Lateral	Circumferential	Human		32
Anterior			159.07 ± 47.4	
Central			228.79 ± 51.4	
Posterior			294.14 ± 90.4	
Medial	Circumferential	Human		32
Anterior			159.58 ± 26.2	
Central			93.18 ± 52.4	
Posterior			110.23 ± 40.7	
Medial (from superior surface)	Circumferential	Cow		27
0-0.2 mm			48.3 ± 29.2	
0.6-1 mm			198.4 ± 87.5	
1.4-1.8 mm			139 ± 79.2	
Meniscus	Radial	Cow		32
Superior			59.8	
Deep			2.8	
Inferior			4.6	
Medial	Radial	Cow		30
Anterior			10-20	
Central			20-40	
Posterior			20-70	
Medial (from superior surface)	Radial	Cow		27
0-0.2 mm			71.4 ± 41.6	
0.6-1 mm			2.8 ± 1.2	
1.4-1.8 mm			4.6 ± 2.1	

Table 2: Compressive properties and permeability of the native meniscus using creep indentation or confined compression

Region	Animal	Aggregate modulus (± SD; MPa)	Permeability (± SD; 10^{-15} m^4 N^{-1} s^{-1})	Ref.
Medial superior	Human	Creep indentation		37
Anterior		0.15 ± 0.03	1.84 ± 0.64	
Central		0.10 ± 0.03	1.54 ± 0.71	
Posterior		0.11 ± 0.02	2.74 ± 2.49	
Medial inferior				37
Anterior		0.16 ± 0.05	1.71 ± 0.48	
Central		0.11 ± 0.04	1.54 ± 0.49	
Posterior		0.09 ± 0.03	1.32 ± 0.61	
Medial superior	Cow			37
Anterior		0.21 ± 0.06	6.22 ± 2.55	
Central		0.14 ± 0.05	5.73 ± 6.19	
Posterior		0.11 ± 0.04	4.73 ± 2.56	
Medial inferior				37
Anterior		0.16 ± 0.06	5.79 ± 4.31	
Central		0.11 ± 0.03	5.65 ± 4.13	
Posterior		0.13 ± 0.06	5.40 ± 5.36	
Medial superficial	Cow	Confined compression		27
Anterior		0.39 ± 0.11	0.76 ± 0.47	
Central-anterior		0.42 ± 0.07	0.83 ± 0.39	
Central-posterior		0.37 ± 0.08	0.78 ± 0.38	
Posterior		0.44 ± 0.11	0.63 ± 0.47	
Medial deep				27
Anterior		0.49 ± 0.04	0.91 ± 0.52	
Central-anterior		0.41 ± 0.05	0.86 ± 0.51	
Central-posterior		0.38 ± 0.09	1.03 ± 0.58	
Posterior		0.38 ± 0.04	0.74 ± 0.14	

Table 3: Shear properties of the native meniscus using creep indentation or dynamic oscillatory strain

Region	Animal	Shear modulus (± SD; MPa)	Reference
Medial superior	Human	Creep indentation	[37]
Anterior		0.08 ± 0.01	
Central		0.05 ± 0.01	
Posterior		0.05 ± 0.01	
Medial inferior			[37]
Anterior		0.08 ± 0.02	
Central		0.06 ± 0.02	
Posterior		0.05 ± 0.01	
Medial superior	Cow		[37]
Anterior		0.11 ± 0.03	
Central		0.08 ± 0.02	
Posterior		0.06 ± 0.02	
Medial inferior			[37]
Anterior		0.08 ± 0.03	
Central		0.06 ± 0.02	
Posterior		0.07 ± 0.03	
Medial	Cow	Dynamic (10% strain, 10 rad/s)	[34]
Axial		0.067 ± 0.024	
Circumferential		0. 087 ± 0.023	
Radial		0.061 ± 0.028	

Table 4: Genes related to hyaline and meniscal cartilages: Fold-increased expression relative to human mesenchymal stem cells*

Hyaline expression	Meniscus expression	Gene symbol	Gene name
>2	<0.5	IGF2	insulin-like growth factor 2 (somatomedin A)
>2	<0.5	IGL@	immunoglobulin lambda locus
>2	<0.5	RTN4R	reticulon 4 receptor (Nogo receptor)
>2	<0.5	EPHX2	epoxide hydrolase 2, cytoplasmic
>2	<0.5	CREG	cellular repressor of E1A-stimulated genes
>2	<0.5	FLJ13840	Homo sapiens cDNA FLJ13840 fis, clone THYRO1000783
>2	<0.5	BCL7A	B-cell CLL/lymphoma 7A
>2	<0.5	PLA2G2A	phospholipase A2, group IIA (platelets, synovial fluid)
>2	<0.5	CTSC	cathepsin C
>2	<0.5	RBP4	Retinol-binding protein 4, interstitial
>100	~15	COL2A1	collagen, type II, alpha 1
<0.5	>2	HPCAL1	hippocalcin-like 1
<0.5	>2	FLJ20831	hypothetical protein FLJ20831
<0.5	>2	PDLIM1	PDZ and LIM domain 1 (elfin)
<0.5	>2	C1QR	complement component C1q receptor
<0.5	>2	COL1A1	collagen, type I, alpha 1
<0.5	>2	COL1A2	collagen, type I, alpha 2
<0.5	>2	CA12	carbonic anhydrase XII

*From Ochi et al.[47]

Table 5: Properties of inner and outer meniscus cells

Property	Associated cell type	Reference
Collagen type II	Inner	39, 45, 50, 53
Aggrecan	Inner	53
NOS2	Inner	53, 54
Collagen type I	Throughout	39, 45, 50, 53
CD34	Outer	51
MMP2	Outer	53
MMP3	Outer	53

Table 6: Effects of mechanical loading on meniscus cells

Stimulus	Details	Effect	Ref.
Normal loading	Finite element model	Strain: inner cell (~7%), outer cell (~2–4%)	55
Biaxial cellular strain, in vitro	Cyclic, 5%, 0.5 Hz, 24 hrs	Increased protein synthesis (larger for outer cells than for inner cells), increased NO levels	56
Static tissue compression	0.1 MPa, 24 hrs	3- to 4-fold decrease in expression of decorin, collagen type I, II; 2- to 3-fold increase in MMP-1 expression	57
Dynamic tissue compression	0.08–0.16 MPa, 0.5 Hz, 24 hrs	2-fold decrease in decorin expression, 4-fold decrease collagen type II expression	57
Dynamic tissue compression	0–0.1 MPa, 0.5 Hz square wave, 24 hrs	Increased NO levels	58
Joint immobilization	*In vivo*	2- to 5-fold decrease in aggrecan expression	59

Figures

Figure 1: The native knee meniscus. Bovine knee joint showing the white, semicircular cartilages that make up the knee meniscus. The meniscus increases congruence between the femoral condyle and tibial plateau, and aids in normal joint function.

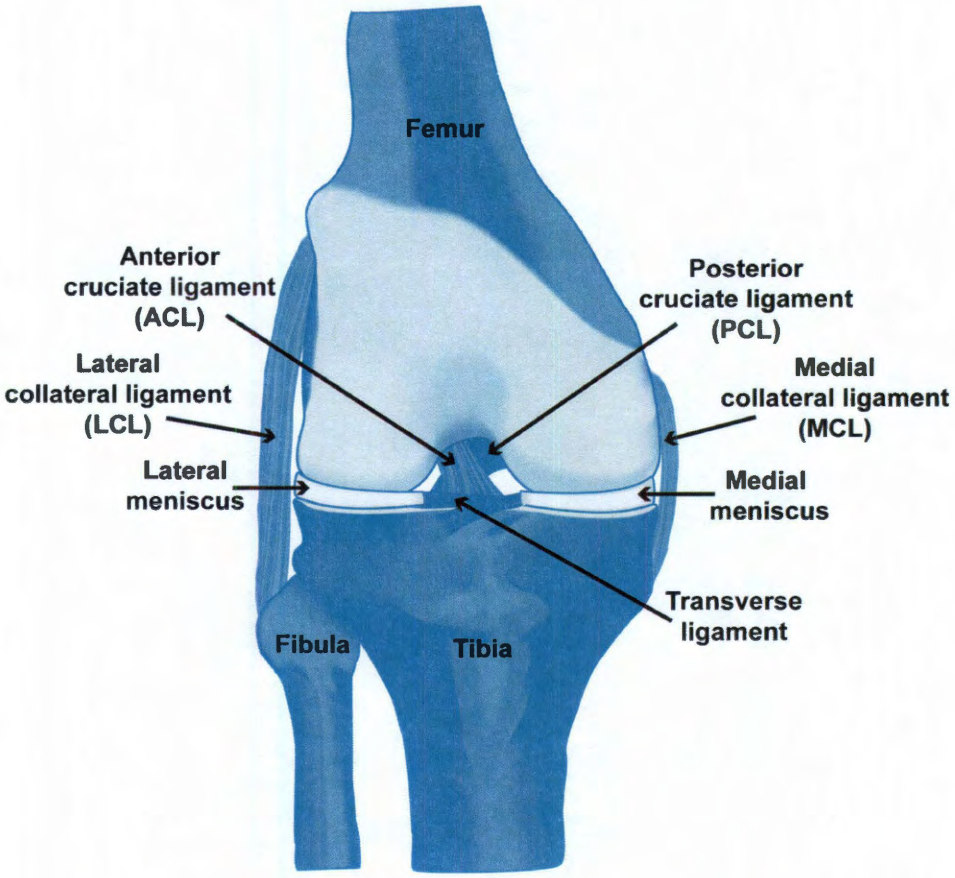

Figure 2: Anterior view of the knee joint and location of the meniscus. The meniscus is located between the femoral condyles and tibial plateau within the knee joint. It is made up of two parts, medial and lateral, which are attached to each other by the transverse ligament. Various ligaments within the joint space and on its periphery help to restrict bone movement, and maintain normal joint functionality. These include the posterior cruciate ligament, anterior cruciate ligament, lateral collateral ligament, and medial collateral ligament.

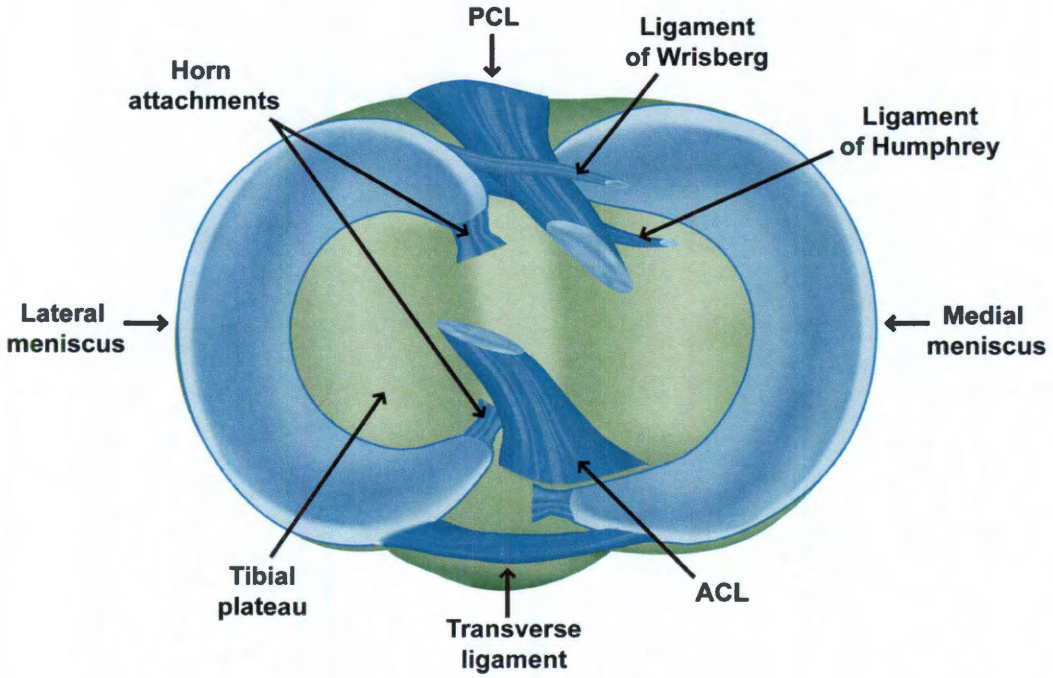

Figure 3: Superior view of the tibial plateau showing meniscal attachments. The medial and lateral menisci rest atop the tibial plateau and are affixed to the tibia via horn attachments and to each other via the transverse ligament. Other ligaments in the joint space help to restrict movement such as the ACL, PCL, and ligaments of Wrisberg and Humphrey.

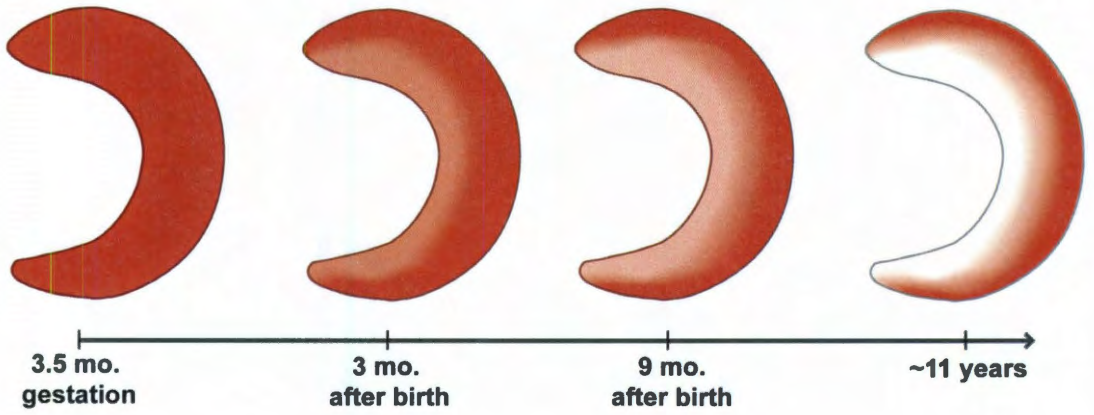

Figure 4: Decrease in meniscus vascularity during development. Before birth, the developing meniscus is completely vascularized. After birth, this vascularity begins to recede rapidly toward the outer periphery during the first 9 months, and then more gradually until approximately 11 years. At this stage, the inner one third of the meniscus is completely avascular.

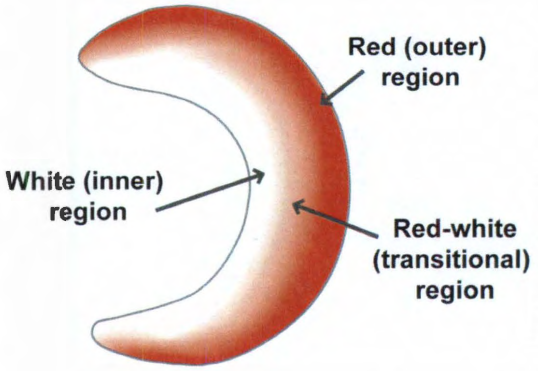

Figure 5: Locations of the three regions of the meniscus. Vascularity defines regions radially in the meniscus. Closest to the synovial membrane is the red (outer) region, which is highly vascularized. Moving toward the center of the joint space, blood vessels become more sparse in the red-white (transitional) region, and are absent in the white (inner) region.

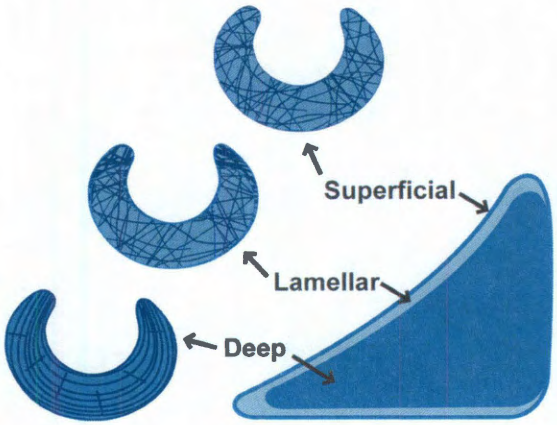

Figure 6: Collagen orientation within the meniscus. The meniscus displays different collagen organization with depth in the tissue. Here, a vertical cross-section of the meniscus is labeled with the three meniscus zones: superficial, lamellar, and deep. Collagen fibers are randomly oriented in the superficial zone and throughout most of the lamellar zone. Some radial fibers can be detected in the posterior and anterior horns of the lamellar layer. The deep layer is characterized by circumferentially oriented fibers, with some radial fibers dispersed throughout.

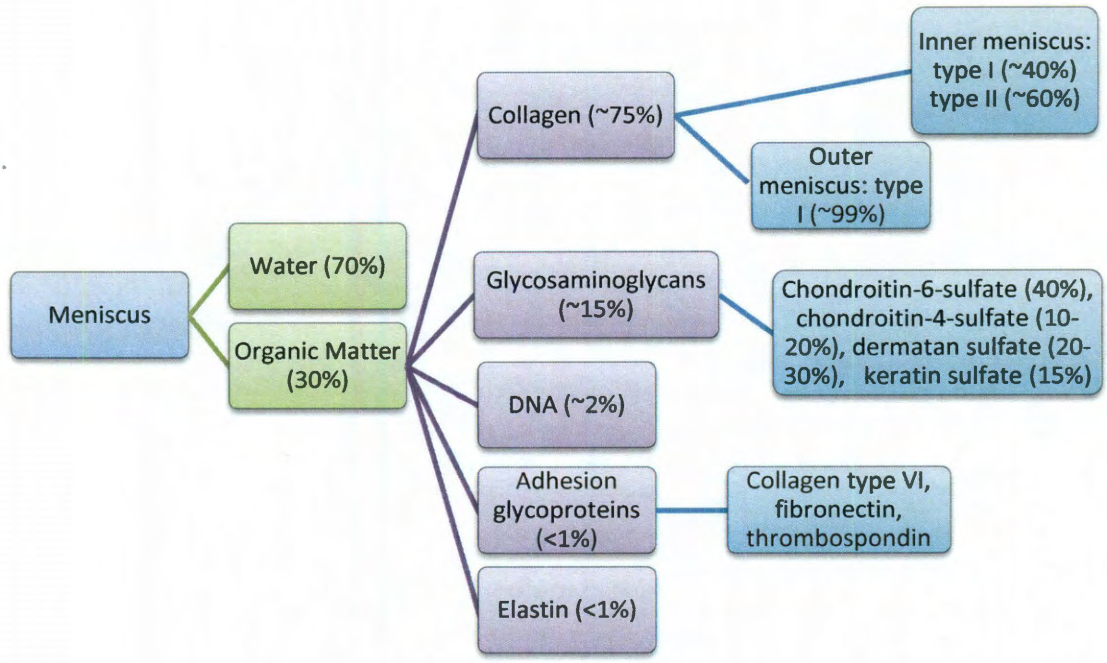

Figure 7: Schematic diagram of meniscus biochemistry. A hierarchical structure of the overall contents of the meniscus is shown in which water is the largest component. Within the solid fraction, collagens comprise the majority, followed by glycosaminoglycans. DNA, adhesion glycoproteins and elastin form a small fraction of organic matter. Variations in meniscus composition can be observed in different locations within the tissue.

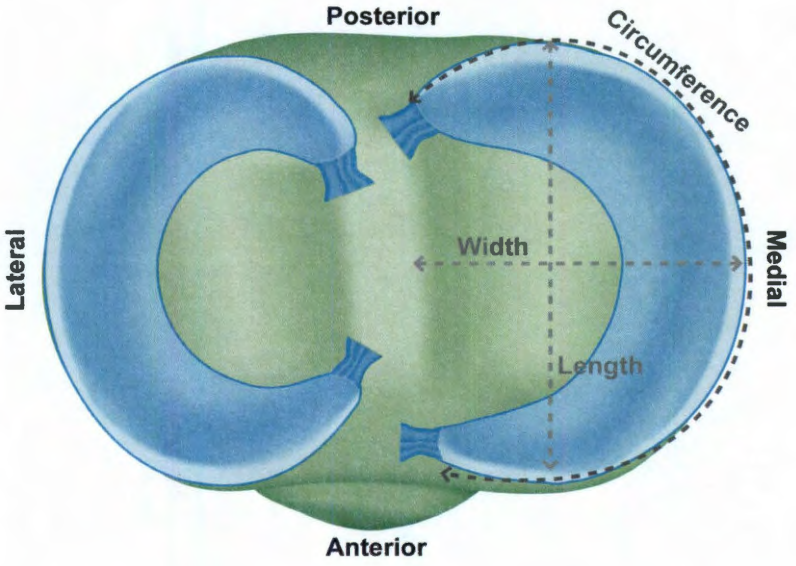

Figure 8: Geometrical measurements of the meniscus. Typical circumferential measurements for the human meniscus range from 80-100 mm and are shorter for the lateral meniscus than for the medial meniscus. Lengths and widths range from 32.4-35.7 mm and 26.6-29.3 mm, respectively.

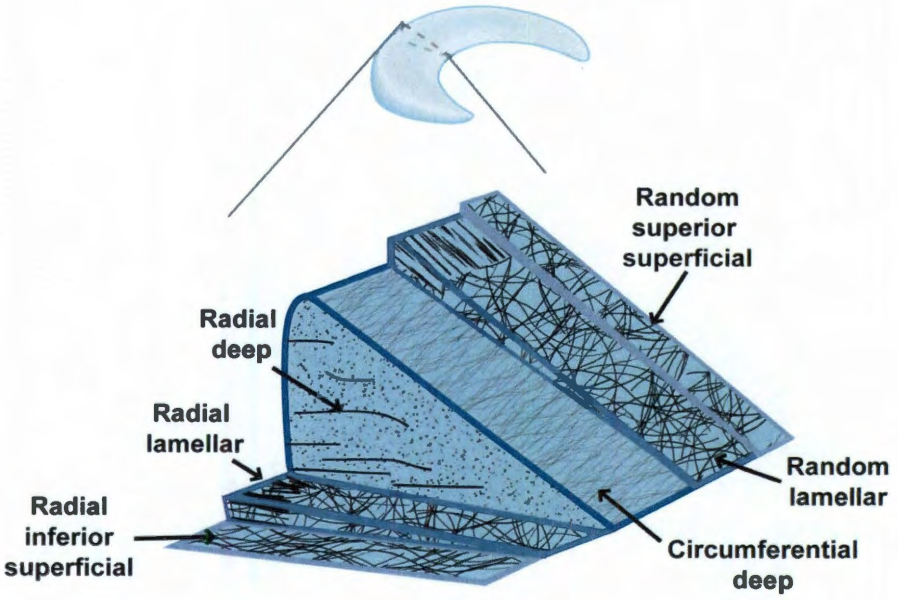

Figure 9: Collagen architecture of the knee meniscus. From core to surface, collagen arrangement changes from structured to unstructured. Collagen orientations in the meniscus are of three main types: circumferential, radial, and random. Circumferential fibers are the most abundant in the tissue and are found in the deep zone. Radial fibers are dispersed throughout the deep zone and are present on the periphery and at the horns of the meniscus in the lamellar zone. Despite the presence of radial fibers, random fiber orientation dominates the lamellar zone. In the superficial zone, fiber orientation is typically random in the superior region and more radially oriented in the inferior region.

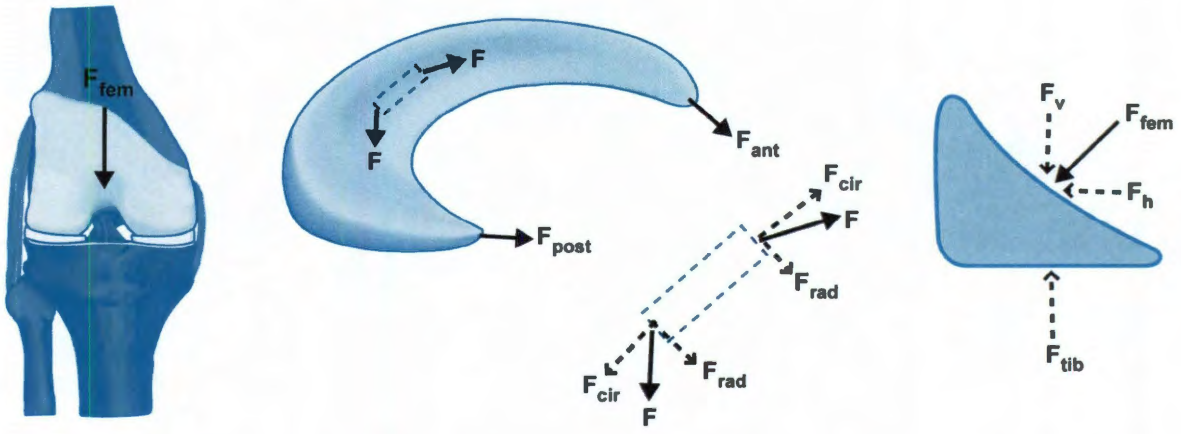

Figure 10: Free body diagram of forces acting on the meniscus during loading. As the femur presses down on the meniscus during normal loading, the meniscus deforms radially but is anchored by its anterior and posterior horns (F_{ant} and F_{post}). During loading, tensile, compressive, and shear forces are generated. A tensile hoop stress (F_{cir}) results from radial deformation, while vertical (F_v) and horizontal (F_h) forces result from the femur pressing on the curved superior surface of the tissue. A radial reaction force (F_{rad}) balances the femoral horizontal force (F_h).

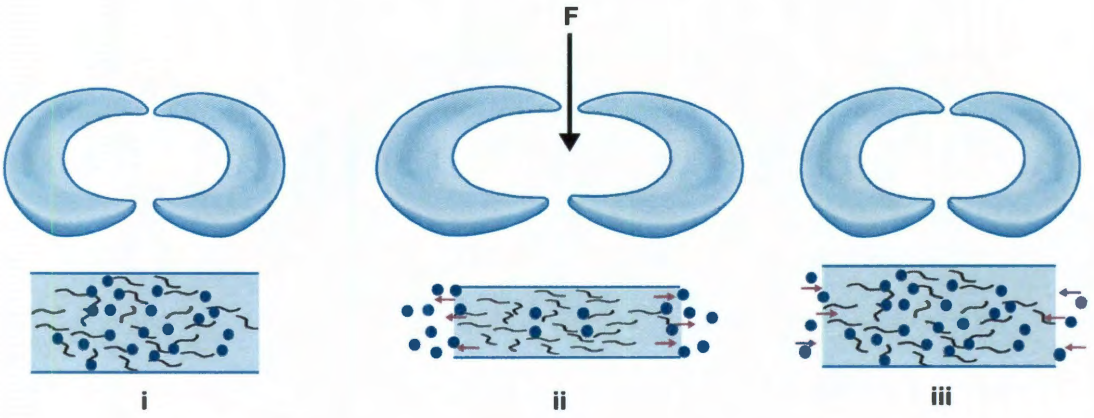

Figure 11: Biphasic behavior of meniscal tissue. (i) GAGs (black lines) and water (blue dots) coexist in the matrix, (ii) as the meniscus is loaded, water is forced from the matrix, and (iii) when the load is released, the negatively charged GAGs attract water back into the matrix, rehydrating the tissue.

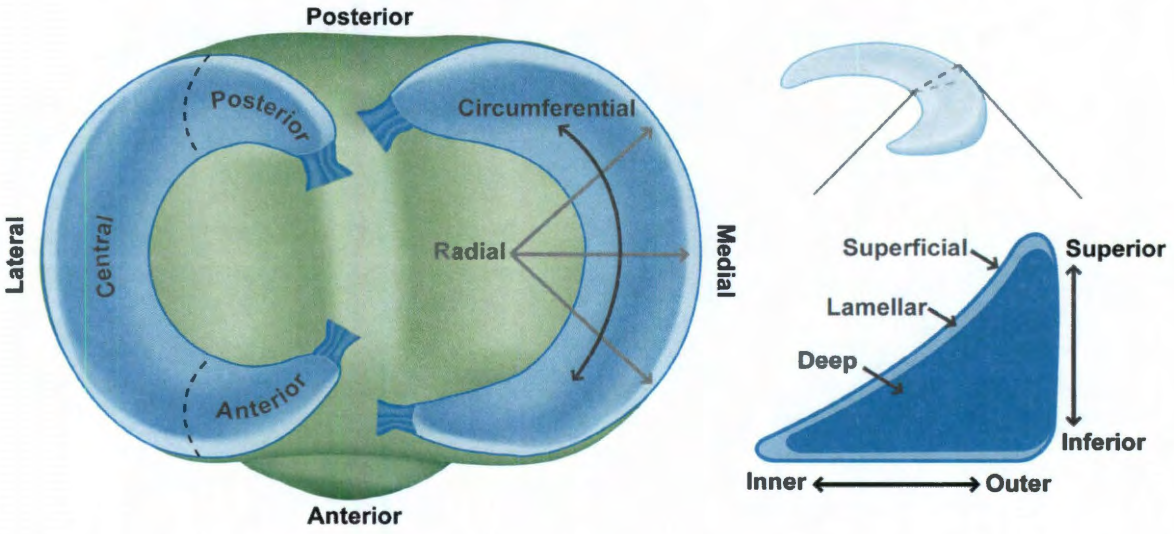

Figure 12: Regions and directions of the meniscus. Because meniscal properties vary with location in the tissue, defining different regions, depth zones, and directions is useful. The meniscus can be divided into anterior, central, and posterior regions based on location in the joint, and into superficial, lamellar, and deep zones that vary with depth in the tissue. Directions such as inner and outer, as well as inferior and superior describe the tissue from the center of the joint to its periphery, and from the tibial plateau to the femoral condyle, respectively. Also of importance are the circumferential and radial directions, which indicate that the meniscus is semi-circular in nature.

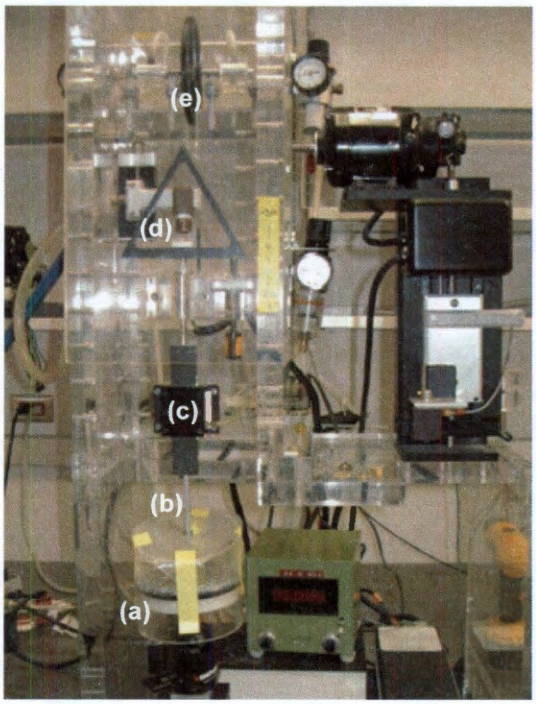

Figure 13: Creep indentation apparatus. To test a specimen using creep indentation, it is submerged in a buffer solution on the sample mounting stage (a) which is adjusted such that the specimen surface is directly under and perpendicular to the indentation tip (b). An LVDT (c) provides positional feedback to a computer to detect when equilibrium conditions are met after the system receives a step load from the loading stage (d). The entire system is suspended by a pulley (e) which relies on frictionless bearing movement provided by compressed air.

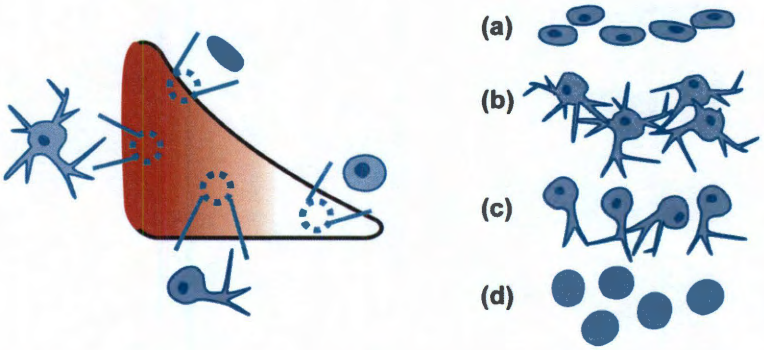

Figure 14: Cell types of the meniscus, distribution, and morphology. Superficial zone cells are flattened (a), red zone cells display many cell processes (b), red-white zone cells display some cell processes (c), and white zone cells are rounded and chondrocyte-like (d).

Chapter 2: Biomechanical Characterization of Single Chondrocytes

Abstract

Normal cartilage functions to cushion and distribute loads throughout the joint. The tissue's constitutive cells, chondrocytes, experience a variety of stresses as a result of these functional aspects, but the effects of these stresses on the individual cells are largely unknown. To understand the mechanical integrity of chondrocytes and how these properties change in response to various stimuli, mechanical testing systems for single cells have been developed. These systems are able to apply a wide variety of load types to characterize cellular biomechanics, and must rely on complex mathematical models to calculate these properties. This chapter reviews the five major mechanical testing systems that are used to test single chondrocytes, their distinct advantages, and discusses the salient results they have produced relating to chondrocyte mechanics and mechanosensitivity. Using these testing systems, it is clear that mechanical signals play a major role in chondrocyte gene expression, and these changes are essential to understand when developing functional cartilage replacements.

Chapter published as: Sanchez-Adams, J., and Athanasiou, K.A. "Biomechanical Characterization of Single Chondrocytes." *Studies in Mechanobiology, Tissue Engineering and Biomaterials*. Gefen, A., ed. Springer, 2010. ISSN: 1868-2006.

Introduction

Beginning with Aristotle's book *On the Movement of Animals*, biomechanics has sought to explain the complex processes of locomotion. As our understanding of the inner workings of the human body increased, a subset of the field emerged to closely investigate the mechanical role of individual tissues and cells. By focusing in on smaller and smaller subcomponents, biomechanics is able to explain how mechanical perturbations affect the normal and diseased states of tissues and how these stimuli can be employed in tissue engineering strategies. Employing this micro-scale approach is especially useful in studying tissues such as articular cartilage, given its major mechanical role in the body, inability to self-repair following injury, and need for functional replacement therapies.

The Mechanical Role of Cartilage

Lining the ends of bones in articulating joints such as the knee, articular cartilage facilitates smooth joint movement as well as bearing and distributing mechanical loads. Within the knee joint, cartilage routinely experiences compressive loads of three times body weight depending on the joint flexion angle and activity. Shear forces in the knee are also significant, and can reach a third of body weight at a knee flexion angle of 40°.[60] These forces are further magnified during activities such as running or jumping. As the articular cartilage

lining is only between 1 and 2.55 millimeters thick in the joints of the lower limb, the tissue must be highly specialized to withstand its mechanical environment.[61]

To achieve mechanical integrity, articular cartilage relies on a network of collagen and proteoglycans produced by its constitutive cells, chondrocytes. The collagen present in the tissue is mainly type II and provides tensile strength, while negatively charged proteoglycans such as aggrecan attract water molecules and resist tissue compression. Containing mostly water and proteins, the tissue can be modeled as biphasic material.[62-65] Mechanical testing of the tissue reveals that the tensile and compressive moduli of articular cartilage vary with depth and joint type, with the aggregate compressive modulus ranging from 0.8 to 2 MPa, and tensile modulus between 5 and 25 MPa.[66-72] But as mechanically robust as cartilage is, injury and disease can compromise its integrity and, lacking vasculature, the tissue is unable to self-repair. In response to this problem, tissue engineering strategies and biomechanical characterization techniques have emerged to further understand the role of chondrocytes in cartilage and to apply this knowledge to cartilage replacement and repair strategies.

Functional Tissue Engineering

Due to the aforementioned forces it must bear, engineered cartilage must reflect the native tissue's functional characteristics, especially its compressive and tensile integrity. To this end, the field of functional tissue engineering has emerged and spurred the creation of mechanical stimulation bioreactors to

produce mechanically robust engineered tissue, and enhance purely biochemical approaches to tissue engineering cartilage. These bioreactors use hydrostatic pressure, direct compression, shear, and combinations thereof to recapitulate the native mechanical environment *in vitro* and cause engineered constructs to become more like native cartilage.[73-77] While these mechanical stimulation strategies have improved matrix deposition and mechanical strength, the exact mechanisms of their action are ill-understood and optimal parameters for stimulation have yet to be determined. It is clear, however, that construct changes in response to mechanical stimuli are caused by cells, the most basic functional unit of any engineered tissue. Therefore, by studying individual cells it is possible to tease out the microscopic phenomena that, in combination, give rise to macroscopic changes in engineered constructs.

Applying the functional unit approach to understand the effects of mechanical stimulation begins with mechanically characterizing single cells. By determining the mechanical properties of single chondrocytes, the material limitations of the cells can be used to define the upper and lower limits of stimulation. Using these limits, the effects of various mechanical perturbations on the gene expression of single cells can be studied. And finally, mechanical stimulation parameters resulting in ideal gene expression changes can be applied to more complex arrangements of cells in tissue engineered constructs. Thus, understanding the response of the single cell to various mechanical stimuli can provide useful information for developing tissue engineering strategies.

Mechanical Testing of Single Cells

A variety of techniques have been developed to study the unique mechanical characteristics of single chondrocytes. Because the chondrocyte's diameter is on the order of 10 μm, mechanical testing machines must be especially sensitive to small changes in force and displacement. For compressive and shear testing, this is often achieved by the use of a cantilever to probe the cell and some mechanism to detect the cantilever's position over time. To test the tensile properties of chondrocytes, micropipette aspiration is the most common method and relies on pressure differentials to deform the cell. The following sections will explore in more detail the most prominent techniques used to elucidate single chondrocyte compressive, shear, and tensile mechanics.

Compression

Physiologically, cartilage tissue undergoes compressive forces on a regular basis. According to its viscoelastic nature, compressive loads are initially borne by the fluid within the tissue, but over time this load transfers to the solid portion of the matrix as the fluid is forced out.[64] Trapped within their collagen and proteoglycan matrix, chondrocytes also deform under the load. Three major tools have been used to test the compressive properties of single chondrocytes: the Cytocompressor, Cytoindenter, and the Atomic Force Microscope. The basic principles of these three apparatuses will be detailed in this section.

Cytocompressor

The Cytocompressor device is a tool to determine the compressive properties of single cells, and has been used extensively to characterize the bulk

mechanical behavior of chondrocytes. In this setup, unconfined compression is applied to single cells seeded on a glass slide via a large, flat, nonporous probe of around 50 μm in diameter. This probe is attached to the end of a cantilever beam, which is controlled by a piezoelectric actuator (Figure 1).

For each test, the probe is positioned directly over the cell which is determined by concurrent focusing of the cell and probe in the microscope. With the probe positioned over the cell, the piezoelectric actuator moves the cantilever a set distance toward the cell surface, causing the probe to compress it. This position is held until the cell reaches equilibrium. The cantilever is then retracted from the cell surface, and the volume recovery of the cell is observed. The entire compression event is recorded via a CCD camera. Video post-processing of each compression event allows for the measurement of key parameters, namely the initial, compressed, and recovery geometries of the cell at different time points, and the position of the probe. These measurements allow for the determination of the cell's compressive modulus, Poisson's ratio, and recovered volume fraction, among others.

To determine the compressive modulus of the cell, the relationship between stress and strain must be known. The following equations are used to determine the cell's stress (σ) from a cytocompression experiment:

$$\sigma = \frac{3EI(\Delta x)}{L^3 A}$$

where E and I are the Young's modulus and moment of inertia of the cantilever, L is the length of the cantilever, Δx is the difference between actual and prescribed

translation of the cantilever, and A is the contact area of the cell and probe. The strain can be written as:

$$\varepsilon = \frac{h_i - h_f}{h_i}$$

where h_i is the initial height of the cell, and h_f is the height of the cell at maximum compression. Using the Cytocompressor, a range of strains can be applied to single cells, and the resultant stresses can be calculated from the deformation of the cantilever beam and the contact area of the probe with the cell. These stresses and strains can then be plotted and fitted with a line, the slope of which gives the compressive modulus of the cell.[78-80]

In addition to the modulus of the cell, the geometric data during the compression event allow for the determination of the cell's compressibility and recovery behavior over time. The apparent Poisson's ratio (v) for the cell can be calculated as follows:[81]

$$v = \frac{\frac{w_f}{w_i} - 1}{1 - \frac{h_f}{h_i}}$$

where w_i and h_i are the cell's initial width and height, and w_f and h_f are the cell's width and height at equilibrium compression. Recovery behavior can be determined by tracking the volumetric changes of the cell over time, and can indicate whether the cell was permanently changed as a result of the applied force. For chondrocytes, which remain mostly rounded after initial seeding, cell volume can be approximated as an ellipsoid with two identical axes.

Approximating the cell's volume initially and after it has recovered from the compression, a measure of recovered volume fraction (V_r) can be determined as follows:

$$V_r = \frac{V_i - V_f}{V_i}$$

where V_i and V_f are the cell's initial and final volume, respectively.

By measuring the compressive stiffness, apparent Poisson's ratio, and recovered volume fraction, the Cytocompressor is able to provide quantitative data to help understand not only the mechanical behavior of cells themselves, but also their ability to recover from mechanical stresses. It is a system that is capable of applying varying stresses to cells, at varying rates, and can even be programmed to apply dynamic strain. This system is also unique in that it performs unconfined compression on single cells. This test is particularly relevant to chondrocytes, as these cells live in a tissue that is regularly compressed.

It is important to note, however, that the Cytocompressor has some limitations. Because its mechanism tests cells in a semi-rounded morphology, for cells that do not normally exist in this geometry the data may not be as relevant. Moreover, teasing out the mechanical characteristics of cells using this setup requires that some approximations in geometrical models be made. These approximations undoubtedly introduce error into the calculations, and careful measurements must be made in order to minimize this error.

Cytoindenter

Closely related to the Cytocompressor is the Cytoindenter (Figure 2). This apparatus applies many of the same principles as the Cytocompressor, but there are a few key differences. Like the Cytocompressor, the Cytoindenter uses a probe attached to a cantilever beam controlled by a piezoelectric actuator for load application, but here the probe is much smaller than the cell (approximately one quarter of its diameter). Unlike the Cytocompressor, the Cytoindenter does not rely on video capture to determine probe position and deflection. Originally these measurements were made using a dual photodiode detector, a technique that is used in the Cytodetacher apparatus and will be discussed in more detail later.[82, 83] The current system, however, monitors the displacement of the cantilever via a laser reflected off the free end of the cantilever.[84] This information is transmitted to the control system and integrated with the displacement data of the piezoelectric actuator. Together, the laser displacement meter and piezoelectric actuator are able to keep constant the force applied to the cell, resulting in creep indentation testing.

As the system does not measure force outright, it must be calculated based on the measured cantilever displacement by the laser and the intrinsic geometry of the apparatus. This is achieved by combining laser displacement data with the force equation for a cantilever beam, as shown below:[84]

$$F = \frac{3EI\Delta x}{(L_1^3 + \frac{3}{2}L_1^2 L_2)}$$

where E is the Young's modulus of the cantilever, I is its moment of inertia, L_1 and L_2 add up to the length of the cantilever and are determined by the position of the probe, and Δx is the deflection of the cantilever beam, as measured by the laser micrometer. This equation is similar to that for pure end-loading of a cantilever, but is complicated by the fact that the force is applied a short distance from the end and the laser micrometer measures the displacement of the beam at its end. Nevertheless, using this equation the force can be monitored in real time and used to apply creep indentation to single chondrocytes.

Once a creep curve is produced, it must be analyzed using a mathematical model in order to obtain the material properties of the cell. To model cell indentation, the punch problem can be used in which the cell is assumed to be a linearly elastic, isotropic, and homogeneous half-space which is indented with a flat, rigid punch. The basic equations for this model have been adapted by Koay et al. to account for viscoelasticity in the cell.[84] The resultant equations from this analysis can define three material properties of the cell: the apparent viscosity (μ), instantaneous modulus (E_0), and relaxed modulus (E_∞). These properties are determined by fitting the following equation to the displacement vs. time curve from each experiment:

$$\Delta x(t) = \frac{3F}{8RE_0}\left(-\frac{E_0}{E_x}e^{\frac{-E_x t}{3\mu}} + \frac{E_0}{E_x} + 1\right)$$

where R is the radius of the indenting probe and E_x is an elastic constant. The relaxed modulus can then be calculated from the following equation:

$$E_{\infty} = \frac{E_0 E_x}{E_0 + E_x}$$

where the variables are as mentioned previously.

The Cytoindentation apparatus possesses several advantages that allow it to characterize the mechanical behavior of individual chondrocytes. Most importantly, it is capable of performing creep indentation on single cells, a test that is able to elucidate the viscoelastic properties of single cells. Due to the simplicity of sample preparation in this setup, any type of anchorage dependent cell type may be tested. The system may also be adapted to use different shaped probes to apply different types of load to the cell. These characteristics all contribute to the system's versatility and applicability.

Along with its many advantages, there are some limitations that must be considered when using the Cytoindenter. As with the Cytocompressor, assumptions about the geometry and homogeneity of the material must be made in order to solve for material properties. In the case of indentation of single cells, the assumption of cell homogeneity may not be accurate as the mechanical properties of subcellular components can vary. Additionally, this system is unable to record recovery data for mechanical tests due to inherent noise in the system. Cell analysis using cytoindentation must be therefore be combined with recovery data from the Cytocompressor.

Atomic Force Microscopy

Atomic force microscopy (AFM) has a wide variety of applications including scanning material surfaces, measuring intermolecular forces, and

testing the mechanical properties of single cells. This technology relies on the use of a cantilever beam, similar to the Cytocompressor and Cytoindenter, but the tip of the cantilever on the AFM is much smaller (Figure 3). For use in testing single chondrocytes, a 5 μm diameter spherical tip is attached to AFM cantilevers and used for indentation of the cell surface.[85, 86] The deflection of the cantilever as it indents the cell is monitored via a laser reflecting off the cantilever into a photodiode detection system. Small changes in the position of the laser beam on the photodiodes indicate how far the cantilever is deflected, thereby allowing for the calculation of applied strain on the cell. For stress-relaxation testing using the AFM, a feedback loop is used to apply a set strain and measure the deflection of the beam over time. Using the appropriate model to fit the data, it is possible to gain both stress and strain data from these tests, and ascertain single cell mechanical properties.

Taking into account the shape and hardness of the indenting probe, and viscoelastic nature of cells, Darling et al. developed a model to fit the data obtained from AFM stress-relaxation tests of single chondrocytes.[86] Beginning with a modified Hertz equation for the force of a rigid sphere on a deformable substrate, the elastic and viscoelastic stress-strain relationships are derived assuming the cell surface is isotropic and incompressible. Combining the viscoelastic and elastic responses and specifying a step displacement for the stress-relaxation test, the following force equation can be obtained:

$$F(t) = \frac{4R^{1/2}\delta_0^{3/2}E_R}{3(1-\nu)}\left(1 + \frac{\tau_\sigma - \tau_\varepsilon}{\tau_\varepsilon}e^{-t/\tau_\varepsilon}\right)$$

where R is the relative radius of the probe tip and cell, E_R is the relaxed modulus of the cell, δ_0 is the prescribed step displacement, v is the cell's Poisson's ratio, and τ_ε and τ_σ are relaxation time constants under constant deformation and load. This equation can then be fit to a force displacement curve to obtain viscoelastic properties such as the instantaneous and Young's moduli of the cell. The equations for these properties are as follows:

$$E_0 = E_R\left(1+\frac{\tau_\sigma - \tau_\varepsilon}{\tau_\varepsilon}\right)$$

$$E_Y = \frac{3}{2}E_R$$

where E_0 is the instantaneous modulus, and E_Y is the Young's modulus of the cell.

AFM technology allows for very precise measurement of forces, and has been used to study many types of materials and surfaces.[87, 88] The system is capable of testing in a variety of modalities including scanning, tapping, and controlled displacement, and can accommodate many tip geometries including conical and spherical. The tips have even been functionalized to study interaction forces between molecules, demonstrating the AFM's ability to study nanoscale events on a cell's surface or between a cell and a substrate.[89-91] Indenting cells with the AFM can produce data that, when combined with an appropriate mathematical model, is a powerful characterization tool.

The development of a mathematical model to describe single cell testing with the AFM can be a challenging task. As all variables cannot be controlled, assumptions about the cell's geometry, homogeneity, and compressibility must

be made in order to solve the constitutive equations involved. Because the cell contains organelles and cytoskeleton, and may assume different shapes when attached to a surface, these assumptions may introduce error in calculating the mechanical properties. Careful consideration must be made, therefore, to ensure the applicability of various models to single cell AFM mechanics data.

Shear

In addition to compressive forces, chondrocytes also experience shear as loads are distributed within the joint space. Understanding the shear characteristics of single chondrocytes will allow for a better understanding of their contribution to the tissue as a whole. In this section, two related systems will be reviewed that are able to measure cell adhesion and the apparent shear modulus of single chondrocytes.

Cytodetacher and Cytoshear

The Cytodetacher was first developed to measure adhesion forces of cells to various substrates, and has since broadened its applications to measure the bulk shear properties of chondrocytes and other cells.[83] The system consists of a 75 μm diameter horizontal cantilever probe attached at the top to a piezoelectric actuator setup (Figure 4).

Once the horizontal cantilever is positioned at the edge of a cell attached to a flat vertical substrate, the piezoelectric actuator moves a precise distance across the cell-seeded surface, detaching the cell from its substrate. The displacement of the probe is measured by a dual photodiode which detects small

changes in the transmitted light in the microscope's view field resulting from the movement of a carbon filament attached to the side of the vertical probe. Using the displacement data from the photodiode, and the mechanical properties of the cantilever probe itself, it is possible to calculate the reaction force of the cell during detachment. From cantilever beam theory, this force can be written as:

$$F = \frac{3EI\Delta x}{L^3}$$

where E is the material stiffness of the horizontal probe, I is the probe's moment of inertia, Δx is the difference between the actual displacement of the probe and its prescribed displacement, and L is the length of the probe.

While the elements of data analysis remain the same, this system has been modified to allow for cells to be seeded on a horizontal surface.[92] This modification was achieved by rotating the probe 90° while maintaining the carbon filament horizontal to the cell seeded surface for photodiode detection. This provided a significant improvement in the system's ease of use, and initiated further modifications to enhance its ability to measure cell stresses and strains.

This system has most recently been modified to measure the shear properties of cells.[93] In this modification, the vertical probe is represented by a 50.8 μm diameter tungsten wire and displacement measurements are made by analyzing individual frames from video-captured shear events. As in the first iteration of this system, cantilever beam theory is used to calculate applied force from the apparent and prescribed displacements. In the case of cell shearing, however, the probe is placed a set distance from the substrate and translated resulting in shearing of the cell rather than simple detachment. The necessary

data for the cellular deformation are also provided via analyzing frames extracted from video-captured events. Throughout the shearing event the cell's leading edge, trailing edge, and the probe are tracked providing data to calculate the cell-probe contact area (needed to calculate stress), and the cell's elongation. The contact area of the probe on the cell can be calculated by assuming the area is a half-ellipse:

$$A = \frac{1}{4}\pi(w_c)(h_c - h_p)$$

where w_c represents the width of the cell, and h_c-h_p denotes the difference in height of the cell and probe from the surface, respectively. Using this contact area and the applied force from cantilever beam theory, a measure of the applied stress can be calculated using the relation:

$$\sigma = \frac{F}{A}$$

To calculate the shear strain (ε) experienced by the cell throughout the shearing event, the following relationship can be used:

$$\varepsilon = \frac{w_i}{w_c}$$

where w_i denotes the indentation depth of the probe into the cell, and w_c is the initial cell width as before. By plotting the stress versus strain curve and fitting a line to the data, it is possible to calculate the apparent shear modulus of the cell.

All of the modifications of the Cytodetacher have provided some improvement in the ability to quantify cell adhesion forces and shear properties. As chondrocytes rapidly de-differentiate in monolayer, adhesiveness of these

cells to various substrates can provide a quantitative measure of phenotypic changes over time. Adhesion forces of chondrocytes to various substrates is also an important measure of the cell's interaction with materials used in tissue engineering strategies. The modification of the Cytodetacher for measurement of the apparent shear modulus of chondrocytes also provides a useful tool to measure the biomechanical properties of the cell itself. This method allows for measurement of the apparent shear modulus, which can be used to ascertain characteristics of the cell under a biomechanically relevant load.

The Cytodetacher, while useful for studying anchorage-dependent cells, was not designed to study floating cells given that its setup necessitates cell adhesion to a substrate. Additionally, care must be taken to apply the correct geometrical model to each experiment as different cell types may appear more rounded than others when adhered to a surface.

Tension

Chondrocytes also experience tensile forces from matrix proteins around them pulling in the direction of local compressive or frictional loads. Tensile forces may also be generated in mechanical stimulation of tissue engineered cartilage constructs. In this section, the use of micropipette aspiration will be examined as it relates to chondrocyte biomechanics.

Micropipette Aspiration

Micropipette aspiration uses pressure differentials to calculate the force the cell experiences, and relates that to the observed strain, as seen in Figure 5.

To perform this type of experiment, a cell is suspended in fluid of pressure p_1 and a micropipette is placed on the cell membrane. The pressure within the pipette is then reduced to p_0 and the cell membrane extends into the pipette at a distance l_p. Given the radius of the micropipette, r_p, the relationship between stiffness and pressure differential for an infinite homogeneous half-space aspirated into a pipette is:

$$\Delta P = \frac{2\pi}{3} E \frac{r_p}{l_p} \phi$$

where ΔP is the pressure differential between p_o and p_1, E is the Young's modulus of the cell, and φ is approximately 2.1 and depends on the geometric properties of the pipette itself.[94] Solving for the Young's modulus, and substituting for φ, this equation reduces to:

$$E = 0.22\left(\frac{r_p \Delta P}{l_p}\right).$$

Another useful parameter to gain from micropipette aspiration experiments is the viscosity of the cell. Given that cells are viscoelastic materials, cell viscosity can be a useful measure of its phenotype. Modeling the cell as a homogeneous, semi-infinite half-space, to calculate cell viscosity (μ) in this setup the following equation may be used:[95]

$$\mu = \frac{r_p \Delta P}{6\frac{dl_p}{dt}\left(1 - \frac{r_p}{r_c}\right)}$$

where ΔP, r_p, and l_p are the same as before, and r_c is the radius of the cell outside of the micropipette. In this equation, the rate of change of membrane

extension into the pipette (dl_p/dt) must also be measured, and can be attained by varying the pressure within the micropipette and recording the resulting deformation with time. This method can also be used to obtain the instantaneous and relaxed modulus of the cell.[86]

Micropipette aspiration can be used on both anchorage dependent and floating cells, making it a widely useful mechanical testing tool. It can produce forces between 10 pN and 10^4 nN, and can reach pressures as low as 0.1 pN/μm^2.[96] This method can also determine whether a cell behaves as a liquid drop or a solid, which becomes useful when deciding on a model for further analysis of cell biomechanics. Mechanical parameters drawn from micropipette aspiration tests can be used to characterize cells and understand their mechanical role in the body.

Along with the many attributes to this method, there are some important considerations that must be made when analyzing its resulting data. Due to the nature of the experiment, measures of viscosity and stiffness are heavily influenced by the mechanical properties of the cell membrane, and thus may not reflect the bulk properties of the cell. Given the microenvironment of the chondrocyte, and that its deformation occurs mostly in compression, testing a portion of the cell in tension will provide some indication of cell properties, but those properties may not be as physiologically relevant.

Chondrocyte Biomechanics

All of the aforementioned single cell mechanical testing systems have been used to mechanically characterize chondrocytes, providing information on a wide variety of previously unknown cellular properties. Considering the mechanical properties of chondrocytes can help to understand the mechanical limitations of the cells within their native environment.

Mechanical Properties of Single Chondrocytes

Often, the same mechanical property can be obtained using a variety of different testing methods. The properties that do overlap, however, do not always match between systems. For example, the instantaneous modulus of chondrocytes using the AFM is around 0.29 kPa, while the same parameter measured using cytoindentation is around 8 kPa.[84, 86] Similar disparities are observed in relaxed modulus, viscosity, and equilibrium time constant measurements between systems. From Table 1, it is apparent that the AFM measures relatively low viscosity compared to measurements from micropipette aspiration, while the viscosity measured by cytoindentation falls between the two. Moreover, equilibrium time constants, when measured with micropipette aspiration can be more than an order of magnitude higher than values obtained from cytoindentation. This wide range could be a result of many different factors, including the constitutive model used, geometric assumptions, biological variability, the source of the tested chondrocytes, and of course the fact that the cell may or may not be anchored during testing.

Perhaps the biggest contributor to these apparent inconsistencies, however, is the type of test performed on the cell. Though literature for chondrocyte mechanics may report the same cellular properties, the particularities of each apparatus and the mathematical model used to calculate those values may only yield a certain aspect of those properties. For example, while the cell's instantaneous modulus can be obtained by AFM and cytoindentation, the different probe geometries and testing modalities may be testing different areas of the cell. More research must be done to better understand these differences, which will inevitably be helped by more rigorous mathematical models for the approximation of the cell.

Contributors to Chondrocyte Mechanics

Though comparing properties from different mechanical testing modalities may not yield meaningful results, comparing cells tested in one modality is a powerful tool and has been used to understand the source of chondrocyte mechanical integrity. Using the Cytocompressor, Ofek et al. showed that knocking out different cytoskeletal components within the chondrocyte can vary the mechanical properties of the cell. Specifically, actin filaments emerged as the greatest contributor to compressive stiffness as actin disruption decreased the compressive modulus of the cell by nearly 40%. Additionally, absence of any of the cytoskeletal components doubled the residual strain of the cell following compression, indicating that the cell's cytoskeleton is important for recovery from mechanical perturbation. This study also showed that cytoskeletal components

greatly influence the apparent Poisson's ratio. The results indicate that at a certain strain threshold, the microtubules that normally serve as rods holding the cell shape are broken down, reducing cell volume and Poisson's ratio.[80] Termed the critical-strain threshold, this change in mechanical behavior of the cell with applied strain may indicate modifications in gene expression and matrix production in response to, or as a result of, cellular deformation.

Along with the cytoskeleton, the nucleus can contribute largely to the overall mechanical integrity of the cell. Chondrocytes, because they exist in a rounded morphology, also have rounded nuclei which respond to loading by changing volume and modifying gene expression.[97] Therefore, nuclear deformation may be necessary for the cell to respond to mechanical load, and the determination of its stiffness could play a major role in identifying effective cartilage stimulation regimens. Nuclear mechanical properties have been measured with a few different methods. Using micropipette aspiration, the free-floating nucleus appears to be 3 to 4 times stiffer than the cell, while modeling techniques used to fit chondrocyte cytocompression data indicate that the nucleus may be only about 1.4 times stiffer than the rest of the cell.[98, 99] Despite the inconsistencies between micropipette aspiration data and theoretical modeling of nuclear stiffness, the methods do agree that the nucleus is somewhat stiffer than the rest of the cell, and therefore can affect its overall mechanics. With more investigation, nuclear mechanics data may prove to be a powerful tool in understanding the underlying mechanotransduction of stimulated chondrocytes.

Chondrocyte Mechanosensitivity

Chondrocytes are known to modify gene expression patterns in response to both biochemical and mechanical perturbations. While research in the area of chondrocyte mechanosensitivity is still in its early stages, the present data indicate that these cells are particularly sensitive to mechanical loading.

Both loading type and loading duration can cause shifts in gene expression of single chondrocytes. When subjected to varying forces applied in unconfined creep compression, chondrocytes display a dose-dependent decrease in collagen type II expression with increasing load, and aggrecan gene expression decreases sharply when force is increased from 25 nN to 50 nN of load. Accompanying the decrease in matrix protein expression with load, an increase in tissue inhibitor of metalloproteinase-1 (TIMP-1) gene expression levels is observed.[97] Together, these data indicate that when loaded in this manner, chondrocytes adapt their gene expression profiles from matrix production to matrix maintenance. Similar results are observed when chondrocytes are statically loaded with forces of 50 and 100 nN, but these forces applied dynamically result in matrix molecule gene expression recovered to control states.[100] These results suggest that the way a load is applied (static or dynamic) can profoundly affect the chondrocyte gene expression, and can provide valuable insight into useful modes of engineered cartilage stimulation.

Gene expression and mechanics of loaded chondrocytes are also affected by the biomolecules present. In the same creep compression experiment, Leipzig

et al. showed that the application of transforming growth factor beta-1 (TGF-β1) or insulin-like growth factor-I (IGF-I) throughout the experiment significantly decreased the strain experienced by the cell, and resulted in differing gene expression profiles than stimulated cells without growth factors.[97] Applying TGF-β1 increased aggrecan gene expression over controls in most cases, while adding IGF-I kept TIMP-1 levels relatively constant for all loads. It has also been shown that these two biomolecules are able to stiffen cells significantly, resulting in altered deformation patterns under the same loading conditions.[78, 101] Biomolecules are therefore important regulators of chondrocyte mechanosensitivity. In fact, as chondrocytes in the presence of growth factors such as IGF-I are known to both stiffen the cells and increase gene expression for collagen type II and aggrecan, they can provide a mechano-protective effect by inhibiting both deformation and gene expression changes caused by mechanical loading.[78, 102] More studies need to be performed to determine the precise ways biomolecules and mechanical stimulation can combine to affect chondrocyte gene expression and mechanics. This information will inevitably prove useful when designing cartilage engineering strategies such that they can harness the synthetic capabilities of chondrocytes.

Conclusions

The mechanical integrity of cartilage is extremely important to its normal function in the body. Due to its lack of reparative potential, damage to this tissue is usually permanent and can lead to further musculoskeletal complications.

Therefore, a functional cartilage replacement is a valuable prospect, and tissue engineering continues to develop new and exciting answers to this problem. Achieving functionality in tissue engineered constructs, however, requires knowledge of the intrinsic biomechanics of cartilage and its cells. By first characterizing the biomechanics of individual chondrocytes, informed decisions can be made regarding the most effective biochemical and mechanical stimulation methods to use in more complex arrangements of these cells.

Healthy cartilage experiences many different types of loads on a daily basis, including compression, shear, and tension. How these forces are transmitted to individual chondrocytes and their effect on the cell's genotype, however, is not well understood. To study this, a number of mechanical testing and stimulation systems have been developed which are able to characterize not only cellular mechanics, but the effect mechanical loading has on gene expression. Additionally, these devices have been able to resolve the effects of growth factors on individual cell biomechanics, showing that chondrocytes become stiffer in the presence of certain biomolecules.

As chondrocyte mechanical properties obtained from different systems do not always agree with one another, it is important to understand each individual system and the type of test it performs. Small differences in load application and the type of model used to fit the data can magnify the discrepancies between mechanical testing systems. Bulk properties of individual chondrocytes are best tested using the Cytocompressor and Cytoshear devices because non-homogeneities are diminished by the probe being much larger than the cell. In

devices where the probe is smaller than the cell, namely the Cytoindenter, AFM, and Micropipette Aspiration systems, these non-homogeneities may be measured, and can provide information about cytoskeletal arrangement and local cell properties. With an understanding of these differences, the mechanical properties of single chondrocytes can be determined and this information can be used to inform tissue engineering strategies. As more information is available about cellular responses to mechanical and biochemical factors, more directed efforts can be made to combine cells with various stimuli to create functional engineered cartilage. Cellular biomechanics testing and stimulation systems like the ones described here are beginning to make this possible.

Future Directions

With the recent advances in chondrocyte biomechanics testing and evaluation, some interesting questions have emerged which deserve further investigation. First, understanding the mechanosensitivity of subcellular components can elucidate the major players in the mechanosensitivity of the cell as a whole. As it is known that the actin cytoskeleton is an important component of cellular stiffness, it may be important in transducing mechanical signals from the cell membrane to the nucleus. Moreover, nuclear mechanical properties are known to differ from the rest of cell, but the importance of this difference in signal mechanotransduction is unknown. These same principles can be applied to any number of chondrocyte subcellular components, and may lead to a more complete understanding of the machinery of chondrocyte mechanotransduction.

These types of experiments can be facilitated by the use of targeted fluorescent molecules to track subcellular components throughout a loading regimen, providing graphic evidence of their response to mechanical stresses.

Another area that should be expanded is the application of these cellular mechanical testing devices to other cell types. At present, aside from the AFM, many of these devices have only been used with a few cell types. Mechanical characterization of cells from other mechanically functional tissues such as tendon, ligament, bone, meniscus, and muscle can provide the same benefits as chondrocyte characterization. As most of these systems are highly adaptable, it would be a natural extension of the technology and would provide interesting comparative values for use in reconstructive therapies.

These future applications can add utility to cellular mechanical testing systems, and allow for a more complete understanding of mechanotransduction pathways of single chondrocytes.

Acknowledgments

We would like to acknowledge the Rice-Houston Alliance for Graduate Education and the Professoriate (AGEP) program for their support and funding of this work. We would also like to acknowledge the former lab members who helped develop, test, and validate the Cytocompressor, Cytoindenter, and Cytoshear systems from this lab: Dr. Adrian Shieh, Dr. Nic Leipzig, Dr. Eugene Koay, Dr. Gidon Ofek, Sriram Eleswarapu, and Dena Wiltz.

Tables

Table 1: Reported mechanical properties of articular chondrocytes using various testing devices

Mechanical Testing Device	Modulus* (kPa)	Viscosity (μ, kPa·s)	Time Constant (τ, s)	Ref.
Cytocompressor	1.63 ± 0.31 (E)	-	1.6 ± 1.3 (recovery)	80
Cytoindenter	8.0 ± 4.41(E_0) 1.09±0.54 (E_∞)	1.5±0.92	1.32 ± 0.65	84
AFM	0.29 ± 0.14 (E_0) 0.17 ± 0.9 (E_∞)	0.61 ± 0.69	9 ± 6.2	86
Cytoshear	4.1 ± 1.3 (*low*) 2.6 ± 1.1 (*med*) 1.7 ± 0.8 (*high*)	-	-	93
Micropipette Aspiration	0.41 ± 0.17 (E_0) 0.24 ± 0.11 (E_∞)	3 ± 0.18	33 ± 20	103
	0.45 ± 0.14 (E_0) 0.14 ± 0.05 (E_∞) 0.2 ± 0.07 (E_Y)	2.57 ± 1.83	37 ± 26	86

* Modulus abbreviations: Instantaneous (E_0), Relaxed (E_∞), Compressive (E), Young's (E_Y), Shear (*low, med, high probe positions*)

Figures

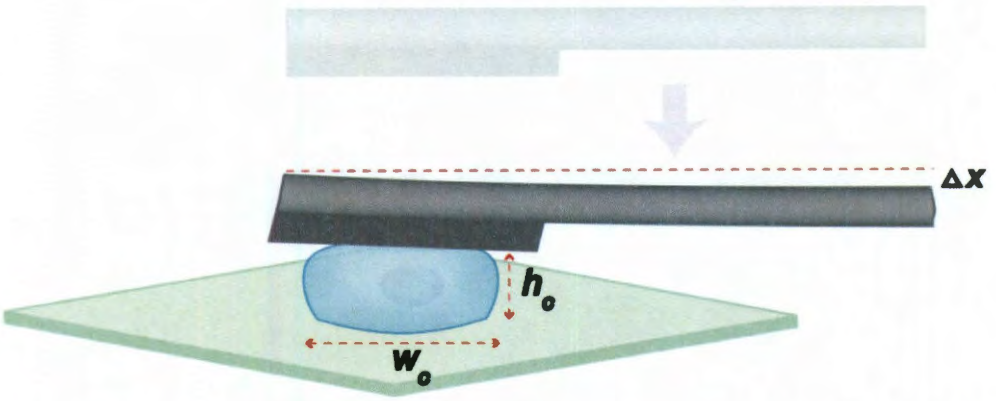

Figure 1: Schematic diagram of the Cytocompressor. To test single cells under unconfined compression, the Cytocompressor uses a cantilever beam with a wide probe attached to its end. A piezoelectric actuator precisely moves the cantilever probe assembly toward the cell surface, and compresses the cell a set amount. Compression events are recorded via a CCD camera, and cell height (h_c) and width (w_c) are determined from extracted frames.

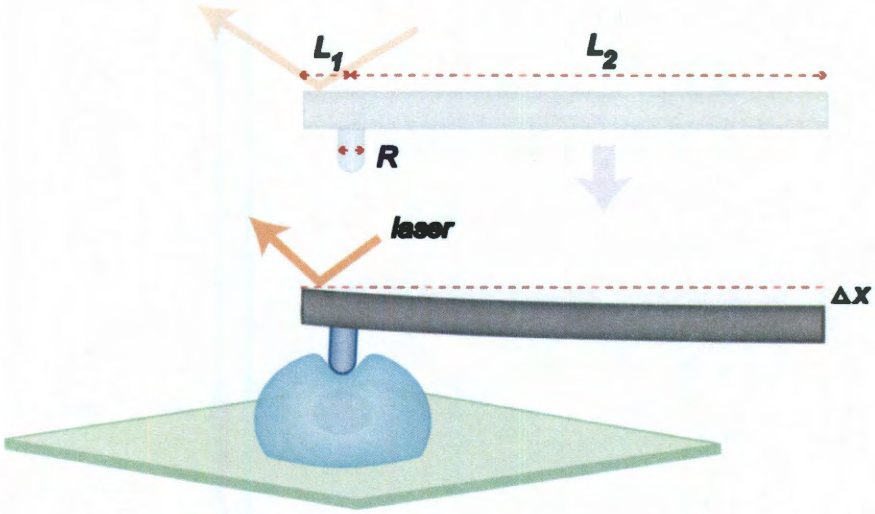

Figure 2: Schematic diagram of the Cytoindenter. The Cytoindenter tests cells under creep indentation, using a thin probe of radius R attached to a cantilever beam. Like the Cytocompressor, the cantilever-probe assembly is controlled by a piezoelectric actuator. The probe placement on the cantilever (described by lengths L_1 and L_2), material properties of the cantilever, and data from the laser micrometer allow for the application of constant force to the cell surface. Probe displacement data over time are recorded and used to extract viscoelastic material properties of the cell.

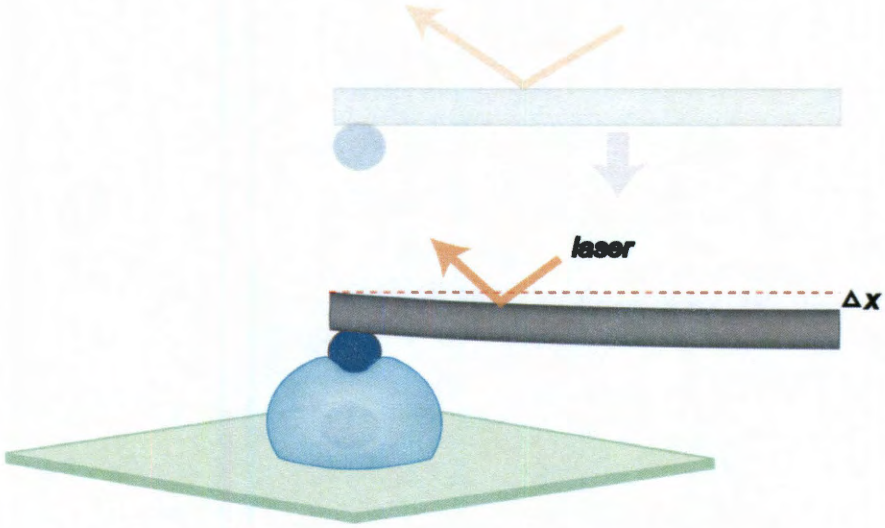

Figure 3: Schematic diagram of Atomic Force Microscopy. In this setup, stress relaxation experiments on single chondrocytes are performed by using a spherical probe attached to a cantilever beam. The probe displacement throughout the experiment is monitored by reflecting a laser off the cantilever and monitoring the angle of reflection over time. This information is then fed back into the actuator system that moves the cantilever to apply a constant strain on the cell. The resultant force versus time graph is then used to determine cellular mechanical properties.

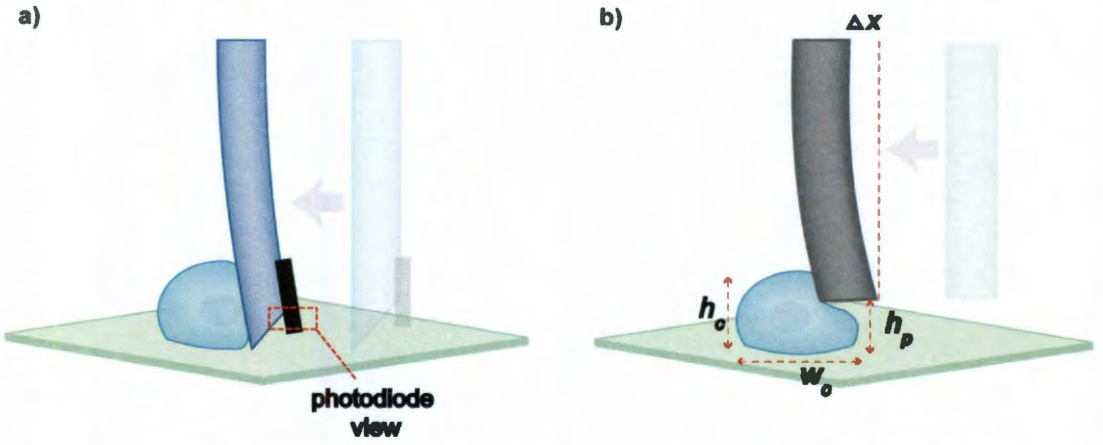

Figure 4: Schematic diagrams of the Cytodetacher and Cytoshear devices. Both the Cytodetacher (a) and Cytoshear (b) systems rely on a piezoelectric actuator to move the probe toward the cell and cause deformation. The Cytodetacher system uses a glass probe with an attached carbon filament positioned at the base of the cell, and monitors the carbon filament displacement via a dual photodiode. Attachment force is then calculated using cantilever beam theory. The Cytoshear device records each event using a CCD camera, and positions its probe some distance above the base of the cell. Shear properties of the cell are then determined using the cell width (w_c) and height (h_c) over time combined with the knowledge of the probe height (h_p) and probe displacement (Δx).

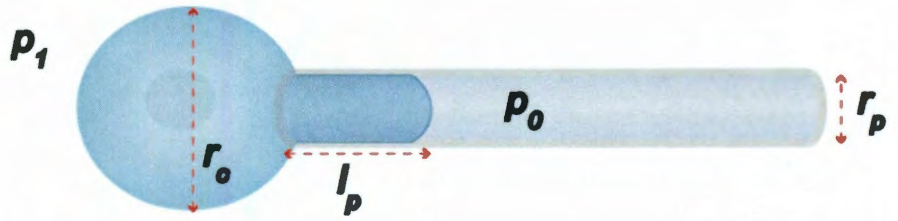

Figure 5: Schematic diagram of Micropipette Aspiration. In this setup, the cell is suspended in fluid of pressure p_1 and a micropipette of radius r_p is placed on the cell membrane. The pressure inside of the pipette is then lowered to p_0 and the resulting deformation of the cell membrane, l_p, into the pipette is measured. This information, along with the radius of the cell outside of the pipette (r_c), can be used to determine the cell's tensile modulus and viscosity.

Chapter 3: The knee meniscus: A complex tissue of diverse cells

Abstract

This review describes the knee meniscus and its diverse cell populations. Situated between the femur and tibia, the meniscus acts to transmit loads within the knee while maintaining joint stability. Not only does this tissue display complex geometry and anatomy, its cellular profile ranges from fibroblast-like to chondrocyte-like. When the tissue first begins to develop in the body, its cells are similar in shape and morphology, but as it matures, these cells take on distinct characteristics. The spindle-shaped cells of the outer meniscus are well-suited to maintaining a fibrous extracellular matrix rich in collagen type I. The round, inner meniscus cells produce both collagen types I and II, and glycosaminoglycans, giving rise to a hyaline-like inner portion of the tissue. Cells intermediately located display characteristics of both cell types. Fibrochondrocytes are also known to be highly dependent on mechanical stimulation to maintain healthy tissue, and display regional variation in response to different biomolecular cues. Investigating this cell population under a variety of conditions can lead to a better understanding of the pathophysiology and regenerative processes of the meniscus.

Chapter published as: Sanchez-Adams, J., and Athanasiou, K. A. "The knee meniscus: A complex tissue of diverse cells." *Cellular and Molecular Bioengineering.* 2(3): 332-340, 2009. DOI: 10.1007/s12195-009-0066-6.

Introduction to meniscus functions and anatomy

The knee meniscus is a fibrocartilaginous tissue comprised of two semilunar pieces that rest on the medial and lateral sides of the tibial plateau (see Figure 1). Its main functions are to aid in joint stability, bear and transmit loads within the knee, and absorb shock. The ability to carry out these specialized functions is imparted by its unique shape and anatomy.

In addition to being semilunar, the medial and lateral menisci are concave on their superior surfaces to increase congruence with the femoral condyles, and flat on their inferior surfaces, to match the tibial plateau. Coupled with this specialized shape, the meniscus is well suited to aid in joint articulation as its surface is smooth both macroscopically and microscopically.[1] With these characteristics the meniscus not only acts as a cushion between the femur and tibia, but also as a nearly frictionless surface during joint movement.

The cushioning function of the meniscus is made possible by a network of ligaments in the knee (see Figure 2). Ligamentous attachments called horn attachments anchor both medial and lateral menisci to the midline of the tibial plateau, keeping them in place while bearing joint loads. Though they look similar overall, the lateral meniscus can be distinguished from the medial meniscus in that its horn attachments are closer together. The medial meniscus is also held in place by the medial collateral ligament (MCL), which connects the medial side of the femoral condyle to the medial side of the tibia. Two other ligaments, those of Humphrey and Wrisberg, connect the posterior horn of the lateral meniscus to the lateral side of the medial femoral condyle. According to cadaveric studies,

both of these ligaments are present in only about 22% of the population, while 50% present only the ligament of Humphrey, and 28% have only the Wrisberg ligament.[104] The coronary ligament is present along the tissue's periphery and provides yet another anchor for the meniscus to the tibia.[3] Medial and lateral menisci are connected via their anterior horns by the transverse ligament. Though not involved in directly anchoring the meniscus, the posterior and anterior cruciate ligaments (PCL and ACL) connect the tibia to the femur keeping the bones in line with each other, thereby guarding against meniscal injury. All of these ligaments work in concert to resist meniscal displacement during normal activity, and are essential to normal meniscus functionality.

Meniscus tissue not only has a complicated shape and anchoring network, but also displays great regional variation in its extracellular matrix components. The periphery of the meniscus is highly fibrous, abundant in cells and collagen type I, while the inner portion of the tissue resembles hyaline cartilage with fewer cells, a higher proteoglycan content, and presence of collagen type II. The outer portion of the tissue is highly vascularized, while the inner meniscus is devoid of blood vessels. Given this range of properties, it is not surprising that a diverse set of cells occupies the tissue, and that classifying them is a difficult task. Through their differing synthetic and gene profiles, and their various sensitivities to mechanical and biochemical cues, the cells of the meniscus work together from gestation to adulthood to develop and maintain a tissue containing a fibrocartilage spectrum. An understanding of these cells, therefore, could aid

significantly in engineering attempts to recreate tissues within this spectrum, which can potentially lead to the development of new cartilage therapies.

Development of the meniscus

Compared to its neighboring hyaline cartilage in the knee, the meniscus is fibrous and highly cellular. In their earliest stages of development, however, both cartilage types begin as masses of condensed cells. Meniscal cartilage then follows a unique developmental path to arrive at its specialized shape and anchoring network. A 1983 study on the developing human meniscus observed various changes in vascularity, cellularity, and matrix molecule architecture which combine over time to form this highly specialized tissue.[5]

The distribution of vasculature and cells in meniscal cartilage changes over time as the tissue develops (see Figure 3). When first formed in the body, the meniscus is completely vascularized and is made up of mostly rounded cells with a high nuclear to cytoplasmic ratio. These cells are compacted together, and somewhat flattened near the surface of the tissue. The high degree of vascularity observed at this stage persists through the development of the tissue in the womb and only begins to diminish at around three months after birth, indicating that an abundant blood supply is important for the early growth and maturation of the meniscus. Nuclear to cytoplasmic ratio also diminishes with time, dropping noticeably by seven and a half months' gestation, when the cells appear more mature and differentiated, and the surface cells are even more distinctly flattened. Approaching nine months' gestation, both the medial and lateral

menisci grow to maintain relatively constant contact area with the tibial plateau. This growth is accomplished by cell synthesis of extracellular matrix molecules rich in collagen, which is organized circumferentially at this stage.[5]

After birth, the meniscus continues to grow and refine its collagen architecture as a whole, and the cells start to vary in their protein synthetic profiles regionally. One of the most visible examples of this change, is the decrease in vascularity of the inner meniscus. This is achieved when the cells in the outer portion of the tissue stop producing endostatin, allowing blood vessels to remain in the periphery.[6, 7] Endostatin is a 20 kDa portion on the C-terminal region of collagen type XVIII which inactivates vascular endothelial growth factor, and is initially present throughout the meniscus at low levels, but accumulates in the inner portion with time as the cells continue to produce it.[6] This change in endostatin abundance results in 10-25% vascularity of the lateral meniscus, and 10-30% vascularity of the medial meniscus in adulthood.[4] Synthesis of other proteins, such as proteoglycans, also changes with tissue maturation. Proteoglycans are highly sulfated, and their rate of synthesis can therefore be detected *in vitro* by measuring levels of sulfate in the culture medium produced by the cells. Using this method it has been determined that meniscus cells from tissue less than 20 years of age display a 1-5 mM sulfate per milligram of DNA per hour synthetic rate. As the tissue gets older, however, this sulfate synthetic rate diminishes to between 0.5 and 1 mM sulfate per milligram of DNA per hour in culture.[8] Additionally, it has been shown that some of the major proteoglycans present are biglycan and decorin, both of which help organize the collagen matrix

and regulate collagen fiber diameter.[8] The higher synthetic rate of proteoglycans in young meniscus tissue and the abundance of biglycan and decorin indicate that early in tissue development, proteoglycans may play an instrumental role in organizing the collagen matrix such that the meniscus can withstand various forces.

Meniscus cell diversity

As discussed previously, when meniscus cells first begin to condense in the embryo, they are similar in size and shape. Following tissue maturation, however, the cells of the meniscus show a great deal of regional variation in morphology and synthetic profiles, making them especially difficult to classify (see Figure 4 and Table 1).

In the superficial layer of the meniscus, the cells are oval or fusiform in shape, which is similar to fibroblast morphology.[38-40] Deeper in the meniscus, cells tend to be more rounded (similar to chondrocytes).[1, 38-40] Because of this morphological variation within the tissue, researchers have classified these cells using terms such as fibroblasts, fibrocytes, chondrocytes, fibrochondrocytes, and meniscus cells.[1, 38, 39, 41-43] The difficulty in describing meniscus cells with one term stems not only from the various morphologies present, but also the various synthetic profiles of the cells. As the outer portion of the meniscus contains predominantly collagen type I, it is not surprising that fibroblast-like cells populate it, helping to create and renew the fibrocartilaginous matrix there. The inner meniscus is more hyaline in nature, being predominantly collagen type II, with

lesser amounts of collagen type I, and necessarily contains cells that are chondrocyte-like. The name fibrochondrocytes, therefore, seems a fitting label, and has been used previously to refer to meniscus cells.[40] Acknowledging both the fibrous and cartilaginous characteristics that embody the meniscus, the terms fibrochondrocytes and meniscus cells will be used interchangeably in this article to describe them as a whole.

Types of meniscus cells

A study on the rabbit meniscus has identified as many as four distinct cell types in different regions in the tissue, which are separated from each other based on their shapes and presence of gap junctions.[38] The outer portion of the meniscus was found to contain two different cell types that display many cell processes.[38] These cells tend to be closer together than those in the inner meniscus and contain gap junctions, allowing them to exchange chemical signals efficiently.[38] Cellularity in the tissue is greatest at the outer periphery, decreasing radially inward. The inner portion of the meniscus contains cells that have a rounded morphology, and do not present gap junctions.[38] Yet another type of cell is present in the superficial zone. These cells are spindle-shaped, and like the inner meniscus cells, do not present gap junctions on their cell membranes.[38] Aside from fibrochondrocytes, there are also endothelial cells that reside in the meniscus, which compose the lumen of blood vessels that permeate the outer portion of the tissue.[44] Therefore, a variety of different cell types can be found in the meniscus, which allow for the tissue's complex architecture to be realized.

Cell synthetic properties

Due to the distribution of its different cells and proteins, the meniscus can be considered in two parts: the outer one third, and the inner two thirds. The cells from these two regions differ in the proteins and enzymes they produce (see Table 1). Though it has been shown that fibrochondrocytes from all regions in the meniscus produce about the same amount of collagen, it is the type of collagen synthesized that sets an outer meniscus cell apart from an inner meniscus cell.[18, 45] While both inner and outer meniscus cells do produce collagen types III, IV, V, and VI at low levels, the predominant collagen types are I and II.[18, 45] Being more fibroblastic in nature, outer meniscus cells almost exclusively produce collagen type I, while inner meniscus cells are more chondrocyte-like in that they produce slightly more collagen type II than type I.[14] Outer meniscus cells also differ from inner meniscus cells as they express CD34, a cell surface marker that functions in cell to cell adhesion, as well as proteases MMP-2 and MMP-3, which are important for matrix remodeling.[38, 45, 51, 53] Inner and outer meniscus cells are again similar in that the types of glycosaminoglycans (GAGs) they produce are largely chondroitin sulfate, with lesser amounts of keratin sulfate.[46] Inner meniscus cells, however, produce more GAGs than outer meniscus cells.[18, 45] They also stain positively for α-smooth muscle actin, which imparts contractile behavior, and highly express nitric oxide synthase (NOS2), which is important for meniscus cell biosynthesis.[42, 47-49, 53, 54] Based on these observations of gene expression and protein synthesis, a clear distinction can be made between the

cells of the avascular inner portion and highly vascular outer portion of the meniscus.

Like the neighboring hyaline cartilage on the ends of the femur and tibia, the meniscus functions in a load-bearing capacity made possible by a matrix rich in collagen and proteoglycans. Given the similarities between meniscal and hyaline cartilages, it is natural to assume that the gene expression profiles of the cells from these tissues would have some commonality. Indeed, a study comparing the gene expression of both cartilages to that of a common precursor cell, the human mesenchymal stem cell, has identified some common genes. [47] As well, specific sets of genes are shown to be expressed highly in only one cartilage type.[47] Using mesenchymal stem cells as a baseline for comparison, both meniscal and hyaline cartilages highly express the COL2A1 gene, specific for collagen type II production, but hyaline cartilage expresses this gene around six-fold higher than meniscal cartilage on the whole.[47] While sharing some commonality in gene expression, there are also certain genes that are only highly expressed in one cartilage type. Most notable of these differences is that meniscal cartilage expresses genes specific for collagen type I, while hyaline cartilage does not.[55] A list of genes that are common and specific to hyaline and meniscal cartilages can be found in Table 2.

Using these genes, it may be possible to better characterize tissue engineered meniscus constructs. A major hurtle in engineering meniscus tissue is determining the similarity between native tissue and engineered neotissue, especially early in the culture process. The identification of genes highly

expressed in the meniscus as compared to hyaline cartilage can facilitate this characterization by providing markers to indicate whether fibrocartilaginous tissue is being formed. As genetic changes precede changes in protein synthesis, and proteins take time to accumulate in a construct, this genetic information can be used to determine what type of tissue is likely to form early in construct development. Additionally, it may be possible to use these genetic markers to track the developmental process of the engineered tissue as well as determine appropriate intervention windows for mechanical or biochemical stimulation. More research must also be done to determine the specific roles of each of these genes in meniscus cells, which will provide a better understanding of meniscus cell functions and inform further engineering efforts.

Mechanosensitivity of meniscus cells

Because of the geometry of the meniscus, and its anchors to the tibial plateau, the tissue undergoes a variety of different mechanical stresses during loading. As shown in Figure 5, as the femur presses down on the tibial plateau, forces are generated in the anterior and posterior horns of the meniscus, which oppose the radial displacement of the tissue from the joint. This results in a circumferential hoop stress along the tissue from horn to horn. The tissue also experiences compression as the tibial plateau resists the downward force from the femur. These mechanical forces generated during the normal functioning of the knee provide mechanical signals to meniscus cells within their extracellular matrix.

Loading patterns can alter gene expression profiles of fibrochondrocytes, and are known to be necessary for developing and maintaining healthy meniscus tissue (see Table 3). Highlighting this fact, a study in chick embryos has shown that immobilization of an immature knee joint results in fusion of the knee cartilage.[105] Alternatively, if the knee joint of an adult rabbit is immobilized for eight weeks, degeneration and decreased permeability of the tissue is observed.[106, 107] A two- to five-fold decrease in GAG gene expression has also been observed in dog menisci following knee joint immobilization at 90° flexion. From these examples, it is evident that mechanical stimulation of meniscus cells is a constant necessity for proper tissue development and maintenance of function.

Mechanical stimulation in the form of 5% biaxial strain on fibrochondrocytes *in vitro* increases total protein synthesis and nitric oxide levels, while NOS2 expression remains constant.[56] These effects are realized in cells from all regions of the meniscus.[56] Cells from the inner and outer meniscus, however, are affected differently by mechanical loading, as evidenced by theoretical modeling of the tissue as well as experimental results. Under normal loading conditions, finite element models have estimated that outer, more elongated, meniscus cells experience between 2% and 4% tensile strain, while round inner meniscus cells experience slightly higher (~7%) strains.[55] This suggests that *in situ*, meniscal fibrochondrocytes will experience different magnitudes of a mechanical cue based on their position within the tissue, which, in turn, can affect their synthetic profiles.

In addition to the degree of stimulation under tension, meniscus cells are known to respond differently to other types of mechanical load, such as compression. Gene expression levels of fibrochondrocytes in response to 0.1 MPa static compressive loading increase three- to four-fold for decorin and collagen types I and II, while this stimulation also causes a two- to three-fold decrease in mRNA levels for MMP-1.[57] In contrast, a dynamic stimulation regimen of 1 MPa at 0.5 Hz causes fibrochondrocytes to increase nitric oxide levels, but decrease expression of collagen type II (four-fold), and decorin (two-fold). Changing the type of mechanical stimulation can therefore have a profound effect on the gene expression and protein synthetic profiles of meniscal fibrochondrocytes.

Therefore, it has been determined that tensile forces on meniscus tissue signal the cells to increase total protein synthesis, while static compressive loading can cause up-regulation of collagens and decorin, and dynamic compression can down-regulate these genes. Understanding the effect of mechanical forces on meniscus cells not only allows for a better understanding of normal meniscus functionality, but also informs tissue engineering efforts. Using this information, researchers can develop strategies to improve or maintain construct properties over time.

Fibrochondrocytes and growth factors

Meniscus cells are not only sensitive to mechanical cues, but also biochemical ones. Studies *in vitro* and *in vivo* have identified a number of

biomolecules that can alter cell behavior toward protein synthesis, migration, and proliferation (see Table 4). When added to *in vitro* monolayer cultures of meniscus cells from sheep, humans, and rabbits, transforming growth factor beta 1 (TGF-β1) has the ability to increase proliferation rates as well as proteoglycan synthesis. [18, 43, 108] Fibroblast growth factor (FGF), hepatocyte growth factor (HGF), platelet-derived growth factor (PDGF-AB), bone morphogenetic protein 2 (BMP-2), and human platelet lysate (Human PL) can also be used to increase cell proliferation *in vitro*.[40, 109, 110] Additionally, rabbit fibrochondrocytes in monolayer culture exposed to TGF-β1 increase their collagen production.[111]

Aside from causing proliferative and protein synthetic changes, some growth factors have been shown to cause meniscus cells to migrate. Cells from the inner (avascular), middle (slightly vascular), or outer (highly vascular) portions of the meniscus, however, respond differently to different growth factors. Interleukin 1 (IL-1) specifically targets outer meniscus cells to migrate, while BMP-2 and insulin-like growth factor I (IGF-I) causes some middle meniscus cells to migrate.[110] Furthermore, all outer meniscus cells, but only half of inner meniscus cells, migrate when exposed to epithelial growth factors (EGF).[110] The cells in the meniscus, therefore, vary regionally in how they are affected by different biochemical factors, highlighting their different roles in the tissue.

From this information, it is apparent that some growth factors can affect the entire meniscus, but others affect certain regions specifically. While all meniscus cells seem to have the capacity to increase proliferative rates in response to certain biomolecules, outer meniscus cells have been shown to

migrate when exposed to both IL-1 and EGF, while only some inner and middle meniscus cells can be induced to migrate. This may point to the outer meniscus cells' role in matrix remodeling following injury. Protein synthesis of fibrochondrocytes as a whole is also affected by biomolecular cues, indicating that meniscus cells, even those of the inner (avascular) portion of the tissue, are active and may be stimulated to replace damaged matrix if presented with appropriate molecular conditioning.

Tissue engineering the meniscus

Given the regional variation in meniscus anatomy, matrix molecules, and cells, it is a complex tissue to engineer. Harnessing information about meniscus cell morphology, mechanosensitivity, and response to growth factors, researchers have made several key advances toward engineering the spectrum of fibrocartilage present in the meniscus. Bioreactors have shown great promise in encouraging the formation of bi-zonal tissue, scaffoldless construct formation has produced tissue with appropriate matrix composition and imparted some mechanical integrity, and growth factors have been used in many efforts to increase matrix production of cells.

Engineering approaches using fluid shear bioreactors have capitalized on meniscus cell mechanosensitivity to create bi-zonal meniscus tissue. Seeding bovine or human chondrocytes on hyaluronic acid scaffolds, and culturing them in a rotating flask has resulted in the formation of a construct with a fibrous outer capsule of tissue with meniscus-like collagen organization.[112] Other studies have

achieved similar results using wavy-walled or flow perfusion bioreactors to culture poly(glycolic acid) (PGA) scaffolds seeded with chondrocytes from bovine hyaline cartilage.[113, 114] The constructs resulting from these experiments also exhibited a bi-zonal structure of fibroblastic outer cells and chondrocytic inner cells, and showed that the culture process had a positive effect on meniscus-specific matrix deposition and cell proliferation.[113, 114] The application of fluid shear during construct culture has made progress in meniscus engineering by producing tissue containing cells that range from fibroblast-like to chondrocyte-like. Informed by meniscus cell mechanosensitivity research and meniscus development and anatomy, researchers have determined that a dynamic culture process incorporating shear is beneficial for the creation of bi-zonal tissue. However, this process alone has yet to produce tissue that has near-native mechanical and geometrical properties.

A scaffoldless approach to tissue engineering the meniscus has addressed the issue of creating geometrically relevant meniscus tissue. Using the anatomic knowledge that the meniscus is comprised of two basic cell-types, fibroblast-like and chondrocyte-like cells, a high-density co-culture of bovine fibrochondrocytes and chondrocytes has been added to agarose molds to form meniscus-shaped constructs.[115] Following an eight week culture period, these constructs displayed meniscus-like geometry and anisotropic mechanical behavior, with a circumferential modulus of around 226 kPa, and a radial modulus of around 67 kPa.[115] These constructs also contained meniscus-like matrix proteins such as collagen types I and II, as well as GAGs, and presented

circumferential collagen orientation.[115] By employing a scaffold-less approach to tissue engineering it is therefore possible to achieve meniscus-like geometry and matrix deposition. The mechanical behavior of these constructs also mimics the anisotropy of native tissue, but their mechanical integrity is still much lower than native values.

Biochemical stimulation of engineered meniscus constructs is a promising avenue toward achieving higher mechanical properties. As it is known that certain biomolecules can induce fibrochondrocytes toward proliferation, migration, and protein synthesis, they can be added to the culture medium of engineered constructs to increase the production of collagens and proteoglycans, which are integral in imparting mechanical integrity to the neotissue. TGF-β1 is known to have a profound effect on the collagen and GAG production of meniscus cells in monolayer, and has also been instrumental in increasing matrix deposition and mechanical properties of various engineered constructs. In particular, the addition of TGF-β1 to the culture medium of scaffoldless constructs formed from a 50:50 co-culture of bovine fibrochondrocytes and chondroctyes allowed for the construct tensile modulus to reach 3 MPa.[116] Furthermore, TGF-β1 added to constructs created by seeding fibrochondrocytes on poly-L-lactide (PLLA) has been shown to increase matrix deposition.[117] Studies such as these indicate that the regenerative capacity of fibrochondrocytes is highly dependent upon culture conditions, and that the addition of biomolecules can compliment various engineering processes. By

optimizing these conditions it may be possible to create tissue *in vitro* that mimics the native meniscus mechanically and biochemically.

Conclusions

Knee meniscus tissue is complex geometrically, with an accompanying diversity of cells. These cells vary regionally within the tissue and display unique characteristics in terms of their morphologies, protein synthetic properties, and response to mechanical and biochemical stimulation. These differences give rise to a tissue with regions that are either vascular or avascular, fibrous or cartilaginous. An understanding of this diverse population of cells and their interaction with their biomolecular milieu can illuminate normal function, pathophysiology, and regenerative processes of the meniscus.

Tissue engineering experiments using fibrochondrocytes have already begun to provide information about some of the regenerative capacities of these cells. Advances in bioreactor technology, scaffold-free construct formation, and the application of growth factors indicate that creating a geometrically, biomechanically, and biochemically relevant meniscus-like tissue from cartilage cells is feasible. More research should be done to determine if a combination of these approaches may help to achieve a complete set of properties.

Acknowledgments

The authors would like to acknowledge NIAMS R01 AR 47839-2 for funding this work, as well as National Science Foundation Rice-Houston Alliance

for Graduate Education and the Professoriate (NSF-AGEP) for their generous support of this work.

Tables

Table 1: Regional variation of meniscus molecules, cell morphology, and mechanical forces

Region	Molecules present	Cell morphology	Dominant force type
Throughout	Collagen type I[39, 45, 50, 53]		Compression, tension, shear
Inner	Collagen type II[39, 45, 50, 53] Aggrecan[53] NOS2[53, 54]	Round, chondrocyte-like	Compression
Outer	CD34[51] MMP2[53] MMP3[53]	Fusiform, fibroblast-like	Tension

Table 2: Selected genes related to hyaline and meniscal cartilages

Gene symbol	Gene name	Cartilage in which highly expressed[47]
IGF2	insulin-like growth factor 2 (somatomedin A)	*Hyaline*
IGL@	immunoglobulin lambda locus	*Hyaline*
RTN4R	reticulon 4 receptor (Nogo receptor)	*Hyaline*
EPHX2	epoxide hydrolase 2, cytoplasmic	*Hyaline*
CREG	cellular repressor of E1A-stimulated genes	*Hyaline*
FLJ13840	Homo sapiens cDNA FLJ13840 fis, clone THYRO1000783	*Hyaline*
BCL7A	B-cell CLL/lymphoma 7A	*Hyaline*
PLA2G2A	phospholipase A2, group IIA (platelets, synovial fluid)	*Hyaline*
CTSC	cathepsin C	*Hyaline*
RBP4	Retinol-binding protein 4, interstitial	*Hyaline*
COL2A1	collagen, type II, alpha 1	*Hyaline and Meniscus*
HPCAL1	hippocalcin-like 1	*Meniscus*
FLJ20831	hypothetical protein FLJ20831	*Meniscus*
PDLIM1	PDZ and LIM domain 1 (elfin)	*Meniscus*
C1QR	complement component C1q receptor	*Meniscus*
COL1A1	collagen, type I, alpha 1	*Meniscus*
COL1A2	collagen, type I, alpha 2	*Meniscus*
CA12	carbonic anhydrase XII	*Meniscus*

Table 3: Effects of mechanical loading on meniscus cells

Stimulus	Details	Effect
Normal loading[55]	Finite element model	Inner cell ~7% strain, outer cell ~2–4%
Biaxial cellular strain, in vitro[56]	Cyclic, 5%, 0.5 Hz, 24 hrs	Increased protein synthesis (higher for outer cells than inner cells); NO levels increase
Static tissue compression[57]	0.1 MPa, 24 hrs	Decrease in decorin and collagen types I and II expression (3- to 4-fold); Increase in MMP-1 expression (2- to 3-fold)
Dynamic tissue compression[57]	0.08–0.16 MPa, 0.5 Hz, 24 hrs	Decrease in decorin expression (2-fold), Decrease collagen type II expression (4-fold)
Dynamic tissue compression[58]	0–0.1 MPa, 0.5 Hz square wave, 24 hrs	NO levels increase
Joint immobilization[59]	*In vivo*	Decrease in aggrecan expression (2- to 5-fold)

Table 4: Effects of growth factors on meniscus cells

Effect	Growth Factor	Cell Source (Details)
Proteoglycan synthesis	TGF-β1[18, 43, 108, 111]	Sheep
		Human
		Rabbit (increased [^{35}S]-sulfate uptake)
		Rabbit (8-fold increase)
Collagen synthesis	TGF-β1[108, 111]	Rabbit (increased [^{3}H]-proline uptake)
		Rabbit (15-fold increase)
Migration	BMP-2 [110]	Cow (middle cells)
	IL-1[110]	Cow (outer cells)
	PDGF-AB [110]	Cow
	IGF-I [110]	Cow (middle cells)
	EGF [110]	Cow (half inner cells, all outer cells)
	HGF [110]	Cow
Proliferation	Human PL [40]	Rabbit
	HGF [110]	Cow
	FGF [40]	Rabbit
	PDGF-AB [110]	Cow
	BMP-2 [110]	Cow

Figures

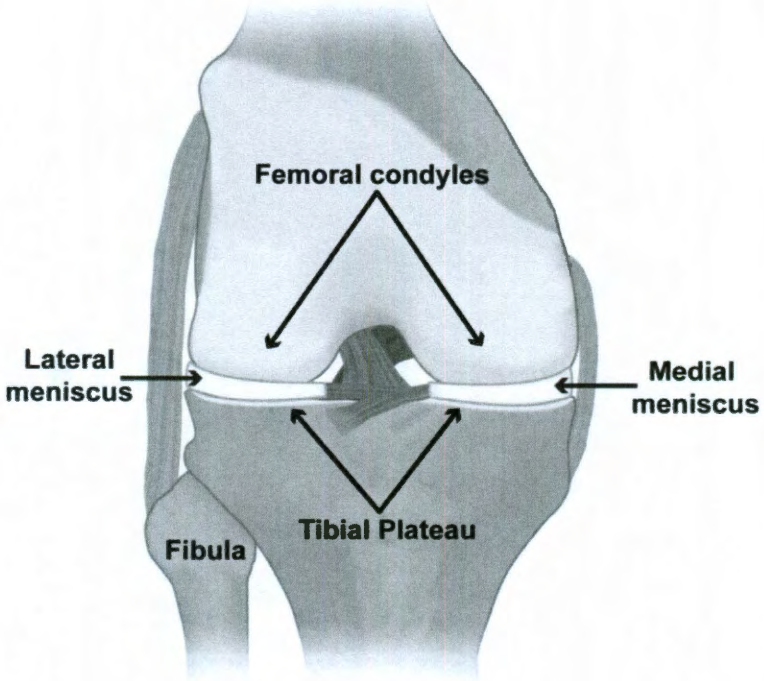

Figure 1: Anterior view of the meniscus within the knee joint. The meniscus rests between the femoral condyles and tibial plateau within the knee joint. Its two semicircular, wedge-shaped parts, the medial and lateral meniscus, are situated on the medial and lateral sides of the knee, respectively. They are held in place by a network of ligaments.

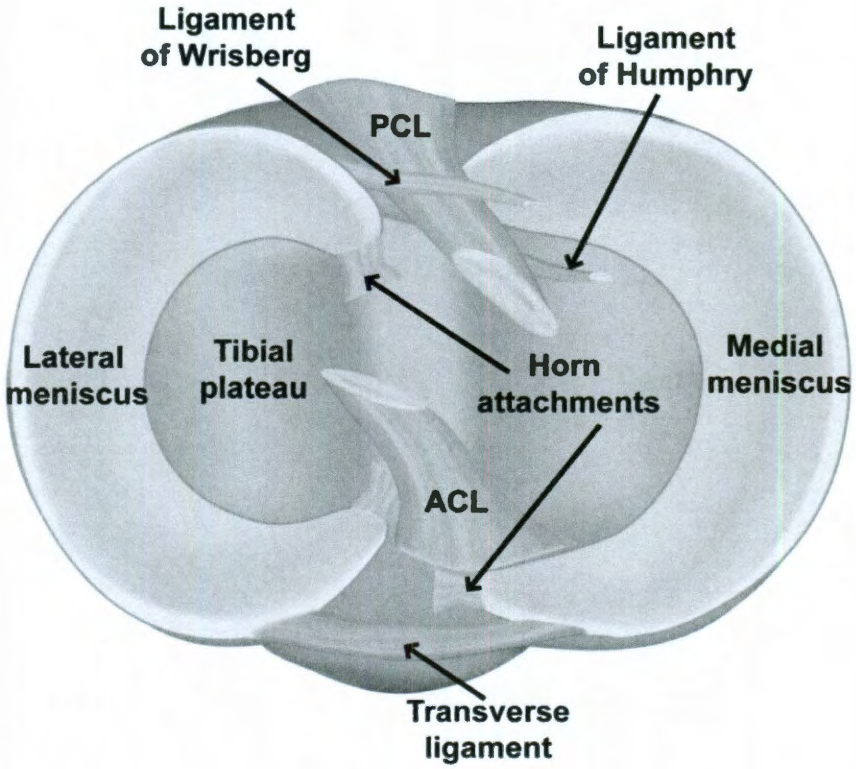

Figure 2: Medial and lateral menisci, superior view. Various ligaments allow for meniscus stabilization and restrict movement of the femur relative to the tibia. Among these are the transverse ligament, which connects the anterior horns of the menisci together, and the horn attachments, which provide anchoring to the tibial plateau. The ligaments of Humphrey and Wrisberg provide the posterior lateral meniscus a connection to the medial femoral condyle, and the ACL and PCL connect the tibia to the femur, stabilizing the joint.

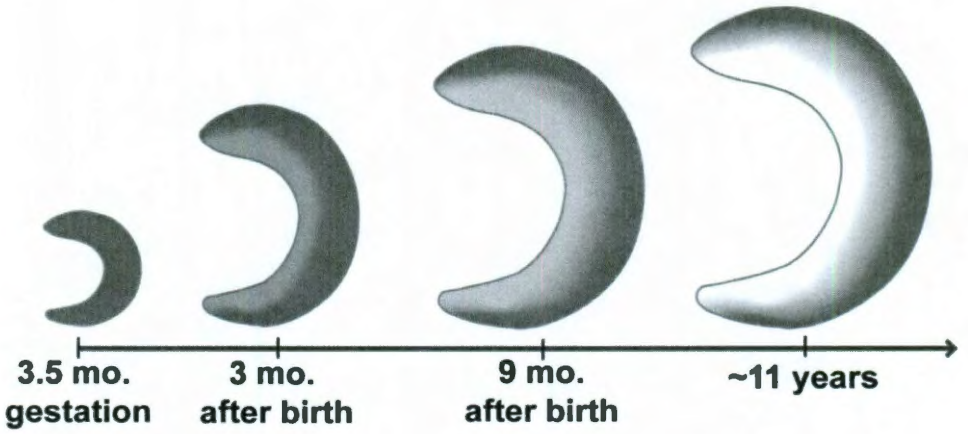

Figure 3: Meniscus vascularity over time. Initially, the meniscus is completely vascularized, but over time, this vascularity recedes to the outer periphery of the tissue. Blood vessels begin to disappear in the inner meniscus around three months after birth, coinciding with the accumulation of endostatin produced by the cells. By 11 years of age, this inner portion is completely avascular.

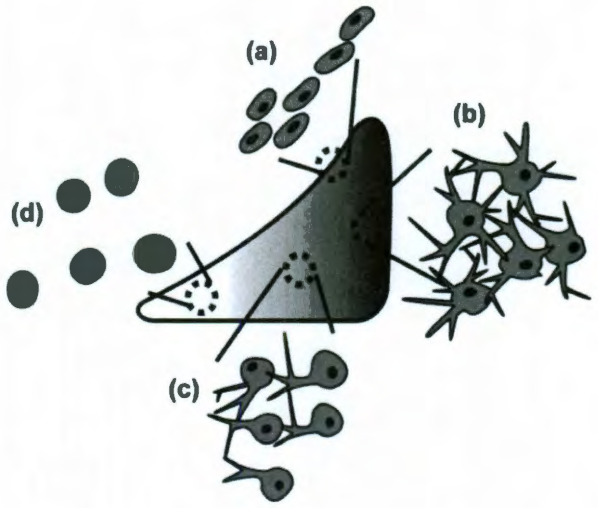

Figure 4: Four different cell types in the meniscus. Cells in the outer layer of the meniscus appear flattened and close together (a), while cells in the outer periphery contain many cell processes like fibroblasts (b). Moving toward the inner portion of the meniscus, the cells contain fewer cell processes (c) and cells from the inner portion are rounded and chondrocyte-like (d).

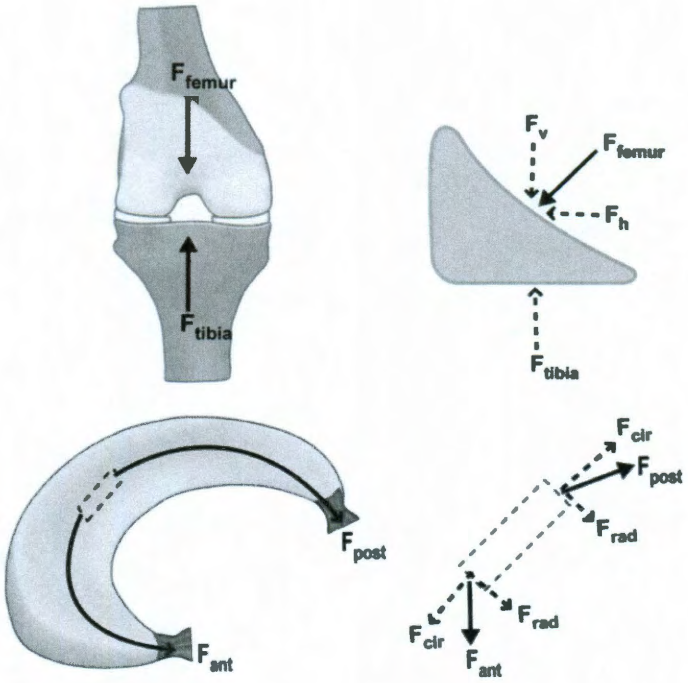

Figure 5: Forces generated during normal meniscus loading. The meniscus experiences various types of forces as the femur transmits vertical loads through the knee joint. Because the tissue is concave on its superior surface, the force from the femur results in a vertical (F_v) and horizontal (F_h) force generated in the tissue. The vertical force is opposed by the tibial reaction force, resulting in compression of the tissue, while the horizontal force is balanced by the anterior and posterior horn attachments of the meniscus(F_{ant} and F_{post}). These horn attachments anchor the meniscus, and generate circumferential (F_{cir}) and radial reaction forces in the tissue (F_{rad}).

Chapter 4: Biomechanics of Meniscus Cells: Regional Variation and Comparison to Articular Chondrocytes and Ligament Cells

Abstract

Central to understanding mechanotransduction in the knee meniscus is the characterization of meniscus cell mechanics. In addition to biochemical and geometric differences, the inner and outer regions of the meniscus contain cells that are distinct in morphology and phenotype. This study investigated the regional variation in meniscus cell mechanics in comparison to articular chondrocytes and ligament cells. It was found that the meniscus contains two biomechanically distinct cell populations, with outer meniscus cells being stiffer (1.59 ± 0.19 kPa) than inner meniscus cells (1.07 ± 0.14 kPa). Additionally, it was found that both outer and inner meniscus cell stiffnesses were similar to ligament cells (1.32 ± 0.20 kPa), and articular chondrocytes showed the highest stiffness overall (2.51 ± 0.20 kPa). Comparison of compressibility characteristics of the cells showed similarities between articular chondrocytes and inner meniscus cells, as well as between outer meniscus cells and ligament cells. These results show that cellular biomechanics vary regionally in the knee meniscus, and that meniscus cells are biomechanically similar to ligament cells. The mechanical

---

Chapter submitted as: Sanchez-Adams, J., and Athanasiou, K.A. "Biomechanics of Meniscus Cells: Regional Variation and Comparison to Articular Chondrocytes and Ligament Cells." *Biophysical Journal.*

properties of musculoskeletal cells determined in this study may be useful for the development of mathematical models or the design of experiments studying mechanotransduction in a variety of soft tissues.

Introduction

Understanding mechanotransduction in the knee meniscus can help elucidate the mechanisms by which meniscus cells maintain healthy tissue or mount a healing response following injury. Located between the femoral condyles and the tibial plateau in the knee joint, the menisci are semi-lunar, wedge-shaped fibrocartilaginous tissues.[19] Each meniscus functions to increase congruence between articulating surfaces, distribute load, and absorb shock during normal movements such as walking or running.[23, 24] Because of its unique shape, meniscus tissue is exposed to a variety of load types including compression, tension, and shear.[30, 32, 37, 118] These forces are also borne by the resident cells in the tissue, which affect their gene expression and synthetic properties.[56, 119] As the regional mechanical properties of meniscus cells are unknown, however, it is difficult to predict how forces at the tissue level are translated to the cells and what effect these forces have on tissue homeostasis or remodeling.

As biochemically distinct regions exist in the inner and outer portions of the meniscus, the mechanical properties of meniscus cells may also vary regionally. Different cell types are known to reside in the inner and outer meniscus regions; the inner region contains rounded, articular chondrocyte-like

cells that produce collagen type II and aggrecan, whereas outer meniscus cells display many cellular processes and are the main producers of collagen type I.[9, 29-31, 52] Regional variations in cellular mechanics have been documented previously in different zones of articular cartilage[86] and in different regions of the intervertebral disc,[120] which also correspond with known differences in cellular morphology and synthetic profiles. If, in addition to phenotypic differences, outer and inner meniscus cells show distinct mechanical properties, these cells may deform differently in response to the same mechanical load, causing varying phenotypic and synthetic changes.

It is also important to understand meniscus cell mechanics in the context of other musculoskeletal cells. As articular cartilage and ligament represent opposite ends of the musculoskeletal soft tissue spectrum, it is likely that cells from the meniscus may have similar properties to cells from these tissues. Identifying key similarities and differences in the mechanical properties of these cells can aid in the development of theoretical models of the meniscus, and inform further studies on the effects of mechanical stimulation on meniscus cells.

Typically, single cells are mechanically tested using one of three techniques: micropipette aspiration,[94, 96, 99] atomic force microscopy (AFM),[85-87, 90, 121] cytoindentation,[82, 84] or unconfined compression.[80, 97, 100, 101] Because of the size of the pipette or probe used in micropipette aspiration and atomic force microscopy, these techniques are most useful for measuring the mechanical properties of subcellular components such as portions of the cellular membrane. Cytoindentation offers some advantages over these techniques as the probe is

larger than that used in AFM, and the cylindrical probe geometry allows for simpler modeling of the viscoelastic mechanical behavior of the cell. Unconfined compression, however, uses a probe that is much larger than the cell, giving it the unique ability to measure bulk cellular properties. This is advantageous because bulk cellular deformation likely occurs during physiologic loading experienced by meniscus cells *in situ*. Bulk cytomechanics have been measured previously using a cytocompression device, which has been used to successfully detect differences in the mechanical properties of a variety of cell types. For example, previous studies found that certain growth factors have a bulk stiffening effect on adult articular chondrocytes, and that the actin cytoskeleton provides the greatest contribution to chondrocyte stiffness.[78, 80] This device has also been used to detect stiffening of myeloma cells compared to normal bone marrow stroma cells, and track the stiffening of human embryonic stem cells as they differentiate along a chondrogenic lineage.[79, 122] Thus, application of this technique is able to detect differences in cellular mechanics in a variety of situations, and presents a useful method of measuring the bulk mechanical properties of meniscus cells.

In light of the lack of information on meniscus cell mechanics, the overall objective of this study is to characterize the biomechanical properties of meniscus cells and compare them to those of articular chondrocytes and ligament cells. To determine if regional variations in meniscus cellular mechanics exist, mechanical properties of inner meniscus cells as well as outer meniscus cells are also measured and compared. Unconfined compression stress-

relaxation tests are performed using a cytocompression device to measure bulk cell stiffness, Poisson's ratio, and recovery characteristics of each cell type. It is hypothesized that inner and outer meniscus cells have distinct mechanical properties, and that inner cells are more similar to articular chondrocytes while outer cells have properties more similar to ligament cells. By characterizing the mechanical properties of inner and outer meniscus cells, this study provides a basis for further understanding of mechanotransduction in the meniscus. Comparing the mechanical properties of meniscus cells to other musculoskeletal cells may also help put this information into context and provide a more complete understanding of these cells and how they may function in the knee.

Materials and Methods

Cell isolation and seeding

Five bovine knee joints from two week old animals were obtained 24 hours after sacrifice and patellar ligaments, articular cartilage from the femoral head, and medial menisci were harvested using aseptic surgical techniques. The outer and inner portions of each medial meniscus were dissected from the tissue and processed separately. Ligament, cartilage, inner meniscus, and outer meniscus tissue was minced to approximately 1 mm^2 pieces, and digested in Dulbecco's Modified Eagle Medium with Glutamax (DMEM) [Invitrogen, Carlsbad, CA], 1% penicillin/streptomycin/fungizone (P/S/F) [Lonza, Basel, Switzerland], 1% non-essential amino acids (NEAA) [Invitrogen], and 0.2% w/v collagenase type 2

[Worthington, Lakewood, NJ]. Digestion was carried out overnight at 37°C with gentle shaking, after which cells were counted and frozen in liquid nitrogen in DMEM containing 20% fetal bovine serum (FBS) [Atlanta Biologicals, Lawrenceville, GA] and 10% dimethyl sulfoxide [Sigma-Aldrich, St. Louis, MO]. Prior to each cytocompression experiment, cells were thawed, counted, and resuspended in DMEM containing 1% P/S/F, 1% NEAA, 10% FBS, and 50 μg/mL ascorbate-2-phosphate. Cells were then seeded onto cut-glass slides at a concentration of 200,000 cells/mL, as described previously.[78, 80] After incubation at 37°C for 1.5 hours, individual cells were subjected to compression, and videos of these compression events were recorded.

Unconfined compression of single cells

As previously described, a cytocompression device was used to subject single chondrocytes, inner meniscus cells, outer meniscus cells, or ligament cells to unconfined compression stress-relaxation tests at 10-50% strain levels.[78, 80, 123] A sample size of n = 30 was used for each group in this study, based on power analysis performed for previous studies using this cytocompression method.[80] A schematic representation of this procedure is shown in Figure 1. Briefly, glass slides seeded with cells were placed on an inverted microscope such that the objective viewed side profiles of the cells. A tungsten probe, 50.8 μm in diameter and driven by a piezoelectric motor, was brought approximately 5-10 μm from the top of each cell, and was used to compress the cell at a rate of 4 μm/second (Figure 1A). Based on the probe's distance from the cell, the cell's stiffness, and

the prescribed distance the probe was to travel toward the cell (15 μm), each cell was exposed to a different amount of strain. After moving the prescribed distance, the probe was held in place for 30 seconds to allow the cell to equilibrate, and then retracted at a rate of 4 μm/second (Figure 1B). Each compression event was recorded using a CCD camera, and recovery behavior following probe retraction was recorded for 45 seconds.

Video capture and image analysis

Recordings of cells compressed and recovering from compression were analyzed as previously described.[80] Briefly, individual compression events were recorded using MetaMorph image analysis software, and cellular dimensions were measured throughout each event. Cell height and width was measured initially, at equilibrium compression, and during cellular recovery following release from compression. Additionally, the distance the probe traveled during each compression event was measured. A pixel to micron ratio was determined for each session by recording the unimpeded probe as it moved through a prescribed distance of 15 μm.

Biomechanical measurements

Cantilever beam theory was employed to determine the stress applied to each cell based on probe's deflection, stiffness, and moment of inertia, as previously described.[80, 84] The reaction force, F, on the cell was described as:

$$F = \frac{3EI\delta}{L^3}$$

where the constants E (Young's modulus), I (moment of inertia), and L (length of the probe) were 394.5 GPa, 3.27 x 10^{-19} m^4, and 31.5 cm, respectively. The deflection of the cantilever (δ) was determined by comparing the prescribed and actual displacement of the probe for each compression event. The applied stress (σ_a) was determined by dividing F by the approximate contact area of the cell with the probe, as in our previous studies.[78, 124] Cells were approximated as ellipsoids with two identical dimensions, and cellular volume was approximated as $V = \pi h d^2/6$. Cell volume was calculated initially (V_{init}), at equilibrium compression (V_{eq}), and following recovery (V_{rec}). Cellular height and width dimensions initially, at equilibrium compression, and at equilibrium recovery were also used to determine lateral (ε_l) and axial (ε_a) strains, as well as residual axial strain (ε_r). From these measures, the apparent Poisson's ratio (v) was calculated as $v = -(\varepsilon_l / \varepsilon_a)$, the recovered volume fraction as V_{rec}/V_{init}, and the apparent compressibility (β_a) as $(V_{init} - V_{eq})/(\sigma_a V_{init})$, as previously described.[80] The characteristic recovery time (τ) for each cell was also determined by modeling axial strain of the cell over time as an exponential decay function:

$$\varepsilon(t) = Ae^{-t/\tau} + \varepsilon_r$$

where A is the recovery coefficient, and t is the time in seconds.

Immunocytochemistry

Cells from each group were fluorescently stained for cell nuclei, actin, focal adhesion kinase (FAK), and microtubules. Each cell type was seeded onto a glass slide at a concentration of 0.25 x 10^6 cells/mL, and incubated at 37°C for

1.5 hours. Following incubation, seeded cells were washed with warm PBS and fixed with 3.7% formaldehyde for 15 minutes. After fixation, cells were washed with PBS and made permeable via incubation with 0.1% Triton X-100 for 15 minutes. Cells were then incubated with Image-iT™ FX Enhancer [Invitrogen] for 30 minutes, and then stained for actin using CF594 Phalloidin [Biotium, Hayward, CA] for 20 minutes. For microtubule staining, cells were incubated with an anti-α-tubulin antibody [Invitrogen] for 1 hour, and for FAK staining, cells were incubated with an anti-FAK antibody [Sigma] for 1 hour. Secondary antibodies specific to each primary, and conjugated to a 488nm fluorophore, were incubated with the cells for 1 hour. Cell nuclei were then stained with 10 μM Hoechst 33342 for 7 minutes. Each slide was mounted using Prolong Gold Antifade medium [Invitrogen]. Images of cells were taken using a fluorescence microscope, and exposure times for each fluorophore were optimized for articular chondrocytes and kept constant for capturing images from all groups.

Data analysis

Linear regression analysis was performed with the data analysis package in Microsoft® Office Excel® 2007, one-way ANOVAs were performed in JMP® 7.0.1, and exponential fits were carried out in MATLAB® 7.11. Linear regression analysis was performed to determine if significant correlations of stress, residual strain, and apparent compressibility existed as a function of applied axial strain and to test if these correlations varied with cell type. A correlation was determined significant if $p < 0.05$. For significant correlations, differences

between slopes were detected by comparing 95% confidence intervals as done previously.[78, 80]

Results

Cell morphology

Initial cell height and width was measured for each cell prior to compression and averaged for each cell type. A comparison of these average dimensions is shown in Figure 2. Following 1.5 hours of static seeding, it was found that the chondrocytes and inner meniscus cells showed statistically greater cell height (10.76 ± 1.08 μm and 11.01 ± 1.44 μm, respectively) than outer meniscus cells and ligament cells (9.93 ± 1.32 μm and 9.55 ± 1.13 μm, respectively). Additionally, inner meniscus cells also displayed statistically greater cell width (12.93 ± 1.47 μm) than all the other cell types (chondrocytes: 11.01 ± 1.05 μm, outer meniscus cells: 10.8 ± 1.03 μm, and ligament cells: 10.57 ± 0.93 μm).

Compressive behavior

Cell stiffness and Poisson's ratio were calculated from measurements of the cell and probe during each compression event. These biomechanical properties are listed in Table 1, and stress-strain plots for each cell type are shown in Figure 3. All linear regression models applied to the stress-strain curves for each cell type had significance values less than 0.001. Comparisons of the 95% confidence intervals from the linear regression analysis of each cell type

showed that the articular chondrocytes were the stiffest of the four cell types, followed by the outer meniscus cells and inner meniscus cells, respectively. The stiffness of the ligament cells was not statistically different from either the inner or the outer meniscus cells, and was significantly lower than the articular chondrocytes. Average apparent Poisson's ratios of the four cell types were not statistically different from each other.

Recovery behavior

Cell morphological changes following compression were recorded, and recovered volume, characteristic recovery time, residual strain, and apparent compressibility were calculated for each cell. The average percent recovered volume was highest for the articular chondrocytes, and lowest for the outer meniscus cells (Table 1). Percent recovered volume for inner meniscus cells and ligament cells was intermediate but was not statistically different from articular chondrocytes or outer meniscus cells. The average characteristic time to recovery was not statistically different between cell types, and was on the order of 7 to 10 seconds for all cell types.

Linear regression analysis of residual strain versus applied strain and apparent compressibility versus applied strain revealed significant linear correlations for all cell types (Figures 4 and 5, respectively). Regression analysis of residual strain versus applied strain showed positive linear correlations for all cell types (Figure 4). The slope of the fitted line for articular chondrocyte residual versus applied strain was found to be significantly lower than the slope for outer

meniscus cells, as determined by comparing 95% confidence intervals. Slopes for inner meniscus cells and ligament cells were similar to each other and not statistically different from either the chondrocytes or outer meniscus cells (Figure 4).

Regression analysis of apparent compressibility versus applied strain showed positive linear correlations for articular chondrocytes and inner meniscus cells, and negative correlations for outer meniscus cells and ligament cells (Figure 5). Chondrocyte and inner meniscus cell slopes were not statistically different from each other but were statistically different from outer meniscus cell and ligament cell slopes. Outer meniscus cell and ligament cell slopes were also not statistically different from each other.

Immunocytochemistry

Representative cells stained for actin and FAK or microtubules are shown in figures 6 and 7, respectively. All cells stained positively for actin, FAK, and microtubules. Articular chondrocytes showed distinct, cortical actin staining, while inner and outer meniscus cells and ligament cells showed more diffuse and less intense staining for actin (Figure 6). FAK staining (Figure 6) and microtubule staining (Figure 7) appeared to be similar for all cell groups.

Discussion

This study compared the biomechanical properties of cells from different meniscus regions to articular chondrocytes and patellar ligament cells. Overall, it

was found that meniscus cells were similar in biomechanical properties and cytoskeletal staining to ligament cells, although outer meniscus cells proved to be stiffer than inner meniscus cells. Additionally, articular chondrocytes were found to be significantly stiffer and show more distinct actin staining than all other cell types studied, suggesting that biomechanical properties of cells may correlate to the primary loading patterns or biochemical makeup of their tissues of origin. To our knowledge, this study is the first to identify two mechanically distinct subpopulations of cells in the meniscus which correspond to known regional biochemical variations. These results may aid in further characterization of musculoskeletal cells, providing key information for mathematical models or mechanical stimulation experiments that seek to understand tissue mechanics and mechanotransduction.

Unconfined compression of inner and outer meniscus cells showed that mechanical properties of meniscus cells are unique to their region of origin. Specifically, outer meniscus cells were found to be smaller and stiffer than inner meniscus cells, but also showed more compressibility with applied strain compared with inner cells. Immunocytochemistry performed on these cells showed similar staining intensity for actin, microtubules, and focal adhesions for inner and outer meniscus cells, indicating that they have similar cytoskeletal makeup and were actively adhered to the glass surface. As the actin cytoskeleton has been implicated as the largest contributor to cell stiffness,[80] and outer meniscus cells did not appear to contain more actin than inner cells, the increased stiffness of these cells may be a result of a more organized actin

cytoskeleton to resist axial compression. Additionally, as outer meniscus cells are known to be fibroblast-like with many cellular processes,[38] and these experiments were carried out with cells attached to a glass surface, the increased compressibility of outer meniscus cells may be due to the propensity of these cells to make focal adhesions and spread on the surface during a compression event which may result in reduced cellular volume. This characteristic increase in compressibility with strain was also shared by ligament cells, which also have fibroblastic characteristics. In contrast, inner cells and articular chondrocytes shared similar compressibility characteristics. This biomechanical similarity could also be related to the preferred spherical morphology of these cells, which would cause less cell spreading to occur during compression and less volume change. Therefore, the differences observed in inner and outer meniscus cell mechanics further illustrate previously identified morphological and phenotypic differences of meniscus cells, and show that apparent compressibility may be linked to preferred cell morphology.

Overall, it appeared that meniscus cells as a whole shared more biomechanical similarities to ligament cells than to articular chondrocytes. As hypothesized, outer meniscus cells and ligament cells showed similarities in nearly all biomechanical measures. Additionally, and in contrast to the proposed hypothesis, inner meniscus cells were also similar in stiffness and residual strain characteristics to ligament cells. These similarities were also detected in fluorescent staining of the actin cytoskeleton, showing similar staining intensity for meniscus cells and ligament cells, and markedly brighter staining for articular

chondrocytes. As the actin cytoskeleton is known to play a major role in imparting cell stiffness,[80] the observed differences in staining may indicate that actin in articular chondrocytes may be either more abundant or more organized than in meniscus or ligament cells. Further, meniscus tissue is similar to ligament tissue in terms of collagen organization, with collagen primary oriented in the circumferential direction in all regions of the meniscus and along the direction of loading in ligaments. The loads experienced by these two tissues are also similar, as tension is generated in both tissues along the axis of collagen orientation. In contrast, primary loading in articular cartilage is compressive. Although inner meniscus tissue bears some resemblance to articular cartilage, containing collagen type II and more sulfated glycosaminoglycans than the outer meniscus, the similarities in inner meniscus cell mechanics to ligament cells may indicate that tensile loading experienced by inner cells is important to their overall phenotype. Thus, differences in stiffness between articular chondrocytes and meniscus or ligament cells seem to be correlated with the actin cytoskeleton and the loading patterns experienced by the cells in their native environment.

Despite differences in cell stiffness, all cell types showed similar characteristic recovery times (Table 1). Additionally, microtubule staining of all cell types showed similar intensity and distribution (Figure 7). Previous research investigating the mechanical role of cytoskeletal elements has shown that microtubules are essential for cellular recovery following axial compression, as disruption of these elements leads to a 100% increase in characteristic recovery time.[80] Given the importance of microtubules in cellular recovery behavior, the

similarities observed in microtubule abundance between cell types supports their similar characteristic recovery times.

The differences in cellular mechanics demonstrated in this study may also indicate that tissues with similar properties may contain cells with similar biomechanical properties. This is in agreement with previous work using AFM to compare the mechanics of different cell types, which reported a correlation between cell stiffness and tissue properties.[125] The higher stiffness of articular chondrocytes compared with meniscus and ligament cells also closely matches the regional mechanical differences observed in intervertebral disc (IVD) cells[120] which reside in different biochemical environments. In the IVD, nucleus pulposus cells have been found to be approximately 3-fold stiffer than annulus fibrosus cells. In the present study, articular chondrocytes were found to be approximately 2-fold stiffer than the other cell types tested. As the nucleus pulposus contains similar biochemical components to articular cartilage, namely high sulfated GAG and collagen type II content, and the annulus fibrosus is made up of fibrous tissue like the meniscus or patellar ligament, the present results agree with the correlation of cell stiffness and tissue properties. These correlations may help predict the biomechanical properties of cells from other musculoskeletal tissues such as tendon, allowing for more accurate biomechanical models to be constructed.

Mathematical models of the mechanical deformation of single cells have already been developed for articular cartilage[126] and the intervertebral disc,[127] and the knee meniscus under axial compression,[55] giving new insights into the

translation of tissue strains to cell strains and indicating potential stimulation parameters for tissue engineering. With respect to the knee meniscus, previous research has used information from modeling to demonstrate that mechanotransduction exists in meniscus cells, showing that inner and outer meniscus cells respond to cyclic tensile loading with increased nitric oxide production and total protein synthesis.[56] Meniscus explants have also been shown to respond to 2% cyclic compressive strain with increased aggrecan gene expression,[128] but other research has shown decreased collagen and increased proteinase gene expression levels following a 0.08-0.16 MPa dynamic compression regimen.[57] These data indicate that there may be optimal levels of strain to apply to meniscus cells to achieve protein synthesis, beyond which catabolic processes are initiated. Thus, as meniscus cells have demonstrated sensitivity to mechanical stimulation, understanding their mechanical properties can help to further tailor the stimulation of engineered constructs to initiate particular mechanotransductive events for achieving functional tissue properties.

Characterization of the mechanical properties of single meniscus cells is an important step toward understanding mechanotransduction in the meniscus. This study demonstrated that meniscus cell mechanics vary regionally in the tissue, and that meniscus cells are most biomechanically similar to ligament cells. The mechanical properties measured in this study will be useful parameters for constructing accurate biomechanical models of various musculoskeletal tissues and for designing experiments to deliver precise mechanical stimulation to tissue engineered constructs.

Acknowledgments

We would like to thank the National Science Foundation Rice-Houston Alliance for Graduate Education and the Professoriate (NSF-AGEP) for their generous support of this work. We would also like to acknowledge funding from the National Institutes of Health R01AR047839.

Tables

Table 1: Mechanical characteristics of musculoskeletal cells*

Mechanical Property	Articular Chondrocytes	Inner Meniscus Cells	Outer Meniscus Cells	Ligament Cells
Cell Stiffness (kPa)	2.51 ± 0.2 [a]	1.07 ± 0.14 [c]	1.59 ± 0.19 [b]	1.32 ± 0.2 [bc]
Poisson's Ratio	0.5 ± 0.27	0.48 ± 0.21	0.54 ± 0.26	0.46 ± 0.17
Recovered Volume (%)	98.2 ± 6.6 [a]	94 ± 6.8 [ab]	92.7 ± 6.8 [b]	96.2 ± 7 [ab]
Recovery Time (sec)	7.15 ± 4.96	8.21 ± 3.74	7.34 ± 3.22	10.73 ± 6.09

* All values are presented as mean ± standard deviation, except cell stiffness which is presented as slope ± 95% confidence bounds (see Figure 3)

Figures

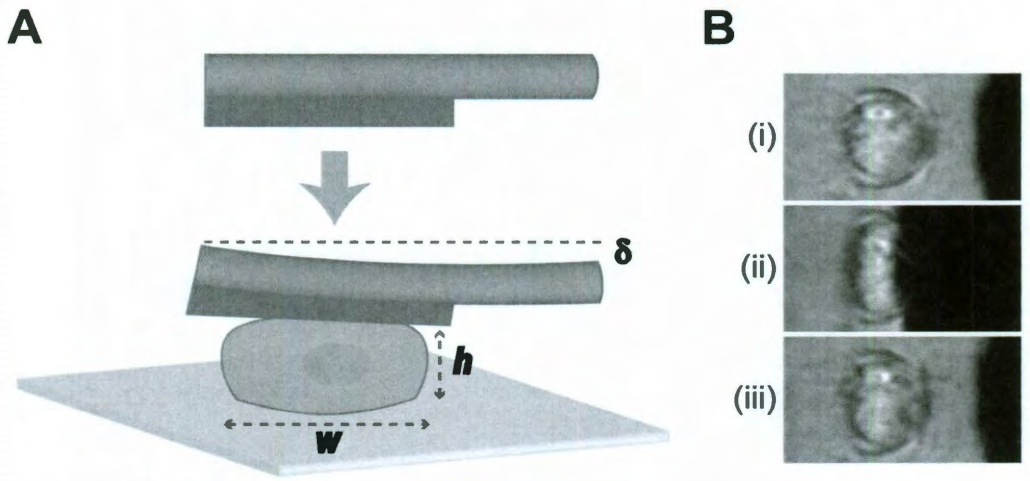

Figure 1: Schematic of cytocompression experiments. (A) Cells were seeded onto a glass slide and compressed at a rate of 4 μm/second by a tungsten probe. The height (*h*) and width (*w*) of the cell, as well as the probe deflection (δ) was measured at various stages of each compression event and used to calculate cellular biomechanical properties. (B) Representative frames of an inner meniscus cell seeded onto a glass slide initially (i), at equilibrium compression (ii), and during the recovery stage (iii), of a cytocompression event.

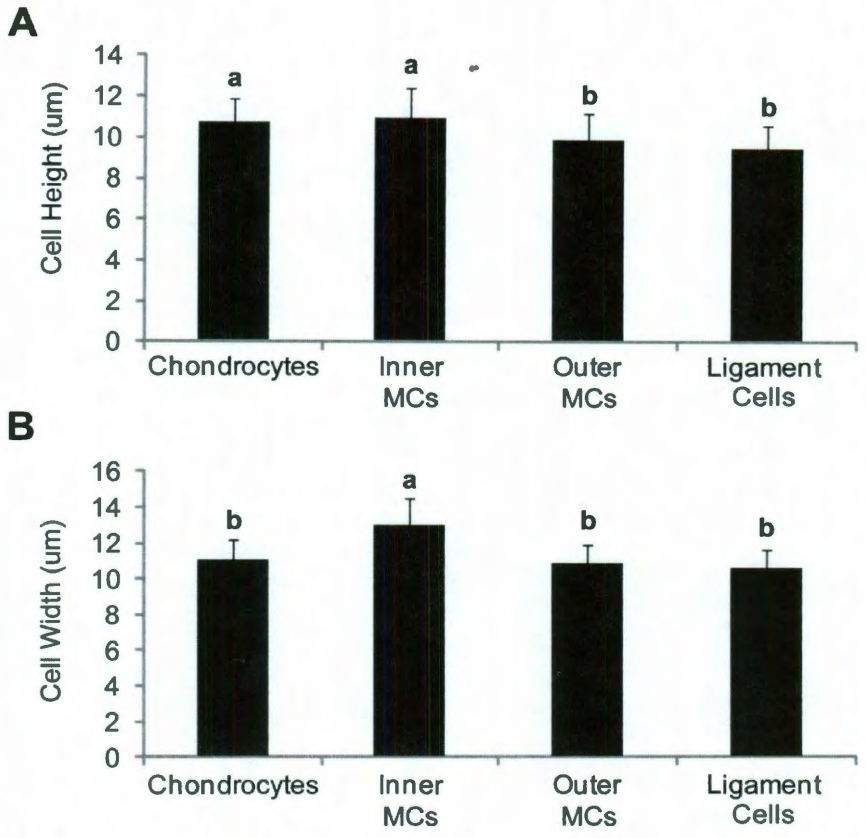

Figure 2: Comparison of initial cell dimensions. Cell height (A) and width (B) were measured for each cell prior to cytocompression. Comparison of average height values showed chondrocytes and inner meniscus cells (MCs) to be greater than outer MCs and ligament cells. Inner cells also showed greater cell width compared with chondrocytes, outer MCs and ligament cells. Data was analyzed using a one-way ANOVA with a Tukey's post hoc test. Significance was set at $p < 0.05$.

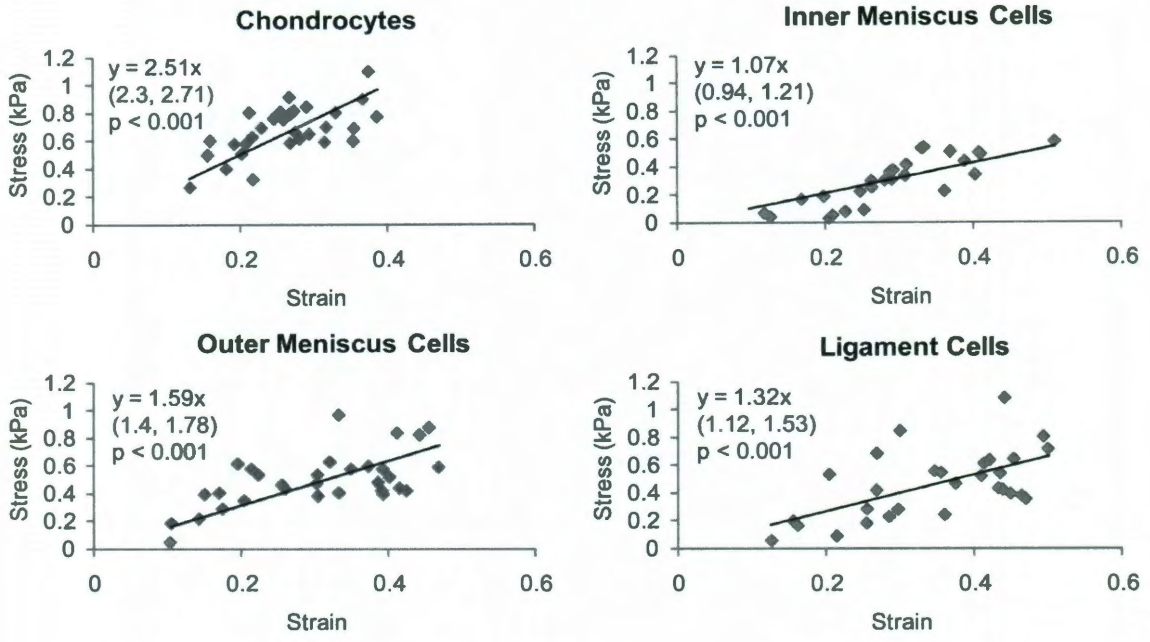

Figure 3: Stress versus strain correlations for different cell types. Linear regression analysis was performed on stress-strain data for chondrocytes, inner and outer meniscus cells, and ligament cells. Significant correlations were observed for all cell types ($p < 0.001$). For each graph, the equation obtained from linear regression is shown with 95% confidence bounds for the slope in parentheses below. Chondrocytes showed the highest cell stiffness (slope) than all other cell types, while ligament cell stiffness was not statistically different from either meniscus cell type. Inner meniscus cells, however, were statistically less stiff than outer meniscus cells.

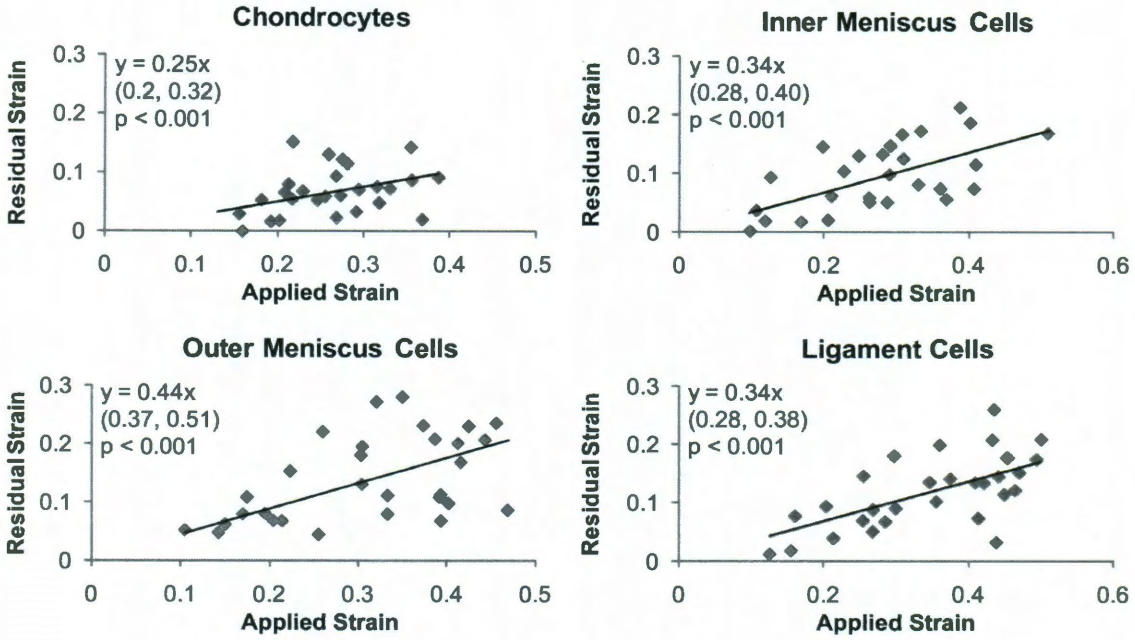

Figure 4: Correlation of residual vs. applied strain of compressed cells. Linear regression analysis was performed on residual strain versus applied strain data for chondrocytes, inner and outer meniscus cells, and ligament cells. Significant correlations were observed for all cell types ($p < 0.001$). The equation obtained from linear regression is shown in each graph with 95% confidence bounds for the slope in parentheses below. Positive correlations were observed for all cell types, but chondrocytes displayed a statistically lower slope than outer meniscus cells.

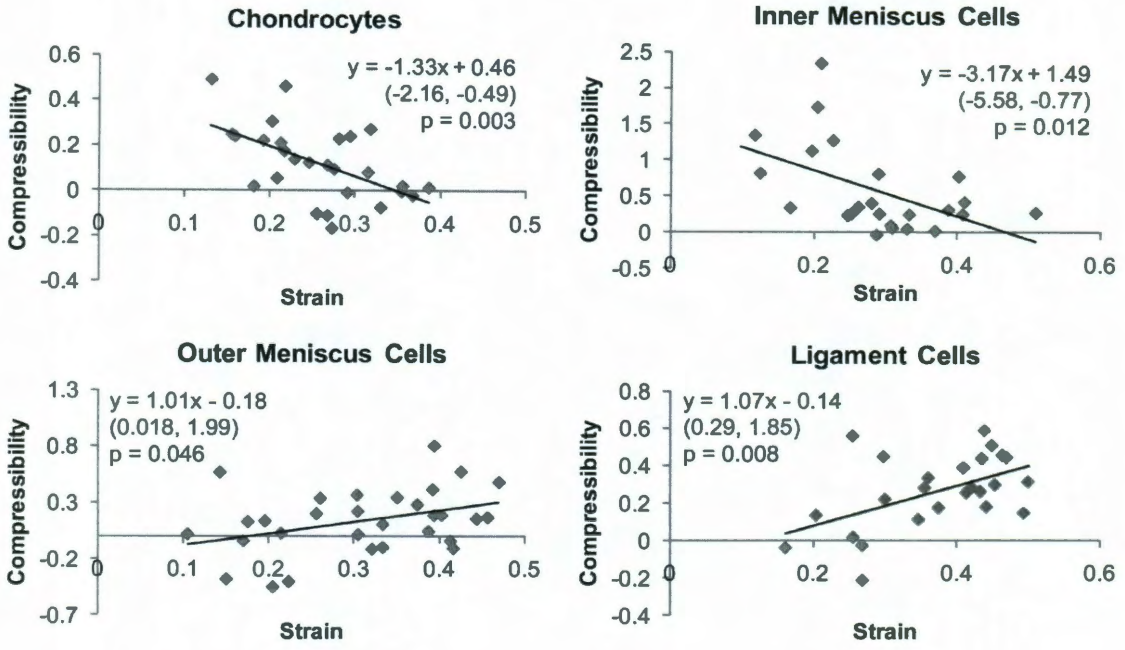

Figure 5: Apparent compressibility versus applied strain correlations. Linear regression analysis was performed on compressibility versus applied strain data for chondrocytes, inner and outer meniscus cells, and ligament cells. Significant correlations were observed for all cell types ($p < 0.05$). The equation obtained from linear regression is shown in each graph with 95% confidence bounds for the slope in parentheses below. Positive correlations were observed for outer meniscus cells and ligament cells, while negative correlations were observed for chondrocytes and inner meniscus cells.

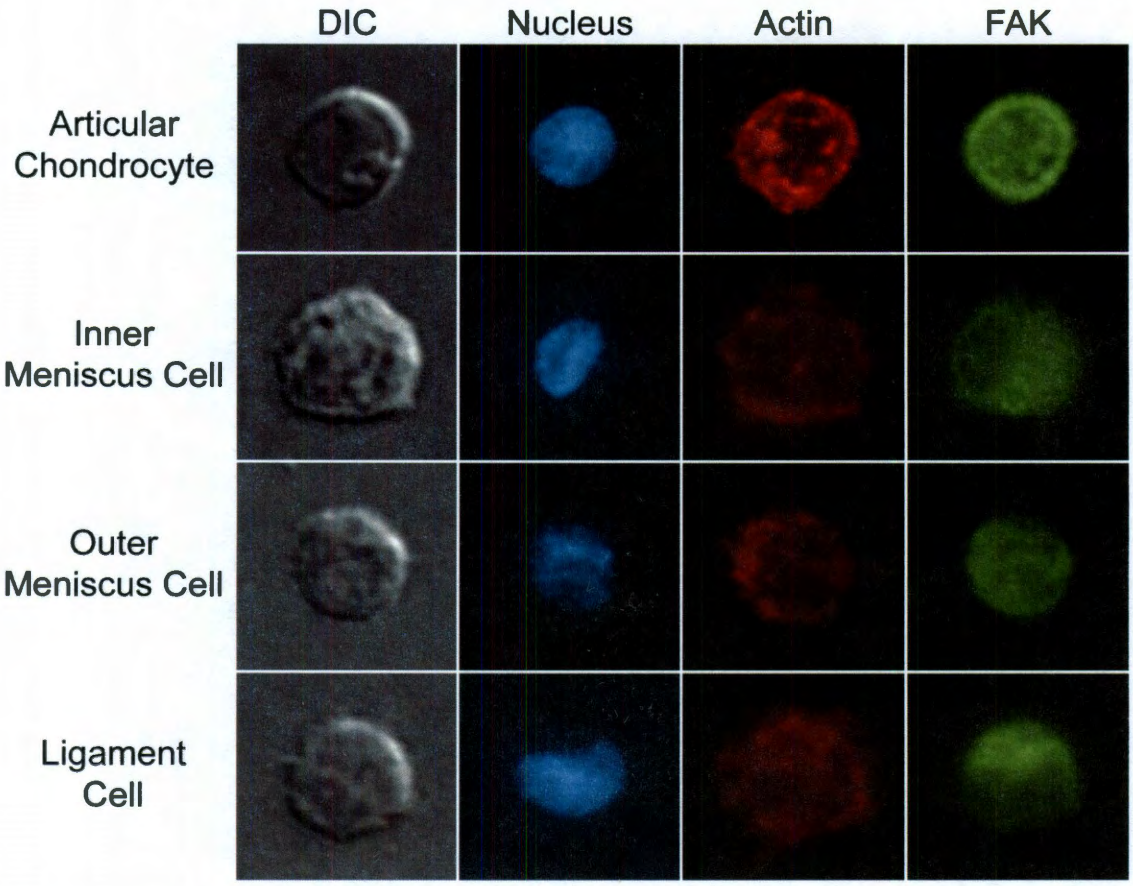

Figure 6: Actin and FAK immunocytochemistry. Articular chondrocytes, inner and outer meniscus cells, and ligament cells were seeded onto glass slides and fluorescently stained for cell nuclei, actin, and focal adhesion kinase (FAK). Cells from all groups stained positively for actin and FAK, and FAK staining was similar in intensity across cell types. Actin staining was most defined in articular chondrocytes, and less intense in meniscus and ligament cells.

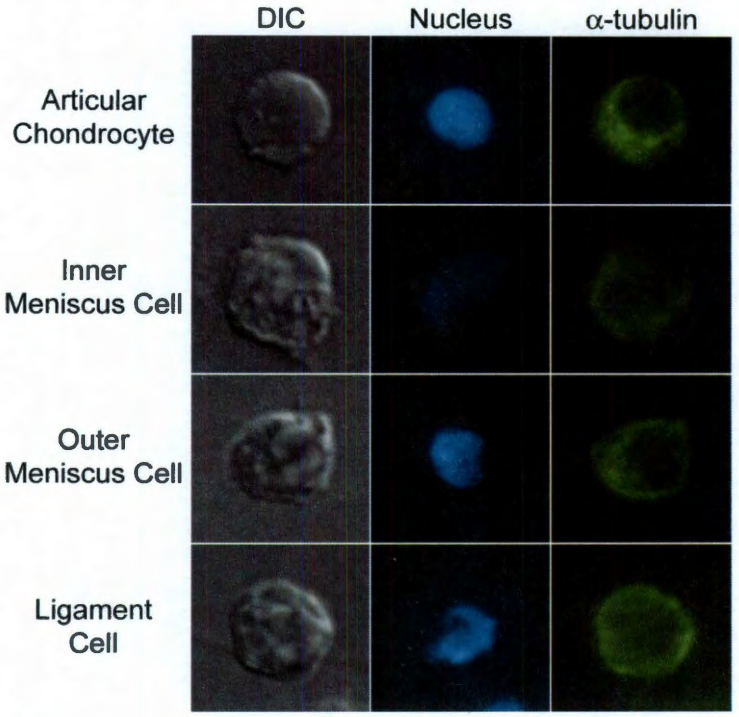

Figure 7: α-tubulin immunocytochemistry. Single articular chondrocytes, inner and outer meniscus cells, and ligament cells were fluorescently stained for microtubules using an anti-α-tubulin antibody. All cells stained positively for microtubules, with no gross differences in intensity noted.

Chapter 5: Regional effects of enzymatic digestion on knee meniscus cell yield and phenotype for tissue engineering

Abstract

An abundant cell source is the cornerstone of most tissue engineering strategies, but extracting cells from the knee meniscus is hindered by its dense fibrocartilaginous matrix. The identification of a method to efficiently isolate meniscus cells is important to the cartilage tissue engineering field, as it can reduce the cost and effort required to perform meniscus engineering research. In this study, six enzymatic digestion regimens used for cartilaginous cell isolation were used to isolate cells from the outer, middle, and inner regions of the bovine knee meniscus. Each regimen in each region was assessed in terms of cell yield, impact on cell phenotype, and cytotoxicity. All digestion regimens caused an overall upregulation of cartilage specific genes Sox9, collagen type I (Col 1), collagen type II (Col 2), COMP, and aggrecan (AGC) in cells from all meniscus regions, but was highest for cells isolated using 1075 U/mL of collagenase for 3 hrs (HC). In response to isolation, outer meniscus cells showed highest upregulation of Sox9 and Col 1 genes, whereas greatest upregulation for middle meniscus cells was seen in Col 1 expression, and Col 2 expression for inner

---

Chapter under review as: Sanchez-Adams, J., and Athanasiou, K.A. "Regional effects of enzymatic digestion on knee meniscus cell yield and phenotype for tissue engineering." *Tissue Engineering, Part C.*

cells. Cell yield was highest in all regions when subjected to 45 min of 61 U/mL pronase followed by 3 hrs of 1075 U/mL collagenase (P/C) digestion regimen (outer: 6.57 ± 0.37, middle: 12.77 ± 1.41, inner: 22.17 ± 1.47 $x10^6$ cells/g tissue). The second highest cell yield was achieved using 433 U/mL of collagenase for 18 hrs (outer: 1.95 ± 0.54, middle: 3.3 ± 4.4, inner: 6.06 ± 2.44 $x10^6$ cells/g tissue). Cytotoxicity analysis showed higher cell death in the LC group compared with the P/C group. Self-assembled constructs formed from LC-isolated cells were less dense than constructs formed from P/C-isolated cells, and P/C constructs showed higher GAG content and compressive moduli than LC constructs. All isolation methods tested resulted in similar phenotypic changes in meniscus cells from each region. These results indicate that, compared with other common isolation protocols, the P/C isolation method is able to more efficiently isolate meniscus cells from all regions and produce better tissue engineered constructs.

Introduction

Successful engineering of meniscus tissue is a valuable goal, as the knee meniscus has a limited ability to self-repair despite being prone to a plethora of debilitating injuries. However, meniscus tissue engineering strategies often require a large number of cells to create tissues with appropriate biochemical and biomechanical properties. Primary meniscus cells are often used for this purpose, and have shown great promise in creating tissue engineered constructs with properties similar to native cartilage.[115, 129-135] To obtain meniscus cells for

tissue engineering efforts, enzymatic digestion is needed, but little is known about the effects of isolation on the phenotype of meniscus cells, or which digestion technique is most effective for extracting cells from the meniscus.

Isolating cells from fibrocartilaginous tissues such as the meniscus is difficult due to the abundance of fibrous extracellular matrix. Various techniques have been employed to extract cells from cartilaginous tissues including collagenase type 2, trypsin, pronase, and hyaluronidase but their efficiency has not been compared or reported for meniscus cell isolation. These enzymes differ in substrate specificity, and therefore meniscus cell isolation techniques often use sequential digestion protocols to break down the tissue.[136-139] Collagenase type 2 is comprised of a variety of enzymes produced by the bacterium *Clostridium histolyticum*, and cleaves various sites along the collagen triple helix.[140-142] Trypsin is a serine peptidase derived from the digestive system which breaks down polypeptide chains into shorter fragments.[143-145] Similar to trypsin, pronase is made up of a variety of serine proteases produced by the bacterium *Streptomyces griseus*.[146-151] Pronase has very broad substrate specificity and is able to break down proteins into their constituent amino acids, in contrast to other enzymes whose end-products are often poly- or oligopeptides.[140, 152, 153] Hyaluronidase is an enzyme present in bovine testes and produced by certain bacteria, which digests the glycosaminoglycan hyaluronan.[154, 155]

While a formal comparison of enzymes has not been performed for meniscus cell isolation, a similar analysis has been carried out for articular chondrocytes. A study on the effects of enzymatic digestion of hyaline cartilage

on chondrocytes revealed that digesting the tissue with a high concentration of collagenase for a short period of time resulted in the least phenotypic changes in the cells.[137] However, other digestion techniques involving a low concentration of collagenase for a long period of time, pronase followed by collagenase, or trypsin followed by collagenase allowed for a greater cell yield than the high collagenase treatment, but also caused more phenotypic changes in the cells overall.[137]

Because of the regional differences in meniscus biochemistry and cell phenotype it is possible that different isolation techniques may be necessary for optimal cell yield from each region. The inner portion of the meniscus is similar to hyaline cartilage in that it contains the majority of sulfated glycosaminoglycans (GAGs) and collagen type II, whereas the middle and outer meniscus regions contain a higher proportion of collagen type I.[9, 29-31, 52] The morphology of meniscus cells also becomes progressively more fibroblast-like peripherally in the meniscus, with the inner region cells more rounded and chondrocyte-like and the outer cells containing more cellular processes.[38] In addition to morphology, regional cell phenotypic differences are observed; cells in the outer meniscus show high gene expression for collagen type I, while cells from the inner region display high gene expression for collagen type II and aggrecan.[18, 53] These differences in biochemical content regionally within the meniscus, as well as cell morphology and phenotype may dictate the type of digestion technique optimal for regional cell yield. The different cell populations resident in each meniscus region may also be affected differently in terms of phenotype to different digestion enzymes and protocols.

Therefore, the objectives of this study were 1) to compare enzymatic digestion techniques for each of the three meniscus regions in terms of overall cell yield and viability, 2) to determine the effect of these isolation techniques on cell phenotype, and 3) to test the cells from the most promising digestion techniques in a tissue engineering modality. The self-assembly method was used as a model tissue engineering strategy, as it has been used previously with meniscus cells yielding constructs with promising biochemical and biomechanical properties.[115, 130, 131] It was hypothesized that different digestion regimens would cause varying phenotypic changes in different regions of the meniscus, and that the digestion regimen yielding the highest number of cells could be used in the self-assembling process. The identification of a meniscus digestion method with high cell yield and minimal detrimental phenotypic changes is of great value to the tissue engineering field, allowing for a more efficient and cost-effective source of cells for further research.

Methods

Tissue dissection

In phase 1, five medial menisci were harvested from one-week-old bovine knee joints. The anterior and posterior horns of the menisci and connective tissue from the outer portion were carefully removed. Each meniscus was then separated into inner, middle, and outer radial regions. Each region was portioned into eight sets of tissue, and the wet weight of each set was measured and

recorded. One of the sets was placed in RNA-*later* and analyzed with RT-PCR, and another was digested in papain and assayed for total DNA content using a PicoGreen® Assay Kit [Invitrogen, Carlsbad, CA].

Cell isolation

The other six sets of tissue were minced to approximately 1 mm^3, and subjected to one of six tissue digestion regimens: 430 U/mL collagenase type II [Worthington, Lakewood, NJ] for 18 hrs (Low Collagenase or LC), 1075 U/mL collagenase type II for 7 hrs (High Collagenase or HC), 61 U/mL pronase [Sigma-Aldrich, St. Louis, MO] for 1.5 hrs followed by 1075 U/mL collagenase type II for 3 hrs (Pronase/Collagenase or P/C), 2.5 mg/mL (0.25%) Trypsin [Invitrogen] for 45 min followed by 1075 U/mL collagenase for 3 hrs (Trypsin/Collagenase or T/C), 433 U/mL hyaluronidase [Sigma] for 45 min followed by 1075 U/mL collagenase for 3 hrs (Hyaluronidase/Collagenase or H/C), and 433 U/mL hyaluronidase for 30 min followed by 2.5 mg/mL Trypsin for 30 min followed by 1075 U/mL collagenase for 3.5 hrs (Hyaluronidase/Trypsin/Collagenase or H/T/C). Tissues were digested at a concentration 43.73 mg/mL of digestion solution, and all digestion steps were carried out at 37°C with gentle shaking. All enzymes were reconstituted in DMEM containing 1% P/S/F and 1% non-essential amino acids, and collagenase solutions contained an additional 10% FBS. After each digestion regimen, cell solutions were filtered through a 70μm cell strainer, and centrifuged at 700 *x g* for 5 minutes. Cells were then washed once with PBS and resuspended in PBS before being counted with a Z2 Coulter

Counter [Beckman-Coulter]. Cells were counted three times and the average and standard deviation of cell counts was calculated. Cell count data were analyzed using a 2-way ANOVA, with a significance level of $p < 0.05$.

Quantitative RT-PCR

Cells from each digestion regimen and regional tissue controls were also analyzed using quantitative RT-PCR for mRNA abundance of cartilage specific genes Sox9, collagen type I (Col 1), collagen type II (Col 2), cartilage oligomeric matrix protein (COMP), and aggrecan (AGC). Total RNA was extracted from native tissue using an RNAqueous Kit, and from cells using an RNAqueous-Micro Kit [Ambion, Austin, TX]. Total RNA was reverse-transcribed using the SuperScript™ III First-Strand Synthesis System [Invitrogen], and then PCR was performed on the resulting cDNA for cartilage-specific genes using SYBR® Green PCR Mastermix, 80-100 ng of sample cDNA, and 900 nM of each primer. PCR analysis was performed using a RotorGene 3000, and each run used the following protocol: 50°C for 2 min, 95°C for 10 min, followed by 40 cycles of 95°C for 15 sec and 60°C for 60 sec. Bovine 18s rRNA was used as a housekeeping gene for each of the digestion techniques and tissue control. All fold-change calculations were determined by normalizing data to native tissue controls from each region and were calculated using the formula $y = 2^{\Delta\Delta C_t}$, where $\Delta\Delta C_t$ represents the difference in takeoff cycle between experimental and control groups. Specific primers for each gene are listed in Table 1. Gene expression data were analyzed using a 2-way ANOVA, with a significance level of $p < 0.05$.

Fluorescent staining of necrosis

Cells from the highest yielding digestion regimens were also fluorescently stained to visualize cell nuclei and necrotic cells. Hoechst 33342 was used to stain cell nuclei, and ethidium homodimer III was used to stain cells in a necrotic state [Biotium, Hayward, CA].

Tissue engineering

In phase 2, the two digestion techniques with highest cell yield were used to extract cells from 3-4 grams of total medial menisci. The cells were counted and total cell yield per gram of tissue was determined. An aliquot of cells from each digestion technique was stained for live and dead cells using a Live/Dead Viability/Cytotoxicity Kit [Invitrogen]. The remaining cells were then seeded into 5 mm agarose molds at 5.5 x 10^6 cells per well in 0.5 mL of chondrogenic medium containing DMEM with 1% penicillin/streptomycin/fungizone, 1% non-essential amino acids, 10^{-7} M dexamethasone, 5mM L-ascorbic acid 2-phosphate, 0.4 mM L-proline, and 10 mM sodium pyruvate. Constructs were cultured for 4 weeks in an incubator 37°C with 5% CO_2 and 0.5 mL of media was changed every day. At the end of the culture period, each construct's diameter and thickness was measured. Constructs were then either analyzed for total glycosaminoglycan content using a dimethyl-methylene blue assay kit [Biocolor, Carrickfergus, UK], or total collagen content using a hydroxyproline assay, or were mechanically tested using an unconfined compression stress-relaxation test at 10% strain.

Compressive testing was initiated with 15 cycles of preconditioning at 0-5% strain, and data were fit with a Kelvin solid viscoelastic model to determine the modulus of relaxation (E_r) and instantaneous modulus (E_i) as previously described.[156]

Results

Cell isolation

Tissue specimens from the inner, middle, and outer meniscus were portioned from five medial menisci and minced in preparation for digestion. Qualitatively, it was observed that the inner meniscus was the easiest to mince, while the outer meniscus was more tough and fibrous, necessitating much more time and effort to achieve the desired ~1 mm^3 fragments. In phase 1, six different isolation methods were used to isolate cells from the inner, middle, and outer regions of the bovine meniscus. Qualitative differences in the viscosity of resultant cell solution were observed among the digestion regimens, with the P/C protocol producing the least viscous solution compared with the HC and LC protocols, which seemed the most viscous. The number of cells per gram of tissue was determined for each isolation regimen (Figure 1). Statistical analysis showed that the overall cell yield was highest for the inner meniscus compared with the outer meniscus. The middle meniscus cell yield trended higher than the outer region but was not statistically different from either the inner or outer regions. All isolation regimens were able to extract cells from all regions, and the

pronase/collagenase (P/C) treatment resulted in the highest overall cell yield from all regions (outer: 6.57 ± 0.37, middle: 12.77 ± 1.41, inner: 22.17 ± 1.47 $x10^6$ cells/g tissue). Additionally, the P/C regimen, when applied to the inner meniscus region, produced a cell yield closely matching that of native tissue (outer: 33.88 ± 0.07, middle: 23.55 ± 1.17, inner: 19 ± 0.16 $x10^6$ cells/g tissue). Overall cell yields from the other isolation regimens were not statistically different from each other, but the low collagenase (LC) treatment trended higher than the rest (outer: 1.95 ± 0.54, middle: 3.3 ± 4.4, inner: 6.06 ± 2.44 $x10^6$ cells/g tissue) .

Fluorescent staining of necrosis

Fluorescent staining of cell nuclei and necrotic cells was carried out for the highest yielding digestion regimens, P/C and LC (Figure 2). Visual comparison of necrotic cells to total cells showed more necrotic cells present in LC digested specimens from all regions than in the P/C digested specimens.

Gene expression

Gene expression of digested cells from each meniscus region using six different isolation protocols were compared to native gene expression from each region (Figure 3). In general, isolated cells from all regions showed an increase in gene expression for all genes studied compared with native tissue controls. In the outer region, Sox9 and Col 1 gene expression displayed the most upregulation, whereas Col 2 gene expression was least affected by isolation. Amongst the digestion regimens, the outer region cells showed the highest gene

upregulation when isolated using the HC protocol, while the gene expression of cells resulting from the LC isolation regimen was the only group not statistically different from native tissue. In response to isolation, middle meniscus cells showed the most upregulation in Col 1, and the least upregulation in Col 2. The digestion regimen resulting in the highest overall gene expression levels was the HC protocol, and the gene expression of cells from the H/T/C protocol was not statistically different from native tissue. Inner meniscus cells showed the highest overall upregulation in Col 2, and AGC gene expression was least affected by isolation. The HC protocol produced the highest overall gene expression upregulation, whereas the gene expression of cells from the LC and P/C protocols were not statistically different from native tissue.

Tissue engineering

In phase 2, constructs were formed from cells isolated using the LC and P/C protocols. Cell yield was similar to results from phase 1, with P/C method yielding approximately 50% more cells than the LC method (Figure 4A). Live-dead staining of the resultant isolated cells showed more dead cells relative to live cells in the LC isolated population relative to the P/C isolated cells (Figure 4B). After 4 weeks in culture, constructs from each group were compared in terms of gross morphology, GAG content, collagen content, and compressive mechanics (Figure 5). Constructs formed from LC-isolated cells displayed statistically higher thickness compared to P/C constructs, though construct diameters were not different between groups. P/C constructs showed higher

GAG content, but no difference was observed in collagen content between groups. Stress-relaxation unconfined compression testing of the two groups showed higher modulus of relaxation and instantaneous modulus for P/C constructs relative to LC constructs.

Discussion

This study sought to compare the regional effects of enzymatic digestion techniques for meniscus tissue engineering. Six different digestion protocols were characterized based on regional meniscus cell yield, viability, and phenotype, and the protocols yielding the highest number of cells were tested in a tissue engineering modality. In agreement with the proposed hypothesis, meniscus cells from different regions showed varying phenotypic changes following isolation, and the protocol yielding the highest number of cells (the P/C isolation method) was successfully implemented in the self-assembling process.

In phase 1, isolation of cells from the different regions of the meniscus showed wide variation. Specifically, the cell yield from the inner meniscus, regardless of digestion regimen, was higher than the yield from the outer region. Although the outer meniscus contained the highest concentration of cells (~34 $x10^6$ cells/g tissue), isolation using the P/C protocol was able to extract less than 20% of these cells. In contrast cell yield from the inner meniscus using the P/C protocol was similar to the expected native tissue cellularity. The reason for this difference needs further investigation, but could be due to higher GAG content in the inner meniscus facilitating digestion solution uptake and enzymatic action, or

insufficient release of cells from the outer region matrix increasing the viscosity of the isolation solution and impeding cell pelleting during centrifugation. To our knowledge, this disparity in cell yield from these two regions has not been reported previously. As the meniscus is wedge shaped, however, the relatively low cell yield from the outer region is mediated by the abundance of outer tissue compared with inner meniscus tissue. Because of this, the relative fractions of isolated meniscus cells from the outer and inner regions are likely similar to those observed in native tissue. The resulting distribution of cells from enzymatic isolation has implications for tissue engineering as meniscus cells from different regions show varying synthetic profiles, which affect the biochemical and mechanical properties of the engineered constructs they form.

Interestingly, cell yield was found to be statistically higher using the P/C isolation regimen in all regions of the meniscus. This protocol involved 45 minutes of pronase treatment followed by 3 hours of high collagenase (HC) treatment. Since the P/C treatment resulted in higher cell yield than the HC treatment, it follows that the introduction of pronase was necessary to achieve such a high cell yield. Although both trypsin and pronase are serine peptidases, they differ in substrate specificity, with pronase having a wider range of proteolytic activity than trypsin. In agreement with the present findings, previous reports comparing the efficacy of trypsin and pronase have reported more favorable tissue digestion with pronase, with digestion occurring more rapidly and the resulting cell solution containing fewer cell clumps.[157, 158] As pronase is known to act on a wide variety of substrates, breaking proteins down into their

individual amino acids, it is likely that pre-treatment of meniscus tissue with this enzyme increases tissue permeability and allows the following collagenase enzyme better access to collagen molecules throughout the tissue. The high cell yield resulting from the P/C isolation protocol represents a vast improvement over other common digestion methods, and may be applicable to other fibrocartilaginous or fibrous tissues such as the temporomandibular joint disc or tendons. More studies are needed, however, to optimize the concentrations and application times of pronase and collagenase to minimize cell death and maximize efficiency of cell isolation.

Additionally, no other combinatorial treatment with HC (T/C, H/C, or H/T/C) resulted in the same increase in cell yield, indicating that the present pronase application acts differently on meniscus tissue than either hyaluronidase or trypsin. Compared with trypsin and pronase, hyaluronidase is known to have higher substrate specificity, concentrating primarily on the hyaluronan molecule.[159, 160] It has also been reported that specificity of this enzyme to hyaluronan is dependent on molecular weight, with more cleavage occurring on high molecular weight molecules.[160] While this enzyme may be effective for digestion of GAG-rich tissue such as articular cartilage, the meniscus contains relatively little GAG, limiting the efficacy of hyaluronan for meniscus cell isolation.[52, 136]

As hypothesized, phenotypic changes in isolated meniscus cells were observed in all regions. Although a general upregulation of cartilage specific genes was noted in all isolated cells compared with native tissue, gene

expression was found to be altered differently in isolated outer, middle, and inner meniscus cells. This variation in phenotypic response based on meniscus regions corresponds to the known differences in native meniscus cell morphology and phenotype.[38, 53] Specifically, outer meniscus cells showed the highest upregulation in Sox9 and Col 1 expression, middle cells in Col 1 expression, and inner cells in Col 2 expression. Outer and middle meniscus cells, therefore, show similar phenotypic changes in response to tissue digestion, and the gene most affected (Col 1) also corresponds to the most abundant extracellular matrix (ECM) protein, collagen type I, in these regions. Similarly, increased inner meniscus cell expression of Col 2 also corresponds to the most abundant collagen protein found in the inner region.[9, 29, 52] These results suggest that, upon liberation from their resident ECM, meniscus cells respond by upregulating genes commensurate with restoring their native environment. This behavior is different than that observed in freshly isolated articular chondrocytes, in which gene expression of collagen type II and aggrecan was unaffected or decreased following tissue digestion, providing more evidence of the distinction between articular chondrocytes and meniscus cells.[29] The general upregulation of cartilage-specific genes in meniscus cells isolated from native tissue may indicate that isolation of these cells stimulates them to produce cartilage matrix components during *in vitro* culture or tissue engineering.

The P/C protocol proved to be an efficient mode of extracting meniscus which had higher viability than LC isolated cells. Cytotoxicity analyses on cells isolated using LC and P/C protocols revealed fewer dead cells in the P/C isolated

population in both phase 1 and phase 2. As cell viability following isolation of meniscus cells is rarely reported in the literature, it is difficult to compare these results to published data. While the mechanism by which P/C isolation preserved cell viability is unknown, it may be related to the relatively short digestion regimen of the P/C protocol relative to the LC protocol. Regardless of the mechanism, however, the increased cell viability observed in P/C isolated cells is an attractive property for use of these cells in tissue engineering.

In addition to increased viability, isolated P/C cells also showed more promising biochemical and mechanical properties when used in a tissue engineering modality. In phase 2, tissue engineering showed increased GAG content and compressive properties in constructs formed from P/C isolated cells compared with constructs formed from LC cells. However, LC constructs were also significantly thicker than their P/C counterparts. This difference in thickness may be attributed to the characteristics of the cell solution seeded. The LC protocol resulted in a much more viscous cell solution than the P/C protocol, perhaps due to the presence of higher molecular weight digestion fragments in the LC isolate. In contrast, the P/C isolated cells settled to the bottom of the agarose well readily, which may have aided cell-cell contacts and subsequent protein synthesis, as has been theorized to be important in self-assembled articular chondrocyte constructs.[161] Further, the higher compressive properties of P/C constructs relative to LC constructs may be related to the increased GAG content of P/C constructs compared to LC constructs as GAGs are known to be important for maintaining compressive properties in tissue such as articular

cartilage.[162, 163] The P/C cells, therefore, appeared to be more active in the self-assembling process than LC cells.

In summary, the P/C isolation regimen resulted in 1) higher cell yield from all meniscus regions than other protocols tested, 2) higher cell viability than cells isolated using the LC protocol, and 3) cells that produced tissue-engineered constructs with higher GAG content and compressive properties than the LC regimen. Therefore, the P/C meniscus cell isolation method is an efficient way to harvest meniscus cells, regardless of region, with relatively low cytotoxicity. This method can be widely applicable to tissue engineering strategies using a variety of fibrocartilaginous or fibrous tissues. However, more studies are warranted to identify the optimal concentrations and durations of pronase/collagenase tissue digestion.

Acknowledgements

We would like to acknowledge the National Science Foundation Rice-Houston Alliance for Graduate Education and the Professoriate (NSF-AGEP) for their generous support of this work. In addition we would like to gratefully acknowledge funding from the National Institutes of Health R01AR047839 and R01DE019666.

Tables

Table 1: Quantitative RT-PCR forward and reverse primers

Gene	Forward Primer (5'-3')	Reverse Primer (5'-3')	Target (bp)	Accession Number	Ref.
18S rRNA	CAAATTACCCACTCCCGACCC	AATGGATCCTCGCGGAAGG	114	DQ066896.1	[164]
SOX9	ACGCCGAGCTCAGCAAGA	CACGAACGGCCGCTTCT	71	AF278708	[165]
Col 1	CATTAGGGGTCACAATGGTC	TGGAGTTCCATTTTCACCAG	97	NM_174520	[166]
Col 2	AACGGTGGCTTCCACTTC	GCAGGAAGGTCATCTGGA	69	X02420	[166]
COMP	TCAGAAGAGCAACGCAGAC	TCTTGGTCGCTGTCACAA	72	X74326	[102]
AGC	GCTACCCTGACCCTTCATC	AAGCTTTCTGGGATGTCCAC	76	U76615	[166]

Figures

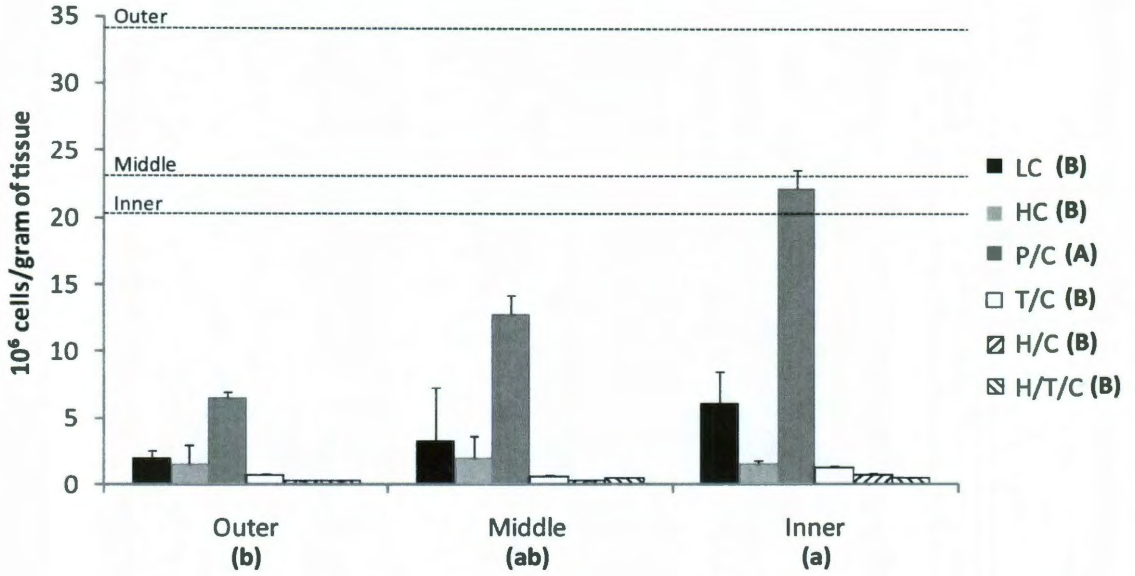

Figure 1: Cell yield from different meniscus regions using six isolation methods. The number of cells per gram of tissue was determined for each isolation regimen in each radial region of the meniscus. For comparison, native tissue average cellularity is depicted for each meniscus region (dashed lines). Overall, cell yield from the inner region was highest, followed by the middle and outer regions, respectively. Amongst the isolation regimens, the pronase/collagenase (P/C) treatment resulted in the highest overall cell yield from all regions. Results were analyzed using a 2-way ANOVA, with significance set at $p < 0.05$. Groups not connected by the same letter are statistically different.

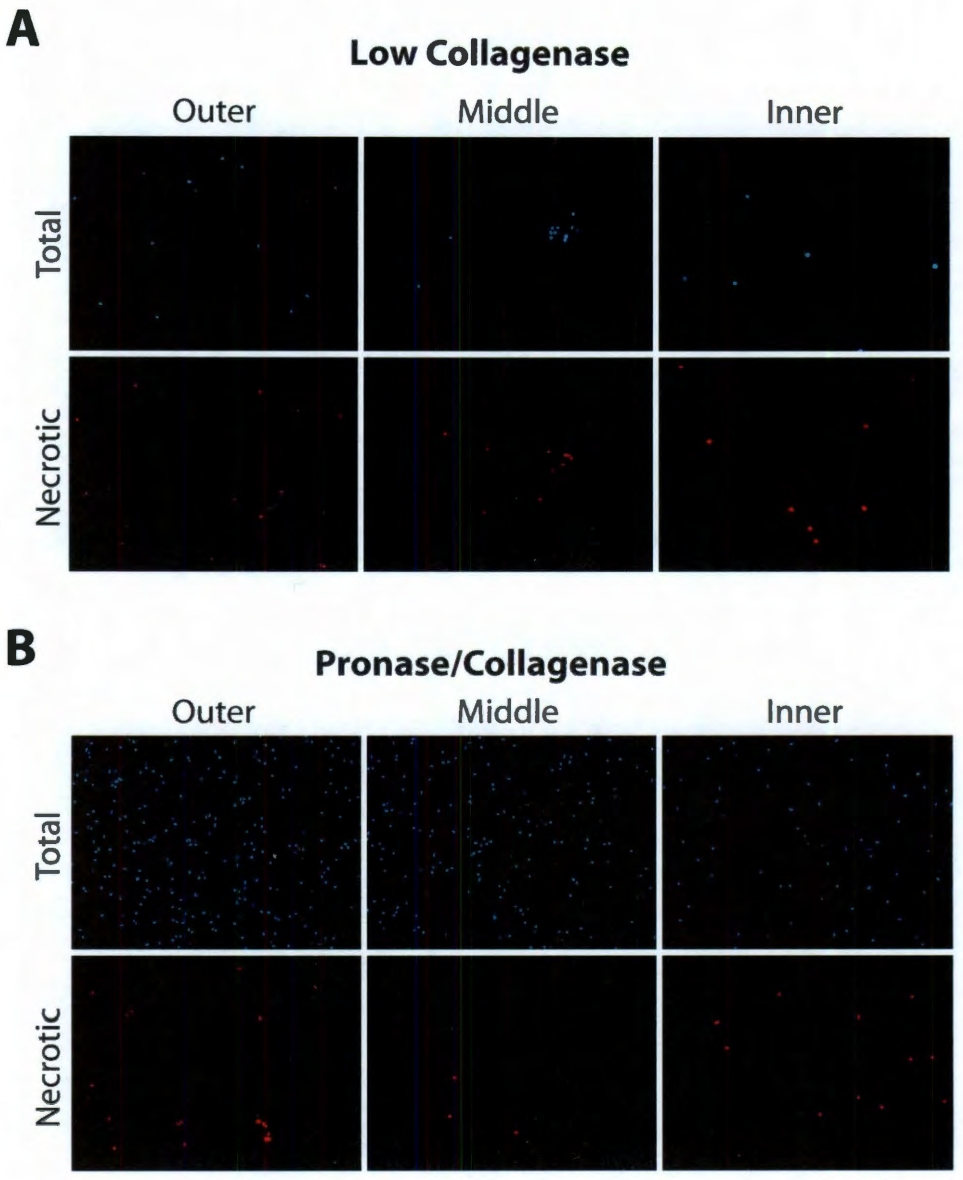

Figure 2: Total and necrotic cells from different meniscus regions using two isolation methods. Fluorescent staining of cell nuclei and indicators of cell necrosis for low collagenase (A) and pronase/collagenase (B) isolated cells. Cells isolated using the pronase/collagenase method displayed fewer necrotic cells than those isolated using the low collagenase protocol.

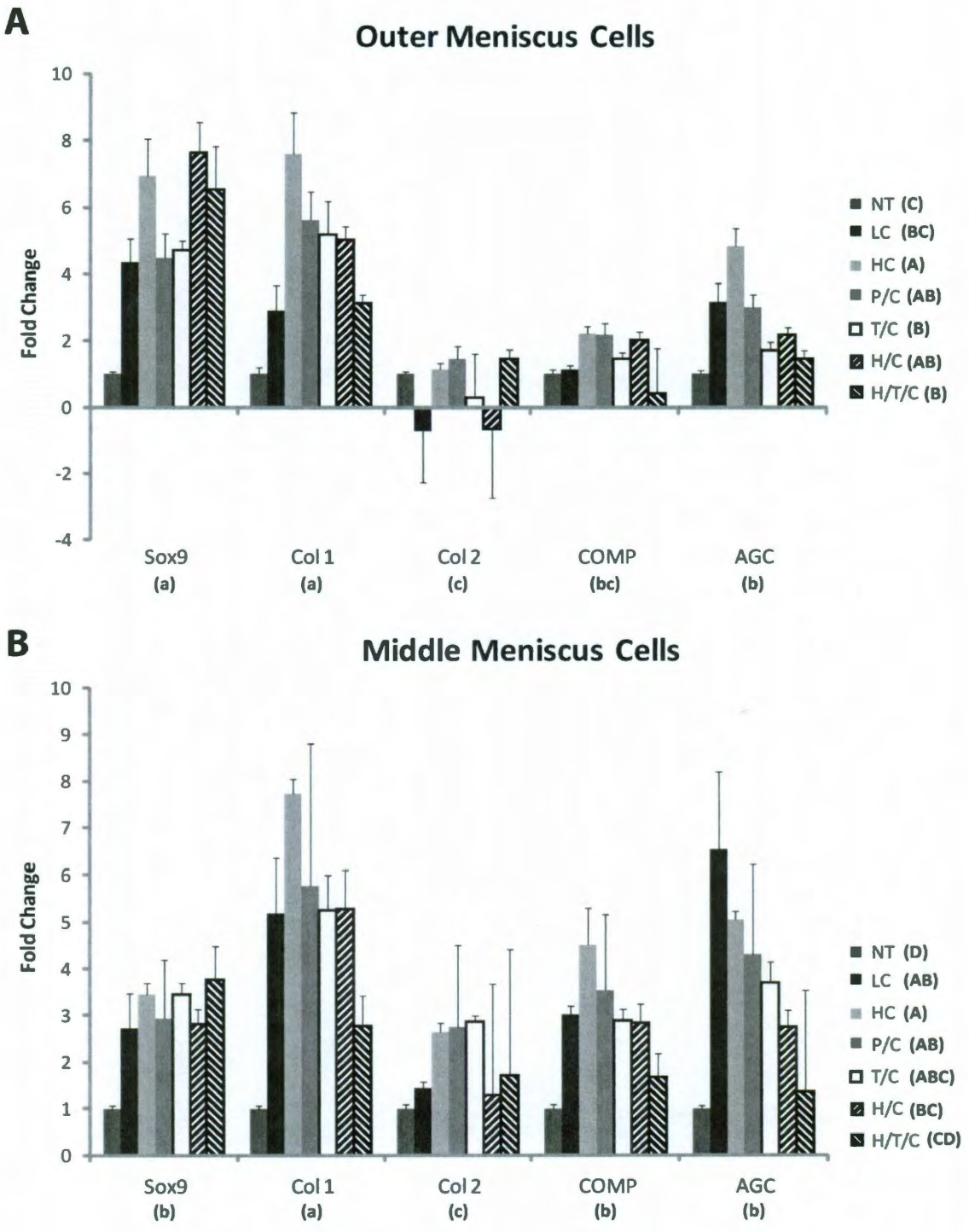
A
Outer Meniscus Cells
Fold Change
10
8
6
4
2
0
-2
-4
Sox9 (a)
Col 1 (a)
Col 2 (c)
COMP (bc)
AGC (b)
NT (C)
LC (BC)
HC (A)
P/C (AB)
T/C (B)
H/C (AB)
H/T/C (B)
B
Middle Meniscus Cells
Fold Change
10
9
8
7
6
5
4
3
2
1
0
Sox9 (b)
Col 1 (a)
Col 2 (c)
COMP (b)
AGC (b)
NT (D)
LC (AB)
HC (A)
P/C (AB)
T/C (ABC)
H/C (BC)
H/T/C (CD)

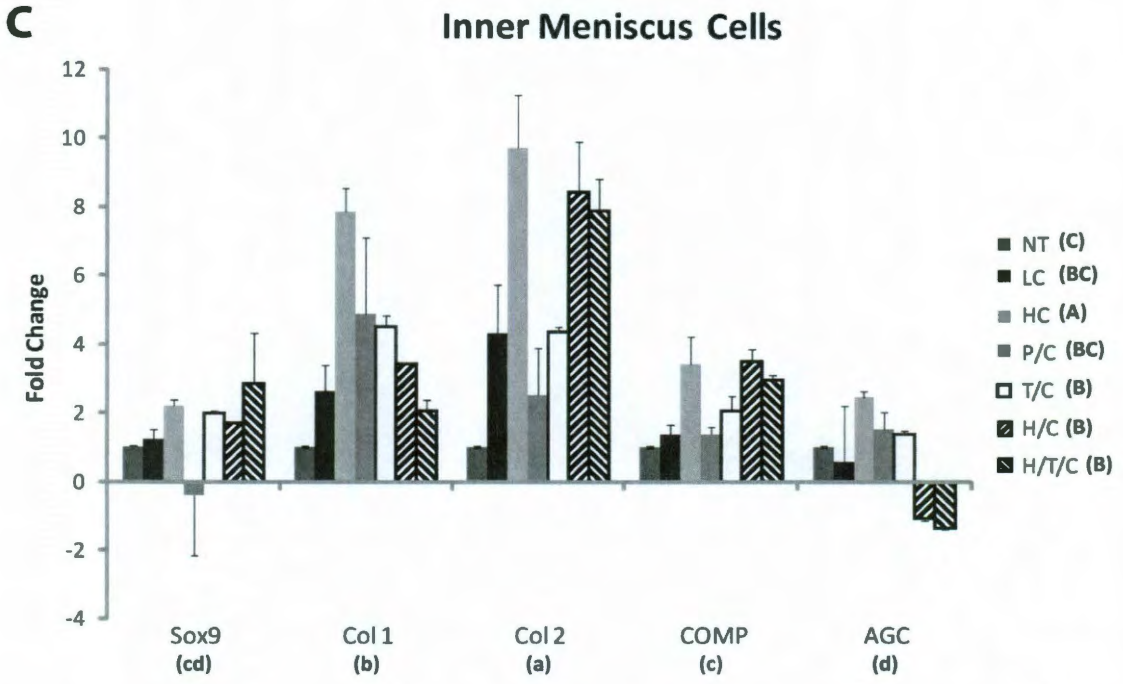

Figure 3: Gene expression of meniscus cells in response to isolation. Outer (A), middle (B), and inner (C) meniscus cells were isolated from native tissue (NT), or subjected to one of 6 isolation regimens: low collagenase (LC), high collagenase (HC), pronase/collagenase (P/C), trypsin/collagenase (T/C), hyaluronidase/collagenase (H/C), or hyaluronidase/trypsin/ collagenase (H/T/C). Gene expression levels were normalized to native tissue values for Sox9, collagen type I, collagen type II, COMP, and aggrecan. Results for each cell type were analyzed using a 2-way ANOVA, $p < 0.05$. Groups not connected by the same letter are statistically different.

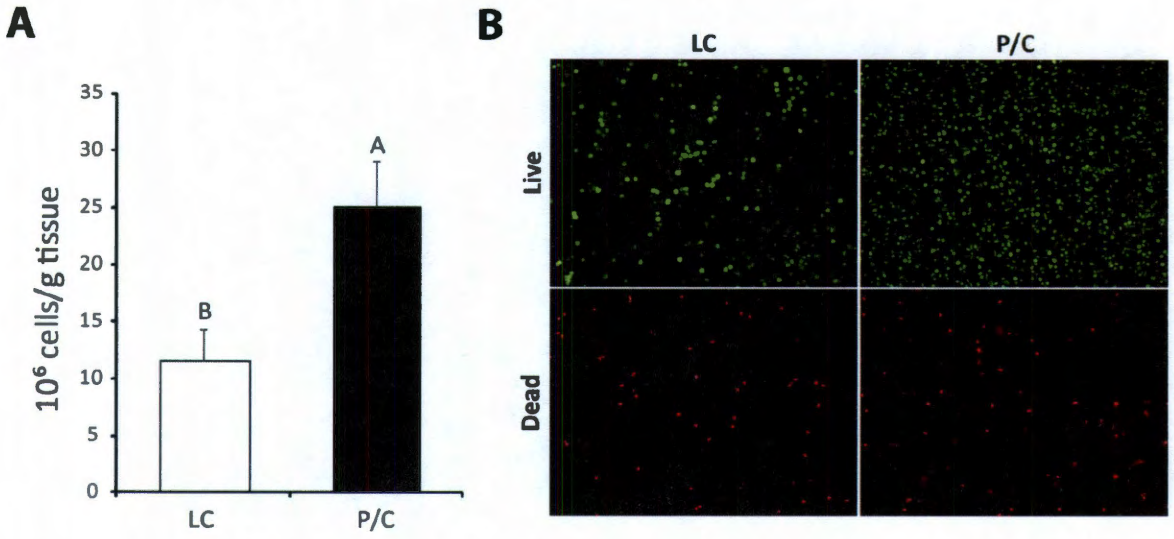

Figure 4: Phase 2 cell yield and live-dead analysis. Cells from whole medial menisci were isolated using the low collagenase (LC) and pronase/collagenase (P/C) protocols from phase 1. Cell yield was higher for the pronase/collagenase method (A). Live-dead staining of the resultant isolated cells showed more dead cells relative to live cells in the LC isolated population compared with the P/C isolated cells. Quantitative data were analyzed using a Student's t-test, with significance set at $p < 0.05$. Groups not connected by the same letter are statistically different.

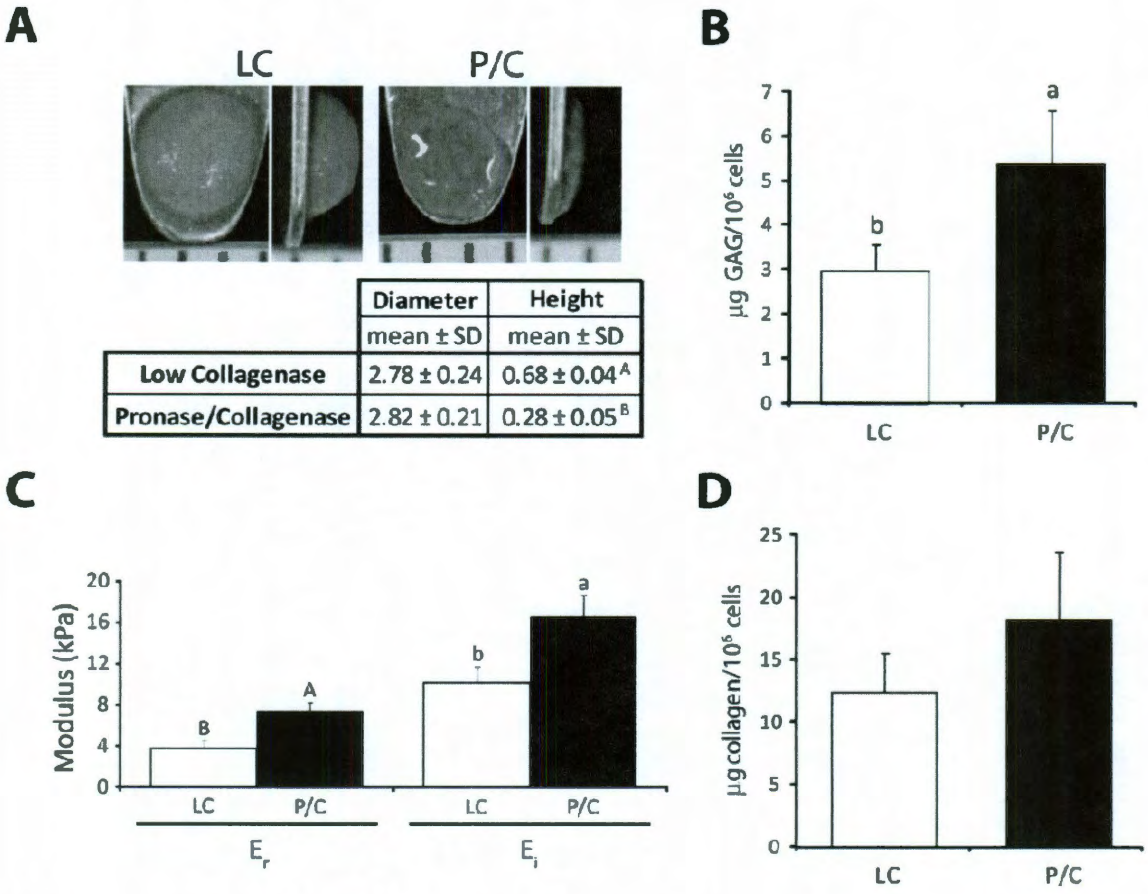

	Diameter	Height
	mean ± SD	mean ± SD
Low Collagenase	2.78 ± 0.24	0.68 ± 0.04^{A}
Pronase/Collagenase	2.82 ± 0.21	0.28 ± 0.05^{B}

Figure 5: Phase 2 gross morphology, biochemistry, and compressive mechanics. Self-assembled constructs were formed using cells isolated by the low collagenase or pronase/collagenase methods (A). LC constructs were significantly thicker than P/C constructs, however construct diameter was not different between groups. Biochemical analysis of GAG and collagen content (B and D, respectively) showed increased GAG content per cell in the P/C constructs, but no difference in collagen content between groups. P/C constructs showed higher modulus of relaxation (E_r) and instantaneous modulus (E_i) compared to LC constructs when subjected to unconfined compression stress-relaxation at 20% strain (C). Student's t-tests were performed on each data set, with significance set at $p < 0.05$. Groups not connected by the same letter are statistically different.

Chapter 6: Pathophysiology of the Knee Meniscus and the Need for Tissue Engineering

Section 6.1: Pathophysiology and injury

Meniscus pathology

The normal meniscus, as discussed previously, is composed of medial and lateral semilunar, wedge-shaped structures. Various deviations from this normal morphology can occur through abnormal development, disease, degeneration, or traumatic injury. Most commonly, abnormal development results in a discoid meniscus, in which the inner portion of the meniscus extends and the tissue is disc-like in shape. This most often afflicts the lateral meniscus and can be complete, in which the meniscus covers almost the entire articulating surface, or incomplete, covering more surface area than normal (see Figure 1). The incidence of discoid abnormality is unclear, but population estimates range from 0.4–5%.[167, 168] Though many cases are thought to be asymptomatic and therefore undiagnosed, some discoid menisci can cause locking of the knee and general knee pain.[168]

The meniscus may also be affected by metabolic disease, degeneration, and traumatic injury. Metabolic diseases including calcium pyrophosphate crystal

---

Chapter published as: Athansiou, K. A., and Sanchez-Adams, J. "Part 2: Pathophysiology and the Need for Tissue Engineering." *Engineering the Knee Meniscus*. Morgan and Claypool Publishers. 2009.

deposition, hemochromatosis, and ochronosis, can cause calcification, gross discoloration, and interference with the overall consistency of the tissue.[169, 170] These disorders heavily compromise the functionality of the meniscus, but cannot be treated locally as they are due to systemic changes in the body. Other types of disorders, such as degeneration and trauma, afflict the meniscus more specifically allowing clinicians to focus treatment on the meniscus itself.

Osteoarthritis and meniscal degeneration

Little is known about the causes of meniscal degeneration, however with degeneration the meniscus becomes more prone to injury.[171, 172] Osteoarthritis can cause widespread degenerative changes in the meniscus as well as the surrounding hyaline cartilage, and has been implicated in meniscal injury. While in the early 1980's meniscus pathology was found to be weakly correlated with osteoarthritis, researchers have more recently identified meniscal injury in around 75% of patients with symptomatic osteoarthritis.[173-175]

Osteoarthritis affects the meniscus in multiple ways, resulting in compromised tissue functionality. This disease is known to affect the geometry of the meniscus, causing thickening of the medial posterior and lateral anterior horns, which may in turn affect the biomechanics of the meniscus making it more prone to injury.[176] Osteoarthritic changes in the biochemical makeup of the meniscus may also play a role, as induced osteoarthritis in dogs causes an increase in meniscal water content and changes in GAG content and type over time.[177] This disease may also be associated with calcification of the meniscus,

but causality has yet to be confirmed.[171] It has also been shown that severe osteoarthritis causes medial joint space narrowing as the medial meniscus displaces radially, which acts to preserve the tissue at the horns slightly, but overall functionality of the tissue is lost and widespread meniscal degeneration is apparent.[178] Therefore, osteoarthritic degeneration can be an important contributor to meniscal injuries.

Tears of the meniscus

Various types of meniscal tears can occur as a result of degeneration and/or trauma. There are four main types of meniscal tears: vertical longitudinal, oblique, radial, and horizontal (see Figure 2).[4, 179] Additionally, there are degenerative (complex) tears which describe an overall fraying of the inner meniscal edge consisting of many different types of tears. The vertical longitudinal tear occurs when the meniscus is split along a circumferential line. These tears can either span the entire thickness of the meniscus vertically (called a bucket-handle tear), or only a portion of it.[4, 180] When a bucket-handle tear occurs, the inner portion of the meniscus is free to intrude into the joint space, causing mechanical opposition to joint movement. The length of vertical longitudinal tears ranges from less than 1 mm to almost the entire circumference of the tissue.[4] Oblique tears are also vertical in nature but extend inward from the inner meniscus in a slanted fashion.[4] These tears are often referred to as parrot beak or flap tears because of their shape. The free end of this type of tear can catch within the joint, inhibiting joint movement. Radial tears are similar to oblique

tears but propagate radially, cleaving the circumferential collagen fibers.[4] These tears often exist without any symptoms as their free ends are not as prone to catching within the joint space as other tear geometries. However, radial tears can be especially damaging to the overall function of the tissue if left to propagate. Horizontal tears cut the meniscus into superior and inferior parts. They begin in the inner portion of the meniscus and extend outward, and are often associated with the formation of fluid-filled cysts.[4] These types of tears are thought to be a result of shear forces within the joint and are more common in older patients.[4]

Epidemiology of meniscus tears

Meniscal tears compromise the overall structural integrity of the joint as well as present symptoms such as locking and catching of the knee, a sensation of giving way, and joint pain.[4, 181] According to one study surveying 1000 patients, meniscus tears occurred more often in the right knee (56.5%).[182] Of medial meniscus lesions, most (75%) were vertical longitudinal tears and 23% were horizontal tears.[182] In the lateral meniscus the tears are more diverse, with 54% being vertical longitudinal tears and the rest divided amongst oblique and complex pathologies.[182] Overall, meniscal tears affect men more often than women, with 70–80% of meniscus tears occurring in men.[4] Afflicted men are most often 21–30 years of age, whereas this pathology affects women most often between the ages of 11 and 20.[4] Traumatic injuries also dominate in younger patients, while older patients are more prone to degenerative changes.

Meniscal health is heavily reliant on the ligamentous attachments of the knee. Joint laxity (instability of the joint) as a result of a ruptured ACL can have a profound effect on the meniscus as it has been estimated that the ACL contributes 85% to the restraint of anterior displacement of the femur.[183, 184] Clinically, meniscal injuries are common in patients with torn ACLs, highlighting the co-dependence of the meniscus with surrounding ligaments for normal joint function.[4, 185, 186] Non-linear finite element modeling of knee joints confirms this clinical finding, showing that without the ACL, the medial meniscus is subjected to higher loads from 0° to 30° flexion.[187] Interestingly, though the biomechanics of the knee are altered by tearing an ACL, the types of tears that the meniscus endure are indistinguishable from those of an ACL-intact knee.[188] This evidence suggests that meniscus tears are more frequent when knee stability is compromised, and that meniscal tears follow certain patterns regardless of ligament health.

Concepts

Meniscal abnormalities such as the discoid meniscus may be benign or symptomatic, but are rare, estimated to afflict only as much as 5% of the population. Systemic diseases can change the pigment and consistency of knee meniscus tissue, but cannot be treated locally. Osteoarthritis is an important contributor to the overall health of the meniscus and has been implicated as a cause of meniscal tears and degeneration. The most common injury specific to the knee meniscus is a meniscus tear. Tears can be classified

into four different categories based on their geometry: vertical longitudinal, oblique, radial, and horizontal. The most common in both the medial and lateral menisci is the vertical longitudinal tear. Overall, men are affected by meniscus tears 70–80% more often than women, and are usually in their 20's when this occurs.[4] Meniscus tears can come about through degenerative changes or trauma, degeneration being a catalyst in older ages. ACL tears significantly compromise knee stability and increase the likelihood of a meniscal tear.

Section 6.2: The meniscus healing problem

Introduction

As the meniscus was originally thought to be a vestigial tissue and because surgery on it was difficult, early treatments (prior to the mid-1960s) for meniscal damage were limited to total removal of the tissue, called meniscectomy.[189, 190] As early as 1948 it was shown that meniscectomy causes joint space narrowing, and many studies have subsequently shown that degenerative changes also occur following this procedure.[191-194] After more became known about the importance of the meniscus in load distribution and stability within the knee joint, treatments shifted to partial meniscectomy, surgical repair, or transplantation, which are still used today.[3, 189, 195, 196]

Healing in the meniscus

Given that the meniscus is not a homogeneous tissue, it is particularly difficult for it to self-repair. While lesions or tears that occur in the outer periphery of the tissue can regenerate due to the high degree of vasculature there, damage to the inner non-vascularized portion of the tissue is unable to heal on its own.[3, 4, 12, 195, 197-199] Following injury in the vascular portion of the meniscus, the defect site is filled with a fibrin clot which uses proinflammatory factors to recruit blood vessels from the surrounding areas.[199] After this initial response and depending on proximity to abundant blood vessels, fibrous scar tissue can take as little as 10 weeks to form.[199, 200] After a few months, the scar tissue will then mature into tissue with inferior mechanical properties to the native meniscus.[199] This timeline is extended with distance from the peripheral blood supply, and does not occur for injuries in the inner meniscus. For inner meniscus injuries, some reorganization of the matrix may occur due to the changed mechanical environment, but a healing response is absent.[201, 202] Some research has focused on creating vascular access channels from the outer to the inner meniscus to allow healing factors from the blood to reach the damaged white zone, which has helped heal longitudinal tears in the avascular region of dogs and goats, and has reduced symptoms in patients.[203-206] As a result, proximity to blood vessels is the best predictor of a meniscal healing response, but the type of healing that takes place does not restore tissue functionality.

Characteristics of repair tissue

Though the outer portion of the meniscus may heal to some degree, the new tissue is quite different from native tissue. Repair tissue in the outer portion of the meniscus is distinct from normal meniscal tissue in that it may contain calcified regions, cysts, unattached collagen fragments, and pools of proteoglycans.[28] This is in stark contrast to normal tissue in which the collagen matrix is highly aligned with proteoglycans throughout and no calcification or void spaces. In torn menisci it is twice as common for the tissue to become calcified over time, and this is often found in conjunction with osteoarthritis.[207] Apoptosis is also increased 2-fold in tissue having undergone traumatic injury or degeneration as compared to normal tissue.[208]

Functionally, meniscal repair tissue is weaker than normal tissue. Meniscal repair tissue in rabbits has been measured to require around 75% less energy (0.8–0.9 mJ) to fail than normal tissue at 12 weeks post-injury.[209] The strength of this tissue increases only marginally with the use of sutures or fibrin glue to hold the torn edges together, and does not reach normal values.[209] Therefore, even in the region of the meniscus that undergoes some repair, the tissue is either lacking in quantity or insufficient in strength and there is an inhibitory environment for new tissue formation. This evidence points to the need for tissue engineering to develop technologies to heal meniscal injuries and prevent calcification or apoptosis from taking place.

Concepts

Meniscus tissue was originally thought to be vestigial, but upon further investigation it has proved to be an important part of normal knee function and maintenance of healthy tissue. Since this realization, preservation of meniscal tissue is a main priority for reparative therapies. The meniscus is able to heal on its own to a certain degree, but this only occurs when the defect site is in the outer periphery of the meniscus, near vasculature. Even after self-repair has taken place, the scar tissue formed requires 75% less energy to fail than native tissue and may contain calcification, pockets of proteoglycans, and unorganized collagen fibrils. This type of matrix therefore compromises the mechanical integrity of the meniscus as a whole, highlighting the need for tissue engineering to provide an alternative viable solution.

Section 6.3: Tissue engineering and historical perspectives

Definition of tissue engineering

Tissue engineering strives to recreate the complex tissues of the body by harnessing biological processes. Using the classic tissue engineering paradigm (Figure 3), cells are seeded onto a scaffold and are subjected to biochemical and/or mechanical stimuli to create a tissue engineered construct ready for implantation. Recently, a new paradigm has emerged which is based on the ability of cells to self-assemble without the use of a scaffold, showing promising results in the field of cartilage regeneration.[115, 210] Tissue from either paradigm may be used to repair damaged areas in the body permanently, thereby

eradicating the need for synthetic implantable prostheses that have a limited lifetime of service. This field is especially relevant to the meniscus, which has a limited reparative potential, and its complex biomechanical properties render synthetic replacement materials insufficient.

Historical perspectives

The first use of the term "tissue engineering" was by Y. C. Fung in 1985 in a proposal to the National Science Foundation for the creation of a tissue engineering facility.[211] He presented the idea of tissue engineering as a field to bridge the gap between biology, which studies the single cell, and medicine, which is primarily concerned with the functioning of entire organs.[211] Though his proposal was not accepted, the concept of tissue engineering surfaced again at many different symposia and meetings throughout the late 1980s, prompting much discussion and debate over the exact definition of the term.[211] Beginning in the early 1990s, a steady increase in journal articles can be found containing the term "tissue engineering" indicating its acceptance and popularity throughout the scientific community.[211] Also during this time many different centers for tissue engineering around the world were established, which continue to conduct advanced research in the field.[212] Tissue engineering, though a relatively new concept, has quickly blossomed into a field with wide application and promise to fulfill Y. C. Fung's vision of bridging the gap between science and clinical implementation.

Functional tissue engineering and the meniscus

As the field has progressed, so have the standards for success. Functional tissue engineering refers to the emerging effort to not only recreate the biochemical traits of a tissue, but also match native mechanical properties of load bearing tissues.[213-217] To do this, researchers rely heavily on tissue characterization research, and use this information to hone in on the most important biochemical and mechanical properties of the tissues they are working to reproduce. For biomechanically active tissues, such as the knee meniscus, it is vital that these characteristics be recapitulated in the engineered version in order that it perform as native tissue and thus be a useful replacement in the body.

Specifically of importance are the tensile and compressive properties of the knee meniscus as well as its geometry, biochemical content, and matrix molecule organization. Attempts at functional tissue engineering of the knee meniscus are ongoing, but key progress has been made in producing similar matrix proteins and geometry to the native tissue.[115, 116, 131] Unfortunately, many tissue engineering studies do not evaluate the mechanical properties of the constructs produced, making functional assessment and comparison to native tissue more difficult. Ideally all functional aspects of a tissue engineered construct should be tested, in order to better understand the potential of each engineering method. A more detailed discussion of the studies in meniscal tissue engineering ensues in chapter 9.

Concepts

Tissue engineering is a multidisciplinary field which aims to recreate biological tissues using a combination of cells, scaffolds, and biochemical and mechanical stimuli. These tissues may then be used to replace or restore function to missing or damaged elements in the body. A relatively new field, tissue engineering efforts increased in the 1990s with the establishment of research centers around the world. Functional tissue engineering is especially important for the meniscus as it emphasizes mimicking not only tissue biochemistry, but also mechanical and geometric properties. Functional assessment of tissue engineered meniscal constructs is the next step in developing useful meniscal replacement tissue.

Figures

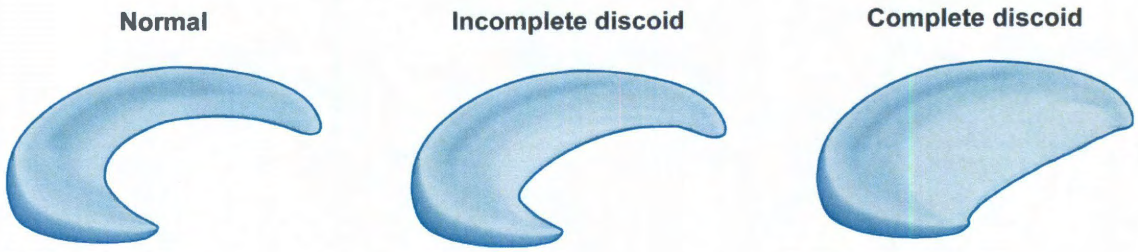

Figure 1: Discoid meniscus morphology. The normal meniscus is semi-lunar in shape, but abnormal development may result in a discoid meniscus. When the inner portion of the tissue covers more area than normal, it is deemed an incomplete discoid meniscus. A complete discoid morphology occurs when the inner portion covers nearly the entire articulating surface.

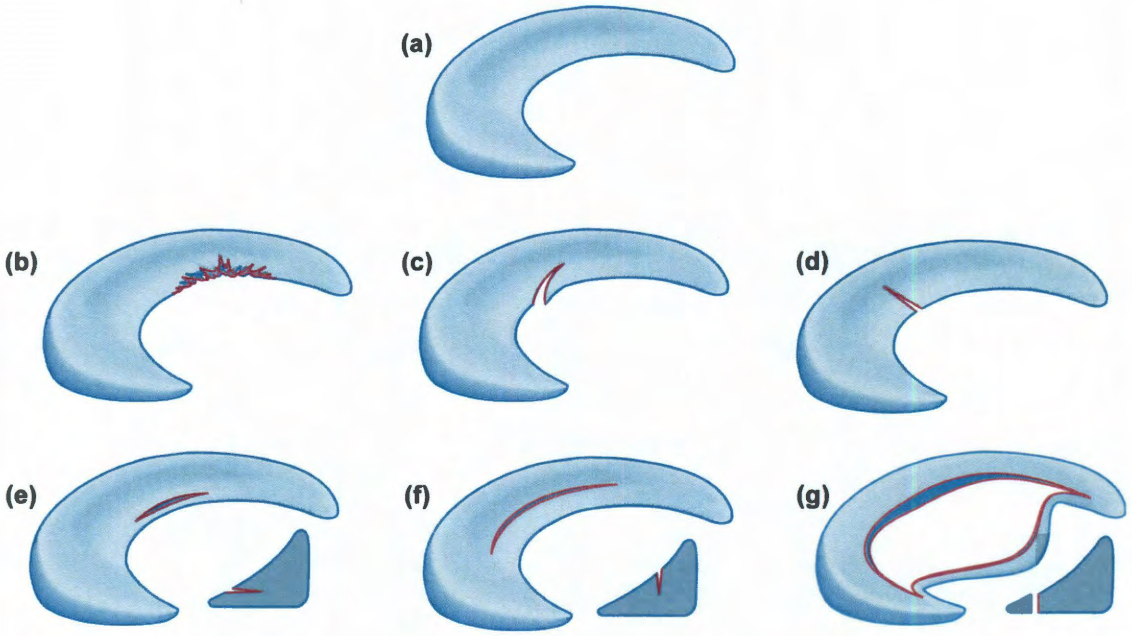

Figure 2: Types of meniscus tears. The normal meniscus (a) is smooth, wedge-shaped, and semi-circular. Complex (degenerative) tears (b) result in a jagged edge and combine many different types of tears. Oblique tears (c) and radial tears (d) typically propagate from the inner portion of the meniscus to its periphery. Horizontal tears (e) split the tissue into superior and inferior parts and also typically propagate outward. Vertical longitudinal tears (f and g), split the meniscus along the direction of collagen orientation. When a vertical longitudinal tear passes through the tissue's thickness it is called a bucket-handle tear (g).

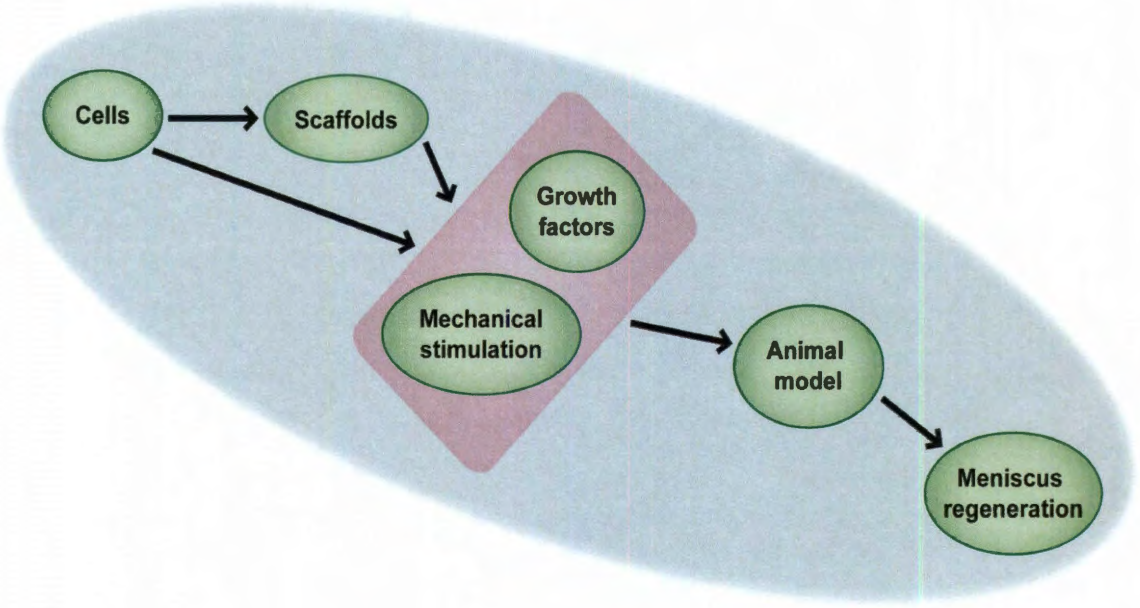

Figure 3: Tissue engineering paradigm. In the classical tissue engineering paradigm, cells combine with a scaffold and are subjected to a regimen of growth factors and/or mechanical stimulation. The resulting construct is then implanted into an animal model with the expectation that meniscus regeneration will ensue. A scaffoldless paradigm has recently emerged in which cells are seeded at a high density and are conditioned biochemically and/or biomechanically.

Chapter 7: Immunogenicity of Bovine and Leporine Articular Chondrocytes and Meniscus Cells

Abstract

Acute immune rejection is a major concern for any allogeneic or xenogeneic graft. For *in vivo* investigations of cartilage tissue engineering strategies, small animal models, such as the leporine model, are commonly employed. Interestingly, many studies report little to no immune rejection upon allogeneic or xenogeneic implantation of native articular and meniscal cartilages. This study investigated whether bovine and leporine articular chondrocytes (ACs) and meniscus cells (MCs) display immunoprivileged characteristics in terms of their ability to stimulate proliferation of leporine peripheral blood mononuclear cells (PBMCs) *in vitro*. After six days of co-culture, none of the cell types caused a significant proliferative response in the leporine PBMCs, indicating that these cells may not elicit an acute immune rejection *in vivo*. RT-PCR analysis for MHC I, II, and co-stimulation factors CD80 and CD86 revealed that all cell types produced mRNA for MHC I and II, but only some were CD80 or CD86 positive, and none were positive for both co-stimulation factors. Flow cytometry for major histocompatibility complex II (MHC II) was also performed. Bovine MCs and ACs displayed MHC II positive populations (MCs: 32.51%, ACs: 14.44%) while only

---

Chapter submitted as: *Huey, D.J., *Sanchez-Adams, J., Willard, V.P., and Athanasiou, K.A. "Immunogenicity of Bovine and Leporine Articular Chondrocytes and Meniscus Cells." *Tissue Engineering, Part A.* (*Authors contributed equally)

leporine ACs were MHC II positive (7.53%). Despite some presence of MHC II and co-stimulation factors, all of the cell types studied were unable to stimulate T cell proliferation. These findings indicate that bovine and leporine MCs and ACs share a similar immunoprivileged profile, bolstering their use as allogeneic and xenogeneic cell sources for engineered cartilage.

Introduction

Due to their lack of vasculature and relative acellularity, articular cartilage lining the ends of long bones and the hyaline-like cartilage of the inner meniscus have little capacity to self-repair following injury. Though tissue engineering strategies are being developed to address this problem, they often require the use of large numbers of primary cells. Donor site morbidity and the lack of available tissue render autologous techniques for cartilage tissue engineering prohibitive, so increasing focus has been on the development of allogeneic and xenogeneic approaches. A major concern with any allogeneic or xenogeneic implant is immune rejection, resulting in a breakdown of the implanted material over time.

Typically, an immune response to implanted tissue is triggered by T cell sensitization, followed by activation. Sensitization occurs when antigens presented on donor cells, specifically major histocompatibility complex classes I and II (MHC I & MHC II), are recognized by T-cell receptors (TCRs) CD8 and CD4, respectively. T cells become activated when co-stimulatory binding of donor cell B7 antigens (CD80 or CD86) with T cell receptor CD28 happens

simultaneously, causing proliferation of the T cell and initiation of an immune response to destroy the foreign material.[218-220] Therefore, the MHCs and B7 antigens present on donor cells are important constituents involved in immune rejection of an implanted tissue engineered construct.

Mounting evidence suggests, however, that cartilaginous tissues are immunoprivileged, thus causing little to no immune response when implanted. While the precise reasons for the immunoprivileged nature of cartilage tissue are not well understood, both cartilage cells and extracellular matrix (ECM) seem to play a role in inhibiting an immune reaction. Flow cytometry analysis of human and sheep articular chondrocytes has shown that these cells present MHC I antigens but not MHC II, CD80, or CD86. In addition to lacking some key immunogenic surface markers, these cells are unable to promote allogeneic T cell proliferation *in vitro.*[221-223] Moreover, studies testing allogeneic (human and leporine) and xenogeneic (porcine to leporine and leporine to caprine) implantation of articular chondrocytes agree with these *in vitro* experiments, reporting that they produce little to no immune response.[224-228] A comparison of literature results suggests that the degree of immune reaction to implanted cartilage material is inversely related to the amount of ECM it contains. This indicates that along with lacking critical surface markers involved with the induction of an immune response, cartilage ECM may shield immunogenic markers on chondrocytes from host T cells, enhancing the reparative capacity of these therapies.[228]

Though little investigation has been made into the immunogenicity of meniscus cells, some evidence suggests that they may share a similar immunoprivileged profile to chondrocytes. When used to fill an articular cartilage defect in the leporine model, both allogeneic and xenogeneic (bovine) meniscus tissue failed to elicit a measureable immune response.[227] Given these promising results, it is possible that the meniscus may provide an abundant cell source for allogeneic and xenogeneic tissue engineering strategies that avoids the concern for immune rejection.

There are a variety of cartilage engineering strategies that could benefit from using an abundant allogeneic or xenogeneic cell source. One promising strategy used in cartilage and meniscus tissue engineering is the self-assembly method, where articular chondrocytes are seeded alone or in co-cultures with meniscus cells to produce functional articular cartilage and fibrocartilage replacements.[76, 130, 131, 210, 229] Though these self-assembled constructs show great promise biochemically and biomechanically, the potential immunogenicity of these highly cellular constructs in an allogeneic or xenogeneic animal model is unknown. Therefore, this study investigates the immunogenicity of bovine and leporine articular chondrocytes and meniscus cells in a rabbit model. Immunogenicity is determined by the ability of cartilaginous cells to induce proliferation of leporine peripheral blood mononuclear cells (PBMCs) in a mixed lymphocyte reaction (MLR) test. In addition, the presence of MHC II is assessed using flow cytometry, and RT-PCR is performed to detect MHC I, MHC II, CD80, and CD86 mRNA. It is hypothesized that both of these cell types have an

immunoprivileged profile, lacking the ability to induce PBMC proliferation and not expressing key factors for immune response initiation, MHC II, CD80 and CD86.

Methods

Isolation of cartilaginous cells

Both bovine and leporine cells were obtained as previously described.[130, 230] Briefly, cartilage and meniscus tissue was sterilely dissected from the knee joint and minced into small pieces. After an 18 hr digestion in 0.2% collagenase (Worthington), cells were isolated with sequential centrifugation and rinses with PBS. Cells were then cryopreserved in media containing 20% fetal bovine serum (Gemini Bio-Products) and 10% dimethyl sulfoxide (Sigma) until needed.

Previously, primary bovine ACs and MCs have been used to form self-assembled constructs, so no further steps were needed to prepare these cells. However, when leporine cells are used to generate self-assembled constructs, they are expanded in monolayer culture. The leporine cells used for subsequent MLR assessment were expanded to test the immunogenicity of the population of leporine cells previously employed for self-assembly. This expansion protocol has been described in detail elsewhere.[230] Briefly, leporine ACs and MCs were separately expanded in a cell culture media consisting of DMEM with 4.5 g/L-glucose and GlutaMAX (Invitrogen), 100 nM dexamethasone, 1% fungizone, 1% penicillin/streptomycin (BD Biosciences), 1% ITS+ premix (BD), 50 mg/mL ascorbate-2-phosphate, 40 mg/mL L-proline, 100 mg/mL sodium pyruvate (Fisher Scientific), and 5 ng/mL basic fibroblastic growth factor. Cells were

seeded at a density of 2.5 x 10^4 cells/cm^2 and allowed to grow until 4 days passed from when confluence was reached. Expansion proceeded until passage 3 was reached.

Mixed Lymphocyte Reaction

The mixed lymphocyte reaction test was based on a protocol described previously.[231] Bovine and leporine ACs and MCs were treated with 25 μg/mL mitomycin-C (Sigma) for 45 minutes and then mitomycin was removed by 3 media rinses with centrifugation between each. Leporine PBMCs (Rockland Immunochemicals) were mixed with the each of the 4 cartilaginous cell types to obtain 2 cell solutions each, that per 100 μL contained: 1) 10^3 cartilaginous cells + 10^5 PBMCs and 2) 10^4 cartilaginous cells + 10^5 PBMCs. Into a well on a 96-well plate, 100 μL of the cell solutions were dispensed. In addition, control groups (cartilaginous cells at either 10^3 or 10^4 cells per well) corresponding to each of the MLR groups were seeded. As a positive control, concanavalin A (Sigma) was added to 10^5 PBMCs at a concentration of 12.5 μg/mL and this mixture was seeded into wells of a 96-well plate. Negative controls consisted of 10^5 PBMCs seeded with or without mitomycin pre-treatment. In all this generated 8 groups of MLR assays, 8 control groups without PBMCs corresponding to the MLR groups, a positive PBMC control (with concanavalin), 2 negative PBMC controls (cells only and cells with mitomycin pretreatment). For each of the 19 groups, 5 replicates were employed.

Following a 6 day culture, plates were centrifuged to pellet all non-adherent cells and trypsin-EDTA (Invitrogen) was applied for 15 minutes to ensure all adherent cells entered into solution. After removal of trypsin via centrifugation and rinsing, plates containing the cell solution were subjected to 3 freeze-thaw cycles to ensure cell lysis. Aliquots from each well were tested in triplicate for DNA content using the PicoGreen® dsDNA reagent (Invitrogen) and dsDNA controls. The amount of DNA was converted to cell number using a conversion factor of 7.8 pg DNA/cell.

RT-PCR

RNA was extracted from bovine ACs and MCs, leporine passage 3 ACs and MCs, and bovine and leporine PBMCs (positive controls) using an RNaqueous Micro Kit (Ambion, Carlsbad, CA). The extracted RNA was then reverse transcribed to cDNA using Superscript III First Strand Synthesis System (Invitrogen, Carlsbad, CA). PCR was run on the resulting cDNA to determine if the following transcripts were present: MHC I, MHC II, CD80, and CD86. Additionally, amplification of GAPDH for bovine cells and β-actin for leporine cells served as positive controls. All PCR was performed on a RotorGene 6000 [Corbette Life Sciences, Valencia, CA], using Platinum PCR Supermix [11306-016, Invitrogen] and run using the following thermal cycling protocol: 94°C 2 min, 40x(94°C 15 sec, [annealing temperature] 30 sec, 72°C 60 sec). Reactions were visualized by gel electrophoresis with gel green dye (Biotium, Hayward, CA). The

specific primers, target lengths, and annealing temperatures were determined from the literature[166, 232-235] and are outlined in Table 1.

Flow Cytometry

Bovine ACs and MCs, leporine passage 3 ACs and MCs, and bovine and leporine PBMCs (positive controls) were analyzed using flow cytometry to determine the presence of immunogenic antigen MHC II. Cells were first blocked with 5% goat serum in PBS for 30 minutes, then incubated with mouse an anti-MHC II primary antibody (VMRD) or mouse anti-IgG2a isotype control (Invitrogen) for 30 minutes and were washed with 1% BSA (Sigma) and 0.1% sodium azide (Sigma) in PBS. The cells were then stained with GtxMs IgG phycoerythrin-conjugated secondary antibody (Abcam) for 20 minutes, washed, and resuspended in 1% paraformaldehyde in PBS (Sigma). Following incubation at 4°C for 24 hours, cells were analyzed for presence of MHC II using a FACScan flow cytometer (BD Biosciences). Up to 10^5 cells were recorded for each group and forward scatter (FSC), side scatter (SSC), and fluorescence channel 2 (FL2) were recorded using CellQuest software. Cyflogic software was used to analyze the generated flow cytometry files. The cell populations of interest were identified by gating FSC versus SSC plots, fluorescence histograms of the isotype control and MHC II stained cells were created using the cell population of interest. Positive staining for each marker was represented as the percentage of the curve exceeding the fluorescence value at 95% of the isotype control curve.

Statistics

Following subtraction of control group cellularity from their corresponding MLR assay group, the number of PBMCs in each group was compared to the number of cells in the PBMC only group with a t-test. Significant differences were defined as $p<0.05$.

Results

Mixed Lymphocyte Reaction

The results of the cell number analysis of the MLR assay are shown in Figure 1. Total cell numbers from the control groups containing only mitomycin-treated cartilaginous cells were subtracted from their corresponding group in which mitomycin-treated cartilaginous cells were co-cultured with PBMCs. No statistically significant differences ($p < 0.05$) were observed between the co-culture groups and the PBMC-only control. A significant increase in cell number was noted when the concanavalin-treated PBMCs were compared to the PBMC-only controls. A small amount of base-line proliferation was observed when comparing mitomycin-treated PBMCs to PBMC-only controls.

RT-PCR

RT-PCR analysis of bovine PBMCs, ACs, and MCs revealed positive expression of GAPDH, MHC I, and MHC II. Bovine PBMCs also expressed CD80 and CD86, while bovine ACs did not express either costimulatory molecule, and

bovine MCs expressed only CD86 (Figure 2). Analysis of leporine PBMCs, ACs, and MCs was similar to that of the bovine cells in that all cell types showed positive expression of β-actin, MHC I, and MHC II, and leporine PBMCs also expressed CD80 and CD86. Leporine ACs and MCs both showed positive expression of CD80, but not CD86.

Flow cytometry

Flow cytometric analysis of MHC II on bovine and leporine MCs and ACs revealed that this marker is present on all cells studied except for leporine MCs. As seen in Figure 3, both types of bovine cells stained positively for MHC II. Bovine articular chondrocytes were 14.44% MHC II positive. Bovine MCs, when stained for MHC II, displayed a bimodal distribution of fluorescence. These cells displayed slightly higher expression for MHC II (32.51%), than bovine ACs. For leporine cells (Figure 3), ACs showed some positive staining for MHC II (7.53%), while leporine MCs showed no positive staining for MHC II. All leporine fluorescence histograms were normally distributed, and no bimodal phenomena were observed.

Discussion

Assessment of the potential for immune response is a critical step in selecting a cell source for tissue engineering. While allogeneic sources have been commonly applied for *in vivo* studies of cartilaginous tissue replacement, the use of xenogeneic sources is less common.[224-228, 236] However, the available

data indicate that xenogeneic cell sources may be applied in cartilage and meniscal tissue engineering because of the immunoprivileged nature of these cells.[224-228, 236] The benefits of applying a xenogeneic cell source for cartilage engineering are significant. Concerns of donor-site morbidity and difficulties associated with obtaining a sufficient number of cells required for tissue engineering efforts such as high-density scaffold-free cartilage formation can be mediated using a xenogeneic approach. Toward this end, this study sought to test *in vitro* whether allogeneic (leporine) or xenogeneic (bovine) meniscus cells and articular chondrocytes show non-immunogenic characteristics when introduced to leporine lymphocytes. The major hypothesis of this study that neither leporine nor bovine ACs or MCs would induce an *in vitro* immune response by leporine PBMCs was proven. This suggests that the functionality of bovine cell-based constructs can be assessed in a leporine *in vivo* model, without the concern for immune rejection.

In agreement with previous results assessing the immune reaction following allogeneic or xenogeneic implantation of articular or meniscal cartilage, none of the cartilaginous cells in this study induced proliferation of PBMCs.[227, 228] Previous studies on the immunogenicity of cartilaginous cells have linked this lack of immunogenicity to the absence of cell surface markers required for promoting an immune response, including MHC II and co-stimulation factors of the B7 family.[221-223] The present study, however, confirmed the presence of MHC II and co-stimulation factors CD80 and CD86 in bovine and leporine ACs and MCs using PCR and flow cytometry. All of the cell types studied showed the

presence of mRNA for at least some of the immunogenic markers studied. MHC II mRNA was found in all cell types, while CD80 mRNA was present in leporine cells, and CD86 mRNA was only found in bovine MCs. Further, translation of the MHC II mRNA was confirmed by flow cytometric analysis, which showed that bovine MCs and ACs, and leporine ACs do express this marker to some degree.

As MHC class II molecules are traditionally associated with professional antigen presenting cells (APC) such as macrophages, dendritic cells, and B cells, the presence of MHC II in the cartilaginous cells examined in this study may appear counterintuitive. While cartilage-derived cells are not typically thought of as APCs, researchers have discovered that chondrocytes possess the potential to obtain properties of APCs.[223, 237, 238] In particular, chondrocytes isolated from arthritic joints have been shown to possess higher amounts of MHC class II molecules and are more immune-reactive when used in an MLR assay than chondrocytes from healthy joints.[237-240] While the cells employed in this study were not isolated from arthritic joints, it is possible that the insult due to enzymatic digestion of the cartilage matrix induced the cells to transition to a phenotype more amenable to antigen presentation. In support of this claim, other researchers have discovered that MHC II is present in isolated chondrocytes while absent in intact, healthy cartilage.[223, 240-242] Overall, the results of this study are in accord with previous studies demonstrating the presence of MHC II on chondrocytes isolated from healthy cartilage.

In contrast to articular chondrocytes, few accounts exist regarding the presence of MHC class II molecules on cells isolated from the meniscus. Prior to

this investigation the presence of MHC class II had not been analyzed for isolated meniscus cells. However, researchers have stained native human and ovine meniscus tissue for MHC class II and found that meniscus cells do not express MHC class II but synovial and endothelial cells within the meniscus do.[243-245] In context with native tissue investigations, the results from the present study suggest that meniscus tissue may be similar to articular cartilage where MHC class II is not present on cells *in situ*, but upon isolation MHC II expression is enhanced.

Along with expressing MHC I and II, some of these cells also showed mRNA expression of B7 family co-stimulation factors, though none of the cell types showed expression of both CD80 and CD86. The presence of B7 mRNA indicates that some of the cell types studied have the molecular machinery to stimulate T-cells, but, when exposed to T-cells, fail to initiate a proliferative response. This suggests that either 1) these cells are unable to induce an immune response due to a lack of B7 family cofactors required to activate T-cells or 2) a factor produced by the cartilage cells is actively quenching immune response. Co-stimulatory molecules CD80 and CD86 are known to be necessary for the effective priming and activation of T-cells, and seem to act on the T-cells through distinct mechanisms.[246-252] Regarding cartilaginous cells, Adkisson et al.[221] showed absence of co-stimulatory molecules on juvenile human articular chondrocytes, which is in agreement with the present results for bovine ACs. The absence of co-stimulatory molecule transcripts in bovine ACs may explain their inability to stimulate xenogeneic T-cells. Bovine MCs and leporine ACs and MCs,

however, showed gene expression for either CD80 or CD86, yet still failed to elicit T-cell activation. One possible explanation for this phenomenon is that though mRNA for these proteins is present, there may be some regulatory mechanism inside the cell inhibiting translation of these mRNAs into functional co-stimulatory proteins.

It is also possible that these cells are actively producing factors that suppress an immune response. There are a number of molecules known to inhibit T-cell activation such as negative co-stimulators in the B7 family, and Chondromodulin-I, an immunosuppressive factor, that juvenile and adult articular chondrocytes have been shown to produce.[236, 253] Another factor produced by chondrocytes is transforming growth factor β (TGF- β), which has been shown to be a potent inhibitor of T-cell activation in studies using chondrocytes and mesenchymal stem cells.[223, 254-256] Thus, it is possible that the lack of PBMC proliferation in co-culture with leporine and bovine ACs and MCs can be explained by an absence of B7 cofactors due to lack of transcription or translation in the cell, or by the production of an immune response inhibitor by the cells.

Given that some of these cell types express co-stimulation factors, future studies are needed to investigate the soluble factors produced by cartilaginous cells that could inhibit an immune response. However, since the present results indicate that neither bovine nor leporine MCs or ACs stimulate leporine PBMC proliferation, it is likely that engineered cartilage constructs using these cells may be implanted into a leporine model without concern for immune rejection.

Conclusions

Overall, this study shows that it is unlikely that the use of tissue engineered cartilaginous constructs formed from either leporine or bovine ACs or MCs will elicit an immune response when implanted into the leporine knee. This opens the door for a plethora of cell types to be evaluated for *in vivo* assessments in animal models. Further, it suggests that xenogeneic transplantation into humans could be a possibility if the presence of alpha-galactosyl of tissues generated from animal cells can be eliminated.

Tables

Table 1: Bovine and Leporine RT-PCR Primers

Species	Gene	5'-3' Forward Primer	5'-3' Reverse Primer	Target Length (bp)	Accession Number
Bovine	GAPDH	ACCCTCAAGATTGTCAGCAA	ACGATGCCAAAGTGGTCA	86	U85042
	MHC I	GGCTCCCACTCCCTGAGGTATTTC	TCTCCAGGTATCTGCGGAGCC	534	X82672 & X82673
	MHC II	GGAAGAAGGAGACGGTGT	CAGGAAGACCGTCTGTGA	305	X78308
	CD80	TGTGGCCTGAATACAAGAACC	CAGGTGCTGATTAGCAGAAGG	488	Y09950
	CD86	GACCTTGAGACTCCACAACG	GTAGAGCTGCAATCCAGAGG	534	AJ291475
Leporine	β-actin	CGTGCGGGACATCAAGGA	AGGAAGGAGGGCTGGAACA	177	AF309819.1
	MHC I	CGACTACATCGCCCTGAACG	CCCAGAAGGCACCACCACA	394	K02441.1
	MHC II	GGAGCACTGGGGCCTGGAGA	GCACCACCTGAGCGCAGTCC	421	M15557.1
	CD80	TGCGCATATACTGGCAGAAG	TTCTCCATCTTCCATCCAGG	356	NM_001082663.1
	CD86	TGACCAGGAAAGTTGGAACC	ACACACAACGATCAGGGTGA	517	NM_001082208.1

Figures

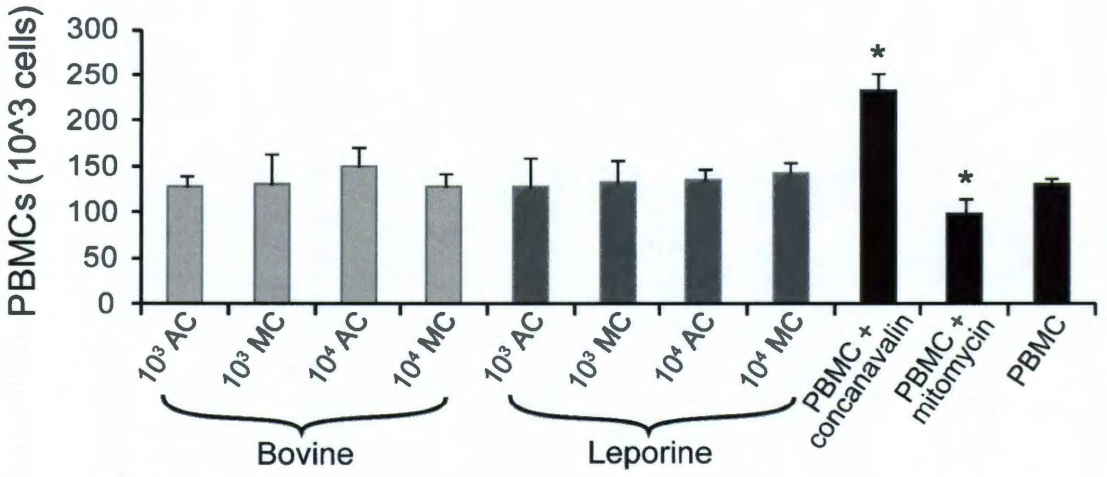

Figure 1. Results of mixed lymphocyte reaction assay. Following subtraction of the control cartilaginous cell-only group, the average number of PBMCs present in each group is compared to the PBMC-only group. Significant differences are defined as $p<0.05$ and denoted with an asterisk (*).

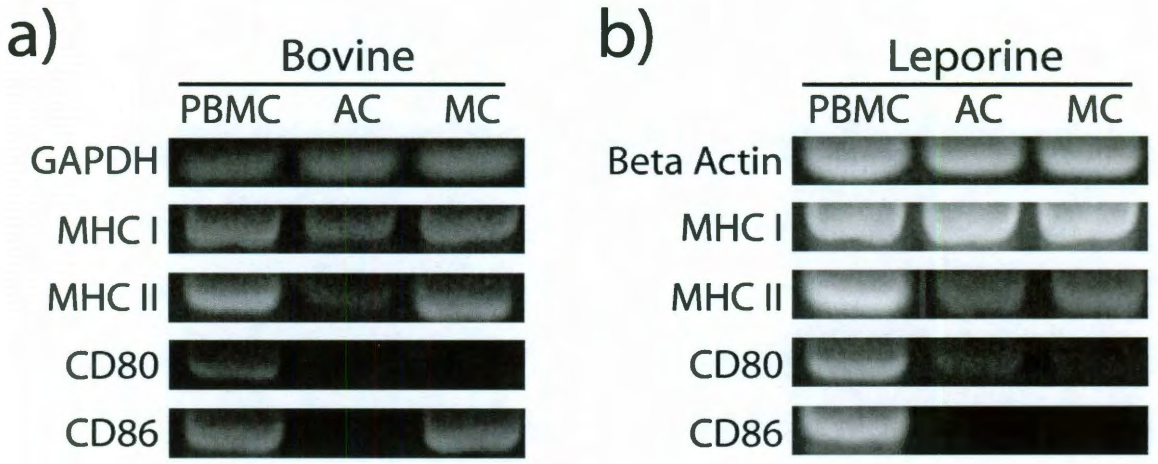

Figure 2. RT-PCR analysis of bovine and leporine PBMCs, ACs, and MCs. RT-PCR of bovine **(a)** and leporine **(b)** PBMCs (positive control), MCs, and ACs. All bovine and leporine cell types express MHC I and MHC II mRNA, while CD80 is only expressed in bovine PBMCs and leporine PBMCs, ACs, and MCs. CD86 is expressed in both bovine and leporine PBMCs, but only in one other cell type, bovine MCs.

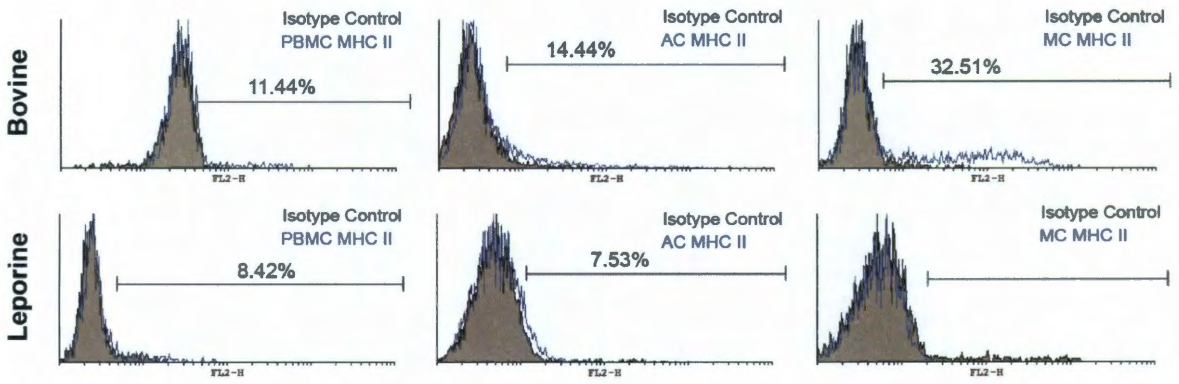

Figure 3. Flow cytometry for MHC II. Histograms of relative cell count versus fluorescence for isotype control and anti-MHC II staining for leporine and bovine ACs, and MCs. Percentages indicate the number of cells with fluorescence values greater than 95% of the isotype control.

Chapter 8: Regional variation in the mechanical role of knee meniscus glycosaminoglycans

Abstract

High compressive properties of cartilaginous tissues are commonly attributed to the sulfated glycosaminoglycan (GAG) fraction of the extracellular matrix (ECM), but this relationship has not been directly measured in the knee meniscus, which shows regional variation in GAG content. In this study, biopsies from each meniscus region (outer, middle, and inner) were either subjected to chondroitinase ABC (CABC) to remove all sulfated GAGs or not. Compressive testing revealed that GAG-depletion in the inner and middle meniscus regions caused a significant decrease in modulus of relaxation (58% and 41% decreases, respectively, at 20% strain), and all regions exhibited a significant decrease in viscosity (outer: 29%, middle: 58%, inner: 62% decrease). Tensile properties following CABC treatment were unaffected for outer and middle meniscus specimens, but the inner meniscus displayed significant increases in Young's modulus (41% increase) and ultimate tensile stress (40% increase) following GAG depletion. These findings suggest that in the outer meniscus GAGs contribute to increasing tissue viscosity, while in the middle and inner meniscus, where GAGs are most abundant, these molecules also enhance the tissue's ability to withstand compressive loads. GAGs in the inner meniscus also

---

Chapter under review as: Sanchez-Adams, J., Willard, V.P., and Athanasiou, K.A. "Regional variation in the mechanical role of knee meniscus glycosaminoglycans." *Journal of Applied Physiology.*

contribute to reducing the circumferential tensile properties of the tissue, perhaps due to the pre-stress on the collagen network from increased hydration of the ECM. Understanding the mechanical role of GAGs in each region of the knee meniscus is important for understanding meniscus structure-function relationships and creating design criteria for functional meniscus tissue engineering efforts.

Introduction

Functioning under shear, compression, and tension, the knee meniscus relies on the complex organization of its biochemical constituents to distribute load and absorb shock in the joint. The meniscus bears between 45% and 75% of knee joint loads which are estimated to be 2.7-4.9 times body weight while walking.[21, 22] Unfortunately, the knee meniscus is prone to tears and degeneration which are unable to heal effectively in the outer and middle portions of the tissue. These injuries are especially devastating in the inner, non-vascularized portion, where a healing response is absent.[3, 4, 12, 195, 197-199] Tissue engineering efforts seek to address this problem by creating functional meniscus tissue for replacement. A complete understanding of the structure-function relationships that exist in the knee meniscus can help advance these tissue engineering efforts by identifying essential design criteria that can enhance the functionality of engineered tissues.

As a biphasic tissue, the knee meniscus relies on the interplay of solid and fluid components to achieve its viscoelastic characteristics.[26, 27, 34, 63, 201]

Composed of approximately 30% organic matter and 70% water, the meniscus is highly hydrated.[3] The flow of the water fraction in and out of the tissue during loading plays a role in the tissue's viscoelastic behavior and allows for the exchange of nutrients between the synovial fluid and meniscus.[32] The solid fraction, dominated by collagenous proteins and, to a lesser degree, sulfated glycosaminoglycans (GAGs), provides structure to the tissue. Collagen, the most abundant biochemical component in the meniscus, has been well-characterized in terms of its distribution, organization, and mechanical contribution to meniscus mechanics. Microscopic and mechanical analyses of meniscal collagens have revealed that these proteins are organized mainly in the circumferential direction of the tissue, with some radially oriented fibers throughout.[29-31] Tensile tests in the circumferential and radial directions indicate that tensile properties are 3- to 10-fold higher in the circumferential direction than in the radial direction.[30, 32]

The mechanical contribution of sulfated GAGs in the meniscus, however, is not as well understood. While collagen is abundant throughout the meniscus, sulfated GAG content is scarce in the outer region of the meniscus and increases in abundance moving radially inward. In tissues with high sulfated GAG content, such as articular cartilage, GAGs mainly contribute to tissue compressive properties; containing many GAG side chains, the negatively charged aggrecan molecule attracts water molecules and therefore helps to resist the flow of water out of the tissue while under compression.[62-65] In articular cartilage, however, sulfated GAGs are, on average, 8-fold more abundant than in the knee

meniscus, which may indicate a difference in the mechanical role of GAGs in these two tissues.[11, 12, 16, 257, 258]

The mechanical role of sulfated GAGs in musculoskeletal tissues has been investigated through selective digestion of sulfated GAGs and subsequent mechanical testing. A common method of depleting GAGs from native tissues is to use the catabolic enzyme chondroitinase ABC (CABC), which depolymerizes chondroitin sulfate, dermatan sulfate, and, to a lesser degree, hyaluronan.[259] CABC has been used previously to investigate the contribution of GAGs to the mechanical properties of various musculoskeletal tissues. GAG-depletion of articular cartilage has been shown to reduce the tissue's compressive modulus and increase tissue permeability.[163] In the tendon, a tissue similar to the knee meniscus in terms of GAG content, results suggest that sulfated GAGs impart higher tissue viscosity in the transverse direction (perpendicular to collagen alignment).[260] A study investigating the human medial collateral ligament, however, showed that dynamic viscoelastic properties of the tissue were largely unchanged by sulfated GAG removal.[261] These results show that GAGs in different tissues play varying roles in the tissue's mechanical properties, indicating that they may affect regional meniscus mechanics as well.

This study, therefore, investigates the regional contribution of sulfated GAGs to meniscus compressive and tensile mechanics. CABC is used to deplete GAGs from each meniscus region, and compressive and tensile material properties are compared between depleted and control specimens. It is hypothesized that GAG-depletion will have varying effects on material properties

regionally in the meniscus. The results from this study will inform further tissue engineering efforts to recapitulate the meniscus, and allow for a better understanding of regional variations in meniscus mechanics.

Materials and Methods

Medial menisci from two-week-old bovine knees [Research 87, Boston, MA] were surgically removed, and frozen in saline solution with protease inhibitors until treatment and mechanical testing were performed. In phase 1 of the study, the minimum treatment time required to remove all of the sulfated GAGs from each region was determined. Samples from each region (inner, middle, and outer meniscus) were dissected from the tissue and either treated with chondroitinase ABC (CABC) in an activation solution, or placed in the activation solution without CABC (untreated control). Treated samples were placed in a 1 U/mL CABC [Sigma-Aldrich, St. Louis, MO] solution containing 50 mM Tris, 60 mM sodium acetate, and 0.02% bovine serum albumin and incubated with gentle shaking at 37°C. Following treatment or incubation in buffer, samples were placed in an inactivation solution (1 mM Zn^{2+} with 50 mM Tris) for 15 minutes with gentle shaking at 37°C. Three samples from each region were treated for either 1, 3, 6, 12, and 24 hours. Biochemical analysis was performed on each sample to determine sulfated glycosaminoglycan (GAG) and collagen content per dry weight of tissue. Sulfated GAG content versus time data were fit with an exponential decay model and the half-life for GAG depletion for

each region was determined. A one-way ANOVA was performed on the data for each region with significance level $p < 0.05$.

The appropriate treatment time determined in phase 1 was then carried forward to phase 2, where compressive and tensile mechanical testing was performed on each GAG-depleted region and untreated control. For compressive samples, three millimeter dermal punches were used to obtain inner, middle, and outer meniscus samples, which were cut to around 1 mm thickness with razorblades. Unconfined compression stress-relaxation testing was performed in the axial direction on each tissue sample. The diameter and sample thickness was determined just prior to testing. Samples were preconditioned with 15 cycles of 0-5% compressive strain, and then stress-relaxation tests were carried out at 10% and 20% strain. As described previously, a Kelvin solid viscoelastic model was fit to the data to yield the following compressive material properties at each strain level: instantaneous modulus (E_i), modulus of relaxation (E_r), and viscosity (μ) [156]. For tensile samples, circumferential strips of the inner, middle, and outer portions of the meniscus were cut into dog bone shapes with an average thickness of 1 mm. Sample thickness and gauge length was determined just prior to mechanical testing. Tensile strain-to-failure testing was carried out in the circumferential direction of the tissue, with preconditioning of 15 cycles of 0-2% strain, followed by tensile testing at 1% strain/second. The linear portion of each stress-strain curve was used to determine the Young's modulus (E_y) of each sample, and the ultimate tensile stress (UTS) was determined from each curve. An integration of the stress-strain curve was used to determine the toughness, or

energy to failure, of each sample. GAG depletion was verified for each region histologically using Safranin-O staining as well as biochemically. Collagen content of the regional samples was also determined biochemically.

Four to six samples were used for each region and treatment group, and Student's t-tests were performed between treated and untreated groups. Statistical significance was set at $p < 0.05$.

Results

Results from phase 1 of the study are shown in Figure 1. Inner, middle, and outer meniscus samples were treated with CABC for 0, 1, 3, 6, 12, or 24 hours. In the untreated state, the inner meniscus contained the most sulfated GAG per dry weight (3.88% ± 1.5%) compared to the outer (0.91% ± 0.33%) and middle (1.2% ± 0.42%) regions. When treated with CABC, it was found that the outer and middle meniscus displayed similar GAG depletion profiles, with half-lives of 0.325 hours and 0.456 hours, respectively. In contrast, the inner meniscus GAG depletion profile displayed the longest time to full depletion, with a half-life of 0.899 hours. Collagen content for each region was unaffected by CABC treatment, and it was found that the inner meniscus had statistically less collagen then the outer and middle meniscus. The outer and middle meniscus contained 89.01% ± 4.8% and 87.07% ± 4.62% total collagen, respectively, while the inner meniscus contained 82.04% ± 3.75%. Based on these results, it was determined that the middle and outer meniscus specimens would be treated with

CABC for three hours, and the inner meniscus specimens would be treated for 24 hours to ensure full GAG depletion in Phase 2.

In Phase 2, outer, middle, and inner meniscus explants were treated with CABC for the duration determined in Phase 1 and tested under compression and tension and compared to untreated controls. Histological and biochemical assessment of untreated and treated explants verified that GAG depletion was achieved for all three regions (Figure 2). Additionally, biochemical analysis of collagen content for treated and untreated samples confirmed that no change in collagen content was observed in any of the regions (Figure 2).

Compressive testing results are shown in Figure 3. Unconfined compression stress-relaxation testing on CABC treated samples showed that GAG depletion reduced the coefficient of viscosity for all regions compared to untreated controls. For the inner and middle regions, GAG depletion also significantly reduced the tissue's modulus of relaxation and caused a trend lower in the tissue's instantaneous modulus. These statistical differences were seen both at the 10% and 20% strain levels.

Tensile material properties of control and GAG-depleted meniscus specimens are shown in Figure 4. The tensile properties of the middle and outer meniscus were not significantly affected by CABC treatment either for ultimate tensile stress or Young's modulus. However, CABC treatment did significantly increase inner meniscus Young's modulus (40.75% over untreated control) and ultimate tensile stress (40.55% over untreated control). Additionally, inner energy

to failure increased significantly with CABC treatment compared to the untreated control.

Discussion

This study investigated the effects of sulfated GAG-depletion on the material properties of the inner, middle, and outer meniscus in order to elucidate structure-function relationships in the knee meniscus. Viscoelastic compressive testing showed that GAG depletion causes decreased tissue viscosity in all regions of the meniscus, as well as decreased modulus of relaxation in the inner and middle regions. Statistically significant decreases in compressive properties for all regions were observed at both 10% and 20% strain levels, indicating that GAGs are mechanically important at even low tissue strains. Tensile properties of the inner region were also found to be increased following GAG depletion, suggesting that sulfated GAGs play a role in the meniscus tensile characteristics. Understanding these contributions of sulfated GAGs to the mechanical properties of the meniscus can help explain the complex structure-function relationships that exist in the tissue. As the meniscus undergoes both static and dynamic compression, tension, and shear under normal loading conditions, it is vital to elucidate the major contributors to this mechanically important tissue. Many investigations have shown that the presence of the meniscus in the knee protects the articulating cartilage from the progression of osteoarthritis.[173-175] Unfortunately, the meniscus is prone to injury, has little self-regenerative capacity, and repair techniques are often insufficient to restore full functionality.

Tissue engineering efforts aim to create functional replacement tissues, and depend on detailed design criteria to achieve this goal. While many studies exist bearing out the types, organization, and mechanics of collagens in the meniscus, much less is known about the mechanical contribution of GAGs regionally in the tissue. To our knowledge, this study is the first to assess the regional contributions of sulfated GAGs to viscoelastic meniscus mechanics.

The success of this study depended on an efficient GAG-removal technique, and CABC proved to be an effective mode of depleting sulfated GAGs from the bovine meniscus (see Figure 2). In the present study, all regions of the meniscus subjected to CABC treatment showed greater than 95% decreases in sulfated GAG content. As CABC is known to act mainly on chondroitin and dermatan sulfate molecules,[259] it follows that these comprise the vast majority of GAGs in the bovine meniscus. This is in agreement with previous characterization of the human meniscus, in which the GAG distribution was found to be 40% chondroitin-6-sulfate, 10-20% chondroitin-4-sulfate, and 20-30% dermatan sulfate.[16] These similarities between bovine and human menisci could indicate that the structure-function relationships borne out in this study may have broader clinical relevance.

GAG depletion affected biochemical content differently in the inner region compared with the outer and middle regions. Following GAG-depletion of the inner region, an increase in percent collagen per dry weight was observed (see Figure 2). This is likely because the inner region contains around 4% GAG per dry weight and when this fraction is removed, there is a concomitant increase in

collagen fraction. The same result is not observed in the outer and middle regions. This is likely because GAGs in these regions do not comprise such a large fraction of the dry weight, and therefore minute increases in collagen content between control and GAG-depleted groups could not be detected. These differences in the effect of GAG-depletion on biochemical content, however, were not predictive of the effect of GAG-depletion on compressive properties.

As hypothesized, the viscoelastic compressive properties of the meniscus were affected by sulfated GAG depletion, and these effects varied regionally. The present data establish that in compression, all regions of the tissue rely on sulfated GAG to impart viscosity, even the outer region where these proteins are most scarce. In the middle and inner regions, where sulfated GAGs are more abundant, both the viscosity and modulus of relaxation of the tissue are reliant on sulfated GAG, indicating that the molecule is also important in supporting compressive loads. This overall change in viscosity is in agreement with the literature on compressive mechanical properties of GAG-depleted ligaments, and cartilages.[163, 260] GAG removal in porcine medial collateral ligament (MCL) causes overall increases in tissue permeability. As ligament tissue is similar in biochemical content and organization to the outer meniscus in the circumferential direction, the observed changes in viscosity in the present study for the outer meniscus were found to closely match the change in permeability for GAG-depleted ligaments. Thus, it appears that the coefficient of permeability reported in these studies is inversely proportional to viscosity. Increased permeability has also been observed in GAG-depleted articular cartilage explants, along with a

decrease in lubrication of the tissue.[163] Though not measured in the current study, it is possible that GAG depletion of the meniscus also has an effect on the lubrication properties of the tissue. Therefore, these results show that changes in compressive properties resulting from GAG-depletion are commensurate with the native GAG content in each region.

Tensile testing on GAG-depleted meniscus regions showed a significant increase in inner region properties, but had no statistically significant effect in the outer and middle regions. As the inner region contains the most sulfated GAG of all the meniscus regions, it is possible that the GAG content imparts a pre-stress on the resident collagen molecules, a phenomenon that has been modeled in GAG-rich tissues such as articular cartilage.[262] If the same principles are applied to the inner meniscus, in its normal state, sulfated GAGs attract water molecules which increases hydrostatic pressure and imparts a pre-stress to the collagen network. Once the GAG is depleted and the pre-stress is removed, the apparent tensile properties of the tissue increase. This increase could be a result of minute decreases in tissue volume as the GAGs are removed. As tissue volume decreases, the same force would be applied to a smaller cross-sectional area, resulting in a higher calculated stress and higher tensile properties. Although not directly measured in this study, decreased tissue volume and increased tensile properties have been noted in CABC-treated articular cartilage, as well as tissue engineered articular cartilage constructs, which are both rich in sulfated GAG.[263, 264] In the other two regions, where GAGs are not as abundant, the pre-stress and volume changes may not be significant enough to make a difference in the

tensile properties measured. These results show, therefore, that sulfated GAGs play a role in inner meniscus tensile properties.

In conclusion, this study showed that GAGs in the knee meniscus contribute significantly to the viscoelastic properties of the meniscus, especially in the inner and middle regions where GAGs are most abundant. These regional variations in the contribution of GAGs to meniscus mechanics illustrate the importance of these molecules to the overall function of this tissue. Therefore, when engineering the meniscus, constructs should use, produce, or mimic the regional distribution of GAGs to attain native viscoelastic mechanics.

Acknowledgements

We would like to acknowledge the National Science Foundation Rice-Houston Alliance for Graduate Education and the Professoriate (NSF-AGEP) for their generous support of this work.

Grants

We would like to gratefully acknowledge funding from the National Institutes of Health R01AR047839 and R01DE019666.

Disclosures

There is no conflict of interest to report.

Figures

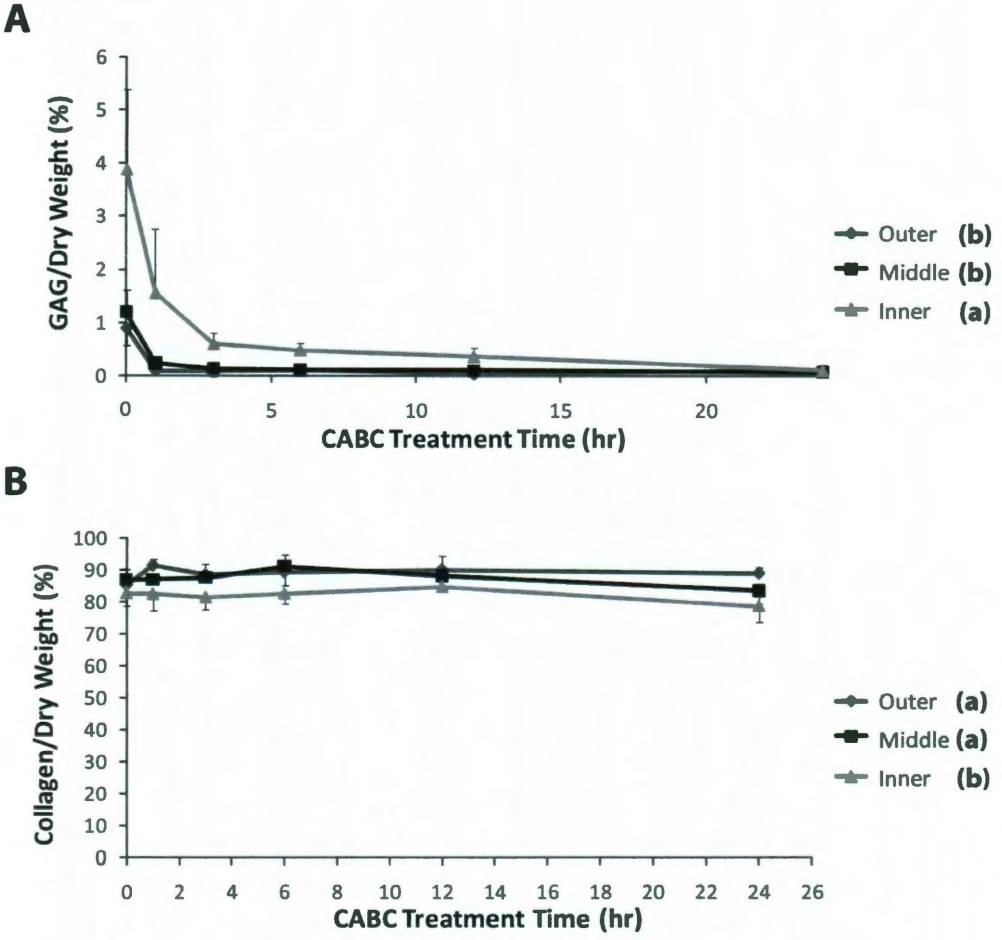

Figure 1: Temporal effects of CABC treatment in different meniscus regions. Percent sulfated GAG content (A), and total collagen content (B) per dry weight was measured for outer, middle, and inner meniscus specimens treated with CABC for 0, 1, 3, 6, 12, and 24 hours. Inner meniscus specimens contained more sulfated GAG per dry weight than the outer and middle specimens prior to CABC treatment, and required longer treatment time to reach full GAG depletion. Collagen content remained unchanged in all groups in response to CABC treatment, and the inner meniscus was found to contain statistically less collagen than the outer and middle meniscus. Each data point represents the average measurement and standard deviation. Significant results from the one-way ANOVA performed on the data are shown in the legend, where groups not connected by the same letter are statistically different from each other.

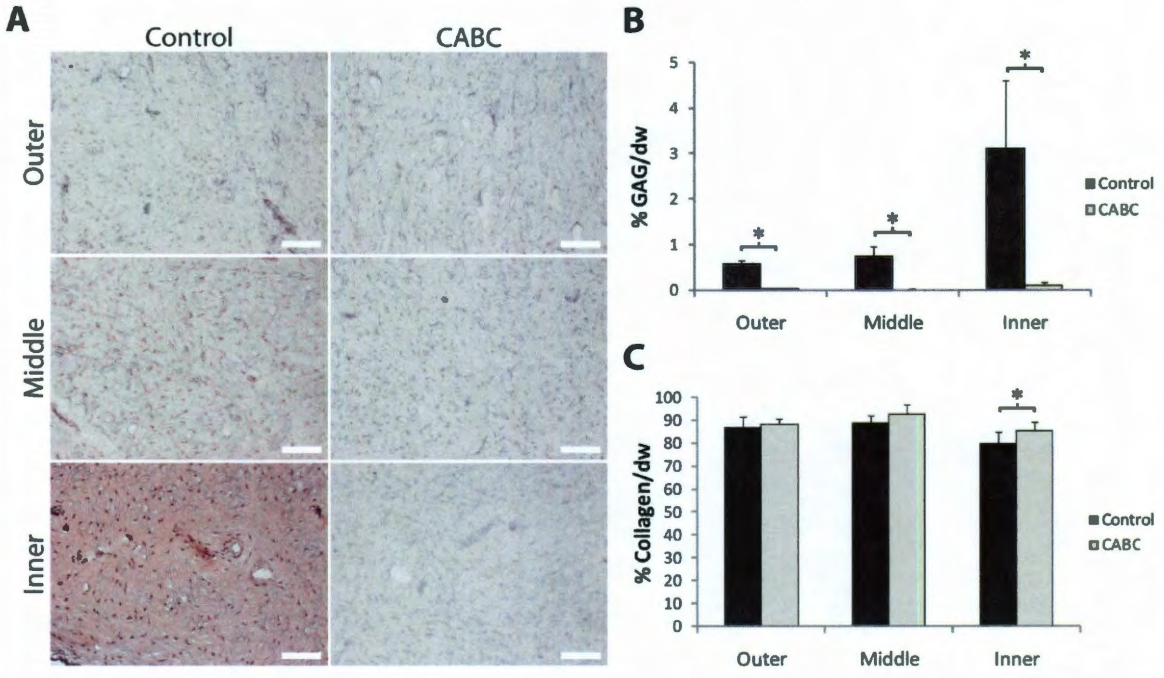

Figure 2: Histology and biochemistry of control and CABC treated specimens. Safranin-O staining (A), and biochemical analyses for sulfated GAG content (B), and total collagen content (C) were performed on control and CABC treated specimens from the outer, middle, and inner regions of the meniscus. Positive staining for sulfated GAGs could be detected readily in the inner region, and, to a lesser degree in the middle and outer regions; all regions were negative for sulfated GAGs following CABC treatment (A). Biochemical analysis confirmed histological results, with all regions showing >95% decreases in GAG content following CABC treatment (B). Percent collagen content per dry weight in the outer and middle regions remained unchanged following GAG-depletion, and increased in the inner region (C). Scale bar: 100 μm. Student's t-tests performed in (B) and (C), with significance set at $p < 0.05$ and indicated by an asterisk.

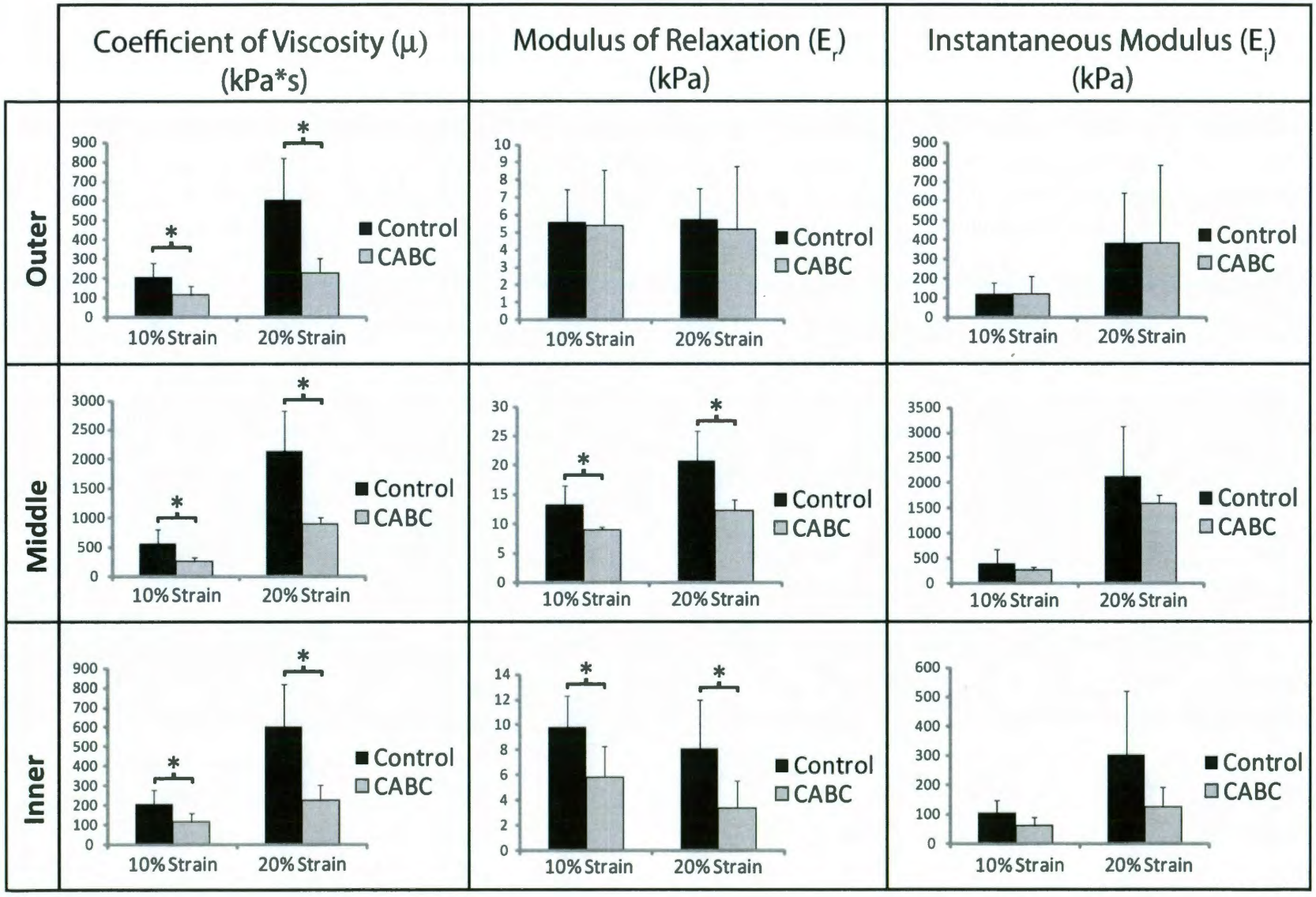
Coefficient of Viscosity (μ) (kPa*s)
Modulus of Relaxation (E_r) (kPa)
Instantaneous Modulus (E_i) (kPa)
Outer
Middle
Inner
Control
CABC
10% Strain
20% Strain
*

Figure 3: Compressive properties of control and GAG-depleted regional meniscus specimens. Unconfined compression stress-relaxation tests at 10% and 20% strain levels were performed on outer, middle, and inner meniscus specimens either treated with CABC or not (Control). Similar results were observed at both 10% and 20% strain levels. All regions displayed a decrease in tissue viscosity in response to GAG depletion. The modulus of relaxation remained unchanged in outer meniscus specimens following CABC treatment, but decreased in middle and inner regions. No region showed differences in instantaneous modulus following GAG depletion. Student's t-tests were performed at each strain level with significance set at $p < 0.05$ indicated by an asterisk.

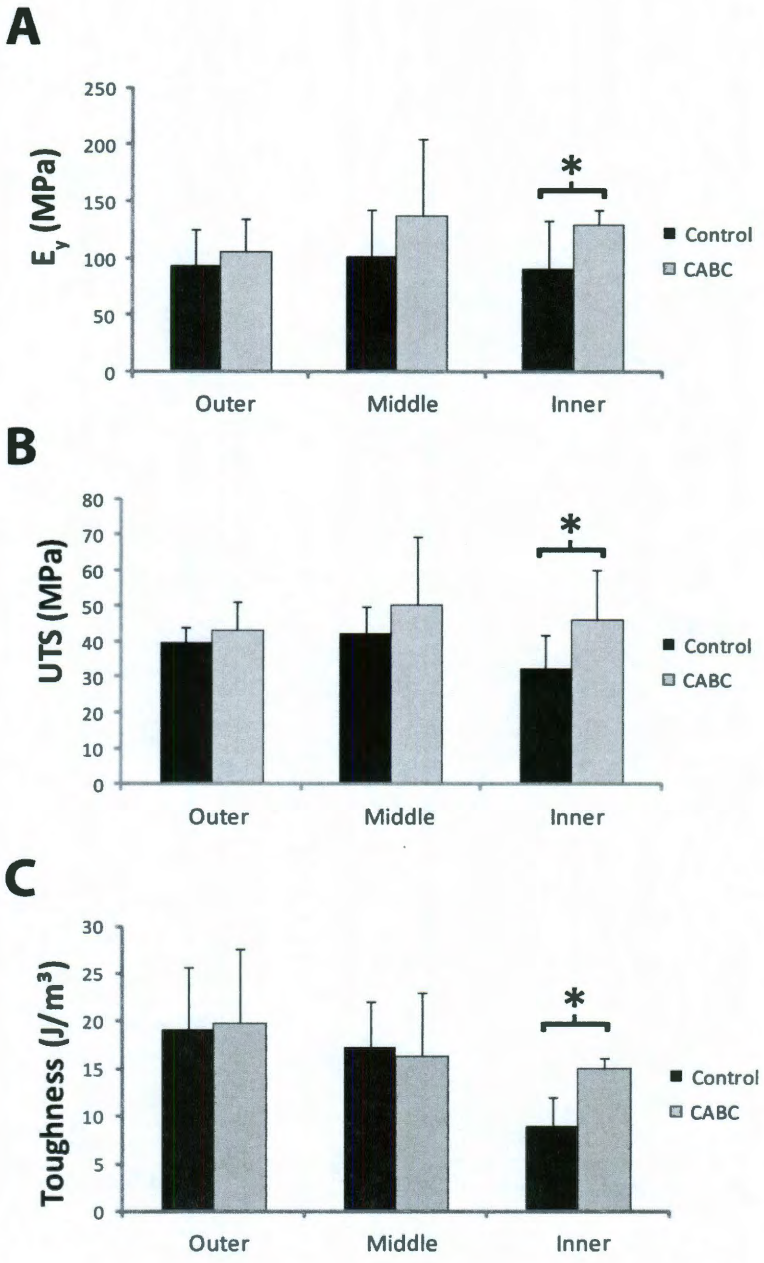

Figure 4: Tensile material properties of GAG-depleted meniscus regions. Young's modulus (A), ultimate tensile stress (B), and toughness (C) were measured for outer, middle, and inner meniscus regions subjected to GAG depletion (CABC) or not (Control). Outer and middle meniscus regions did not show any significant difference in either Young's modulus or UTS following GAG depletion. Inner meniscus specimens, however, showed a statistically significant increase in both parameters after CABC treatment. Student's t-tests were performed on these data with significance set at $p < 0.05$ indicated by an asterisk.

Chapter 9: Tissue Engineering of the Knee Meniscus

Section 9.1: Bioreactors

Introduction

The meniscus is a mechanically-sensitive tissue that can respond favorably or unfavorably to biomechanical stimuli.[265] It is known that during development, the meniscus experiences a myriad of mechanical stresses that are important for normal maturation. Studies have shown that immobilizing chick embryos results in the complete absence of the meniscus and fusion of the cartilaginous parts in the joint.[105] Additionally, the mature meniscus is also heavily reliant on mechanical stimulation to maintain its health. Joint immobilization of rabbit knees for 8 weeks results in degeneration of the deep zone of the meniscus and reduced tissue permeability.[106, 107] Given the importance of mechanical cues for normal meniscal development and function, it is natural to expect that mechanical stimulation of tissue engineered meniscal replacements would be beneficial. To impart mechanical forces to tissue engineered constructs many different bioreactors have been developed which can apply compression, shear, hydrostatic pressure, vibration, or combinations of these forces in a controlled environment. As the exact type and pattern of optimal

---

Chapter published as: Athanasiou, K. A., and Sanchez-Adams, J. "Part 3: Tissue Engineering of the Knee Meniscus." *Engineering the Knee Meniscus*. Morgan and Claypool Publishers. 2009.

mechanical stimulation of the meniscus is not known, various stimulation regimens should be investigated.

There are only a few bioreactors that are specifically designed for stimulation of meniscal tissue, and they comprise a subset of bioreactors designed for stimulation of cartilage constructs. As cartilages in the knee experience similar types of forces, bioreactors generally designed for cartilage stimulation can also be considered applicable to engineering the meniscus. Cartilage bioreactors fall into five different categories: direct compression, hydrostatic pressure, high shear systems, low shear systems, and ultrasound. Other bioreactors use combinations of these in an effort to achieve more tailored results.

Direct compression

Direct compression bioreactors, sometimes called cyclic strain bioreactors, impart a compressive load to cartilage constructs to simulate normal loading patterns (see Figure 1). Typically strains of 1–10% have been used with frequencies of 0.1–1 Hz. Varying degrees of success have been achieved using this type of stimulation including increases in hydroxyproline content, indicating collagen increases, and [^{35}S] sulfate incorporation, indicating an increase in glycosaminoglycans following the loading regimen (see Table 1).[266-270] This type of bioreactor has been used to stimulate meniscal explants, showing an increase in aggrecan gene expression by 108% with dynamic stimulation (2% oscillatory strain, 1 Hz).[128] Direct compression bioreactors may also be used to simulate

loading patterns of the meniscus following partial meniscectomy, showing that removing part of the meniscus results in loading patterns that detrimentally affect proteoglycan retention in the tissue.[271]

Hydrostatic pressure

Static and dynamic hydrostatic pressure bioreactors have also been used to simulate the pressurization of the interstitial fluid or the joint capsule (see Table 2). Using this type of loading, constructs or explants are placed in a chamber which is pressurized via a piston to physiologic levels (Figure 2). Magnitudes of 0.1–15 MPa either applied statically or dynamically at 0.01–1 Hz have been used to stimulate cartilage constructs and have been shown to be effective at increasing mRNA levels responsible for collagen types I and II and aggrecan, and also to reduce tissue breakdown of meniscal explants.[107, 111, 272-278] Hydrostatic pressure can be applied to constructs intermittently, in which a period of static culture is interrupted with hydrostatic pressure stimulation, or continuously, in which constructs are cultured within a pressurized chamber. Continuous culture provides the added advantage of minimal construct manipulation, minimizing user variables.

Shear

Bioreactors that impart shear forces to constructs can be considered in two classes: high shear systems and low shear systems (see Table 3). Both use fluid flow to impart mechanical forces. Two types of high shear systems are currently in use: flow perfusion chambers and spinner flasks. In flow perfusion

chambers medium flows through the construct, creating shear forces as the fluid makes its way through the pores of the construct.[114, 279-281] Another type of high shear environment can be achieved using a spinner flask in which medium is stirred around the constructs, creating high shear as it flows around the boundary of the construct. The main difference between these two approaches is that the perfusion chamber creates shear within the construct and the spinner flask creates shear at the construct's surface. Flow in the perfusion chamber imparts higher shear at the first contact with the construct, and lower shear as the medium exits the construct, which can cause differences in cellular response based on the construct thickness.[282] Spinner flasks, however, only impart shear on the outside of the construct which affects cells at the surface differently than in the center. Despite their differences, both of these bioreactors have been shown to increase collagen and GAG production, while the spinner flask has been especially effective at creating bi-zonal tissues with an outer fibrous capsule.[283] For meniscal tissue engineering, high shear systems such as spinner flasks may be beneficial to create the fibrocartilaginous outer portion while maintaining a more hyaline-like core.

Low shear systems such as parallel plate flow bioreactors and rotating wall bioreactors also impart fluid forces to the constructs, but the forces felt are much lower than those in the high shear systems. A laminar flow bioreactor has been shown to increase collagen type II production and increase tensile properties of cultured chondrocytes, indicating that low shear can be a beneficial way to stimulate cartilage formation *in vitro*.[113] Much work has been done using

rotating wall bioreactors in which small amounts of fluid shear are imparted to constructs as they are cultured in a medium-filled chamber that slowly rotates. This environment simulates microgravity by maintaining constructs in a mostly free-floating state. The mechanical environment has shown mixed results in tissue engineering cartilage, in some cases increasing matrix production and in other cases not appreciably improving construct properties.[129, 284, 285] An intermediate form of the rotating wall bioreactor is the wavy-walled bioreactor in which constructs are subjected to a more complicated set of fluid stresses due to the irregular shape of the bioreactor walls.[286-288] In this type of bioreactor, ECM synthesis is stimulated to varying degrees based on the position of the construct in the chamber.[289]

Ultrasound

Another type of stimulation that may be used for tissue engineered cartilage is low-intensity ultrasound (Table 4). The impetus for using ultrasound stimulation came from research done in the late 1990s which showed that ultrasound increased the gene expression for aggrecan in cultured chondrocytes.[290-292] This type of stimulation has shown a similar, but less persistent enhancement of ECM formation when compared to the rotating wall bioreactor.[293] Pulsed ultrasound stimulation of cartilage constructs at 1 MHz and 67 mW/cm^2 for 10 minutes per day was shown to be beneficial for cell proliferation and matrix production in a cell-seeded construct for up to 4 weeks, beyond which decay of the construct was observed.[293] The effect of low-intensity

ultrasound also has a minimal effect on cartilage construct maturation.[294] Ultrasound therefore may be effective during the cell culture stages of tissue engineering, but has not shown great promise for stimulating cartilage construct maturation.

Combinations

Limited studies have been performed on combinations of mechanical stimulation (Table 5). Direct compression has been combined with shear in two different bioreactor systems, emulating physiologic loading patterns and increasing cartilage matrix production.[75, 295] Both bioreactors use a round piece that rotates and imparts a shear force while pressing down on the construct to impart compression. Using an oscillating pin and ball mechanism simulates physiologic compression and shear within a joint and has been shown to increase cartilage oligomeric protein synthesis, which helps to organize cartilage matrix.[295] Another type of combination bioreactor uses fluid shear with cyclic compression and shows higher GAG retention with varying matrix compositions on the surface of the construct versus the core.[281] Combinations of mechanical stimulation can therefore be beneficial to enhancing construct properties beyond that which can be reached using one type of stimulation.

Application to meniscus engineering

Based on the research that has been done using these various systems to tissue engineer hyaline cartilage, some projections for their potential use in

meniscal tissue engineering can be made. High shear systems may be especially useful for meniscal tissue engineering as they can create bi-zonal tissue, an important attribute of the meniscus. Hydrostatic pressure bioreactors have achieved marked success in increasing mechanical properties of tissue engineered cartilage constructs, a central concern for engineering biomechanically important tissues like the meniscus. Direct compression may be beneficial for meniscal constructs during the later stages of maturation, when mechanical stimulation is known to be important for normal tissue function. Low shear systems could provide stimulation for overall ECM production, but due to the mixed review of this stimulation in articular cartilage engineering it is unclear how beneficial it might be. Ultrasound stimulation is fairly new to cartilage tissue engineering and may be beneficial for stimulating GAG synthesis of cultured cells, but has not shown beneficial effects on construct maturation. Rather than choosing one type of bioreactor, it is likely that some combination of these stimuli will provide the best environment for meniscus tissue regeneration, given the vast number of events that occur during meniscal development.

Concepts

Tissue engineering the knee meniscus has garnered much attention in the scientific community due to the prevalence of meniscus degeneration and defects and the tissue's limited ability to self-repair. As the meniscus is dependent on mechanical stimulation for normal function, bioreactors that simulate physiologic stresses have been developed and may provide the

appropriate conditions for meniscal regeneration *in vitro*. Though there are few bioreactors specifically designed for meniscus tissue engineering, a basic understanding of cartilage bioreactors as a whole provides the necessary background for the progression of this field. Five different categories of cartilage bioreactors exist: direct compression, hydrostatic pressure, high shear systems, low shear systems, and ultrasound. Amongst these, direct compression, hydrostatic pressure, and high shear systems seem the most promising for developing tissue mechanically and biochemically similar to the native meniscus. Combination bioreactors incorporate two or more types of these stimuli, and could allow for more directed formation of the meniscus.

Section 9.2: *In vitro* tissue engineering

Introduction

According to the classic tissue engineering paradigm, the basis of any meniscus tissue engineering attempt are cells and scaffolds. Currently in the meniscus tissue engineering field, the focus has been mostly on characterization of meniscal fibrochondrocytes and their sensitivity to various biochemical stimuli. This information has been used to create various methods for tissue engineering the meniscus that maximize matrix synthesis and increase the biochemical and mechanical relevance of engineered constructs.

Cell Source

Success of tissue engineering strategies relies heavily on the type of cells used and their potential to create enough of the appropriate extracellular matrix molecules. Fibrochondrocytes are well characterized and have been used in many meniscus engineering attempts.[18, 40, 42, 43, 46, 110, 117] While the presence of these cells is optimal for understanding the culture environments and stimuli appropriate for engineering a meniscus-like tissue, they are relatively scarce in the body and would likely be an impractical source for large-scale engineering attempts. This has prompted research into other sources of cells that may present an abundant, autologous or allogenic source.

Other cell types that have been used in tissue engineering the meniscus include chondrocytes, mesenchymal stem cells, and embryonic stem cells. Chondrocytes are nicely suited to meniscal engineering as they can be induced to produce collagen type I through passaging. Their synthetic capacity for collagen and GAGs in tissue engineering is also higher than fibrochondrocytes.[131] Chondrocytes are, however, also relatively scarce in the body and therefore would prove difficult to procure for tissue engineering. Mesenchymal and embryonic stem cells, on the other hand, present a potentially limitless cell source. The difficulty in using these cells lies in understanding the necessary stimuli for directing their differentiation to a fibrochondrocytic lineage. Encouraging results have been obtained using various growth factors including IGF-I, TGF-β1, TGF-β3, BMP2, and BMP6, for directing MSCs from the bone to produce collagen types I and II.[296-298] Human embryonic stem cells have also shown promise toward producing fibrocartilaginous tissue when conditioned with

transforming growth factors, bone morphogenetic proteins, and when co-cultured with native fibrochondrocytes.[299] These embryonic stem cells, when differentiated and formed into scaffoldless constructs, can produce matrix molecules important for meniscus tissue including collagen types I and II, as well as GAGs.[131, 300] More work needs to be done to solidify the differentiation regimen for both of these cell types, and also to identify MSCs that are sensitive to fibrochondrocytic differentiation.

There are also some cell types that are promising for use in this field, but have yet to be fully investigated for meniscal tissue engineering. These include auricular chondrocytes, dermal fibroblasts, adipocytes, and synovial tissue cells. All of these cell types are advantageous for tissue engineering in that they are easily procured, and have minimal donor site morbidity. Auricular chondrocytes, from the elastic cartilages of the nose and ear, have high proliferative and synthetic capacities and can produce a matrix of collagens I and II that is similar in makeup to meniscal tissue.[301] Recently a subpopulation of dermal fibroblasts has been identified that has the capacity to be chondroinduced through various means including gene transfection and culture on or with various proteins.[302-304] This conditioning produces cells that synthesize collagens I, II, and GAGs, which are all important components of the normal meniscus. Like dermal fibroblasts, a subset of adipocytes has also been identified as a cell source for cartilage tissue engineering. Using culture medium containing BMP6 has proved effective for differentiating these cells towards a chondrocytic pathway.[305-307] Synovial tissue cells may also prove beneficial for meniscal engineering as they have shown

chondrogenic capacity, and an ability to vary production of collagen types I and II in response to the culture environment.[165] All four of these cell sources may provide autologous cell sources for meniscal tissue engineering but more research must be completed to illuminate their potential.

Growth factors

Though a different cell source may ultimately be used for meniscal engineering, an understanding of the behavior of fibrochondrocytes to growth factors is advantageous as it provides the framework for culturing meniscus-like cells. Meniscal fibrochondrocytes respond in different ways to different growth factors, as outlined in Table 6. It has been shown in multiple studies that monolayer cultures of fibrochondrocytes exposed to transforming growth factor beta 1 (TGF-β1) exhibit enhanced proteoglycan synthesis and cell proliferation.[18, 43, 108] Fibroblast growth factor (FGF), hepatocyte growth factor (HGF), platelet-derived growth factor (PDGF-AB), bone morphogenetic protein 2 (BMP-2), and human platelet lysate (Human PL) also increase cell proliferation, but at a high enough concentration FGF decreases GAG synthesis.[40, 109, 110] Cell migration of all fibrochondrocytes is stimulated by PDGF-AB and HGF, and slightly by epidermal growth factor (EGF), but only outer meniscus cells migrate when exposed to interleukin-1 (IL-1).[110] All of these growth factors have some effect on meniscal cells and therefore can be used along with scaffolds to enhance matrix synthesis, cell proliferation, and cell penetration into tissue engineered constructs.

Several of these growth factors have already been incorporated into the culture medium for engineered constructs, and their effects investigated. One growth factor, TGF-β1, has proved especially effective for enhancing construct properties in various engineering modalities. Using a scaffoldless approach in which cells are cultured in a non-adherent well, application of TGF-β1 has been shown to increase tensile properties of engineered fibrochondrocytic constructs up to 3 MPa.[116] TGF-β1 has also been shown to increase matrix production of fibrochondrocytes seeded on poly-L-lactide (PLLA) constructs, outperforming PDGF-AB, FGF, and insulin-like growth factor 1 (IGF-1).[117] Bone marrow mesenchymal stem cells seeded on collagen matrices are also stimulated by TGF-β1 to make collagen type II and glycosaminoglycans, important proteins for reconstruction of the inner one-third of the meniscus.[308]

Synthetic scaffolds

In scaffold-based approaches, scaffold material can have similar effects on cell synthetic profiles as growth factors. Scaffolds that have been used for meniscal engineering are either synthetic, such as PLLA, or natural, such as decellularized tissue or scaffolds made from various matrix proteins (see Table 7). Synthetic scaffold materials must be biocompatible, but have the innate advantage over natural scaffolds of low batch variability, which is important for reproducibility. For meniscus engineering polyglycolic acid (PGA) and PLLA have been used previously. These two scaffold materials are biocompatible and degradable, and their degradation products are non-toxic, though acidic. Seeding

fibrochondrocytes on PGA scaffolds has the effect of increasing cell proliferation, sulfated GAG production, and collagen synthesis over an agarose scaffold control.[129] PLLA has also been proven biocompatible with fibrochondrocytes, though the effect of PLLA alone on fibrochondrocyte processes has not been investigated.[117]

Natural scaffolds

Natural scaffolds have also garnered success in meniscal engineering (see Table 9). Collagen meshes have been shown to allow cell proliferation and collagen and GAG production, and to allow for growth factors to enhance these properties.[46, 308] The type of collagen used for the scaffold also has an effect on cell behavior. Collagen type II-GAG meshes fared better than type I-GAG meshes when seeded with fibrochondrocytes, reducing contraction of the constructs and increasing collagen and GAG production.[42] Matrices made of hyaluronic acid (HA) are also biocompatible, as they are made of a major component of cartilage, and when cultured in a mixed flask can create bi-zonal tissue reminiscent of the non-uniform properties of the meniscus.[309, 310] Agarose is another type of natural scaffold that has been used extensively in cartilage tissue engineering. This scaffold material can encapsulate fibrochondrocytes as it crosslinks and can be made into any shape. This material has not been shown to be as effective at stimulating matrix production or imparting mechanical integrity as other scaffold materials, however, and therefore is not as popular for meniscal engineering.[129] The last type of natural scaffold material used in meniscal

engineering is decellularized meniscal tissue. This material is advantageous because it contains matrix that is already organized and can best simulate the natural microenvironment for meniscal cells. While decellularization of meniscal tissue has been achieved, mechanical integrity of the matrix has been maintained, and cytocompatibility has been demonstrated, work has yet to be done to demonstrate its use in tissue engineering.[244]

Scaffold-free approaches

An emerging technique in meniscal tissue engineering is to use a scaffold-free method to grow meniscal tissue. Eliminating scaffold material from the tissue engineering approach eliminates variables such as the degradation profile, acidic degradation products from polymers such as polylactides/polyglycolides, and biocompatibility of the scaffold. Recently, a self-assembling method has been devised for scaffoldless tissue engineering in which cells are seeded into an agarose mold which inhibits cell attachment.[210] Using the self-assembling method, a 50:50 co-culture of bovine fibrochondrocytes and chondrocytes were formed into constructs which were cultured for 4 weeks and were found to contain both collagen types I and II as well as proteoglycans.[131]

This method has also been employed to create meniscus-shaped constructs using this same co-culture of bovine meniscal fibrochondrocytes and chondrocytes, showing that these constructs were 200–400% stiffer after 4 weeks than cell-seeded PGA scaffolds (Figure 3).[115] This scaffold-free method therefore seems promising for recreating meniscus biochemistry and geometry

as well as improving upon mechanical properties of constructs formed using synthetic scaffolds (see Table 7).

Concepts

In vitro tissue engineering of the knee meniscus has yet to produce constructs that match native meniscal properties. A variety of cell types are under investigation for meniscal engineering, prompted by the overall scarcity of fibrochondrocytes. Progenitor cells, either adult or embryonic, hold much promise as they have shown chondrogenic capacity when exposed to various growth factor treatments. Much work has been done to identify biochemical factors and scaffold materials to which fibrochondrocytes are sensitive, and various studies have used them in combination to maximize construct biochemistry and biomechanics. Much is still unknown as to the effect of other combinations of cells and scaffold materials as well as the addition of mechanical stimulation to many of the current approaches. Some promising results have been obtained using co-cultures of chondrocytes and fibrochondrocytes in a scaffold-free approach (self-assembly process), which mimic the native meniscus in terms of biochemical makeup and geometrical properties as well as improve upon the mechanical properties when compared to constructs that use synthetic scaffolds.

Section 9.3: *In vivo* tissue engineering

Introduction

As a next step to *in vitro* studies or to demonstrate feasibility of a tissue engineering technology, *in vivo* work with the knee meniscus provides practical measures of construct properties. There have been many different attempts to repair damaged meniscal tissue by implanting scaffolds with or without cells into the body, using the joint itself as a bioreactor to stimulate tissue formation.

Animal models

An ideal model for testing engineered meniscus products would replicate the environment found in the human knee joint. Though this has not yet been achieved, various animal models are used as approximations, providing a first understanding of how engineered meniscus tissue will fare when placed inside an organism. The most popular animal model for testing engineered meniscus technologies is the New Zealand white rabbit.[133, 311-316] Well-characterized and relatively inexpensive, the rabbit model is large enough for surgical procedures and small enough to raise easily. Though it has been shown that the mechanical properties of the rabbit meniscus are not as similar to the human meniscus as those of baboons, dogs, and pigs, the rabbit still remains the model of choice for most studies.[37] Larger animal models such as dogs, sheep, pigs, and goats have also been used to show the biocompatibility and feasibility of tissue engineered meniscus constructs.[317-323] Showing good performance in these models may more closely approach expected outcomes in a human, as they are more comparable in size and the meniscus in these animals has similar biomechanical properties to human tissue. Additionally, testing in these types of animals is often

required by the Food and Drug Administration (FDA) prior to embarking on clinical trials.

Table 8 lists the advantages and disadvantages of the various animal models used in meniscus tissue engineering. It is important to note that in addition to the type of animal used, the age of the animal has a large influence on tissue plasticity. Researchers must take the age of the animal model into account when evaluating *in vivo* success rates.

Fibrin

The earliest attempts to tissue engineer cartilage *in vivo* involved using fibrin or fibrin clots as a scaffold. Fibrin, a natural material formed in the body following injury, can be processed into a gel and in combination with endothelial cell growth factor was shown to increase healing of defects created in the dog meniscus.[322] Following this success, fibrochondrocytes were encapsulated in fibrin gels and implanted into rabbit meniscal defects. After two months, the scaffolds showed signs of cell proliferation and sulfated GAG production.[316] Fibrin gel has shown better success than fibrin clots even with the incorporation of mesenchymal stem cells. Fibrin clots that were implanted into defect sites did not induce much healing when implanted into avascular defect sites of the meniscus.[318] Although some success has been observed with these fibrin scaffolds, full defect healing was not observed and no mechanical testing was performed on the repair tissue.

Synthetic scaffolds

In the mid-1990's, cell-seeded synthetic scaffolds were investigated *in vivo* as possible replacement therapies for meniscal defects (see Table 9). PGA scaffolds were seeded with meniscal fibrochondrocytes and implanted subcutaneously in nude mice for 16 weeks, showing organization with time of a fibrous matrix containing sulfated GAGs.[324] These scaffolds were also seeded with fibrochondrocytes transfected with a gene to encourage vascularization, and implanted subcutaneously. In this experiment the gene transfection successfully encouraged vascularization of the construct.[325] Recently, a PGA scaffold was seeded with fibrochondrocytes and implanted into a rabbit knee that had undergone total meniscectomy. Following 10 weeks *in vivo*, fibrocartilaginous tissue had formed, although the biochemical and mechanical characteristics of the neotissue were still a fraction of native tissue.[133] Another synthetic scaffold type comprised of a PLLA and poly(p-dioxanone) PPD blend was also used recently as a meniscal prosthesis to stimulate meniscal regeneration.[312] After 14 weeks there was some ingrowth of tissue and extensive degradation of the scaffold.[312] Additionally the cartilage underlying the scaffold was intact, while in control specimens the cartilage had signs of damage.[312] Therefore, the PLLA/PPD scaffold was shown effective as a meniscal prosthetic but was not able to stimulate complete tissue repair prior to degradation of the material.

Natural scaffolds

Currently, focus has turned to the potential of natural scaffolds to repair the meniscus (see Table 9). Studies using decellularized tissue such as the

meniscus and small intestine submucosa have been able to achieve partial regeneration of meniscal tears, but their *in vivo* success has been limited.[317, 323] More success has been achieved using collagen scaffolds from bovine Achilles tendon called collagen meniscus implants (CMI). These implants aim to act as prostheses and to stimulate tissue ingrowth. Longitudinal studies in patients have shown that 6 months post-implantation, the underlying cartilage was intact, the scaffold was infiltrated with fibrochondrocytes and that the implant contained fibrous tissue after 5 years.[326, 327] Another study in sheep used CMI in a tissue engineering strategy in which fibrochondrocytes were seeded into the scaffold and then implanted in an inner-meniscus defect.[319] The results after 3 months suggested that cell-seeded CMI performed better than non-seeded controls, although the matrix produced was more fibrous than that found in the inner meniscus, and the constructs tended to contract significantly.[319] CMI is therefore a promising technology for meniscal replacement, although more research must be done to induce inner-meniscus like tissue to form.

Another natural scaffold used currently in meniscal tissue engineering research *in vivo* is hyaluronan. This scaffold has been used to encapsulate chondro-differentiated mesenchymal stem cells and was implanted in a rabbit meniscal defect for 12 weeks.[311] The repair tissue formed by this method was more similar to native meniscus tissue than non-treated controls and good integration was observed between the scaffold and native meniscus.[311]

Concepts

In vivo testing of engineered materials is important for ensuring the biocompatibility of the technology as well as its feasibility to repair damaged tissue. The most popular animal model for *in vivo* testing of meniscus constructs is the New Zealand white rabbit. Other animals that have been used include sheep, dogs, pigs, and goats. Many different types of cells and scaffold materials have been investigated *in vivo* for use as meniscal replacements. Fibrin has demonstrated a limited capacity to induce sufficient repair of meniscal tissue. The addition of cells to scaffolds tends to increase overall reparative potential of a construct, but complete healing of a meniscus defect has yet to be achieved. A number of scaffold materials have been used for meniscus tissue engineering including synthetic types (PGA, PPD, PLLA) and natural types (collagen, hyaluronan). Recent focus has been on using natural scaffolds rather than synthetic ones to better achieve meniscus-like repair tissue. There are a few promising approaches currently being investigated using both types of scaffolds, but more research must be done to understand their long-term behavior in the body.

Tables

Table 1: Summary of direct compression bioreactors

Stimulation	Specimen	Effect	Ref.
3% cyclic strain, 0.1–1 Hz, 6 wks	$20x10^6$ bovine chondrocytes/ml agarose gel	15–25% increase [^{35}S]-sulfate incorporation, 10–35% increase [^{3}H]-proline incorporation	266
10% cyclic strain, 1 Hz, 5 days/wk, 3 hrs/day, 4 wks	$60x10^6$ bovine chondrocytes/ml agarose gel	1.74% GAG/wet weight 2.64% collagen/wet weight	267
10% cyclic strain, 1 Hz, 5 days/wk, 3 hrs/day, 4 wks	$20x10^6$ bovine chondrocytes/ml agarose gel	Aggregate modulus: 53 kPa, Young's modulus: 66 kPa, 1.43% GAG/wet weight 1.23% collagen/wet weight	268
10% cyclic strain, 1 Hz, 5 days/wk, 3 hrs/day, 4 wks	$60x10^6$ bovine chondrocytes/ml agarose gel	No increase in mechanical properties or GAG/wet weight (~1.6%); collagen/wet weight significantly higher (1.86%)	268
1–5% cyclic strain, 1 Hz	Bovine hyaline explant	20–40% increase in [^{35}S]-sulfate and [^{3}H]-proline incorporation	269
2% cyclic strain, 1 Hz, 4 hours	Bovine meniscus expants (medial and lateral)	108% increase aggrecan gene expression, no effect on collagen type II expression	128

Table 2: Summary of hydrostatic pressure bioreactors

Stimulation	Specimen	Effect	Ref.
10 MPa, 1 Hz, 4 hrs/day, 4 days	10^5 cow wrist cells/cm^2 monolayer	20-fold increase aggrecan mRNA, 9-fold increase collagen type II mRNA	272
1 MPa, 0.5 Hz, 1/14 min (on/off), 4 hrs	Rabbit meniscus explant	Prevents up-regulation of catabolic agents (MMPs, TIMPs) that occurs in unstimulated controls	107
6.87 MPa, 5/15 s (on/off), for 20 min every 4 hrs, 5 wks	5–7.5x10^6 juvenile horse chondrocytes/cm^3 PGA scaffold	20-fold increase in GAG, 2.4-fold increase in collagen	273
3.45 MPa, 5/15 s (on/off), for 20 min every 4 hrs, 5 wks	2x10^6 juvenile horse chondrocytes/cm^3 PGA scaffold	2-fold increase GAG concentration, no increase in collagen	274
10 MPa, static, 1 hr/day, days 10–14 in culture, 4 wks	5.5x10^6 cow chondrocytes, scaffold-less construct	Aggregate modulus 273 kPa, Young's modulus 1.6 MPa, 6.1% GAG/wet weight 10.6% collagen/wet weight	275
10 MPa, static, 1 hr/day, 1/3 days (on/off),4 wks	1x10^6 rabbit meniscus cells/ml PLLA scaffold	4-fold increase in collagen production, 3-fold increase in GAG production	111
10 MPa, 1 Hz, 4 hrs/day, 5 days/wk, 8 wks	5.5x10^6 cow chondrocytes, scaffold-less construct	Prevents decrease in GAG content observed in static culture	277
10 MPa, static, 4 hrs/day, 2/1 days (on/off), 1 wk	10^5 temporomandibular joint disc (cow) cells/ml, PGA scaffold	Increased collagen type I gene expression and collagen production	278

Table 3: Summary of shear bioreactors

Stimulation	Specimen	Effect	Ref.
Spinner flask, 8 wks	$25x10^6$ bovine chondrocytes /cm^3 PGA scaffold	60% increase in GAG, 125% increase in collagen, fibrous capsule formation	283
Flow perfusion	$12x10^6$ ovine chondrocytes/cm^3 PET scaffold	Outer layer of fibroblast-like cells, inner core of meniscus-like cells	114
Parallel plate, 1 dyne/cm^2, 3 days	$1.7x10^6$ bovine chondrocytes/cm^2, scaffold-less	113% increase in total collagen, 230% increase in collagen type II, Young's modulus 2.28 MPa, ultimate strength 0.81 MPa	113
Rotating wall, 6 wks	$127x10^6$ bovine chondrocytes/cm^3, PGA scaffold	GAG levels 68% of native, collagen levels 33% of native, collagen type II crosslinked	285
Rotating wall, 7 wks	$5x10^7$ rabbit fibrochondrocytes/cm^3, PGA scaffold or agarose	No significant effects over static control	129
Wavy-wall, 4 wks	$5x10^6$ bovine chondrocytes PGA scaffold	30% increase in cell number and 60% increase in ECM deposition over controls, fibrous outer capsule with type I collagen, inner core with type II collagen and GAG	287

Table 4: Summary of ultrasound bioreactors

Stimulation	Specimen	Effect	Ref.
1 MHz pulsed, 50 or 120 mW/cm^2, 10 min/day, 3 or 5 days	Rat chondrocytes, monolayer	Increase in aggrecan gene expression and [^{35}S]-sulfate incorporation	291
1 MHz pulsed, 67 mW/cm^2, 10 min/day, 6 days	4x10^6 human chondrocytes/cm^3 scaffold	Increased cell proliferation, beneficial effects last around 28 days (shorter than rotating wall bioreactor)	293
1.5 MHz, 30 mW/cm^2, 20 min/day, 7 days/wk, 12 wks	30x10^6 bovine chondrocytes/cm^2, PLGA scaffold, implanted into nude mice	No effect on accelerating chondrogenesis or maturation of engineered constructs *in vivo*	294

Table 5: Summary of combination bioreactors

Stimulation	Specimen	Effect	Ref.
Compression and shear, 0.5 N	Bovine chondrocytes, scaffoldless, immature cartilage-like construct	260% increase in aggrecan gene expression, 310% increase in collagen gene expression at 2 hrs, return to normal after 4 hrs; 4 days increases GAG content	75
Oscillating pin (5% strain, 0.1 Hz), and ball(0.6 Hz, ±60°), 1 hr/day, 3 days	Bovine nasal cartilage explant	Slight increase in COMP gene expression	295
Perfusion and compression, static (10% strain), or dynamic (5% strain, 0.3 Hz), 37 days	Bovine chondrocytes seeded in PGA scaffold	Flat top and bottom, increased GAG retention in construct	281

Table 6: Effects of growth factors on meniscus cells

Type	Source	Effect	References
TGF-β1	Sheep	Increases proteoglycan synthesis	18, 43, 108, 111
	Human	Increases proteoglycan synthesis	
	Rabbit	Increases [^{35}S]-sulfate [^{3}H]-proline uptake	
	Rabbit	15-fold increase in collagen production and 8-fold increase in GAG production	
BMP-2	Cow	Stimulates some cell migration in red-white region, also stimulates proliferation	110
IL-1	Cow	Stimulates migration of outer meniscus cells	110
PDGF-AB	Cow	Stimulates cell migration, proliferation	110
IGF-I	Cow	Stimulates some cell migration in red-white region	110
EGF	Cow	Stimulates half of inner and outer cells to migrate	110
HGF	Cow	Stimulates cell migration, proliferation	110
FGF	Rabbit	Increases proliferation	40
Human PL	Rabbit	Increases proliferation	40

Table 7: Scaffolds and scaffold-free methods for in vitro meniscus engineering

Type	Details	Result	Ref.
Synthetic			
PLLA	$2.5x10^7$ rabbit fibrochondrocytes/cm^3, 9 days, addition of growth factors	Supports cell survival, attachment	117
PGA	$23x10^6$ 50:50 bovine fibrochondrocytes and chondrocytes, meniscus-shaped, 8 wks	Irregularly shaped, presence of GAGs and collagen, random orientation of collagen, stiffness 16 ± 5 kPa, fibers degraded by 8 wks	115
PGA	$5x10^7$ rabbit fibrochondrocytes/cm^3, 7 wks	Increases sulfated GAGs, cellularity	129
Natural			
Collagen type II-GAG	$18x10^6$ calf or dog fibrochondrocytes/cm^3, 3 wks	<10% contraction, 2-fold increase in DNA content, GAG and type I collagen synthesis	42
Collagen type I-GAG	$18x10^6$ calf or dog fibrochondrocytes/cm^3, 3 wks	50% contraction, cells confined to margins of scaffold, produced GAG and collagen	42
Hyaluronic acid	$3.9x10^7$ bovine or human fibrochondrocytes/cm^3, 4 wks, mixed or rotating flask	Bi-zonal tissue created with meniscus-like collagen organization, matrix deposition, and mechanical behavior	309, 310
Agarose	$5x10^7$ rabbit fibrochondrocytes/cm^3, 7 wks	Some initial cell death, rounded cell morphology, some GAG and collagen production	129
Decellularized meniscus	10^5 sheep fibrochondrocytes/ml, 4 wks	Scaffold nontoxic, higher stiffness (17%) and compression (26%) than native	244
Scaffold-free			

Type	Details	Result	Ref.
Self-assembly	50:50 co-culture of bovine fibrochondrocytes and chondrocytes, meniscus-shaped agarose well, 8 wks	Stiffness anisotropic, circumferential modulus 226 ± 76 kPa, radial modulus 67 ± 32 kPa, meniscus-like collagen orientation, presence of GAGs and collagen types I and II	115
Self-assembly	50:50 co-culture of bovine fibrochondrocytes and chondrocytes, agarose well, 4 wks	Collagen I and II present, GAGs, constructs largely uncontracted	131
Self-assembly	Bovine fibrochondrocytes, agarose well, 4 wks	Collagen I and GAGs present, constructs contracted significantly	131

Table 8: Animal models used in meniscus tissue engineering

Animal model	Advantages	Disadvantages	Ref.
Rabbit	Commonly used for meniscus studies, cost, feasibility, relatively easily operable, small	Small, meniscal properties differ from humans	133, 311-316
Dog	Large, meniscus Poisson's ratio and permeability similar to humans, easily operable	Cost, feasibility	321, 322
Sheep	Large, easily operable	Cost, feasibility	319, 320
Pig	Large, meniscus Poisson's ratio similar to humans, easily operable	Cost, feasibility	323
Goat	Large, easily operable	Cost, feasibility	317, 318
Human	Most clinically relevant	Regulatory approval	326, 327

Table 9: Scaffolds for *in vivo* meniscus engineering

Type	Details	Result	Ref.
Synthetic			
PGA	$2.5x10^7$ bovine fibrochondrocytes/mL alginate, subcutaneous nude mouse, 16 wks	Fibrous matrix formation, presence of GAGs and collagen	324
PGA	$2x10^7$ bovine fibrochondrocytes/cm^3, subcutaneous nude mouse, 8 wks	Fibrous matrix formation, firm consistency, collagen and GAG presence	325
PGA	$2x10^6$ rabbit fibrochondrocytes/scaffold, meniscus-shaped scaffold, replaced meniscus in rabbit knee, 10 wks	Fibrous tissue formation, up to 40% collagen/dry weight, GAG and collagen type II found in inner portion of scaffold, type I collagen in outer portion	133
PLLA/PPD	acellular, filled rabbit partial meniscectomy defect, 14 wks	Fibrous matrix formation, some collagen alignment, some preservation of underlying hyaline cartilage	312
Natural			
Fibrin	Rabbit fibrochondrocytes, 8 wks	Cells able to produce sulfated GAGs, proliferate	316
Small intestine submucosa	Filled goat meniscal defect, 12 wks	Fibrous tissue formation, no organization, partially filled defect, hyaline cartilage degeneration	317
Acellular meniscus	Pig chondrocytes on surface of scaffold, filled longitudinal tear in avascular region of pig meniscus, 9 wks	Some healing of tear observed, matrix contained GAGs	323
Hyaluronan	Rabbit bone-marrow mesenchymal stem cells, rabbit meniscal defect, 12 wks	Some repair tissue formed, contained collagen type II	311

Type	Details	Result	Ref.
Collagen meniscus implant	Acellular, human meniscal defect, 5 years	Pain scores improved significantly, implant maintained structure	326
Collagen meniscus implant	Sheep fibrochondrocytes, sheep meniscal defect, 21 wks	Scaffold contraction, some fibrous repair tissue formed	319

Figures

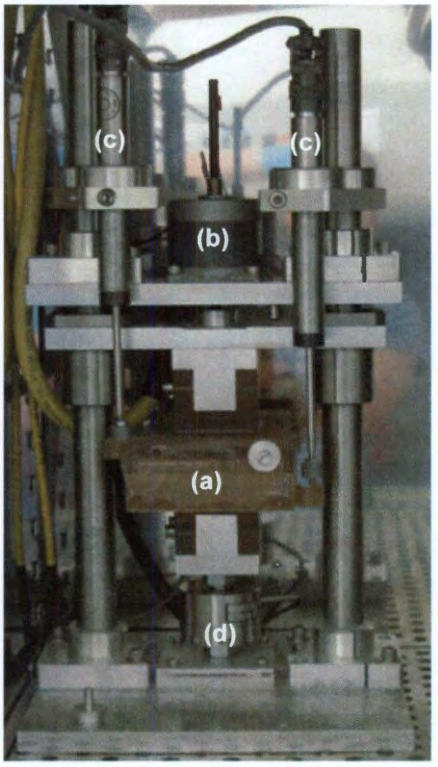

Figure 1: Direct compression bioreactor. The main component of a direct compression bioreactor is the loading chamber (a), inside of which constructs are placed for stimulation. A stepper motor (b) induces axial deformation to constructs in the load chamber and receives spatial feedback from the LVDTs (c) and force feedback from the load cell (d).

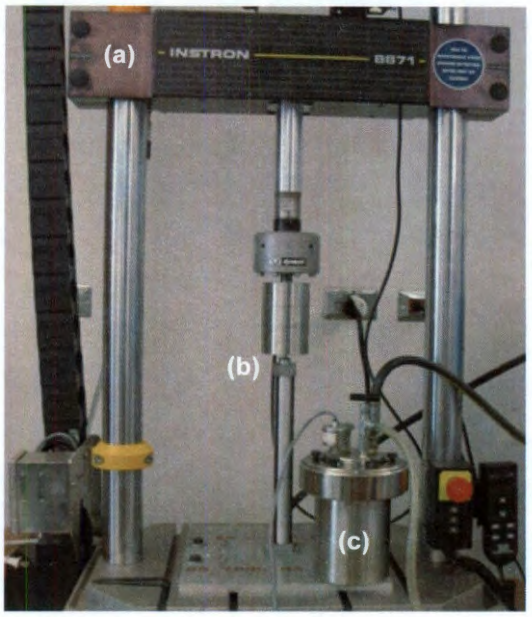

Figure 2: Hydrostatic pressure bioreactor. An Instron machine (a) drives a hydraulic piston (b) which pressurizes a sealed chamber (c). For stimulation, constructs are sealed in media-filled bags and placed in the water-filled chamber. The chamber is submerged in a water bath and pressurized via the hydraulic piston.

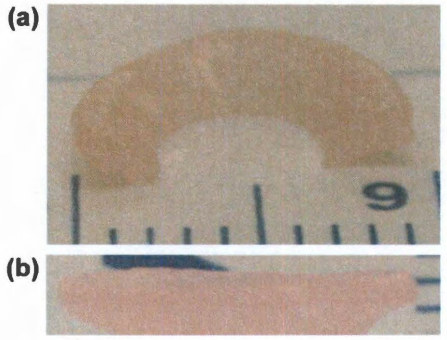

Figure 3: Self-assembled meniscus-shaped construct. The length (a) and height (b) in millimeters of a self-assembled construct after 4 weeks in culture is shown. The construct correctly mimics the wedge-shaped, semi-circular geometry of the native meniscus.

Chapter 10: Current Therapies for Meniscus Injuries

Section 10.1: Products and current therapies

Products involving biological materials

Currently, the only clinical product available for meniscus repair that uses biological materials is the Menaflex™ collagen meniscus implant, which has been approved for use in Europe and, more recently, in the United States. Developed in the United States by ReGen Biologics (Hackensack, New Jersey), the implant is approved for use in both the medial and lateral menisci in Europe, but in the U.S. it is currently only FDA approved for use in the medial meniscus. Menaflex™ is made of a collagen type I scaffold which can be sutured to the remaining meniscus following partial meniscectomy and degrades almost completely after one year. It has gone through several clinical trials and has shown an ability to allow cell infiltration and increase activity levels of patients who had a history of meniscus surgeries.[328] For patients with acute injuries who had not undergone previous surgeries on the meniscus, activity level increased the same amount with or without treatment with Menaflex™.[328] While activity levels do increase for patients with chronic meniscus problems, arthroscopic evaluation has revealed that this treatment will only partially fill a meniscus defect

---

Chapter published as: Athanasiou, K. A., and Sanchez-Adams, J. "Part 4: Current Therapies and Future Directions." *Engineering the Knee Meniscus*. Morgan and Claypool Publishers. 2009.

site (around 50–60% on average).[328] Additionally, the repair tissue resulting from Menaflex™ treatment is not extensively characterized, leaving the biomechanical benefits of the implant unknown. Therefore, though there exists a product on the market to address the need for replacement meniscus tissue, it may not be optimal in all cases and there is still a need for more alternatives.

Other current therapies

Clinical therapies for meniscus repair are varied. Meniscus surgery is most often performed arthroscopically, as this method is the least invasive and leaves the smallest scars. Depending on the type of meniscus injury, surgical techniques may involve arthroscopic suturing, other fixation devices, or meniscectomy. Abrasion may also be used to smooth the remaining meniscus tissue following meniscectomy. The success of sutures or other fixation devices to encourage healing of meniscus tears depends on the location of the tear. Tears in the outer portion of the meniscus are more likely to bond when held together due to the proximity of blood vessels, whereas tears in the inner region are unlikely to repair.

Suturing is a popular repair mode for bucket-handle tears as it can hold a tear closed to encourage bonding. Suture materials in use today are usually biodegradable, eliminating the need for subsequent procedures for removal. Suturing techniques can be inside-out, outside-in, or all-inside depending on where the suture material first enters the meniscus (see Figure 1).[329, 330] Suturing meniscus tears can take around 20 minutes using the inside-out technique, and

around 40 minutes using the outside-in technique.[331] Both of these suturing methods have around 100% success rates for healing a peripheral tear.[331] All-inside suturing techniques are less common, but can provide the benefit of reducing arthroscopic incision size compared to the other methods.[330, 332-334]

Recently, all-inside repair techniques that do not use sutures have gained popularity. These include meniscus arrows, screws, and anchors. These all-inside fixation devices take less time to place than normal sutures, though there is debate as to whether these methods work as well as suturing.[331, 335-342] Amongst the all-inside repair options, the most popular is the meniscus arrow. The meniscus arrow is quick and easy to implement, uses fewer incisions than suturing techniques, and has a higher success rate than either screws or anchors. Success rates for meniscus arrow treatments typically range from 70–95%.[338, 339, 343] In contrast, success rates for meniscus screws and anchors are reported to be around 27% and 65%, respectively.[331, 342] Though there are many benefits to using meniscus arrows, they also involve some risks including migration out of the tissue, inflammation of the surrounding tissue, and/or damage to the hyaline cartilage surfaces.[337, 340]

In some cases, the meniscus is so damaged that total meniscectomy is necessary. In this case the knee is either left without a meniscus or a meniscus allograft is implanted. Allografts, though scarce, can improve the stability of the knee and increase the success rate of ACL repair.[344] In arthritic joints, a meniscus allograft has an estimated lifetime of around 4.4 years and can decrease joint pain significantly.[345] Challenges to using meniscus allografts on a

large scale include difficulty in preserving, sterilizing, and attaching the tissue, as well as the limited lifetime of the material.[346]

Partial meniscectomy and abrasion are used to remove torn inner meniscus tissue that causes pain or impedes joint movement. In arthroscopic partial meniscectomy, a scalpel or other tool is used to cut away the torn tissue, leaving the rest of the meniscus intact. Following partial meniscectomy, abrasion may be performed to smooth out the remaining meniscal surface, thereby discouraging tear propagation or new tear formation. This mode of therapy was shown especially effective for tears of the posterior horn of the lateral meniscus, or radial tears that appear stable.[347]

Concepts

Presently, the only product available for meniscus repair that uses biological materials is the Menaflex™ collagen meniscus implant by ReGen Biologics. This product is a collagen type I sponge that can be sutured to the remaining meniscus after a partial meniscectomy. Menaflex™ is biocompatible, providing a scaffold for cell infiltration and new tissue formation, and has increased activity levels in some patients. Use of this product, however, has not demonstrated full defect healing. Other current therapies that do not involve engineered biological materials include sutures and other fixation devices (arrows, screws, anchors), meniscectomy, abrasion, and allografting. Suturing is most successful for vertical-longitudinal (bucket-handle) tears in the outer region of the meniscus and can be done three ways: outside-in, inside-out, or all-inside.

The all-inside technique has become popular with the introduction of meniscus arrows, which are easy and quick to implant as compared to suturing techniques. There is still controversy as to whether arrows work as well as sutures, and indeed the reported success rates for arrows are lower than for sutures. For inner region tears that are symptomatic, partial meniscectomy is often performed. Following partial meniscectomy abrasion of the remaining tissue can be performed to smooth out the tissue surface and discourage new tear formation. If the meniscus is thoroughly damaged, total meniscectomy may be performed and a meniscus allograft can be implanted. Allografts tend to work well for most patients, but they are generally scarce and conditioning them for implantation may compromise tissue integrity.

Section 10.2: Design standards for tissue engineering the meniscus

Determining design standards

Meniscus tissue engineering has made great advances in recent years, but has yet to produce a therapy that can fully restore function to a damaged meniscus. In the normal meniscus, a complex set of characteristics work together to form a tissue that is able to bear load, transfer stresses, absorb shock, and stabilize the knee joint. Ideally, a meniscal replacement would have the same properties as the native meniscus, but in practice it is difficult to get all of them to coexist using current tissue engineering modalities. Therefore, tissue engineers must carefully consider which meniscus properties they will reproduce such that

the resulting tissue is able to perform well in the body. Based on what is known about the role of the meniscus, there are certain characteristics that a meniscal replacement must have in order to restore function. Primarily, a meniscus replacement must be biocompatible and have specific geometrical and biomechanical attributes to operate well in the knee joint. Of secondary concern are the biochemical characteristics, vascularization, enervation, and cellularity of the replacement. Prioritizing meniscal attributes as such is advantageous to the tissue engineer as it allows for the design of a tissue that is maximally functional, a main concern for meniscus replacement options.

Primary standards

The main design standards important for tissue engineering a functional meniscus are proper geometry, biomechanics, and biocompatibility. The geometry of the meniscus has a central role in allowing for smooth joint movement and stabilization. Being wedge-shaped and semi-circular, the meniscus increases the congruence of the femur and tibia. The shape and size of tissue engineered constructs should therefore match that of the native meniscus to best restore meniscal function.

Biomechanical properties of the meniscus are also primary contributors to normal meniscus function. The anisotropic material behavior of the meniscus in tension, compression, and shear allows for dynamic load bearing and distribution and is imparted to the tissue through the organization of matrix molecules. Engineered meniscus tissue must also withstand these loading patterns, either

by organized matrix deposition or other means. Specifically, circumferential tensile properties for the engineered tissue must be higher than radial properties, and compressive properties must be higher in the inner portion than in the outer portion. Having mechanical properties regionally similar to native values will ensure that the construct is not destroyed upon implantation. This is especially important if the engineered tissue is used to fill a defect site, in which case mechanical similarity will ensure a normal distribution of load. Creating a biomechanically robust tissue is also advantageous for surgical implantation. Fixation methods involving screws and sutures place great amounts of local stress on the tissue. As it is known that the meniscus relies heavily on tibial horn attachments for anchoring within the joint, it is imperative that a replacement tissue is able to withstand these fixation stresses in addition to loading stresses.

The safety of an implantable meniscal replacement is not only linked to its function within the joint, but also to its immune response. Biocompatibility is, of course, a primary concern for tissue engineering the meniscus as this attribute can increase safety, which is highly important for eventual clinical approval. Increasing the biocompatibility of the engineered tissue by using natural scaffolds or scaffolds with non-toxic degradation products, or using autologous cells can reduce the likelihood of an immune reaction in the body.

Secondary standards

Creating a tissue that mimics the geometrical, biomechanical, and biocompatibility of the native meniscus may be sufficient to restore function, but

there are some secondary characteristics that could increase its longevity and overall compatibility within the body. These include biochemical makeup, vascularization, and cellularity. Once the primary functional characteristics are achieved in a meniscal replacement, these secondary characteristics should be examined.

There are many different chemical components that make up meniscus tissue, yet all of their functions are not known. Given their relative abundance in the tissue, however, collagens and proteoglycans seem to be the main biochemical contributors. Their distributions and orientations within the meniscus contribute greatly to the regional variation in mechanical properties, highlighting the need for tissue with complex regional makeup for replacement. Specifically, collagen is primarily oriented circumferentially, and proteoglycans are most abundant in the inner portion of the meniscus. Collagen type I is the primary type of collagen in the outer portion, while collagen type II is more abundant in the inner portion. Mimicking the regionally varying relative abundance of these two components of the meniscus, as well as their structural organization, may lead to appropriate mechanical properties. It should be noted, however, that other molecules such as those used for adhesion may be important for tissue organization and overall function. The functions of many of these minor biochemical components of the meniscus are not well understood, but they could play an important role in creating a functional construct.

Because not all of the functions of a meniscal blood supply are known, the importance of vascularization for a tissue engineered meniscus is difficult to

determine. In the normal adult meniscus, the blood supply is confined to the peripheral two-thirds and helps in tissue remodeling following injury. It is likely also responsible for proper delivery of nutrients and removal of waste products. Depending on the cellularity and permeability of the engineered tissue, vascularization could play an important role in allowing the tissue to thrive indefinitely.

The cellular aspects of an engineered meniscus are also of secondary concern. As many as four different types of cells have been identified in the meniscus, though their functions are not well understood. The morphologies of these cells range from rounded in the inner portion of the meniscus to having many cell processes in the outer portion. While in general cells are important for the creation or remodeling of tissue, little is known about the extent of remodeling that takes place in the adult meniscus. For engineered tissue, cells are important for creating specific types of matrix molecules that can aid in developing a mechanically robust construct. It is unclear, however, whether having the exact types and morphologies of cells found in the native meniscus is necessary for maintaining the overall function of an engineered meniscus.

Concepts

In designing an engineered meniscal replacement, much thought must be put into which characteristics are most important to the overall function of the construct. For the meniscus, a biomechanically active tissue, primary design standards focus on recreating functional aspects. These include mimicking

meniscus geometry, biomechanics, and biocompatibility. Of secondary concern are the specific biochemical makeup of the construct, its vascularity, and the types of cells that it contains. By focusing primarily on the functional aspects, a robust and clinically suitable tissue may be achieved. As more is discovered about the specific functions of meniscus matrix molecules, vascular supply, and cells, these secondary criteria may become useful to extend construct longevity and compatibility in the body.

Section 10.3: Assessments for tissue engineered constructs

Need for functional assessment

Whether or not engineered meniscus tissue will perform well *in vivo* may depend on many different factors, including biochemical and biomechanical properties of the engineered neotissue. Not only do laboratories engaged in tissue engineering need standards to evaluate the functionality of their work, but regulatory agencies must likewise determine the type of assessments required for approval of such products.

Functionality index

Common methods to functionally evaluate engineered meniscus tissue are tensile tests, compression tests, shear tests, and biochemical assays. Ideally, all of these measurements would be taken, and the collective set of properties would be compared to native tissue. Typically, however, only one measurement

is compared to the gold standard at a time, giving a limited view of the overall functionality of the engineered construct. Determining this overall functionality is not trivial, as some construct properties will inevitably be closer to native values than others. Using a functionality index (FI) is one way to assess the overall similarity of an engineered tissue to known native values. This method uses a weighted average taken of the similarity fractions of the engineered tissue's properties compared to native values. The FI has been used previously to compare engineered hyaline cartilage to native hyaline cartilage.[348]

$$FI = \frac{1}{4}\left(\begin{array}{l} \left(1-\frac{\left(G_{nat}-G_{ec}\right)}{G_{nat}}\right)+\left(1-\frac{\left(C_{nat}-C_{ec}\right)}{C_{nat}}\right)+\frac{1}{2}\left(1-\frac{\left(E^{T}_{nat}-E^{T}_{ec}\right)}{E^{T}_{nat}}\right)+ \\ \frac{1}{2}\left(1-\frac{\left(E^{C}_{nat}-E^{C}_{ec}\right)}{E^{C}_{nat}}\right)+\frac{1}{2}\left(1-\frac{\left(S^{T}_{nat}-S^{T}_{ec}\right)}{S^{T}_{nat}}\right)+\frac{1}{2}\left(1-\frac{\left(S^{C}_{nat}-S^{C}_{ec}\right)}{S^{C}_{nat}}\right) \end{array} \right) \quad \text{(Equation 1)}$$

In the functionality index above (Equation 1), G and C represent the total GAG and total collagen per wet weight, E represents stiffness and S represents strength. Superscripts of T and C indicate tensile and compressive properties, respectively, and the subscripts 'nat' and 'ec' indicate natural or engineered construct properties, respectively. According to this equation, equal weight is given to biochemical and mechanical properties. This could be adjusted, however, if one property demonstrates a dominant role in the overall functionality of the tissue. As the right hand side of the equation approaches a value of 1, the engineered tissue approaches the properties of native tissue. A value close to zero indicates that the engineered tissue has much lower properties than native tissue, and a value higher than 1 indicates that some or all of the engineered

tissue's properties are higher than native values. The functionality index can therefore provide an extra measure of engineered tissue's similarity to native tissue by considering all measured properties simultaneously.

Variable considerations

There are many different considerations to make when writing a functionality index equation. Weights must be assigned to each parameter based on its overall importance to tissue functionality. Whether to assign mature or immature tissue properties to the native tissue variables in the equation must also be determined. Once the equation is formulated, a level must be set to determine satisfactory or unsatisfactory similarity to the comparison tissue.

In the above example, equal weight is applied to biochemical and mechanical properties. For the meniscus, as it is known that mechanical integrity plays a large functional role, more weight might be shifted toward mechanical performance. Other parameters that take into account the circumferential versus radial stiffness and strength could also be included in the equation to assess appropriate functional behavior.

As engineered meniscal tissue is likely to be implanted into adult patients, using adult tissue properties as a comparison in the FI equation could provide valuable information. During the process of tissue development, however, engineered meniscus constructs may exhibit immature properties. Immature native tissue properties could therefore be used in the FI during this process to determine if engineered tissue mimics native tissue in early developmental

stages. While it is unclear whether native properties should be attained prior to implantation or if a construct can mature *in vivo*, the FI is a useful tool to determine similarity between engineered and native tissues and may eventually be used to identify the readiness of a construct for implantation.

A highly important consideration for the tissue engineer is how similar an engineered tissue must be to native tissue in order to be useful in the body. The functionality index is suited to quantify this similarity, but it remains to be determined what FI threshold must be reached to indicate acceptable properties. More research must be done to determine suitable characteristics for implantation, but once this threshold is determined, engineers will have a tangible success criterion that takes into account many different aspects of an engineered tissue.

Concepts

Engineers use various tests to functionally assess their tissue engineered constructs. The properties that are measured are usually considered alone, allowing for only a limited understanding of tissue functionality. The functionality index (FI) can be used to consider all measured properties of an engineered construct compared to native tissue. This allows for an overall assessment of tissue functionality. The FI is calculated by taking the average of similarity fractions of engineered tissue properties compared to native tissue properties. An unlimited number of properties can be included in this equation, and different weights can be assigned to each property based on its importance to tissue

performance. When writing a functionality index equation for engineered meniscus tissue, it may be necessary to weight certain mechanical properties higher than biochemical properties, given its highly biomechanical role in the body. Also of importance is determining what type of tissue (mature or immature) to use for comparison, as well as identifying an FI value that indicates an acceptably functional tissue.

Figures

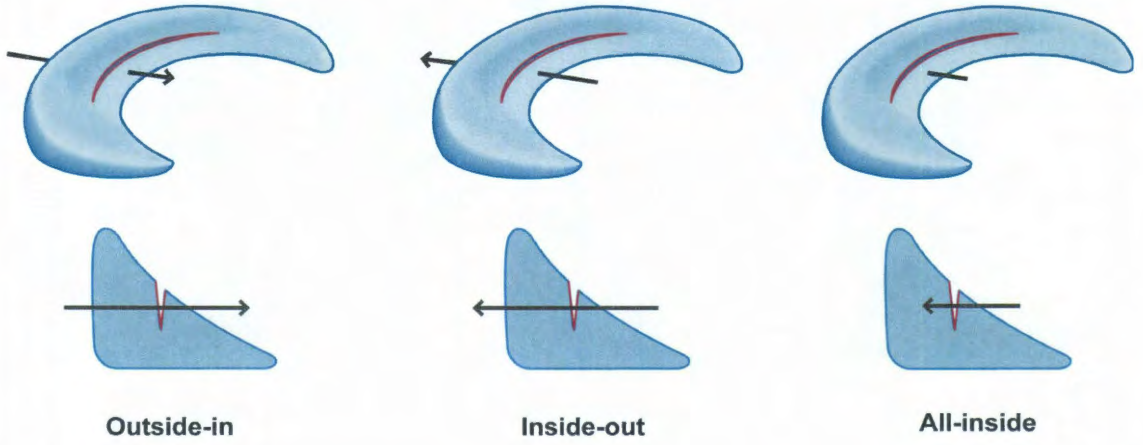

Figure 1: Meniscus suturing techniques. There are three main modes of suturing the meniscus arthroscopically. The outside-in technique passes the suture material from the periphery of the tissue to the inner surface, while the inside-out technique passes the suture into the meniscus from within the joint space, exiting at the periphery. The all-inside technique does not affect as much of the meniscus, as the suture enters and exits only at the inner portion of the tissue. Other repair methods such as the meniscus arrow are considered all-inside techniques as they are implanted into the tissue via the inner surface.

Chapter 11: Dermis Isolated Adult Stem Cells for Cartilage Tissue Engineering

Abstract

Adult stem cells from the dermal layer of skin are an attractive alternative to primary cells for meniscus engineering, as they may be easily obtained through out-patient biopsy techniques and used autologously. Recently, chondroinducible dermis cells from caprine skin have been identified that show promising characteristics for cartilage tissue engineering. In this study, their multilineage differentiation capacity is determined, and methods of expanding and tissue engineering these cells are investigated. It was found that these cells could differentiate along adipogenic, osteogenic, and chondrogenic lineages, allowing them to be termed dermis isolated adult stem cells (DIAS cells). Focusing on cartilage tissue engineering, it was found that passaging these cells in chondrogenic medium containing basic fibroblast growth factor and forming them into self-assembled tissue engineered constructs caused upregulation of collagen type II and COMP gene expression. Further investigation into biochemical stimulation of self-assembled DIAS cell constructs showed that application of either transforming growth factor β1 (TGF-β1) or bone morphogenetic protein 2 (BMP-2) caused increased sulfated glycosaminoglycan content. Additionally, TGF-β1 treatment caused significant increases in

---

Chapter submitted as: Sanchez-Adams, J., and Athanasiou, K.A. "Dermis Isolated Adult Stem Cells for Cartilage Tissue Engineering." *Biomaterials.*

viscoelastic compressive properties: 14-fold, 5.5-fold, and 7-fold increases in modulus of relaxation, instantaneous modulus, and coefficient of viscosity, respectively, compared with controls, but also resulted in the most contracted constructs. In contrast, BMP-2 treatment resulted in the largest and most hydrated constructs, but did not increase compressive properties over untreated controls. These results show that DIAS cells can be easily manipulated for cartilage tissue engineering strategies, and may also be a useful cell source for other mesenchymal tissues.

Introduction

Injuries to the knee meniscus are common and severely compromise the tissue's ability to stabilize, distribute load, and absorb shock in the knee joint.[1, 23, 24, 29] Unfortunately, meniscus regenerative capacity is limited and clinical therapies are often insufficient to restore full functionality.[3, 4, 12, 195, 197-199] Meniscus tissue engineering efforts seek to address this problem by creating functional replacement tissue, often using primary cells from hyaline and meniscal cartilages.[111, 116, 131, 349, 350] However, these cells are scarce and concerns of donor site morbidity hinder their use as autologous cell sources. In contrast, stem cells are an abundant alternate cell source for meniscus tissue engineering, and can be derived from embryos, umbilical cords, or adult tissues. Among these, adult stem cells are especially useful as they may be harvested from a patient's own body as needed and used to create autologous tissue, avoiding the concern for immune rejection. While adult stem cells have been

identified in many tissues in the body,[302, 306, 351-356] skin is an especially attractive source since it is the body's largest organ and has high regenerative capacity.

Stem cells have been identified in all regions of the skin: epidermis,[356-358] dermis,[302, 304, 355, 359-361] and hair follicles,[362-365] but dermal stem cells are of particular importance as they are of mesodermal origin, and have the potential to regenerate mesenchymal tissues such as cartilage. Recently, a chondroinducible population of dermis cells from adult caprine skin has been identified,[302] which could be used to repair meniscal tissue. These cells have many benefits for cartilage tissue engineering as they are easily isolated from the dermal population through rapid adherence to tissue culture treated plastic, and show high chondroinductive potential when plated on an aggrecan-coated surface. Engineered cartilage formed from these cells could also be implanted autologously into the goat, a mid-sized animal model, which is an important benefit for developing strategies that could be translated for eventual clinical application. In fact, autologous implantation of cartilage constructs has successfully been employed in the goat, indicating that this animal model may also be appropriate for *in vivo* meniscus tissue engineering studies.[366] Although these cells can be induced toward a chondrogenic phenotype, their multilineage differentiation capacity and a viable mode of expanding them for tissue engineering have yet to be determined.

To achieve a high number of these cells for tissue engineering, expansion must occur prior to construct formation. Identifying a method to expand these cells while not compromising their chondroinductive capacity is of paramount

importance to their use in tissue engineering strategies. For other cell types, such as bone marrow derived mesenchymal stem cells (MSCs), monolayer expansion conditions are known to be important for maintaining differentiation capacity. Basic fibroblast growth factor (bFGF) has been used to successfully expand MSCs while maintaining their chondrogenic differentiation capacity, allowing for the production of a large number of cells suitable for tissue engineering.[367, 368] This growth factor may therefore be an important media additive for expansion of chondroinducible dermis cells.

It is unclear, however, whether expansion should occur before or after the chondroinduction phase. Previous work used minimal cell expansion, and seeded cells onto aggrecan-coated surfaces to form chondroinduced cell nodules.[302] This mode of chondroinduction has been proven effective, yet inconsistencies in nodule formation could be diminished by employing alternative methods. Micromass culture of MSCs is an effective mode of achieving chondrogenic differentiation.[369-371] In this method, a high density of cells is seeded in a droplet and allowed to coalesce into a cell mass, which is cultured with various stimuli to cause differentiation. Micromass culture alone or on bioactive molecule-coated surfaces may therefore provide a more consistent mode of chondroinducing dermis cells, though cell dissociation will still be necessary to form homogeneous constructs.

It is unknown whether a chondroinduction step is necessary before expanded chondroinducible dermis cells are formed into tissue engineered constructs. Self-assembled constructs formed from chondroinducible dermis

nodules have shown promising cartilage-like biochemical properties,[302] but residual matrix from developed nodules likely inhibits construct homogeneity. Cell dissociation following chondroinduction and prior to self-assembly would alleviate this problem, as is often performed with human embryonic stem cell (hESC) embryoid bodies,[372-374] but self-assembling cells immediately after expansion would offer the simplest and most advantageous solution. As it is known that these cells are sensitive to three-dimensional chondroinduction, self-assembling expanded cells in the appropriate medium may simultaneously chondroinduce the cells and produce tissue engineered constructs.

Once tissue engineered constructs are formed, various stimuli can be applied to enhance cartilage-like biochemical and biomechanical properties. Previously, engineered constructs formed from chondroinduced dermis cell nodules were cultured with transforming growth factor β1 (TGF-β1) and insulin-like growth factor I (IGF-I), but the individual effects of these agents have not been determined.[302] These tissue engineered constructs may also be sensitive to other biomolecules known to be potent promoters of chondrogenesis, such as bone morphogenetic protein 2 (BMP-2).[375-379] Understanding the biochemical and biomechanical effects of these different growth factors on engineered constructs formed from chondroinducible dermis cells will help to identify an effective method of using these cells for functional tissue engineering of cartilaginous tissues such as the knee meniscus.

Previously identified chondroinducible dermis cells are a potentially abundant cell source for meniscus tissue engineering, motivating more

comprehensive development of methods for their expansion, chondroinduction, and tissue engineering. Therefore, in phase 1 of this study combinations of monolayer expansion, micromass chondroinduction, and self-assembly will be applied to a sub-population of adult dermis cells to determine a promising expansion and chondroinduction method for further tissue engineering. It is hypothesized in phase 1 that expansion will not hinder chondroinductive capacity, and that glycosaminoglycan (GAG) coated surfaces will enhance chondroinduction compared with non-coated surfaces. In phase 2, the most promising cell population from phase 1 will be exposed to a variety of mesenchymal differentiation protocols to determine their multilineage differentiation capacity. These cells will also be used to form self-assembled constructs for cartilage tissue engineering and the effects of various growth factors on the phenotypic, biochemical, and biomechanical cartilage-like properties of the constructs will be measured. In this phase, it is first hypothesized that the population of cells identified in phase 1 will show multilineage differentiation capacity. It is also hypothesized that, when used in a cartilage tissue engineering modality, constructs formed from these cells will show varying cartilage-like biochemical and biomechanical effects in response to different growth factors. The results from this phased approach will determine if previously identified chondroinducible dermis cells are multipotent stem cells and provide a method for expansion and tissue engineering with these cells towards the repair of meniscal defects.

Materials and Methods

Cell isolation

Abdominal skin from 5 six-month-old Spanish goats were obtained from a local abattoir [Nature's Bounty, Dixon, CA]. Skins were washed, sub-dermal fat and muscle was removed, and dermal tissue was dissected from epidermal tissue, and placed in a collagenase solution containing Dulbecco's Modified Eagle Medium with Glutamax (DMEM) [Invitrogen, Carlsbad, CA], 1% penicillin/streptomycin/fungizone (P/S/F) [Lonza, Basel, Switzerland], 1% non-essential amino acids (NEAA) [Invitrogen], and 0.2% w/v collagenase type 2 [Worthington, Lakewood, NJ]. Tissue was digested overnight at 37°C with gentle shaking. Following digestion, cells were counted and frozen in liquid nitrogen in DMEM containing 20% fetal bovine serum (FBS) [Atlanta Biologicals, Lawrenceville, GA] and 10% dimethyl sulfoxide [Sigma-Aldrich, St. Louis, MO].

Phase 1

In Phase 1, cells were thawed and seeded in expansion medium (EM) containing 10% FBS, 1% P/S/F, and 1% NEAA and allowed to reach 90% confluence. Cells were visually inspected to ensure that no epithelial cells were present in the population. Cells were then passaged and an isolated sub-population of cells with high chondrogenic potential was obtained by rapid adherence (RA) to tissue culture-treated plastic (TCP) for 10 minutes in EM, as previously described.[302] Adherent cells were grown to 90% confluence in EM

(RA-2D cells). Three different modes of chondroinduction (chondrogenic passaging, self-assembly process, and micromass formation) were then evaluated to determine the most promising mode of chondroinduction for further tissue engineering using RA-2D cells. Figure 1 depicts a schematic of phase 1, with cell populations analyzed shown in dashed boxes. Following expansion, RA-2D cells were either set aside for quantitative RT-PCR (qRT-PCR), formed into micromasses (uM), or plated in monolayer and passaged up to three times.

Micromass formation

Non-TCP (NT) 24-well plates were either coated with 0.08% chondroitin sulfate (CS) solution or not. In coated wells, 20 µL of CS solution was placed in the center of each well, and allowed to dry overnight. RA-2D cells were then seeded at high density (20 µL of $10x10^6$ cells/mL) on coated or non-coated wells to form micromasses. After 4 hours, 1 mL of chondrogenic medium (DMEM with 1% P/S/F, 1% NEAA, 10-7 M dexamethasone, 5mM L-ascorbic acid 2-phosphate, 0.4 mM L-proline, and 10 mM sodium pyruvate) containing 10 ng/mL of transforming growth factor β1 (TGF-β1), and 100 ng/mL of insulin-like growth factor I (IGF-I), was added to each well. Four micromasses were formed per group and cultured for 2 weeks in hypoxic conditions (5% O_2); media was changed every other day. The resulting micromasses were termed RA-CS-uM and RA-NT-uM, and were either set aside for qRT-PCR analysis, or were dissociated into single cells using 0.2% collagenase solution and passaged in chondrogenic medium three times to yield cells for tissue engineering.

Chondrogenic Passaging

RA-2D cells were also seeded in monolayer and passaged in chondrogenic medium containing 1% FBS and 100 ng/mL of basic fibroblast growth factor (bFGF) up to three times. At each passage, cells were grown to 80% confluence. At passages 2 and 3, cells were set aside (cP2-2D and cP3-2D) for qRT-PCR analysis. Passage 3 cells were also used to form micromasses on non-TCP and CS-coated surfaces as described above (cP3-NT-uM and cP3-CS-uM), and resulting micromasses were analyzed with qRT-PCR for cartilage-specific gene expression.

Self-assembly

cP2-2D and cP3-2D cells, and passaged cells from RA-CS-uM and RA-NT-uM, were also formed into tissue engineered (TE) constructs using the self-assembling method as described previously.[161, 210] Briefly, $2x10^6$ cells were seeded into cylindrical, 3 mm-diameter agarose wells and cultured for 4 weeks in normoxic conditions (21% O_2) in chondrogenic medium (CM). Four constructs were formed from each group and medium was changed every other day. The resulting self-assembled constructs were termed cP2-TE, cP3-TE, RA-CS-TE, and RA-NT-TE and were analyzed using qRT-PCR for cartilage-specific gene expression.

qRT-PCR

RNA from cell populations, micromasses, and constructs in phase 1 was extracted using an RNAqueous-Micro Kit [Invitrogen]. Resulting RNA was then reverse-transcribed using the SuperScriptTM III First-Strand Synthesis System [Invitrogen], and then PCR was performed on the resulting cDNA for cartilage-specific genes using SYBR® Green PCR Mastermix, 80-100 ng of sample cDNA, and 900 nM of each primer. PCR analysis was performed using a RotorGene 3000, with the following protocol: 50°C for 2 min, 95°C for 10 min, followed by 40 cycles of 95°C for 15 sec and 60°C for 60 sec. Bovine 18s rRNA was used as a housekeeping gene for each group. All fold-change calculations were determined by normalizing data to RA-2D cells using the formula $y = 2^{\Delta\Delta C_t}$, where $\Delta\Delta C_t$ represents the difference in take-off cycle between experimental and control groups. Forward and reverse primers for Sox9, collagen type I, collagen type II, COMP, and aggrecan were obtained from the literature.[102, 164-166] Gene expression data were analyzed using a one-way ANOVA, with a significance level of $p < 0.05$.

Phase 2

Based on gene expression data, cP2-2D cells were carried forward from phase 1 (termed cP2 cells in phase 2), and subjected to multilineage differentiation or tissue engineering.

Multilineage Differentiation

To determine their multipotency, cP2 cells were subjected to adipogenic, osteogenic, or chondrogenic differentiation protocols commonly used for differentiation of mesenchymal stem cells. For adipogenic and osteogenic differentiation, cells were seeded into 6-well plates and allowed to reach 80% confluence in base medium (DMEM containing 16.5% FBS, 1% P/S/F, and 1% NEAA). Wells were then cultured an additional 3 weeks with base medium (control), adipogenic medium (base medium with 0.5 μM dexamethasone, 0.5 mM isobutylmethylxanthine and 50 μM indomethacin), or osteogenic medium (base medium with 10 nM dexamethasone, 20 mM β-glycerolphosphate, and 50 μM L-ascorbic acid 2-phosphate). For chondrogenic differentiation, cell pellets were formed by centrifuging 0.2 $x10^6$ cells at 450 x *g* for 10 minutes. Pellets were fed with base medium (Control) or chondrogenic medium with 10 ng/mL TGF-β1 and 100 ng/mL BMP-2. Resulting cell populations or pellets were analyzed histologically for adipogenic differentiation (Oil Red O), osteogenic differentiation (Alizarin Red), and chondrogenic differentiation (Safranin-O and collagen type II immunohistochemistry).

Self-Assembly and Gross Morphology

Tissue engineered constructs were formed as in phase 1, and cultured for 5 weeks in chondrogenic medium alone (Control) or with 100 ng/mL IGF-I, 100 ng/mL bone morphogenetic protein 2 (BMP-2), or 10 ng/mL TGF-β1. Culture conditions and medium changes were carried out as in phase 1, and 16 constructs were formed per group. Pictures were taken of constructs from each

group weekly during the culture period to qualitatively assess morphological changes. Following the culture period, construct diameter, thickness, wet weight and dry weight were measured, and constructs from each group were assessed biomechanically, histologically, biochemically, and with qRT-PCR.

Histology & Immunohistochemistry

Constructs from each group were cryosectioned and stained with Safranin-O or Picrosirius Red to visualize sulfated glycosaminoglycans (GAGs) and total collagen, respectively. Sections were also stained using immunohistological methods to visualize collagen types I, II and VI.

Biochemistry

Total collagen and glycosaminoglycan content was measured in constructs from each group using a hydroxyproline assay or a dimethyl-methylene blue assay [Biocolor, Carrickfergus, UK], respectively. DNA content was also measured in each group using a PicoGreen® Assay Kit [Invitrogen, Carlsbad, CA], and normalized to cell number using 7.7 ng DNA/cell. Additionally, collagen types I and II were measured using indirect enzyme-linked immunosorbent assays (ELISAs). Anti-collagen type I [Accurate Chemical, Westbury, NY] and anti-collagen type II [Fitzgerald, Acton, MA] antibodies were used to detect collagen types I & II in tissue engineered constructs, and were normalized to control constructs.

Compressive testing

Following the 5 week culture period, constructs from each group were tested in unconfined compression stress-relaxation. Samples were preconditioned with 15 cycles of 0-5% compressive strain, and then stress-relaxation tests were carried out at 10% and 20% strain. As described previously, a Kelvin solid viscoelastic model was fit to the data to yield the following compressive material properties at each strain level: instantaneous modulus (Ei), modulus of relaxation (Er), and viscosity (μ).[156]

Statistics

One-way ANOVAs were used to analyze quantitative data, with significance set at $p < 0.05$. If warranted, a Tukey's post-hoc test was performed to determine differences between groups.

Results

Phase 1

qRT-PCR

Quantitative RT-PCR analysis of cartilage-specific genes for cells (2D), micromasses (uM), and constructs (TE) formed in phase 1 showed distinct differences (Figure 2). In particular, regardless of pre-treatment, aggrecan gene expression in uM groups was significantly higher than the 2D or TE groups (332-

fold to 788-fold increase over RA-2D cells). Collagen type I gene expression also trended higher in the uM groups, and was significantly higher in the RA-NT-uM (3.8 ± 0.72 fold change) and cP3-CS-uM (3.8 ± 0.48 fold change) groups compared with the 2D and TE groups. In contrast, the TE groups and chondrogenically passaged cells (cP2-2D and cP3-2D) showed down-regulation in collagen type I compared with RA-2D cells. Gene expression for COMP trended higher in TE groups and was statistically higher than 2D and uM groups in the RA-NT-TE group (132 ± 50 fold change). Similarly, collagen type II expression trended higher in the TE group, and was statistically higher in the cP2-TE group (28 ± 14 fold change). Little variation in Sox9 gene expression was observed, however cP2-2D cells showed statistically lower Sox9 expression compared with RA-2D cells.

Phase 2

Multilineage Differentiation

cP2 cells showed the ability to differentiate along the adipogenic, osteogenic, and chondrogenic lineages (Figure 3). Cells exposed to adipogenic media stained positively for lipids, whereas cells exposed to base media did not. Cells in monolayer exposed to osteogenic media formed cell masses over the 4 week culture period, and stained positively for calcium deposits using Alizarin Red. Cell pellets exposed to chondrogenic medium and growth factors also

stained positively for sulfated GAGs and collagen type II, while control pellets were negative for these markers.

Gross Morphology

Over the 5 week culture period, various morphological changes were obsereved (Figure 4). At week 1, all groups showed some contraction. Contractile behavior was enhanced at week 2 for all groups, but appeared to plateau by week 3 in Control and IGF-I constructs. In TGF-β1 constructs, a slight increase in diameter was observed at week 3 compared with week 2 which was maintained throughout the rest of the culture period. Between weeks 2 and 3 BMP-2 constructs also increased in size, and continued to grow throughout the rest of the culture period. BMP-2 constructs showed statistically higher diameter and thickness measurements at the end of the culture period, as well as higher wet weight and dry weight compared to other groups. TGF-β1 constructs had statistically smaller diameter and wet weight measurements than other groups, but had higher dry weight than control and IGF-I constructs.

qRT-PCR

Gene expression for the starting population of cells (cP2 cells) were compared with that of tissue engineered constructs at the end of their 5 week culture period (Figure 5). Aggrecan and collagen type I gene expression was up-regulated for TGF-β1 constructs (77.3 ± 32.9 and 5.82 ± 0.27 fold change, respectively) compared with all other constructs and cP2 cells. COMP and

collagen type II expression was up-regulated in Control (28.6 ± 20.8 and 67.3 ± 33.6 fold change, respectively) and IGF-I (59.2 ± 31.6 and 73.5 ± 15.3 fold change, respectively) constructs compared with cP2 cells. Sox9 expression trended higher in all tissue engineered constructs compared with cP2 cells, and was statistically higher in IGF-I (27 ± 13.2 fold change) and TGF-β1 (24 ± 2.1 fold change) constructs.

Histology & Immunohistochemistry

Histological assessment of tissue engineered constructs is shown in Figure 6. Collagen types I, II, and VI were present in all tissue engineered constructs, though collagen type II was most prominent in BMP-2 and TGF-β1 constructs. Total collagen staining showed a dense collagenous matrix in TGF-β1 constructs, loosely packed collagen in BMP-2 constructs, and similar collagen densities in Control and IGF-I constructs. Sulfated GAG was detected in all constructs, and was diffusely distributed in BMP-2 constructs.

Biochemistry

Analysis of biochemical content and hydration is shown in Figure 7 A-F. All constructs contained similar cellularity, though TGF-β1 constructs contained statistically fewer cells than BMP-2 constructs. Overall, BMP-2 constructs showed the most hydration, while the TGF-β1 constructs were the least hydrated. Total GAG and collagen content was statistically higher in BMP-2 and TGF-β1 constructs compared with control constructs, though TGF-β1 constructs showed

the least amount of collagen type I compared with control constructs. All groups showed similar amounts of collagen type II.

Compressive testing

Results from viscoelastic compressive testing are shown in Figure 7 G-I. Compressive properties of TGF-β1 constructs were statistically higher than all other groups. Compared with control constructs, TGF-β1 constructs showed approximately 14-fold, 5.5-fold, and 7-fold increases in modulus of relaxation, instantaneous modulus, and coefficient of viscosity, respectively.

Discussion

This study identified a method to expand a sub-population of adult dermis cells that showed 1) multilineage differentiation capacity and 2) the ability to form tissue engineered constructs with cartilage-like properties. It also evaluated the effects of various growth factors on tissue engineered constructs formed from these cells, and found that both BMP-2 and TGF-β1 enhance cartilage-like compressive and biochemical properties. Given their demonstrated multilineage capacity and ability to form cartilaginous tissue, these cells are termed dermis isolated adult stem (DIAS) cells. The results from this study show that DIAS cells can be used as an alternate, and possibly autologous, cell source for meniscus tissue engineering, and may have wider applicability to engineering of other mesenchymal tissues.

In phase 1 it was found that DIAS cells subjected to chondrogenic passaging showed few differences from non-expanded cells, indicating that these cells may be expanded without compromising chondrogenic capacity. This was further demonstrated as micromasses formed from chondrogenically passaged DIAS cells showed nearly identical gene expression profiles to those formed from non-expanded DIAS cells. This similarity between non-expanded and chondrogenically passaged DIAS cells may be a result of the expansion conditions used, and could indicate that these cells are similar to other types of stem cells. Chondrogenic passaging was carried out in chondrogenic medium supplemented with bFGF, a growth factor used previously to maintain the multilineage differentiation capacity of MSCs and hESCs through many population doublings.[367, 368, 380] Although the mechanism by which bFGF maintains differentiation capacity is still under investigation, recent studies have drawn correlations between bFGF-treatment and decreased telomerase activity, suggesting that bFGF may play a protective role during cell proliferation.[368] The present results show that chondrogenic passaging using bFGF is an effective mode of achieving a large number of DIAS cells for cartilage tissue engineering.

Comparing the phenotypic changes of cell populations in phase 1, it was apparent that both three-dimensional culture systems (micromass and self-assembly) had marked chondroinductive effects on DIAS cells. Cells in micromass culture showed increased aggrecan gene expression, while self-assembly caused up-regulation in collagen type II and COMP. Although not yet fully understood, three-dimensional culture systems are thought to have a

beneficial effect on chondroinduction of stem cells by forcing a rounded cell morphology, similar to chondrocytes *in situ*. This rounded morphology is known to be important for the preservation of articular chondrocyte gene expression, as passaged chondrocytes show rapid phenotypic changes upon loss of this morphology.[166] In fact, beneficial effects of three-dimensional culture have been well-documented for the chondroinduction of MSCs[369, 371, 381, 382] and hESCs,[300, 383] indicating that DIAS cells are similar to these other cell types in their sensitivity to three-dimensional culture.

Although both micromass and self-assembly forced rounded cell morphology, their effects on cartilage specific gene expression were distinct. As micromass culture was carried out in hypoxic conditions and with growth factors, and self-assembled constructs were cultured in blank chondrogenic medium, this may have contributed to the difference in gene expression between micromass and self-assembled cells. Hypoxia has been shown previously to cause increased gene expression for collagen types I and II in meniscus tissue, and enhance collagen type II content and compressive properties of meniscus cell-seeded constructs.[384, 385] The growth factors used during micromass culture, TGF-β1 and IGF-I, have also caused increased cartilage specific protein content, mechanical properties, and cell proliferation in tissue engineered cartilage constructs.[108, 229, 298, 308, 348, 386] To begin to understand the contribution of these factors in the present study, growth factors were combined with self-assembled constructs formed from DIAS cells and phenotypic changes were measured. Results from phase 2 suggest that growth factors do have a marked phenotypic

effect on the cells, especially on upregulating aggrecan gene expression as seen in the TGF-β1 group. This result indicates that the large upregulation in aggrecan gene expression seen in micromass culture in phase 1 could be due to the application of TGF-β1. Although not tested in this study, hypoxia may also have an effect on aggrecan or collagen type II upregulation which could improve construct properties beyond those observed with growth factors, as shown in previous studies on cartilage explants and tissue engineered constructs.[384, 385] Growth factors such as TGF-β1, therefore, play a role in enhancing DIAS cell chondroinduction in three-dimensional culture.

In contrast to the proposed hypothesis, micromasses formed on GAG-coated surfaces did not show a general upregulation of cartilage-specific genes compared with those formed on non-TCP. In fact, the up-regulation of aggrecan gene expression observed in the micromasses was statistically higher for RA-2D cells on non-TCP than all other groups (Figure 2). Previous work using chondroinducible dermis cells has shown increased cartilage-specific gene expression of cells on GAG-coated surfaces,[302] but the effects of hypoxia in this process have not been previously tested. As hypoxia has been shown to upregulate TGF-β1 production by dermal fibroblasts,[387] and TGF-β1 was shown to increase aggrecan gene expression in phase 2, it is possible that the effects of surface coating may have been overshadowed by the effect of hypoxia. As micromasses formed from RA-2D cells on non-TCP showed the highest aggrecan gene expression, surface coating may actually interfere with the effects of hypoxia in non-expanded cells. These results indicate that hypoxia may be a

useful stimulus to apply during self-assembly in addition to, or in lieu of, TGF-β1 treatment.

As hypothesized, in addition to causing phenotypic changes, different growth factors caused varying effects on the mechanics and biochemistry of self-assembled DIAS constructs formed in phase 2. All constructs, regardless of growth factor stimulation, showed presence of collagens I, II, and VI, as well as sulfated GAG, indicating that self-assembly and culture in chondrogenic medium has some chondroinductive effect on DIAS cells. BMP-2 and TGF-β1 further enhanced the sulfated GAG content and compressive properties of self-assembled constructs, while IGF-I treated constructs were nearly identical to controls in almost all measures. Thus it was found that DIAS cells were most sensitive to BMP-2 and TGF-β1.

The biochemical properties of BMP-2 and TGF-β1 self-assembled DIAS constructs showed similarity to meniscus tissue. Though both growth factors increased glycosaminoglycan (GAG) content, BMP-2 constructs were considerably larger and more hydrated than other groups. The increased GAG content observed is agreement with other published work, which has shown that primary chondrocytes passaged in the presence of bFGF and subjected to tissue engineering with BMP-2 causes increased hydration and GAG content.[388] Other studies have shown TGF-β1 to be a potent enhancer of GAG content in tissue engineered constructs formed from many different cell types including chondrocytes, meniscus cells, MSCs, and hESCs.[348, 389-391] The GAG content per dry weight achieved in the present study for BMP-2 and TGF-β1 constructs was

approximately 1.2-1.6%. These values are on par with native values for the meniscus, which reportedly contains ~3.9% GAG per dry weight.[16] As GAG concentration is known to vary in the different meniscus regions,[9, 257] the GAG content achieved in DIAS cell constructs by applying BMP-2 or TGF-β1 may be representative of the middle meniscus region.

Compressive properties achieved by treating self-assembled DIAS cell constructs with TGF-β1 were also much higher than those achieved using other growth factors. Although TGF-β1 constructs were more contracted, they showed 14-fold, 5.5-fold, and 7-fold increases in instantaneous modulus, modulus of relaxation, and coefficient of viscosity compared with untreated controls. As TGF-β1 caused substantial contraction of DIAS cell constructs as well as increased GAG and collagen content, this increase in compressive properties could be a result of both biochemical and biophysical factors. Sulfated GAGs are known to be important in resisting compressive loads in cartilaginous tissues,[62-65] so increased GAG content in TGF-β1 treated constructs could be partly responsible for increased compressive properties. However, increased GAG content was also observed in BMP-2 constructs which did not show increased compressive properties. The observed contraction and increased total collagen content of TGF-β1 constructs could have made the difference between these groups by increasing matrix content and density. In fact, the difference in matrix density between groups is apparent in the histological sections of TGF-β1 and BMP-2 constructs (Figure 6). Interestingly, although TGF-β1 constructs showed higher total collagen content than all other groups, they contained statistically lower

collagen type I content with no difference in collagen type II content. Thus it is likely that the increased collagen content was due to other collagenous proteins present, such as type VI (Figure 6), or types III, IV, V, and XVIII which are also present in cartilage.[6, 12] The contraction observed in TGF-β1 constructs is also consistent with prior literature which shows that contraction is a well-documented phenomenon of TGF-β1-stimulated fibroblasts.[392-396] The observed effects of TGF-β1 on DIAS constructs are also in agreement with previous work on self-assembled cartilage cell constructs that show that TGF-β1 treatment causes increased GAG and collagen content as well as higher compressive properties.[229, 348] Comparing the present results with previous literature suggests that TGF-β1 affects DIAS cell constructs in similar ways as self-assembled native cartilage cell constructs, further indicating the cartilaginous nature of DIAS cell constructs. Given the promising results seen by adding BMP-2 and TGF-β1, further studies should investigate the effects of different combinations of these growth factors to achieve sufficient size and compressive properties of these tissue engineered constructs.

As well as forming cartilage-like tissue, DIAS cells used to create self-assembled constructs in phase 2 also showed multilineage differentiation capacity. The ability of these cells to differentiate along adipogenic, osteogenic, and chondrogenic lineages indicates that these cells are multipotent in nature, similar to other dermal stem cell populations. Although dermal multipotent stem cells have been identified previously, they have been isolated either from rodents[355, 360] or humans[304, 359, 397-399] but not from mid-sized animal models.

DIAS cells, isolated from goat skin, present an abundant source of dermal multipotent cells with the potential to be used for both *in vitro* and *in vivo* tissue engineering experimentation. Given the multipotent nature of DIAS cells, they may not only be a useful cell source for cartilage tissue engineering, but also as an autologous source for engineering of other mesenchymal tissues such as bone and fat, which are often needed for reconstructive surgeries.[400-404]

Conclusions

The methods developed in this study demonstrate the ability of DIAS cells to not only produce cartilage-like matrix, but also form tissue engineered constructs with robust mechanical properties. As determined in this study, DIAS cells may be passaged in monolayer without losing their multipotent nature, making them appealing for tissue engineering efforts which often require large cell numbers for construct formation. Due to the multipotent nature of these cells, it is possible that other biochemical or mechanical stimuli could be applied to self-assembled DIAS constructs to form functional bilayered tissue interfaces such as those observed between the meniscal horns and the tibial plateau.

Acknowledgments

We thank the National Science Foundation Rice-Houston Alliance for Graduate Education and the Professoriate (NSF-AGEP) for their generous support of this work. We would also like to acknowledge funding from "Use of

dermis derived cells for articular cartilage tissue engineering" Arthritis Foundation, Innovative Research Grant.

Figures

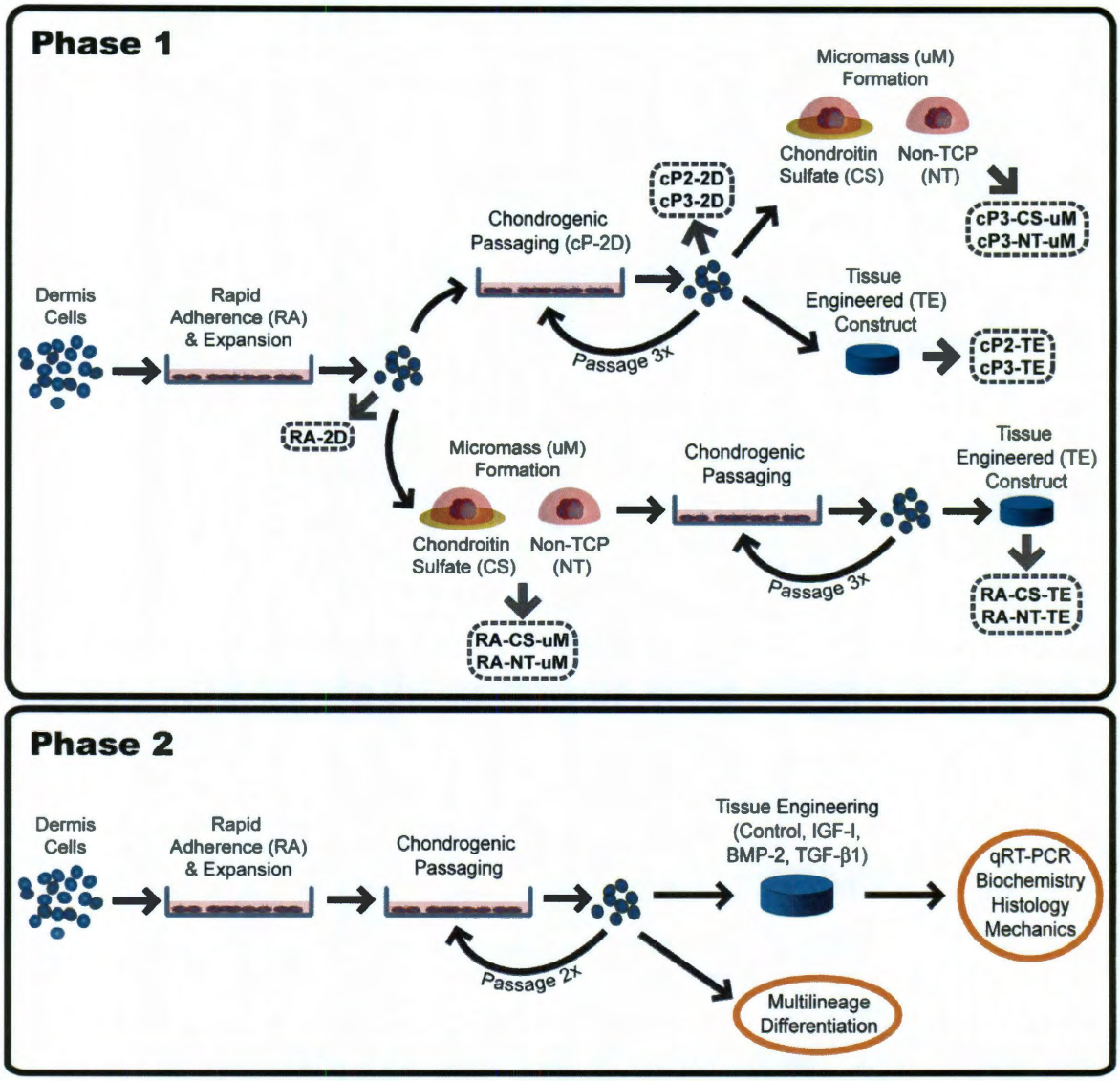

Figure 1: Schematic diagram of phases 1 and 2. In phase 1 an optimal method of expansion and chondroinduction for tissue engineering is determined by testing different combinations of expansion, chondroinduction, and tissue engineering. In phase 2, cells are tested for multilineage differentiation capacity, and the effects of growth factors tissue engineered constructs are measured.

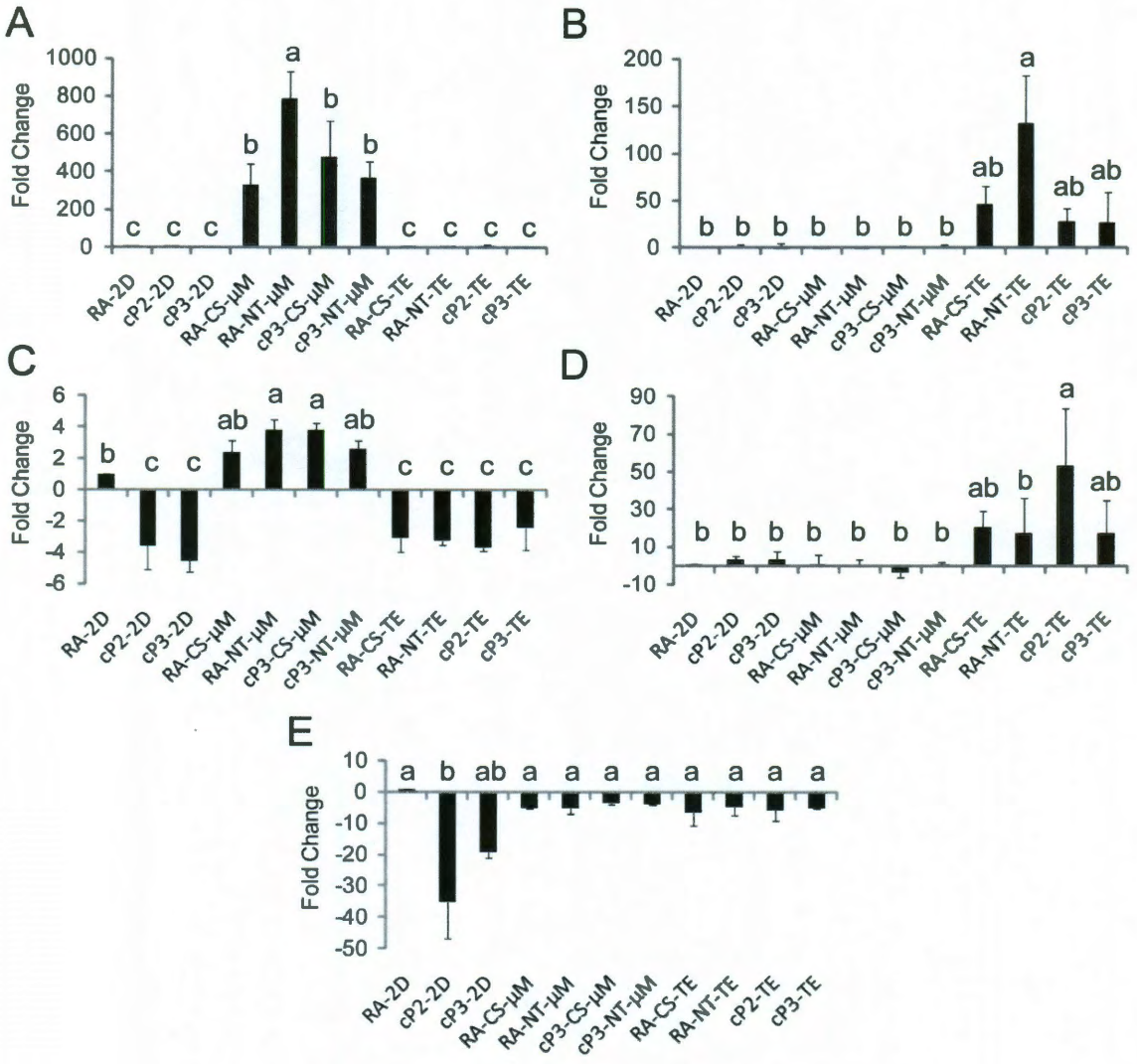

Figure 2: Phase 1 quantitative RT-PCR. Fold change in gene expression of aggrecan (A), COMP (B), collagen type I (C), collagen type II (D), and Sox9 (E) are compared among all cell populations produced in phase 1. Data were analyzed using a one-way ANOVA with Tukey's post-hoc, and significance was set at $p < 0.05$.

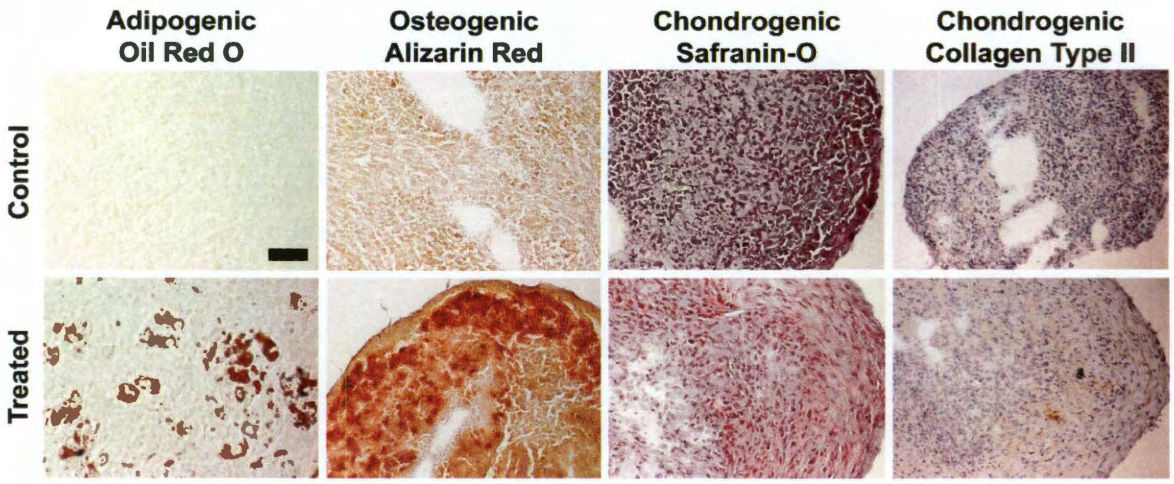

Figure 3: Phase 2 multilineage differentiation. Cells exposed to adipogenic, osteogenic, and chondrogenic differentiation regimens showed positive staining for lipids, calcium deposits, and sulfated glycosaminoglycan and collagen type II, respectively. Control cells and cell masses were negative for these markers.

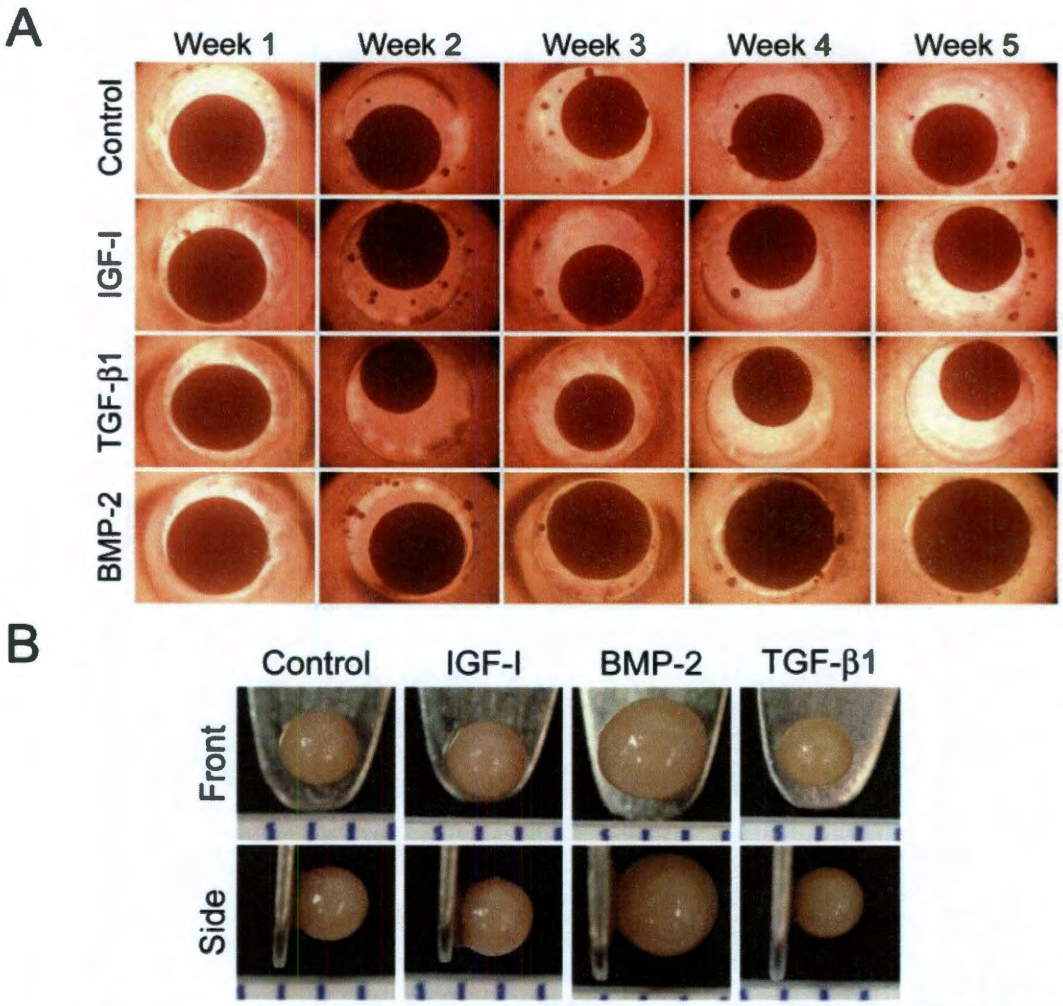

	Control	IGF-I	BMP-2	TGF-β1
Diameter (mm)	1.95 ± 0.04^{B}	1.96 ± 0.05^{B}	2.63 ± 0.15^{A}	1.8 ± 0.05^{C}
Thickness (mm)	1.77 ± 0.09^{B}	1.81 ± 0.06^{B}	2.38 ± 0.22^{A}	1.69 ± 0.08^{B}
Wet Weight (mg)	3.91 ± 0.14^{B}	4.03 ± 0.2^{B}	9.63 ± 1.09^{A}	3.16 ± 0.23^{C}
Dry Weight (mg)	0.63 ± 0.03^{C}	0.59 ± 0.07^{C}	0.97 ± 0.13^{A}	0.73 ± 0.07^{B}

Figure 4: Gross morphology of tissue engineered constructs. (A) 4x images of constructs in 3 mm wells during culture, and (B) constructs from each group following culture with diameter, thickness, wet weight, and dry weight measurements for each group. Data are presented as mean ± SD, and analyzed with a one-way ANOVA, $p < 0.05$.

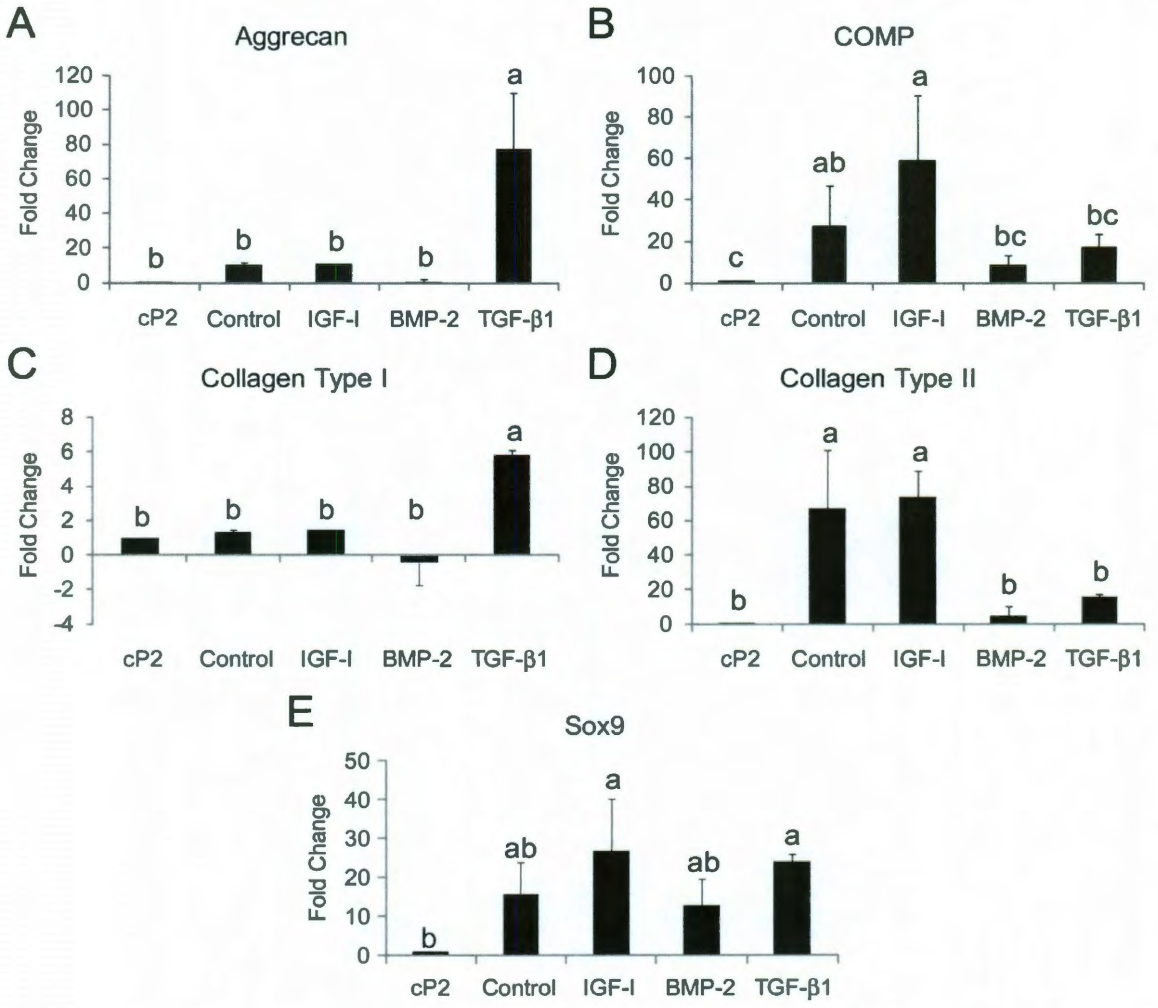

Figure 5: qRT-PCR of tissue engineered constructs. Fold change in expression of aggrecan (A), COMP (B), collagen type I (C), collagen type II (D), and Sox9 (E) are normalized to cP2 cells and compared between cP2 cells and tissue engineered constructs. Data analyzed with a one-way ANOVA and Tukey's post-hoc, $p < 0.05$.

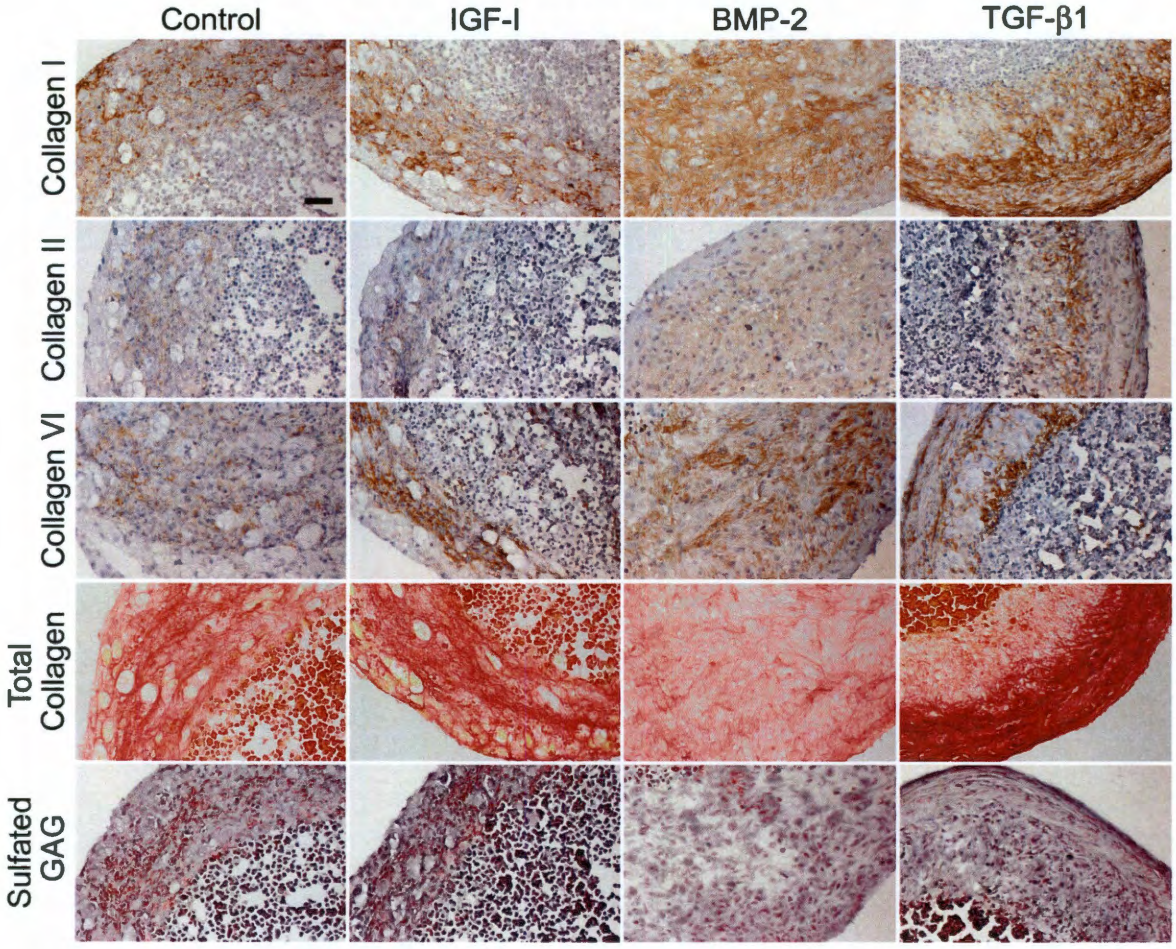

Figure 6: Histological assessment of tissue engineered constructs. Control, IGF-I, BMP-2, and TGF-β1 constructs were sectioned at 14 μm and stained for collagen types I, II, and VI, as well as total collagen and sulfated GAG. Photographs were taken at 20x magnification, scale bar = 100 μm.

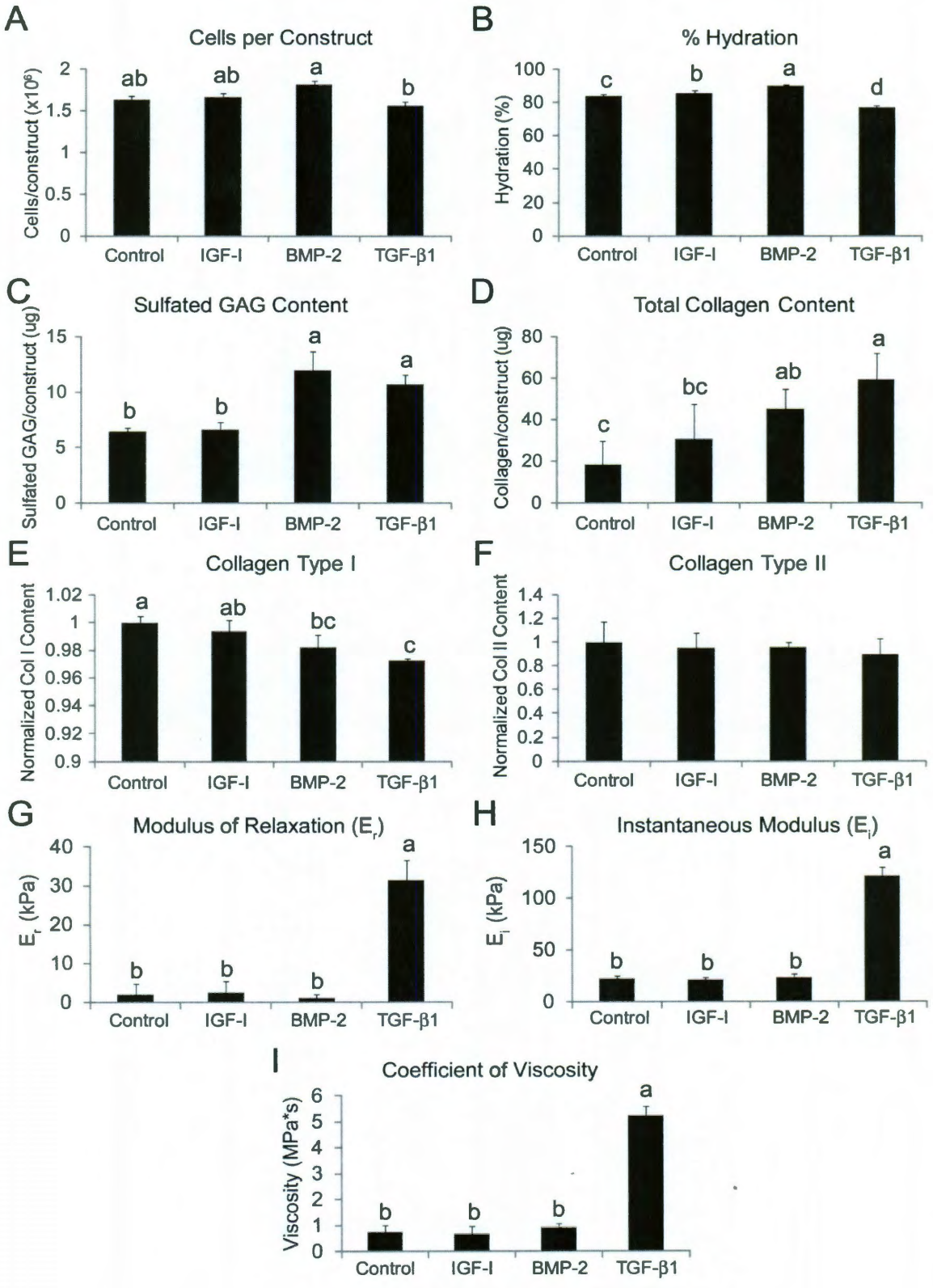
A
Cells per Construct
Cells/construct (x10^6)
2
1.5
1
0.5
0
ab
ab
a
b
Control
IGF-I
BMP-2
TGF-β1
B
% Hydration
Hydration (%)
100
80
60
40
20
0
c
b
a
d
Control
IGF-I
BMP-2
TGF-β1
C
Sulfated GAG Content
Sulfated GAG/construct (ug)
15
10
5
0
b
b
a
a
Control
IGF-I
BMP-2
TGF-β1
D
Total Collagen Content
Collagen/construct (ug)
80
60
40
20
0
c
bc
ab
a
Control
IGF-I
BMP-2
TGF-β1
E
Collagen Type I
Normalized Col I Content
1.02
1
0.98
0.96
0.94
0.92
0.9
a
ab
bc
c
Control
IGF-I
BMP-2
TGF-β1
F
Collagen Type II
Normalized Col II Content
1.4
1.2
1
0.8
0.6
0.4
0.2
0
Control
IGF-I
BMP-2
TGF-β1
G
Modulus of Relaxation (E_r)
E_r (kPa)
40
30
20
10
0
b
b
b
a
Control
IGF-I
BMP-2
TGF-β1
H
Instantaneous Modulus (E_i)
E_i (kPa)
150
100
50
0
b
b
b
a
Control
IGF-I
BMP-2
TGF-β1
I
Coefficient of Viscosity
Viscosity (MPa*s)
6
5
4
3
2
1
0
b
b
b
a
Control
IGF-I
BMP-2
TGF-β1

Figure 7: Biochemical and mechanical evaluation of tissue engineered constructs. Biochemical content and viscoelastic compressive properties were compared between Control, IGF-I, BMP-2, and TGF-β1 constructs. Results were analyzed using a one-way ANOVA with Tukey's post hoc test. Significance was set at $p < 0.05$.

Conclusions

Tissue engineering efforts seeking to create functional replacement tissue for the repair of knee meniscus injuries must consider a variety of cellular, biochemical, and biomechanical design criteria. While significant progress has been made toward the generation of functional replacement meniscus tissue, the gaps in characterization of this mechanically important tissue and the lack of an abundant cell source for tissue engineering challenge the realization of this goal. The reviews of current literature in this thesis identified several key areas of meniscus tissue engineering research that warranted further investigation: regional variation in meniscus cells and tissue, and alternate cell sources for fibrocartilage engineering. Addressing these knowledge gaps, the studies presented in this thesis showed that regional variations exist in meniscus cell mechanics, and in the effect of isolation on these cells. This thesis also demonstrated that meniscus cells may be implanted in an allogeneic or xenogeneic animal model without the concern for immediate immune rejection, and showed that knee meniscus glycosaminoglycans (GAGs) contribute distinctly to regional tissue mechanics. Finally, this thesis established the multilineage differentiation capacity of dermis isolated adult stem (DIAS) cells and determined a method to expand these cells and tissue engineer with them to form fibrocartilaginous tissue. The characterization of meniscus cells and tissue performed in this thesis will provide important design criteria for engineering functional meniscus replacements which may be created using an alternate cell source such as DIAS cells.

Reviewing the literature on meniscus cells it was found that little was known about regional meniscus cell mechanics and that this information could help understand mechanisms of mechanotransduction in the meniscus. Therefore, in chapter 4, the cells of the inner and outer meniscus were mechanically tested and compared to articular chondrocytes and ligament cells. It was found that the meniscus contains two biomechanically distinct cell populations, and that meniscus cells are mechanically similar to ligament cells. This study was the first to show regional variation in meniscus cell mechanics, and the results may have important implications for understanding meniscus cell mechanotransduction. As both inner and outer meniscus cells were found to be more similar to ligament cells than to articular chondrocytes, these results may indicate that meniscus cells respond to circumferential hoop stresses as ligament cells respond to axial tension. Interestingly, although inner meniscus cells are often regarded as chondrocyte-like due to their rounded morphology and gene expression profile, inner meniscus cells were shown to be mechanically distinct from articular chondrocytes, perhaps indicating that these cells function less like articular chondrocytes than previously hypothesized. The additional finding that chondrocytes show more distinct actin cytoskeletal staining than both meniscus and ligament cells further demonstrates the difference between hyaline cartilage and fibrous tissue, and also supports the possibility that mechanical stimulation of meniscus cells may be most effective in tension.

Although many studies use meniscus cells for fibrocartilage tissue engineering, this thesis was the first to investigate the effects of isolation on

meniscus cell phenotype (chapter 5). It was found that meniscus cells from all regions responded to isolation with increased cartilage-specific gene expression, in contrast to chondrocytes which are known to down-regulate their chondrogenic genes in response to enzymatic digestion. This difference highlights the distinct characteristics of fibrocartilaginous and cartilaginous cells, and may indicate that isolated meniscus cells enter a tissue engineering modality synthesizing more cartilage-specific proteins than articular chondrocytes. This study was also the first to show that using a digestion regimen of pronase followed by collagenase allows for the highest cell yield from all meniscus regions, and these cells can be used to create engineered meniscus constructs. This is an important finding which can improve the ease of obtaining meniscus cells for tissue engineering, and may be applicable to cell isolation from other fibrous tissues such as tendon and ligament.

As promising biochemical and biomechanical properties have been achieved in constructs formed using primary meniscus cells for tissue engineering *in vitro*, it was important to determine the feasibility of using these constructs as allogeneic or xenogeneic meniscus replacements. To this end, bovine and leporine meniscus cells were cultured *in vitro* with leporine immune cells. This analysis, described in chapter 7, showed that both bovine and leporine meniscus cells failed to activate leporine immune cells, though they showed some known immunogenic markers. However, neither of the meniscus cell populations studied showed presence of both co-stimulatory factors known to be necessary for achieving full activation of immune cells. Therefore, it is possible

that these cells lack the appropriate surface markers, or actively produce immunomodulatory molecules. Excitingly, the lack of activation observed in this study indicates that allogeneic or xenogeneic transplantation of meniscus cells may be possible.

Although much is already known about the types, organization, and mechanical contribution of collagens in the knee meniscus, relatively little was known about the mechanical contribution of meniscus GAGs until the study performed in chapter 8. By comparing the mechanical properties of control specimens from different meniscus regions to specimens subjected to GAG-depletion, it was found that knee meniscus GAGs contribute significantly to the tissue's compressive and tensile properties. Notably, GAGs impart viscosity to all meniscus regions, but are most mechanically important in the inner region where the modulus of relaxation is increased and the tensile stiffness is decreased by the presence of these molecules. Given the major contribution of GAGs to inner meniscus mechanics and the importance of mechanical integrity to overall meniscus functionality, tissue engineered constructs may need to use, produce, or mimic these molecules to achieve appropriate mechanical behavior.

While primary meniscus cells have been used successfully to produce engineered fibrocartilaginous tissue, the eventual translatability of this research is limited by the scarcity of this cell source. In chapter 11 chondroinducible dermis cells were investigated as a possible alternate cell source for meniscus engineering. This study was the first to determine that these cells could be differentiated along the adipogenic and osteogenic lineages, as well as along the

chondrogenic lineage, allowing them to be termed DIAS cells. The multipotent nature of DIAS cells increases their applicability to musculoskeletal tissue engineering strategies, as they have the potential to be used as a single cell source for the generation of bilayered tissues, such as that found between the tibial plateau and the horns of the knee meniscus. Expanded DIAS cells also showed the ability to self-assemble into tissue engineered constructs, and displayed sensitivity to growth factors TGF-β1 and BMP-2. Constructs treated with these growth factors showed increased GAG content, but TGF-β1-treated constructs were distinct from BMP-2 constructs as they were smaller and showed increased collagen content and compressive properties. Further investigation into optimal growth factor treatments for cartilage engineering with DIAS cells may benefit from combining these two growth factors to form constructs with sufficient size and compressive integrity. These results show great promise for cartilage tissue engineering with DIAS cells, and because they are isolated from adult skin, these cells may also be used for autologous tissue engineering.

Overall, this thesis 1) presents a comprehensive review of meniscus tissue engineering, 2) demonstrates previously unknown regional variations in meniscus cell characteristics, 3) elucidates the mechanical importance of knee meniscus GAGs, and 4) identifies a method to use DIAS cells to engineer fibrocartilaginous tissue. These advances allow for a more complete understanding of meniscus tissue, and provide a possible autologous cell source for meniscus tissue engineering.

References

1. Ghadially, F.N., et al., *Ultrastructure of rabbit semilunar cartilages.* J Anat, 1978. **125**(Pt 3): p. 499-517.

2. Tham, S.C., I.Y. Tsou, and T.S. Chee, *Knee and ankle ligaments: magnetic resonance imaging findings of normal anatomy and at injury.* Ann Acad Med Singapore, 2008. **37**(4): p. 324-6.

3. Brindle, T., J. Nyland, and D.L. Johnson, *The Meniscus: Review of Basic Principles With Application to Surgery and Rehabilitation.* J Athl Train, 2001. **36**(2): p. 160-169.

4. Greis, P.E., et al., *Meniscal injury: I. Basic science and evaluation.* J Am Acad Orthop Surg, 2002. **10**(3): p. 168-76.

5. Clark, C.R. and J.A. Ogden, *Development of the menisci of the human knee joint. Morphological changes and their potential role in childhood meniscal injury.* J Bone Joint Surg Am, 1983. **65**(4): p. 538-47.

6. Pufe, T., et al., *Endostatin/collagen XVIII--an inhibitor of angiogenesis--is expressed in cartilage and fibrocartilage.* Matrix Biol, 2004. **23**(5): p. 267-76.

7. O'Reilly, M.S., et al., *Endostatin: an endogenous inhibitor of angiogenesis and tumor growth.* Cell, 1997. **88**(2): p. 277-85.

8. McAlinden, A., et al., *Age-related changes in the synthesis and mRNA expression of decorin and aggrecan in human meniscus and articular cartilage.* Osteoarthritis Cartilage, 2001. **9**(1): p. 33-41.

9. McDevitt, C.A. and R.J. Webber, *The ultrastructure and biochemistry of meniscal cartilage.* Clin Orthop Relat Res, 1990(252): p. 8-18.

10. Ghosh, P. and T.K. Taylor, *The knee joint meniscus. A fibrocartilage of some distinction.* Clin Orthop Relat Res, 1987(224): p. 52-63.

11. McNicol, D. and P.J. Roughley, *Extraction and characterization of proteoglycan from human meniscus.* Biochem J, 1980. **185**(3): p. 705-13.

12. Sweigart, M.A. and K.A. Athanasiou, *Toward tissue engineering of the knee meniscus.* Tissue Eng, 2001. **7**(2): p. 111-29.

13. Wojtys, E.M. and D.B. Chan, *Meniscus structure and function.* Instr Course Lect, 2005. **54**: p. 323-30.

14. Cheung, H.S., *Distribution of type I, II, III and V in the pepsin solubilized collagens in bovine menisci.* Connect Tissue Res, 1987. **16**(4): p. 343-56.

15. Hopker, W.W., et al., *Changes of the elastin compartment in the human meniscus.* Virchows Arch A Pathol Anat Histopathol, 1986. **408**(6): p. 575-92.

16. Herwig, J., E. Egner, and E. Buddecke, *Chemical changes of human knee joint menisci in various stages of degeneration.* Ann Rheum Dis, 1984. **43**(4): p. 635-40.

17. Scott, P.G., T. Nakano, and C.M. Dodd, *Isolation and characterization of small proteoglycans from different zones of the porcine knee meniscus.* Biochim Biophys Acta, 1997. **1336**(2): p. 254-62.

18. Tanaka, T., K. Fujii, and Y. Kumagae, *Comparison of biochemical characteristics of cultured fibrochondrocytes isolated from the inner and outer regions of human meniscus.* Knee Surg Sports Traumatol Arthrosc, 1999. **7**(2): p. 75-80.

19. McDermott, I.D., et al., *An anatomical study of meniscal allograft sizing.* Knee Surg Sports Traumatol Arthrosc, 2004. **12**(2): p. 130-5.

20. Shaffer, B., et al., *Preoperative sizing of meniscal allografts in meniscus transplantation.* Am J Sports Med, 2000. **28**(4): p. 524-33.

21. Paul, J.P., *Force actions transmitted by joints in the human body.* Proc R Soc Lond B Biol Sci, 1976. **192**(1107): p. 163-72.

22. Shrive, N.G., J.J. O'Connor, and J.W. Goodfellow, *Load-bearing in the knee joint.* Clin Orthop Relat Res, 1978(131): p. 279-87.

23. Walker, P.S. and J.V. Hajek, *The load-bearing area in the knee joint.* J Biomech, 1972. **5**(6): p. 581-9.

24. Walker, P.S. and M.J. Erkman, *The role of the menisci in force transmission across the knee.* Clin Orthop Relat Res, 1975(109): p. 184-92.

25. Kurosawa, H., T. Fukubayashi, and H. Nakajima, *Load-bearing mode of the knee joint: physical behavior of the knee joint with or without menisci.* Clin Orthop Relat Res, 1980(149): p. 283-90.

26. Favenesi, J.A., J.C. Shaffer, and V.C. Mow, *Biphasic mechanical properties of knee meniscus.* Trans. 29th Annual Orthopaedic Research Society, 1983.

27. Proctor, C.S., et al., *Material properties of the normal medial bovine meniscus.* J Orthop Res, 1989. **7**(6): p. 771-82.

28. Ghadially, F.N., J.M. Lalonde, and J.H. Wedge, *Ultrastructure of normal and torn menisci of the human knee joint.* J Anat, 1983. **136**(Pt 4): p. 773-91.

29. Gabrion, A., et al., *Relationship between ultrastructure and biomechanical properties of the knee meniscus.* Surg Radiol Anat, 2005. **27**(6): p. 507-10.

30. Skaggs, D.L., W.H. Warden, and V.C. Mow, *Radial tie fibers influence the tensile properties of the bovine medial meniscus.* J Orthop Res, 1994. **12**(2): p. 176-85.

31. Aspden, R.M., Y.E. Yarker, and D.W. Hukins, *Collagen orientations in the meniscus of the knee joint.* J Anat, 1985. **140 (Pt 3)**: p. 371-80.

32. Fithian, D.C., M.A. Kelly, and V.C. Mow, *Material properties and structure-function relationships in the menisci.* Clin Orthop Relat Res, 1990(252): p. 19-31.

33. McDermott, I.D., S.D. Masouros, and A.A. Amis, *Biomechanics of the menisci of the knee.* Current Orthopaedics, 2008. **22**: p. 193-201.

34. Zhu, W., K.Y. Chern, and V.C. Mow, *Anisotropic viscoelastic shear properties of bovine meniscus.* Clin Orthop Relat Res, 1994(306): p. 34-45.

35. Joshi, M.D., et al., *Interspecies variation of compressive biomechanical properties of the meniscus.* J Biomed Mater Res, 1995. **29**(7): p. 823-8.

36. Leslie, B.W., et al., *Anisotropic response of the human knee joint meniscus to unconfined compression.* Proc Inst Mech Eng [H], 2000. **214**(6): p. 631-5.

37. Sweigart, M.A., et al., *Intraspecies and interspecies comparison of the compressive properties of the medial meniscus.* Ann Biomed Eng, 2004. **32**(11): p. 1569-79.

38. Hellio Le Graverand, M.P., et al., *The cells of the rabbit meniscus: their arrangement, interrelationship, morphological variations and cytoarchitecture.* J Anat, 2001. **198**(Pt 5): p. 525-35.

39. Nakata, K., et al., *Human meniscus cell: characterization of the primary culture and use for tissue engineering.* Clin Orthop Relat Res, 2001(391 Suppl): p. S208-18.

40. Webber, R.J., M.G. Harris, and A.J. Hough, Jr., *Cell culture of rabbit meniscal fibrochondrocytes: proliferative and synthetic response to growth factors and ascorbate.* J Orthop Res, 1985. **3**(1): p. 36-42.

41. Moon, M.S., J.M. Kim, and I.Y. Ok, *The normal and regenerated meniscus in rabbits. Morphologic and histologic studies.* Clin Orthop Relat Res, 1984(182): p. 264-9.

42. Mueller, S.M., et al., *Meniscus cells seeded in type I and type II collagen-GAG matrices in vitro.* Biomaterials, 1999. **20**(8): p. 701-9.

43. Pangborn, C.A. and K.A. Athanasiou, *Effects of growth factors on meniscal fibrochondrocytes.* Tissue Eng, 2005. **11**(7-8): p. 1141-8.

44. Miller, R.R. and P.A. Rydell, *Primary culture of microvascular endothelial cells from canine meniscus.* J Orthop Res, 1993. **11**(6): p. 907-11.

45. Melrose, J., et al., *Comparative spatial and temporal localisation of perlecan, aggrecan and type I, II and IV collagen in the ovine meniscus: an ageing study.* Histochem Cell Biol, 2005. **124**(3-4): p. 225-35.

46. Gruber, H.E., et al., *Three-dimensional culture of human meniscal cells: extracellular matrix and proteoglycan production.* BMC Biotechnol, 2008. **8**: p. 54.

47. Ochi, K., et al., *Expression profiles of two types of human knee-joint cartilage.* J Hum Genet, 2003. **48**(4): p. 177-82.

48. Ahluwalia, S., et al., *Distribution of smooth muscle actin-containing cells in the human meniscus.* J Orthop Res, 2001. **19**(4): p. 659-64.

49. Mueller, S.M., et al., *alpha-smooth muscle actin and contractile behavior of bovine meniscus cells seeded in type I and type II collagen-GAG matrices.* J Biomed Mater Res, 1999. **45**(3): p. 157-66.

50. Kambic, H.E. and C.A. McDevitt, *Spatial organization of types I and II collagen in the canine meniscus.* J Orthop Res, 2005. **23**(1): p. 142-9.

51. Verdonk, P.C., et al., *Characterisation of human knee meniscus cell phenotype.* Osteoarthritis Cartilage, 2005. **13**(7): p. 548-60.

52. Valiyaveettil, M., J.S. Mort, and C.A. McDevitt, *The concentration, gene expression, and spatial distribution of aggrecan in canine articular cartilage, meniscus, and anterior and posterior cruciate ligaments: a new molecular distinction between hyaline cartilage and fibrocartilage in the knee joint.* Connect Tissue Res, 2005. **46**(2): p. 83-91.

53. Upton, M.L., J. Chen, and L.A. Setton, *Region-specific constitutive gene expression in the adult porcine meniscus.* J Orthop Res, 2006. **24**(7): p. 1562-70.

54. Cao, M., et al., *Generation of nitric oxide by lapine meniscal cells and its effect on matrix metabolism: stimulation of collagen production by arginine.* J Orthop Res, 1998. **16**(1): p. 104-11.

55. Upton, M.L., et al., *Finite element modeling predictions of region-specific cell-matrix mechanics in the meniscus.* Biomech Model Mechanobiol, 2006. **5**(2-3): p. 140-9.

56. Upton, M.L., et al., *Biaxial strain effects on cells from the inner and outer regions of the meniscus.* Connect Tissue Res, 2006. **47**(4): p. 207-14.

57. Upton, M.L., et al., *Differential effects of static and dynamic compression on meniscal cell gene expression.* J Orthop Res, 2003. **21**(6): p. 963-9.

58. Fink, C., et al., *The effect of dynamic mechanical compression on nitric oxide production in the meniscus.* Osteoarthritis Cartilage, 2001. **9**(5): p. 481-7.

59. Djurasovic, M., et al., *Knee joint immobilization decreases aggrecan gene expression in the meniscus.* Am J Sports Med, 1998. **26**(3): p. 460-6.

60. Kaufman, K.R., et al., *Dynamic joint forces during knee isokinetic exercise.* Am J Sports Med, 1991. **19**(3): p. 305-16.

61. Shepherd, D.E. and B.B. Seedhom, *Thickness of human articular cartilage in joints of the lower limb.* Ann Rheum Dis, 1999. **58**(1): p. 27-34.

62. Mak, A.F., W.M. Lai, and V.C. Mow, *Biphasic indentation of articular cartilage--I. Theoretical analysis.* J Biomech, 1987. **20**(7): p. 703-14.

63. Mow, V.C., et al., *Biphasic indentation of articular cartilage--II. A numerical algorithm and an experimental study.* J Biomech, 1989. **22**(8-9): p. 853-61.

64. Mow, V.C., et al., *Biphasic creep and stress relaxation of articular cartilage in compression? Theory and experiments.* J Biomech Eng, 1980. **102**(1): p. 73-84.

65. Spilker, R.L., J.K. Suh, and V.C. Mow, *A finite element analysis of the indentation stress-relaxation response of linear biphasic articular cartilage.* J Biomech Eng, 1992. **114**(2): p. 191-201.

66. Schinagl, R.M., et al., *Depth-dependent confined compression modulus of full-thickness bovine articular cartilage.* J Orthop Res, 1997. **15**(4): p. 499-506.

67. Athanasiou, K.A., et al., *Biomechanical topography of human articular cartilage in the first metatarsophalangeal joint.* Clin Orthop Relat Res, 1998(348): p. 269-81.

68. Athanasiou, K.A., G.G. Niederauer, and R.C. Schenck, Jr., *Biomechanical topography of human ankle cartilage.* Ann Biomed Eng, 1995. **23**(5): p. 697-704.

69. Athanasiou, K.A., et al., *Interspecies comparisons of in situ intrinsic mechanical properties of distal femoral cartilage.* J Orthop Res, 1991. **9**(3): p. 330-40.

70. Kempson, G.E., M.A. Freeman, and S.A. Swanson, *Tensile properties of articular cartilage.* Nature, 1968. **220**(5172): p. 1127-8.

71. Woo, S.L., et al., *Large deformation nonhomogeneous and directional properties of articular cartilage in uniaxial tension.* J Biomech, 1979. **12**(6): p. 437-46.

72. Akizuki, S., et al., *Tensile properties of human knee joint cartilage: I. Influence of ionic conditions, weight bearing, and fibrillation on the tensile modulus.* J Orthop Res, 1986. **4**(4): p. 379-92.

73. Davisson, T., et al., *Static and dynamic compression modulate matrix metabolism in tissue engineered cartilage.* J Orthop Res, 2002. **20**(4): p. 842-8.

74. Kisiday, J.D., et al., *Effects of dynamic compressive loading on chondrocyte biosynthesis in self-assembling peptide scaffolds.* J Biomech, 2004. **37**(5): p. 595-604.

75. Stoddart, M.J., L. Ettinger, and H.J. Hauselmann, *Enhanced matrix synthesis in de novo, scaffold free cartilage-like tissue subjected to compression and shear.* Biotechnol Bioeng, 2006. **95**(6): p. 1043-51.

76. Elder, B.D. and K.A. Athanasiou, *Effects of temporal hydrostatic pressure on tissue-engineered bovine articular cartilage constructs.* Tissue Eng Part A, 2009. **15**(5): p. 1151-8.

77. Smith, R.L., et al., *In vitro stimulation of articular chondrocyte mRNA and extracellular matrix synthesis by hydrostatic pressure.* J Orthop Res, 1996. **14**(1): p. 53-60.

78. Koay, E.J., G. Ofek, and K.A. Athanasiou, *Effects of TGF-beta1 and IGF-I on the compressibility, biomechanics, and strain-dependent recovery behavior of single chondrocytes.* J Biomech, 2008. **41**(5): p. 1044-52.

79. Ofek, G., et al., *Mechanical characterization of differentiated human embryonic stem cells.* J Biomech Eng, 2009. **131**(6): p. 061011.

80. Ofek, G., D.C. Wiltz, and K.A. Athanasiou, *Contribution of the cytoskeleton to the compressive properties and recovery behavior of single cells.* Biophys J, 2009. **97**(7): p. 1873-82.

81. Shieh, A.C. and K.A. Athanasiou, *Biomechanics of single zonal chondrocytes.* J Biomech, 2006. **39**(9): p. 1595-602.

82. Shin, D. and K. Athanasiou, *Cytoindentation for obtaining cell biomechanical properties.* J Orthop Res, 1999. **17**(6): p. 880-90.

83. Athanasiou, K.A., et al., *Development of the cytodetachment technique to quantify mechanical adhesiveness of the single cell.* Biomaterials, 1999. **20**(23-24): p. 2405-15.

84. Koay, E.J., A.C. Shieh, and K.A. Athanasiou, *Creep indentation of single cells.* J Biomech Eng, 2003. **125**(3): p. 334-41.

85. Darling, E.M., et al., *A thin-layer model for viscoelastic, stress-relaxation testing of cells using atomic force microscopy: do cell properties reflect metastatic potential?* Biophys J, 2007. **92**(5): p. 1784-91.

86. Darling, E.M., S. Zauscher, and F. Guilak, *Viscoelastic properties of zonal articular chondrocytes measured by atomic force microscopy.* Osteoarthritis Cartilage, 2006. **14**(6): p. 571-9.

87. Ikai, A., *A Review on: Atomic Force Microscopy Applied to Nano-mechanics of the Cell.* Adv Biochem Eng Biotechnol, 2009.

88. Neuman, K.C. and A. Nagy, *Single-molecule force spectroscopy: optical tweezers, magnetic tweezers and atomic force microscopy.* Nat Methods, 2008. **5**(6): p. 491-505.

89. Lal, R. and S.A. John, *Biological applications of atomic force microscopy.* Am J Physiol, 1994. **266**(1 Pt 1): p. C1-21.

90. You, H.X. and L. Yu, *Atomic force microscopy imaging of living cells: progress, problems and prospects.* Methods Cell Sci, 1999. **21**(1): p. 1-17.

91. Ushiki, T., et al., *Atomic force microscopy in histology and cytology.* Arch Histol Cytol, 1996. **59**(5): p. 421-31.

92. Hoben, G., et al., *Quantification of varying adhesion levels in chondrocytes using the cytodetacher.* Ann Biomed Eng, 2002. **30**(5): p. 703-12.

93. Ofek, G., et al., *Biomechanics of single chondrocytes under direct shear.* Biomech Model Mechanobiol, 2010. **9**(2): p. 153-62.

94. Theret, D.P., et al., *The application of a homogeneous half-space model in the analysis of endothelial cell micropipette measurements.* J Biomech Eng, 1988. **110**(3): p. 190-9.

95. Needham, D. and R.M. Hochmuth, *Rapid flow of passive neutrophils into a 4 microns pipet and measurement of cytoplasmic viscosity.* J Biomech Eng, 1990. **112**(3): p. 269-76.

96. Hochmuth, R.M., *Micropipette aspiration of living cells.* J Biomech, 2000. **33**(1): p. 15-22.

97. Leipzig, N.D. and K.A. Athanasiou, *Static compression of single chondrocytes catabolically modifies single-cell gene expression.* Biophys J, 2008. **94**(6): p. 2412-22.

98. Ofek, G., R.M. Natoli, and K.A. Athanasiou, *In situ mechanical properties of the chondrocyte cytoplasm and nucleus.* J Biomech, 2009. **42**(7): p. 873-7.

99. Guilak, F., J.R. Tedrow, and R. Burgkart, *Viscoelastic properties of the cell nucleus.* Biochem Biophys Res Commun, 2000. **269**(3): p. 781-6.

100. Shieh, A.C. and K.A. Athanasiou, *Dynamic compression of single cells.* Osteoarthritis Cartilage, 2007. **15**(3): p. 328-34.

101. Leipzig, N.D., S.V. Eleswarapu, and K.A. Athanasiou, *The effects of TGF-beta1 and IGF-I on the biomechanics and cytoskeleton of single chondrocytes.* Osteoarthritis Cartilage, 2006. **14**(12): p. 1227-36.

102. Eleswarapu, S.V., N.D. Leipzig, and K.A. Athanasiou, *Gene expression of single articular chondrocytes.* Cell Tissue Res, 2007. **327**(1): p. 43-54.

103. Trickey, W.R., G.M. Lee, and F. Guilak, *Viscoelastic properties of chondrocytes from normal and osteoarthritic human cartilage.* J Orthop Res, 2000. **18**(6): p. 891-8.

104. Park, L.S., et al., *Posterior horn lateral meniscal tears simulating meniscofemoral ligament attachment in the setting of ACL tear: MRI findings.* Skeletal Radiol, 2007. **36**(5): p. 399-403.

105. Mikic, B., et al., *Differential effects of embryonic immobilization on the development of fibrocartilaginous skeletal elements.* J Rehabil Res Dev, 2000. **37**(2): p. 127-33.

106. Ochi, M., et al., *Changes in the permeability and histologic findings of rabbit menisci after immobilization.* Clin Orthop Relat Res, 1997(334): p. 305-15.

107. Natsu-Ume, T., et al., *Menisci of the rabbit knee require mechanical loading to maintain homeostasis: cyclic hydrostatic compression in vitro prevents derepression of catabolic genes.* J Orthop Sci, 2005. **10**(4): p. 396-405.

108. Collier, S. and P. Ghosh, *Effects of transforming growth factor beta on proteoglycan synthesis by cell and explant cultures derived from the knee joint meniscus.* Osteoarthritis Cartilage, 1995. **3**(2): p. 127-38.

109. Spindler, K.P., et al., *Regional mitogenic response of the meniscus to platelet-derived growth factor (PDGF-AB).* J Orthop Res, 1995. **13**(2): p. 201-7.

110. Bhargava, M.M., et al., *The effect of cytokines on the proliferation and migration of bovine meniscal cells.* Am J Sports Med, 1999. **27**(5): p. 636-43.

111. Gunja, N.J., R.K. Uthamanthil, and K.A. Athanasiou, *Effects of TGF-beta1 and hydrostatic pressure on meniscus cell-seeded scaffolds.* Biomaterials, 2009. **30**(4): p. 565-73.

112. Marsano, A., et al., *Bi-zonal cartilaginous tissues engineered in a rotary cell culture system.* Biorheology, 2006. **43**(3-4): p. 553-60.

113. Gemmiti, C.V. and R.E. Guldberg, *Fluid flow increases type II collagen deposition and tensile mechanical properties in bioreactor-grown tissue-engineered cartilage.* Tissue Eng, 2006. **12**(3): p. 469-79.

114. Neves, A.A., N. Medcalf, and K.M. Brindle, *Tissue engineering of meniscal cartilage using perfusion culture.* Ann N Y Acad Sci, 2002. **961**: p. 352-5.

115. Aufderheide, A.C. and K.A. Athanasiou, *Assessment of a bovine co-culture, scaffold-free method for growing meniscus-shaped constructs.* Tissue Eng, 2007. **13**(9): p. 2195-205.

116. Hoben, G.M. and K.A. Athanasiou, *Creating a spectrum of fibrocartilages through different cell sources and biochemical stimuli.* Biotechnol Bioeng, 2008. **100**(3): p. 587-98.

117. Pangborn, C.A. and K.A. Athanasiou, *Growth factors and fibrochondrocytes in scaffolds.* J Orthop Res, 2005. **23**(5): p. 1184-90.

118. Sweigart, M.A. and K.A. Athanasiou, *Tensile and compressive properties of the medial rabbit meniscus.* Proc Inst Mech Eng H, 2005. **219**(5): p. 337-47.

119. Upton, M.L., et al., *Transfer of macroscale tissue strain to microscale cell regions in the deformed meniscus.* Biophys J, 2008. **95**(4): p. 2116-24.

120. Guilak, F., et al., *Viscoelastic properties of intervertebral disc cells. Identification of two biomechanically distinct cell populations.* Spine (Phila Pa 1976), 1999. **24**(23): p. 2475-83.

121. Darling, E.M., et al., *Spatial mapping of the biomechanical properties of the pericellular matrix of articular cartilage measured in situ via atomic force microscopy.* Biophys J, 2010. **98**(12): p. 2848-56.

122. Feng, Y., et al., *Unique biomechanical interactions between myeloma cells and bone marrow stroma cells.* Prog Biophys Mol Biol, 2010. **103**(1): p. 148-56.

123. Shieh, A.C., E.J. Koay, and K.A. Athanasiou, *Strain-dependent recovery behavior of single chondrocytes.* Biomech Model Mechanobiol, 2006. **5**(2-3): p. 172-9.

124. Leipzig, N.D. and K.A. Athanasiou, *Unconfined creep compression of chondrocytes.* J Biomech, 2005. **38**(1): p. 77-85.

125. Darling, E.M., et al., *Viscoelastic properties of human mesenchymally-derived stem cells and primary osteoblasts, chondrocytes, and adipocytes.* J Biomech, 2008. **41**(2): p. 454-64.

126. Kim, E., F. Guilak, and M.A. Haider, *An axisymmetric boundary element model for determination of articular cartilage pericellular matrix properties in situ via inverse analysis of chondron deformation.* J Biomech Eng, 2010. **132**(3): p. 031011.

127. Cao, L., F. Guilak, and L.A. Setton, *Three-dimensional finite element modeling of pericellular matrix and cell mechanics in the nucleus pulposus of the intervertebral disk based on in situ morphology.* Biomech Model Mechanobiol, 2011. **10**(1): p. 1-10.

128. Aufderheide, A.C. and K.A. Athanasiou, *A direct compression stimulator for articular cartilage and meniscal explants.* Ann Biomed Eng, 2006. **34**(9): p. 1463-74.

129. Aufderheide, A.C. and K.A. Athanasiou, *Comparison of scaffolds and culture conditions for tissue engineering of the knee meniscus.* Tissue Eng, 2005. **11**(7-8): p. 1095-104.

130. Gunja, N.J., et al., *Effects of agarose mould compliance and surface roughness on self-assembled meniscus-shaped constructs.* J Tissue Eng Regen Med, 2009. **3**(7): p. 521-30.

131. Hoben, G.M., et al., *Self-assembly of fibrochondrocytes and chondrocytes for tissue engineering of the knee meniscus.* Tissue Eng, 2007. **13**(5): p. 939-46.

132. Baker, B.M., et al., *Tissue engineering with meniscus cells derived from surgical debris.* Osteoarthritis Cartilage, 2009. **17**(3): p. 336-45.

133. Kang, S.W., et al., *Regeneration of whole meniscus using meniscal cells and polymer scaffolds in a rabbit total meniscectomy model.* J Biomed Mater Res A, 2006. **78**(3): p. 659-71.

134. Marsano, A., et al., *Differential cartilaginous tissue formation by human synovial membrane, fat pad, meniscus cells and articular chondrocytes.* Osteoarthritis Cartilage, 2007. **15**(1): p. 48-58.

135. Tan, Y., Y. Zhang, and M. Pei, *Meniscus reconstruction through coculturing meniscus cells with synovium-derived stem cells on small intestine submucosa--a pilot study to engineer meniscus tissue constructs.* Tissue Eng Part A, 2010. **16**(1): p. 67-79.

136. Green, W.T., Jr., *Behavior of articular chondrocytes in cell culture.* Clin Orthop Relat Res, 1971. **75**: p. 248-60.

137. Hayman, D.M., et al., *The effects of isolation on chondrocyte gene expression.* Tissue Eng, 2006. **12**(9): p. 2573-81.

138. Webber, R.J., T. Zitaglio, and A.J. Hough, Jr., *In vitro cell proliferation and proteoglycan synthesis of rabbit meniscal fibrochondrocytes as a function of age and sex.* Arthritis Rheum, 1986. **29**(8): p. 1010-6.

139. Webber, R.J., T. Zitaglio, and A.J. Hough, *Serum-Free Culture of Rabbit Meniscal Fibrochondrocytes - Proliferative Response.* Journal of Orthopaedic Research, 1988. **6**(1): p. 13-23.

140. French, M.F., K.A. Mookhtiar, and H.E. Vanwart, *Limited Proteolysis of Type-I Collagen at Hyperreactive Sites by Class-I and Class-Ii Clostridium-Histolyticum Collagenases - Complementary Digestion Patterns.* Biochemistry, 1987. **26**(3): p. 681-687.

141. Bicsak, T.A. and E. Harper, *Purification of nonspecific protease-free collagenase from Clostridium histolyticum.* Anal Biochem, 1985. **145**(2): p. 286-91.

142. Bond, M.D. and H.E. Van Wart, *Characterization of the individual collagenases from Clostridium histolyticum.* Biochemistry, 1984. **23**(13): p. 3085-91.

143. Barrett, A.J. and N.D. Rawlings, *Families and clans of serine peptidases.* Arch Biochem Biophys, 1995. **318**(2): p. 247-50.

144. Page, M.J. and E. Di Cera, *Serine peptidases: classification, structure and function.* Cell Mol Life Sci, 2008. **65**(7-8): p. 1220-36.

145. Rawlings, N.D. and A.J. Barrett, *Families of serine peptidases.* Methods Enzymol, 1994. **244**: p. 19-61.

146. Nomoto, M. and Y. Narahashi, *A Proteolytic Enzyme of Streptomyces-Griseus .4. General Properties of Streptomyces-Griseus Protease.* Journal of Biochemistry, 1959. **46**(12): p. 1645-1651.

147. Nomoto, M. and Y. Narahashi, *A Proteolytic Enzyme of Streptomyces Griseus .1. Purification of a Protease of Streptomyces Griseus.* Journal of Biochemistry, 1959. **46**(5): p. 653-667.

148. Nomoto, M., Y. Narahashi, and M. Murakami, *A Proteolytic Enzyme of Streptomyces Griseus .5. Protective Effect of Calcium Ion on the Stability of Protease.* Journal of Biochemistry, 1960. **48**(3): p. 453-463.

149. Awad, W.M., et al., *Proteolytic-Enzymes of K-1 Strain of Streptomyces-Griseus Obtained from a Commercial Preparation (Pronase) .1. Purification of 4 Serine Endopeptidases.* Journal of Biological Chemistry, 1972. **247**(13): p. 4144-&.

150. Johnson, P. and L.B. Smillie, *The amino acid sequence and predicted structure of Streptomyces griseus protease A.* FEBS Lett, 1974. **47**(1): p. 1-6.

151. Jurasek, L., et al., *Amino-Acid Sequence of Streptomyces-Griseus Protease-B, a Major Component of Pronase.* Biochemical and Biophysical Research Communications, 1974. **61**(4): p. 1095-1100.

152. Nomoto, M., Y. Narahashi, and M. Murakami, *A Proteolytic Enzyme of Streptomyces Griseus .7. Substrate Specificity of Streptomyces Griseus Protease.* Journal of Biochemistry, 1960. **48**(6): p. 906-918.

153. Nomoto, M., Y. Narahashi, and M. Murakami, *A Proteolytic Enzyme of Streptomyces Griseus .6. Hydrolysis of Protein by Strepomyces Griseus Protease.* Journal of Biochemistry, 1960. **48**(4): p. 593-602.

154. Knudsen, P.J., et al., *High-Performance Liquid-Chromatography of Hyaluronic-Acid and Oligosaccharides Produced by Bovine Testes Hyaluronidase.* Journal of Chromatography, 1980. **187**(2): p. 373-379.

155. Starr, C.R. and N.C. Engleberg, *Role of hyaluronidase in subcutaneous spread and growth of group A streptococcus.* Infect Immun, 2006. **74**(1): p. 40-8.

156. Allen, K.D. and K.A. Athanasiou, *Viscoelastic characterization of the porcine temporomandibular joint disc under unconfined compression.* J Biomech, 2006. **39**(2): p. 312-22.

157. Foley, J.F. and Aftonomo.B, *Use of Pronase in Tissue Culture - a Comparison with Trypsin.* Journal of Cellular Physiology, 1970. **75**(2): p. 159-&.

158. Gwatkin, R.B.L. and J.L. Thomson, *New Method for Dispersing Cells of Mammalian Tissues.* Nature, 1964. **201**(492): p. 1242-&.

159. Derby, M.A. and J.E. Pintar, *The histochemical specificity of Streptomyces hyaluronidase and chondroitinase ABC.* Histochem J, 1978. **10**(5): p. 529-47.

160. Lepperdinger, G., B. Strobl, and G. Kreil, *HYAL2, a human gene expressed in many cells, encodes a lysosomal hyaluronidase with a novel type of specificity.* J Biol Chem, 1998. **273**(35): p. 22466-70.

161. Ofek, G., et al., *Matrix development in self-assembly of articular cartilage.* PLoS One, 2008. **3**(7): p. e2795.

162. Basalo, I.M., et al., *Cartilage interstitial fluid load support in unconfined compression following enzymatic digestion.* J Biomech Eng, 2004. **126**(6): p. 779-86.

163. Katta, J., et al., *The effect of glycosaminoglycan depletion on the friction and deformation of articular cartilage.* Proc Inst Mech Eng H, 2008. **222**(1): p. 1-11.

164. Finot, L., P.-G. Marnet, and F. Dessauge, *Reference gene selection for quantitative real-time PCR normalization: Application in the caprine mammary gland.* Small Ruminant Research, 2011. **95**: p. 20-26.

165. Park, Y., et al., *BMP-2 induces the expression of chondrocyte-specific genes in bovine synovium-derived progenitor cells cultured in three-dimensional alginate hydrogel.* Osteoarthritis Cartilage, 2005. **13**(6): p. 527-36.

166. Darling, E.M. and K.A. Athanasiou, *Rapid phenotypic changes in passaged articular chondrocyte subpopulations.* J Orthop Res, 2005. **23**(2): p. 425-32.

167. Vandermeer, R.D. and F.K. Cunningham, *Arthroscopic treatment of the discoid lateral meniscus: results of long-term follow-up.* Arthroscopy, 1989. **5**(2): p. 101-9.

168. Washington, E.R., 3rd, L. Root, and U.C. Liener, *Discoid lateral meniscus in children. Long-term follow-up after excision.* J Bone Joint Surg Am, 1995. **77**(9): p. 1357-61.

169. Bjelle, A., *Cartilage matrix in hereditary pyrophosphate arthropathy.* J Rheumatol, 1981. **8**(6): p. 959-64.

170. DiCarlo, E.F., *Pathology of the Meniscus*, in *Knee Meniscus: Basic and Clinical Foundations*, V.C. Mow, S.P. Arnoczky, and D.W. Jackson, Editors. 1992, Raven Press: New York. p. 123-128.

171. Hough, A.J., Jr. and R.J. Webber, *Pathology of the meniscus.* Clin Orthop Relat Res, 1990(252): p. 32-40.

172. DeHaven, K.E., *Meniscectomy Versus Repair: Clinical Experience*, in *Knee Meniscus: Basic and Clinical Foundations*, V.C. Mow, S.P. Arnoczky, and D.W. Jackson, Editors. 1992, Raven Press: New York. p. 132.

173. Berthiaume, M.J., et al., *Meniscal tear and extrusion are strongly associated with progression of symptomatic knee osteoarthritis as assessed by quantitative magnetic resonance imaging.* Ann Rheum Dis, 2005. **64**(4): p. 556-63.

174. Fahmy, N.R., E.A. Williams, and J. Noble, *Meniscal pathology and osteoarthritis of the knee.* J Bone Joint Surg Br, 1983. **65**(1): p. 24-8.

175. Lange, A.K., et al., *Degenerative meniscus tears and mobility impairment in women with knee osteoarthritis.* Osteoarthritis Cartilage, 2007. **15**(6): p. 701-8.

176. Bamac, B., et al., *Evaluation of medial and lateral meniscus thicknesses in early osteoarthritis of the knee with magnetic resonance imaging.* Saudi Med J, 2006. **27**(6): p. 854-7.

177. Adams, M.E., M.E. Billingham, and H. Muir, *The glycosaminoglycans in menisci in experimental and natural osteoarthritis.* Arthritis Rheum, 1983. **26**(1): p. 69-76.

178. Sugita, T., et al., *Radial displacement of the medial meniscus in varus osteoarthritis of the knee.* Clin Orthop Relat Res, 2001(387): p. 171-7.

179. Smillie, I.S., *The current pattern of the pathology of meniscus tears.* Proc R Soc Med, 1968. **61**(1): p. 44-5.

180. Schlossberg, S., et al., *Bucket handle tears of the medial meniscus: meniscal intrusion rather than meniscal extrusion.* Skeletal Radiol, 2007. **36**(1): p. 29-34.

181. Choi, N.H. and B.N. Victoroff, *Anterior horn tears of the lateral meniscus in soccer players.* Arthroscopy, 2006. **22**(5): p. 484-8.

182. Dandy, D.J., *The arthroscopic anatomy of symptomatic meniscal lesions.* J Bone Joint Surg Br, 1990. **72**(4): p. 628-33.

183. Noyes, F.R., et al., *Clinical laxity tests and functional stability of the knee: biomechanical concepts.* Clin Orthop Relat Res, 1980(146): p. 84-9.

184. Roberts, D., G. Andersson, and T. Friden, *Knee joint proprioception in ACL-deficient knees is related to cartilage injury, laxity and age: a retrospective study of 54 patients.* Acta Orthop Scand, 2004. **75**(1): p. 78-83.

185. Allen, C.R., et al., *Importance of the medial meniscus in the anterior cruciate ligament-deficient knee.* J Orthop Res, 2000. **18**(1): p. 109-15.

186. Belzer, J.P. and W.D. Cannon, Jr., *Meniscus Tears: Treatment in the Stable and Unstable Knee.* J Am Acad Orthop Surg, 1993. **1**(1): p. 41-47.

187. Moglo, K.E. and A. Shirazi-Adl, *Biomechanics of passive knee joint in drawer: load transmission in intact and ACL-deficient joints.* Knee, 2003. **10**(3): p. 265-76.

188. Meister, K., et al., *Histology of the torn meniscus: a comparison of histologic differences in meniscal tissue between tears in anterior cruciate ligament-intact and anterior cruciate ligament-deficient knees.* Am J Sports Med, 2004. **32**(6): p. 1479-83.

189. Fairbank, T.J., *Knee joint changes after meniscectomy.* J Bone Joint Surg Am, 1948. **30B**(4): p. 664-70.

190. McGinity, J.B., L.F. Geuss, and R.A. Marvin, *Partial or total meniscectomy: a comparative analysis.* J Bone Joint Surg Am, 1977. **59**(6): p. 763-6.

191. Allen, P.R., R.A. Denham, and A.V. Swan, *Late degenerative changes after meniscectomy. Factors affecting the knee after operation.* J Bone Joint Surg Br, 1984. **66**(5): p. 666-71.

192. Berjon, J.J., L. Munuera, and M. Calvo, *Degenerative lesions in the articular cartilage after meniscectomy: preliminary experimental study in dogs.* J Trauma, 1991. **31**(3): p. 342-50.

193. Jackson, J.P., *Degenerative changes in the knee after meniscectomy.* Br Med J, 1968. **2**(5604): p. 525-7.

194. Moon, M.S. and I.S. Chung, *Degenerative changes after meniscectomy and meniscal regeneration.* Int Orthop, 1988. **12**(1): p. 17-9.

195. Messner, K. and J. Gao, *The menisci of the knee joint. Anatomical and functional characteristics, and a rationale for clinical treatment.* J Anat, 1998. **193 (Pt 2)**: p. 161-78.

196. Goodfellow, J., *He who hesitates is saved.* J Bone Joint Surg Br, 1980. **62-B**(1): p. 1-2.

197. Adams, S.B., Jr., M.A. Randolph, and T.J. Gill, *Tissue engineering for meniscus repair.* J Knee Surg, 2005. **18**(1): p. 25-30.

198. Hoben, G.M. and K.A. Athanasiou, *Meniscal repair with fibrocartilage engineering.* Sports Med Arthrosc, 2006. **14**(3): p. 129-37.

199. Arnoczky, S.P., *Gross and Vascular Anatomy of the Meniscus and Its Role in Meniscal Healing, Regeneration, and Remodeling*, in *Knee Meniscus: Basic and Clinical Foundations*, V.C. Mow, S.P. Arnoczky, and D.W. Jackson, Editors. 1992, Raven Press: New York. p. 6-12.

200. Arnoczky, S.P. and R.F. Warren, *The microvasculature of the meniscus and its response to injury. An experimental study in the dog.* Am J Sports Med, 1983. **11**(3): p. 131-41.

201. Mow, V.C., S.P. Arnoczky, and D.W. Jackson, *Knee Meniscus: Basic and Clinical Foundations.* 1992: p. 6-12.

202. McAndrews, P.T. and S.P. Arnoczky, *Meniscal repair enhancement techniques.* Clin Sports Med, 1996. **15**(3): p. 499-510.

203. Zhang, Z. and J.A. Arnold, *Trephination and suturing of avascular meniscal tears: a clinical study of the trephination procedure.* Arthroscopy, 1996. **12**(6): p. 726-31.

204. Fox, J.M., K.G. Rintz, and R.D. Ferkel, *Trephination of incomplete meniscal tears.* Arthroscopy, 1993. **9**(4): p. 451-5.

205. Zhang, Z.N., et al., *Treatment of longitudinal injuries in avascular area of meniscus in dogs by trephination.* Arthroscopy, 1988. **4**(3): p. 151-9.

206. Zhang, Z., et al., *Repairs by trephination and suturing of longitudinal injuries in the avascular area of the meniscus in goats.* Am J Sports Med, 1995. **23**(1): p. 35-41.

207. Noble, J. and D.L. Hamblen, *The pathology of the degenerate meniscus lesion.* J Bone Joint Surg Br, 1975. **57**(2): p. 180-6.

208. Uysal, M., et al., *Apoptosis in the traumatic and degenerative tears of human meniscus.* Knee Surg Sports Traumatol Arthrosc, 2008. **16**(7): p. 666-9.

209. Roeddecker, K., U. Muennich, and M. Nagelschmidt, *Meniscal healing: a biomechanical study.* J Surg Res, 1994. **56**(1): p. 20-7.

210. Hu, J.C. and K.A. Athanasiou, *A self-assembling process in articular cartilage tissue engineering.* Tissue Eng, 2006. **12**(4): p. 969-79.

211. Lal, B., et al., *Emergence and Evolution of a Shared Concept*, in *The Emergence of Tissue Engineering as a Research Field.* 2003, Prepared for the National Science Foundation: Arlington, VA.

212. Vacanti, C.A., *The history of tissue engineering.* J Cell Mol Med, 2006. **10**(3): p. 569-76.

213. Butler, D.L., S.A. Goldstein, and F. Guilak, *Functional tissue engineering: the role of biomechanics.* J Biomech Eng, 2000. **122**(6): p. 570-5.

214. Goldstein, S.A., *Tissue engineering: functional assessment and clinical outcome.* Ann N Y Acad Sci, 2002. **961**: p. 183-92.

215. Guilak, F., *Functional tissue engineering: the role of biomechanics in reparative medicine.* Ann N Y Acad Sci, 2002. **961**: p. 193-5.

216. Guilak, F., D.L. Butler, and S.A. Goldstein, *Functional tissue engineering: the role of biomechanics in articular cartilage repair.* Clin Orthop Relat Res, 2001(391 Suppl): p. S295-305.

217. Mauck, R.L., et al., *Functional tissue engineering of articular cartilage through dynamic loading of chondrocyte-seeded agarose gels.* J Biomech Eng, 2000. **122**(3): p. 252-60.

218. Trivedi, H.L., *Immunobiology of rejection and adaptation.* Transplant Proc, 2007. **39**(3): p. 647-52.

219. Bretscher, P.A., *A two-step, two-signal model for the primary activation of precursor helper T cells.* Proc Natl Acad Sci U S A, 1999. **96**(1): p. 185-90.

220. Kindt, T.J., et al., *Kuby immunology*. 6th ed. 2007, New York: W.H. Freeman. xxii, 574, A-31, G-12, AN-27, I-27 p.

221. Adkisson, H.D., et al., *Immune evasion by neocartilage-derived chondrocytes: Implications for biologic repair of joint articular cartilage.* Stem Cell Res, 2010. **4**(1): p. 57-68.

222. Elves, M.W., *A study of the transplantation antigens on chondrocytes from articular cartilage.* J Bone Joint Surg Br, 1974. **56**(1): p. 178-85.

223. Jobanputra, P., et al., *Cellular responses to human chondrocytes: absence of allogeneic responses in the presence of HLA-DR and ICAM-1.* Clin Exp Immunol, 1992. **90**(2): p. 336-44.

224. Ramallal, M., et al., *Xeno-implantation of pig chondrocytes into rabbit to treat localized articular cartilage defects: an animal model.* Wound Repair Regen, 2004. **12**(3): p. 337-45.

225. Yan, H. and C. Yu, *Repair of full-thickness cartilage defects with cells of different origin in a rabbit model.* Arthroscopy, 2007. **23**(2): p. 178-87.

226. van Susante, J.L., et al., *Resurfacing potential of heterologous chondrocytes suspended in fibrin glue in large full-thickness defects of femoral articular cartilage: an experimental study in the goat.* Biomaterials, 1999. **20**(13): p. 1167-75.

227. Heatley, F.W. and W.J. Revell, *The Use of Meniscal Fibrocartilage as a Surface Arthroplasty to Effect the Repair of Osteochondral Defects - an Experimental-Study.* Biomaterials, 1985. **6**(3): p. 161-168.

228. Revell, C.M. and K.A. Athanasiou, *Success rates and immunologic responses of autogenic, allogenic, and xenogenic treatments to repair articular cartilage defects.* Tissue Eng Part B Rev, 2009. **15**(1): p. 1-15.

229. Huey, D.J. and K.A. Athanasiou, *Maturational growth of self-assembled, functional menisci as a result of TGF-beta1 and enzymatic chondroitinase-ABC stimulation.* Biomaterials, 2011. **32**(8): p. 2052-8.

230. Huey, D.J. and K.A. Athanasiou, *Chondrogenically-tuned expansion enhances the cartilaginous matrix forming capabilities of primary, adult, leporine chondrocytes in the self-assembly modality.* Submitted to Tissue Engineering.

231. Muul, L.M., et al., *Measurement of proliferative responses of cultured lymphocytes.* Curr Protoc Immunol, 2008. **Chapter 7**: p. Unit 7 10 1-7 10 24.

232. Ashrafi, G.H., et al., *Down-regulation of MHC class I by bovine papillomavirus E5 oncoproteins.* Oncogene, 2002. **21**(2): p. 248-59.

233. Cannon, M.J., J.S. Davis, and J.L. Pate, *The class II major histocompatibility complex molecule BoLA-DR is expressed by endothelial cells of the bovine corpus luteum.* Reproduction, 2007. **133**(5): p. 991-1003.

234. Donaldson, L., et al., *Construction and validation of a Bovine Innate Immune Microarray.* BMC Genomics, 2005. **6**: p. 135.

235. Moreno, R., et al., *Characterization of mesenchymal stem cells isolated from the rabbit fetal liver.* Stem Cells Dev, 2010. **19**(10): p. 1579-88.

236. Adkisson, H.D., et al., *Immune evasion by neocartilage-derived chondrocytes: Implications for biologic repair of joint articular cartilage.* Stem Cell Res. **4**(1): p. 57-68.

237. Alsalameh, S., et al., *Cellular immune response toward human articular chondrocytes. T cell reactivities against chondrocyte and fibroblast membranes in destructive joint diseases.* Arthritis Rheum, 1990. **33**(10): p. 1477-86.

238. Kuhne, M., et al., *HLA-B27-restricted antigen presentation by human chondrocytes to CD8+ T cells: potential contribution to local immunopathologic processes in ankylosing spondylitis.* Arthritis Rheum, 2009. **60**(6): p. 1635-46.

239. Klareskog, L., et al., *Reactivity of monoclonal anti-type II collagen antibodies with cartilage and synovial tissue in rheumatoid arthritis and osteoarthritis.* Arthritis Rheum, 1986. **29**(6): p. 730-8.

240. Lance, E.M., L.H. Kimura, and C.N. Manibog, *The expression of major histocompatibility antigens on human articular chondrocytes.* Clin Orthop Relat Res, 1993(291): p. 266-82.

241. Apte, S.S. and N.A. Athanasou, *An immunohistological study of cartilage and synovium in primary synovial chondromatosis.* J Pathol, 1992. **166**(3): p. 277-81.

242. Goldring, M.B., et al., *Immune interferon suppresses levels of procollagen mRNA and type II collagen synthesis in cultured human articular and costal chondrocytes.* J Biol Chem, 1986. **261**(19): p. 9049-55.

243. Khoury, M.A., V.M. Goldberg, and S. Stevenson, *Demonstration of HLA and ABH antigens in fresh and frozen human menisci by immunohistochemistry.* J Orthop Res, 1994. **12**(6): p. 751-7.

244. Maier, D., et al., *In vitro analysis of an allogenic scaffold for tissue-engineered meniscus replacement.* J Orthop Res, 2007. **25**(12): p. 1598-608.

245. Rodeo, S.A., et al., *Histological analysis of human meniscal allografts. A preliminary report.* J Bone Joint Surg Am, 2000. **82-A**(8): p. 1071-82.

246. Fleischer, J., et al., *Differential expression and function of CD80 (B7-1) and CD86 (B7-2) on human peripheral blood monocytes.* Immunology, 1996. **89**(4): p. 592-8.

247. Gaspari, A.A., et al., *CD86 (B7-2), but not CD80 (B7-1), expression in the epidermis of transgenic mice enhances the immunogenicity of primary cutaneous Candida albicans infections.* Infect Immun, 1998. **66**(9): p. 4440-9.

248. Hathcock, K.S., et al., *Comparative analysis of B7-1 and B7-2 costimulatory ligands: expression and function.* J Exp Med, 1994. **180**(2): p. 631-40.

249. Kano, M., et al., *A crucial role of host CD80 and CD86 in rat cardiac xenograft rejection in mice.* Transplantation, 1998. **65**(6): p. 837-43.

250. Okano, M., et al., *Differential role of CD80 and CD86 molecules in the induction and the effector phases of allergic rhinitis in mice.* Am J Respir Crit Care Med, 2001. **164**(8 Pt 1): p. 1501-7.

251. Perrin, P.J., et al., *Mitogenic stimulation of T cells reveals differing contributions for B7-1 (CD80) and B7-2 (CD86) costimulation.* Immunology, 1997. **90**(4): p. 534-42.

252. Tatsumi, T., et al., *Expression of costimulatory molecules B7-1 (CD80) and B7-2 (CD86) on human hepatocellular carcinoma.* Hepatology, 1997. **25**(5): p. 1108-14.

253. Setoguchi, K., et al., *Suppression of T cell responses by chondromodulin I, a cartilage-derived angiogenesis inhibitory factor - Therapeutic potential in rheumatoid arthritis.* Arthritis and Rheumatism, 2004. **50**(3): p. 828-839.

254. Bodmer, S., et al., *Immunosuppression and Transforming Growth Factor-Beta in Glioblastoma - Preferential Production of Transforming Growth Factor-Beta 2.* Journal of Immunology, 1989. **143**(10): p. 3222-3229.

255. Wahl, S.M., N. McCartney-Francis, and S.E. Mergenhagen, *Inflammatory and immunomodulatory roles of TGF-beta.* Immunol Today, 1989. **10**(8): p. 258-61.

256. Di Nicola, M., et al., *Human bone marrow stromal cells suppress T-lymphocyte proliferation induced by cellular or nonspecific mitogenic stimuli.* Blood, 2002. **99**(10): p. 3838-43.

257. McDevitt, C.A., *Biochemistry of articular cartilage. Nature of proteoglycans and collagen of articular cartilage and their role in ageing and in osteoarthrosis.* Ann Rheum Dis, 1973. **32**(4): p. 364-78.

258. Adams, M.E. and H. Muir, *The glycosaminoglycans of canine menisci.* Biochem J, 1981. **197**(2): p. 385-9.

259. Hamai, A., et al., *Two distinct chondroitin sulfate ABC lyases. An endoeliminase yielding tetrasaccharides and an exoeliminase preferentially acting on oligosaccharides.* J Biol Chem, 1997. **272**(14): p. 9123-30.

260. Henninger, H.B., et al., *Effect of sulfated glycosaminoglycan digestion on the transverse permeability of medial collateral ligament.* J Biomech, 2010. **43**(13): p. 2567-73.

261. Lujan, T.J., et al., *Contribution of glycosaminoglycans to viscoelastic tensile behavior of human ligament.* J Appl Physiol, 2009. **106**(2): p. 423-31.

262. Setton, L.A., et al., *Predictions of the swelling induced pre-stress in articular cartilage*, in *Mechanics of Porous Media*, A.P.S. Selvadurai, Editor. 1995, Kluwer Academic Publishers. p. 299-322.

263. Asanbaeva, A., et al., *Mechanisms of cartilage growth - Modulation of balance between proteoglycan and collagen in vitro using chondroitinase ABC.* Arthritis and Rheumatism, 2007. **56**(1): p. 188-198.

264. Natoli, R.M., C.M. Revell, and K.A. Athanasiou, *Chondroitinase ABC treatment results in greater tensile properties of self-assembled tissue-engineered articular cartilage.* Tissue Eng Part A, 2009. **15**(10): p. 3119-28.

265. Setton, L.A., et al., *Biomechanical factors in tissue engineered meniscal repair.* Clin Orthop Relat Res, 1999(367 Suppl): p. S254-72.

266. Buschmann, M.D., et al., *Mechanical compression modulates matrix biosynthesis in chondrocyte/agarose culture.* J Cell Sci, 1995. **108 (Pt 4)**: p. 1497-508.

267. Hung, C.T., et al., *A paradigm for functional tissue engineering of articular cartilage via applied physiologic deformational loading.* Ann Biomed Eng, 2004. **32**(1): p. 35-49.

268. Mauck, R.L., et al., *Influence of seeding density and dynamic deformational loading on the developing structure/function relationships of chondrocyte-seeded agarose hydrogels.* Ann Biomed Eng, 2002. **30**(8): p. 1046-56.

269. Sah, R.L., et al., *Biosynthetic response of cartilage explants to dynamic compression.* J Orthop Res, 1989. **7**(5): p. 619-36.

270. Meyer, U., et al., *Design and performance of a bioreactor system for mechanically promoted three-dimensional tissue engineering.* Br J Oral Maxillofac Surg, 2006. **44**(2): p. 134-40.

271. McHenry, J.A., B. Zielinska, and T.L. Donahue, *Proteoglycan breakdown of meniscal explants following dynamic compression using a novel bioreactor.* Ann Biomed Eng, 2006. **34**(11): p. 1758-66.

272. Smith, R.L., et al., *Time-dependent effects of intermittent hydrostatic pressure on articular chondrocyte type II collagen and aggrecan mRNA expression.* J Rehabil Res Dev, 2000. **37**(2): p. 153-61.

273. Carver, S.E. and C.A. Heath, *Semi-continuous perfusion system for delivering intermittent physiological pressure to regenerating cartilage.* Tissue Eng, 1999. **5**(1): p. 1-11.

274. Carver, S.E. and C.A. Heath, *Increasing extracellular matrix production in regenerating cartilage with intermittent physiological pressure.* Biotechnol Bioeng, 1999. **62**(2): p. 166-74.

275. Elder, B.D. and K.A. Athanasiou, *Effects of Temporal Hydrostatic Pressure on Tissue-Engineered Bovine Articular Cartilage Constructs.* Tissue Eng Part A, 2008.

276. Elder, B.D. and K.A. Athanasiou, *Synergistic and additive effects of hydrostatic pressure and growth factors on tissue formation.* PLoS ONE, 2008. **3**(6): p. e2341.

277. Hu, J.C. and K.A. Athanasiou, *The effects of intermittent hydrostatic pressure on self-assembled articular cartilage constructs.* Tissue Eng, 2006. **12**(5): p. 1337-44.

278. Almarza, A.J. and K.A. Athanasiou, *Effects of hydrostatic pressure on TMJ disc cells.* Tissue Eng, 2006. **12**(5): p. 1285-94.

279. Mahmoudifar, N. and P.M. Doran, *Tissue engineering of human cartilage in bioreactors using single and composite cell-seeded scaffolds.* Biotechnol Bioeng, 2005. **91**(3): p. 338-55.

280. Nagel-Heyer, S., et al., *Bioreactor cultivation of three-dimensional cartilage-carrier-constructs.* Bioprocess Biosyst Eng, 2005. **27**(4): p. 273-80.

281. Seidel, J.O., et al., *Long-term culture of tissue engineered cartilage in a perfused chamber with mechanical stimulation.* Biorheology, 2004. **41**(3-4): p. 445-58.

282. Darling, E.M. and K.A. Athanasiou, *Articular cartilage bioreactors and bioprocesses.* Tissue Eng, 2003. **9**(1): p. 9-26.

283. Vunjak-Novakovic, G., et al., *Bioreactor cultivation conditions modulate the composition and mechanical properties of tissue-engineered cartilage.* J Orthop Res, 1999. **17**(1): p. 130-8.

284. Freed, L.E., et al., *Microgravity cultivation of cells and tissues.* Gravit Space Biol Bull, 1999. **12**(2): p. 57-66.

285. Freed, L.E., et al., *Chondrogenesis in a cell-polymer-bioreactor system.* Exp Cell Res, 1998. **240**(1): p. 58-65.

286. Bilgen, B., et al., *Tissue Growth Modeling in a Wavy-Walled Bioreactor.* Tissue Eng Part A, 2008.

287. Bueno, E.M., B. Bilgen, and G.A. Barabino, *Wavy-walled bioreactor supports increased cell proliferation and matrix deposition in engineered cartilage constructs.* Tissue Eng, 2005. **11**(11-12): p. 1699-709.

288. Bilgen, B., et al., *Flow characterization of a wavy-walled bioreactor for cartilage tissue engineering.* Biotechnol Bioeng, 2006. **95**(6): p. 1009-22.

289. Bilgen, B. and G.A. Barabino, *Location of scaffolds in bioreactors modulates the hydrodynamic environment experienced by engineered tissues.* Biotechnol Bioeng, 2007. **98**(1): p. 282-94.

290. Yang, K.H., et al., *Exposure to low-intensity ultrasound increases aggrecan gene expression in a rat femur fracture model.* J Orthop Res, 1996. **14**(5): p. 802-9.

291. Parvizi, J., et al., *Low-intensity ultrasound stimulates proteoglycan synthesis in rat chondrocytes by increasing aggrecan gene expression.* J Orthop Res, 1999. **17**(4): p. 488-94.

292. Parvizi, J., et al., *Calcium signaling is required for ultrasound-stimulated aggrecan synthesis by rat chondrocytes.* J Orthop Res, 2002. **20**(1): p. 51-7.

293. Hsu, S.H., et al., *The effect of ultrasound stimulation versus bioreactors on neocartilage formation in tissue engineering scaffolds seeded with human chondrocytes in vitro.* Biomol Eng, 2006. **23**(5): p. 259-64.

294. Duda, G.N., et al., *Does low-intensity pulsed ultrasound stimulate maturation of tissue-engineered cartilage?* J Biomed Mater Res B Appl Biomater, 2004. **68**(1): p. 21-8.

295. Wimmer, M.A., et al., *Tribology approach to the engineering and study of articular cartilage.* Tissue Eng, 2004. **10**(9-10): p. 1436-45.

296. Kawamura, K., et al., *Adenoviral-mediated transfer of TGF-beta1 but not IGF-1 induces chondrogenic differentiation of human mesenchymal stem cells in pellet cultures.* Exp Hematol, 2005. **33**(8): p. 865-72.

297. Sekiya, I., et al., *In vitro cartilage formation by human adult stem cells from bone marrow stroma defines the sequence of cellular and molecular events during chondrogenesis.* Proc Natl Acad Sci U S A, 2002. **99**(7): p. 4397-402.

298. Worster, A.A., et al., *Chondrocytic differentiation of mesenchymal stem cells sequentially exposed to transforming growth factor-beta1 in monolayer and insulin-like growth factor-I in a three-dimensional matrix.* J Orthop Res, 2001. **19**(4): p. 738-49.

299. Hoben, G.M., V.P. Willard, and K.A. Athanasiou, *Fibrochondrogenesis of hESCs: Growth factor combinations and co-cultures.* Stem Cells Dev, 2008.

300. Hoben, G.M., E.J. Koay, and K.A. Athanasiou, *Fibrochondrogenesis in two embryonic stem cell lines: effects of differentiation timelines.* Stem Cells, 2008. **26**(2): p. 422-30.

301. Van Osch, G.J., et al., *Considerations on the use of ear chondrocytes as donor chondrocytes for cartilage tissue engineering.* Biorheology, 2004. **41**(3-4): p. 411-21.

302. Deng, Y., J.C. Hu, and K.A. Athanasiou, *Isolation and chondroinduction of a dermis-isolated, aggrecan-sensitive subpopulation with high chondrogenic potential.* Arthritis Rheum, 2007. **56**(1): p. 168-76.

303. Ikeda, T., et al., *The combination of SOX5, SOX6, and SOX9 (the SOX trio) provides signals sufficient for induction of permanent cartilage.* Arthritis Rheum, 2004. **50**(11): p. 3561-73.

304. Mizuno, S. and J. Glowacki, *Chondroinduction of human dermal fibroblasts by demineralized bone in three-dimensional culture.* Exp Cell Res, 1996. **227**(1): p. 89-97.

305. Betre, H., et al., *Chondrocytic differentiation of human adipose-derived adult stem cells in elastin-like polypeptide.* Biomaterials, 2006. **27**(1): p. 91-9.

306. Estes, B.T., A.W. Wu, and F. Guilak, *Potent induction of chondrocytic differentiation of human adipose-derived adult stem cells by bone morphogenetic protein 6.* Arthritis Rheum, 2006. **54**(4): p. 1222-32.

307. Gimble, J. and F. Guilak, *Adipose-derived adult stem cells: isolation, characterization, and differentiation potential.* Cytotherapy, 2003. **5**(5): p. 362-9.

308. Steinert, A.F., et al., *Genetically enhanced engineering of meniscus tissue using ex vivo delivery of transforming growth factor-beta 1 complementary deoxyribonucleic acid.* Tissue Eng, 2007. **13**(9): p. 2227-37.

309. Marsano, A., G. Vunjak-Novakovic, and I. Martin, *Towards tissue engineering of meniscus substitutes: selection of cell source and culture environment.* Conf Proc IEEE Eng Med Biol Soc, 2006. **1**: p. 3656-8.

310. Marsano, A., et al., *Use of hydrodynamic forces to engineer cartilaginous tissues resembling the non-uniform structure and function of meniscus.* Biomaterials, 2006. **27**(35): p. 5927-34.

311. Angele, P., et al., *Stem cell based tissue engineering for meniscus repair.* J Biomed Mater Res A, 2008. **85**(2): p. 445-55.

312. Testa Pezzin, A.P., et al., *Bioreabsorbable polymer scaffold as temporary meniscal prosthesis.* Artif Organs, 2003. **27**(5): p. 428-31.

313. Sonoda, M., et al., *The effects of hyaluronan on tissue healing after meniscus injury and repair in a rabbit model.* Am J Sports Med, 2000. **28**(1): p. 90-7.

314. Walsh, C.J., et al., *Meniscus regeneration in a rabbit partial meniscectomy model.* Tissue Eng, 1999. **5**(4): p. 327-37.

315. Suzuki, Y., et al., *Effects of hyaluronic acid on meniscal injury in rabbits.* Arch Orthop Trauma Surg, 1998. **117**(6-7): p. 303-6.

316. Isoda, K. and S. Saito, *In vitro and in vivo fibrochondrocyte growth behavior in fibrin gel: an immunohistochemical study in the rabbit.* Am J Knee Surg, 1998. **11**(4): p. 209-16.

317. Bradley, M.P., et al., *Porcine small intestine submucosa for repair of goat meniscal defects.* Orthopedics, 2007. **30**(8): p. 650-6.

318. Port, J., et al., *Meniscal repair supplemented with exogenous fibrin clot and autogenous cultured marrow cells in the goat model.* Am J Sports Med, 1996. **24**(4): p. 547-55.

319. Martinek, V., et al., *Second generation of meniscus transplantation: in-vivo study with tissue engineered meniscus replacement.* Arch Orthop Trauma Surg, 2006. **126**(4): p. 228-34.

320. Burger, C., et al., *Polylactide (LTS) causes less inflammation response than polydioxanone (PDS): a meniscus repair model in sheep.* Arch Orthop Trauma Surg, 2006. **126**(10): p. 695-705.

321. Nabeshima, Y., et al., *Effect of fibrin glue and endothelial cell growth factor on the early healing response of the transplanted allogenic meniscus: a pilot study.* Knee Surg Sports Traumatol Arthrosc, 1995. **3**(1): p. 34-8.

322. Hashimoto, J., et al., *Meniscal repair using fibrin sealant and endothelial cell growth factor. An experimental study in dogs.* Am J Sports Med, 1992. **20**(5): p. 537-41.

323. Peretti, G.M., et al., *Cell-based therapy for meniscal repair: a large animal study.* Am J Sports Med, 2004. **32**(1): p. 146-58.

324. Ibarra, C., et al., *Tissue engineered meniscus: a potential new alternative to allogeneic meniscus transplantation.* Transplant Proc, 1997. **29**(1-2): p. 986-8.

325. Hidaka, C., et al., *Formation of vascularized meniscal tissue by combining gene therapy with tissue engineering.* Tissue Eng, 2002. **8**(1): p. 93-105.

326. Steadman, J.R. and W.G. Rodkey, *Tissue-engineered collagen meniscus implants: 5- to 6-year feasibility study results.* Arthroscopy, 2005. **21**(5): p. 515-25.

327. Reguzzoni, M., et al., *Histology and ultrastructure of a tissue-engineered collagen meniscus before and after implantation.* J Biomed Mater Res B Appl Biomater, 2005. **74**(2): p. 808-16.

328. Rodkey, W.G., et al., *Comparison of the collagen meniscus implant with partial meniscectomy. A prospective randomized trial.* J Bone Joint Surg Am, 2008. **90**(7): p. 1413-26.

329. Boyd, K.T. and P.T. Myers, *Meniscus preservation; rationale, repair techniques and results.* Knee, 2003. **10**(1): p. 1-11.

330. Espejo-Baena, A., et al., *All-inside suture technique using anterior portals in posterior horn tears of lateral meniscus.* Arthroscopy, 2008. **24**(3): p. 369 e1-4.

331. Hantes, M.E., et al., *Arthroscopic meniscal repair: a comparative study between three different surgical techniques.* Knee Surg Sports Traumatol Arthrosc, 2006. **14**(12): p. 1232-7.

332. Kim, S.J., et al., *Arthroscopic all-inside repair of tears of the anterior horn of the lateral meniscus.* Arthroscopy, 2005. **21**(11): p. 1399.

333. Fukushima, K., et al., *New meniscus repair by an all-inside knot suture technique.* Arthroscopy, 2005. **21**(6): p. 768.

334. Cho, J.H., *Arthroscopic all-inside repair of anterior horn tears of the lateral meniscus using a spinal needle.* Knee Surg Sports Traumatol Arthrosc, 2008. **16**(7): p. 683-6.

335. Gill, S.S. and D.R. Diduch, *Outcomes after meniscal repair using the meniscus arrow in knees undergoing concurrent anterior cruciate ligament reconstruction.* Arthroscopy, 2002. **18**(6): p. 569-77.

336. Albrecht-Olsen, P., et al., *Failure strength of a new meniscus arrow repair technique: biomechanical comparison with horizontal suture.* Arthroscopy, 1997. **13**(2): p. 183-7.

337. Kurzweil, P.R., C.D. Tifford, and E.M. Ignacio, *Unsatisfactory clinical results of meniscal repair using the meniscus arrow.* Arthroscopy, 2005. **21**(8): p. 905.

338. Koukoulias, N., et al., *Clinical results of meniscus repair with the meniscus arrow: a 4- to 8-year follow-up study.* Knee Surg Sports Traumatol Arthrosc, 2007. **15**(2): p. 133-7.

339. Lee, G.P. and D.R. Diduch, *Deteriorating outcomes after meniscal repair using the Meniscus Arrow in knees undergoing concurrent anterior cruciate ligament reconstruction: increased failure rate with long-term follow-up.* Am J Sports Med, 2005. **33**(8): p. 1138-41.

340. Jones, H.P., et al., *Two-year follow-up of meniscal repair using a bioabsorbable arrow.* Arthroscopy, 2002. **18**(1): p. 64-9.

341. Albrecht-Olsen, P., et al., *The arrow versus horizontal suture in arthroscopic meniscus repair. A prospective randomized study with arthroscopic evaluation.* Knee Surg Sports Traumatol Arthrosc, 1999. **7**(5): p. 268-73.

342. Hantes, M.E., et al., *Arthroscopic meniscal repair with an absorbable screw: results and surgical technique.* Knee Surg Sports Traumatol Arthrosc, 2005. **13**(4): p. 273-9.

343. Siebold, R., et al., *Arthroscopic all-inside repair using the Meniscus Arrow: long-term clinical follow-up of 113 patients.* Arthroscopy, 2007. **23**(4): p. 394-9.

344. Garrett, J.C. and R.N. Steensen, *Meniscal transplantation in the human knee: a preliminary report.* Arthroscopy, 1991. **7**(1): p. 57-62.

345. Stone, K.R., et al., *Meniscus allograft survival in patients with moderate to severe unicompartmental arthritis: a 2- to 7-year follow-up.* Arthroscopy, 2006. **22**(5): p. 469-78.

346. McDermott, I. and N.P. Thomas, *Human meniscal allograft transplantation.* Knee, 2006. **13**(1): p. 69-71.

347. Shelbourne, K.D. and J. Heinrich, *The long-term evaluation of lateral meniscus tears left in situ at the time of anterior cruciate ligament reconstruction.* Arthroscopy, 2004. **20**(4): p. 346-51.

348. Elder, B.D. and K.A. Athanasiou, *Systematic assessment of growth factor treatment on biochemical and biomechanical properties of engineered articular cartilage constructs.* Osteoarthritis Cartilage, 2009. **17**(1): p. 114-23.

349. Gunja, N.J. and K.A. Athanasiou, *Effects of co-cultures of meniscus cells and articular chondrocytes on PLLA scaffolds.* Biotechnol Bioeng, 2009. **103**(4): p. 808-16.

350. Gunja, N.J. and K.A. Athanasiou, *Effects of hydrostatic pressure on leporine meniscus cell-seeded PLLA scaffolds.* J Biomed Mater Res A, 2010. **92**(3): p. 896-905.

351. Estes, B.T., et al., *Isolation of adipose-derived stem cells and their induction to a chondrogenic phenotype.* Nat Protoc, 2010. **5**(7): p. 1294-311.

352. Huang, A.H., et al., *Tensile properties of engineered cartilage formed from chondrocyte- and MSC-laden hydrogels.* Osteoarthritis Cartilage, 2008. **16**(9): p. 1074-82.

353. Kuroda, R., et al., *Cartilage repair using bone morphogenetic protein 4 and muscle-derived stem cells.* Arthritis Rheum, 2006. **54**(2): p. 433-42.

354. Matsumoto, T., et al., *Cartilage repair in a rat model of osteoarthritis through intraarticular transplantation of muscle-derived stem cells*

expressing bone morphogenetic protein 4 and soluble Flt-1. Arthritis Rheum, 2009. **60**(5): p. 1390-405.

355. Fernandes, K.J., et al., *A dermal niche for multipotent adult skin-derived precursor cells.* Nature Cell Biology, 2004. **6**(11): p. 1082-93.

356. Fuchs, E., *Scratching the surface of skin development.* Nature, 2007. **445**(7130): p. 834-42.

357. Alonso, L. and E. Fuchs, *Stem cells in the skin: waste not, Wnt not.* Genes Dev, 2003. **17**(10): p. 1189-200.

358. Blanpain, C. and E. Fuchs, *Epidermal stem cells of the skin.* Annu Rev Cell Dev Biol, 2006. **22**: p. 339-73.

359. Glowacki, J., et al., *In vitro engineering of cartilage: effects of serum substitutes, TGF-beta, and IL-1alpha.* Orthod Craniofac Res, 2005. **8**(3): p. 200-8.

360. Toma, J.G., et al., *Isolation of multipotent adult stem cells from the dermis of mammalian skin.* Nature Cell Biology, 2001. **3**(9): p. 778-784.

361. Zhong, J.Q., et al., *A novel promising therapy for skin aging: Dermal multipotent stem cells against photoaged skin by activation of TGF-beta/Smad and p38 MAPK signaling pathway.* Medical Hypotheses, 2011. **76**(3): p. 343-346.

362. Amoh, Y., et al., *Implanted hair follicle stem cells form Schwann cells that support repair of severed peripheral nerves.* Proceedings of the National Academy of Sciences of the United States of America, 2005. **102**(49): p. 17734-17738.

363. Hoogduijn, M.J., E. Gorjup, and P.G. Genever, *Comparative characterization of hair follicle dermal stem cells and bone marrow mesenchymal stem cells.* Stem Cells and Development, 2006. **15**(1): p. 49-60.

364. Liu, F., et al., *The bulge area is the major hair follicle source of nestin-expressing pluripotent stem cells which can repair the spinal cord compared to the dermal papilla.* Cell Cycle, 2011. **10**(5): p. 830-839.

365. Ohyama, M., et al., *Characterization and isolation of stem cell-enriched human hair follicle bulge cells.* J Clin Invest, 2006. **116**(1): p. 249-60.

366. Brehm, W., et al., *Repair of superficial osteochondral defects with an autologous scaffold-free cartilage construct in a caprine model: implantation method and short-term results.* Osteoarthritis Cartilage, 2006. **14**(12): p. 1214-26.

367. Tsutsumi, S., et al., *Retention of multilineage differentiation potential of mesenchymal cells during proliferation in response to FGF.* Biochem Biophys Res Commun, 2001. **288**(2): p. 413-9.

368. Yanada, S., et al., *Possibility of selection of chondrogenic progenitor cells by telomere length in FGF-2-expanded mesenchymal stromal cells.* Cell Prolif, 2006. **39**(6): p. 575-84.

369. Denker, A.E., et al., *Chondrogenic differentiation of murine C3H10T1/2 multipotential mesenchymal cells: I. Stimulation by bone morphogenetic protein-2 in high-density micromass cultures.* Differentiation, 1999. **64**(2): p. 67-76.

370. Yang, J.W., et al., *Evaluation of human MSCs cell cycle, viability and differentiation in micromass culture.* Biorheology, 2006. **43**(3-4): p. 489-96.

371. Zhang, L., et al., *Chondrogenic differentiation of human mesenchymal stem cells: a comparison between micromass and pellet culture systems.* Biotechnol Lett, 2010. **32**(9): p. 1339-46.

372. Koay, E.J. and K.A. Athanasiou, *Hypoxic chondrogenic differentiation of human embryonic stem cells enhances cartilage protein synthesis and biomechanical functionality.* Osteoarthritis Cartilage, 2008. **16**(12): p. 1450-6.

373. Koay, E.J., G.M. Hoben, and K.A. Athanasiou, *Tissue engineering with chondrogenically differentiated human embryonic stem cells.* Stem Cells, 2007. **25**(9): p. 2183-90.

374. Hwang, N.S., et al., *Chondrogenic differentiation of human embryonic stem cell-derived cells in arginine-glycine-aspartate-modified hydrogels.* Tissue Eng, 2006. **12**(9): p. 2695-706.

375. Yang, H.S., et al., *Hyaline cartilage regeneration by combined therapy of microfracture and long-term bone morphogenetic protein-2 delivery.* Tissue Eng Part A, 2011. **17**(13-14): p. 1809-18.

376. Tian, H., et al., *Chondrogenic differentiation of mouse bone marrow mesenchymal stem cells induced by cartilage-derived morphogenetic protein-2 in vitro.* J Huazhong Univ Sci Technolog Med Sci, 2007. **27**(4): p. 429-32.

377. Nawata, M., et al., *Use of bone morphogenetic protein 2 and diffusion chambers to engineer cartilage tissue for the repair of defects in articular cartilage.* Arthritis Rheum, 2005. **52**(1): p. 155-63.

378. Sellers, R.S., et al., *Repair of articular cartilage defects one year after treatment with recombinant human bone morphogenetic protein-2 (rhBMP-2).* J Bone Joint Surg Am, 2000. **82**(2): p. 151-60.

379. Iwata, H., et al., *Bone morphogenetic protein-induced muscle- and synovium-derived cartilage differentiation in vitro.* Clin Orthop Relat Res, 1993(296): p. 295-300.

380. Xu, C.H., et al., *Basic fibroblast growth factor supports undifferentiated human embryonic stem cell growth without conditioned medium.* Stem Cells, 2005. **23**(3): p. 315-323.

381. Banu, N. and T. Tsuchiya, *Markedly different effects of hyaluronic acid and chondroitin sulfate-A on the differentiation of human articular chondrocytes in micromass and 3-D honeycomb rotation cultures.* J Biomed Mater Res A, 2007. **80**(2): p. 257-67.

382. Carlberg, A.L., et al., *Efficient chondrogenic differentiation of mesenchymal cells in micromass culture by retroviral gene transfer of BMP-2.* Differentiation, 2001. **67**(4-5): p. 128-38.

383. Koay, E.J. and K.A. Athanasiou, *Development of serum-free, chemically defined conditions for human embryonic stem cell-derived fibrochondrogenesis.* Tissue Eng Part A, 2009. **15**(8): p. 2249-57.

384. Hofstaetter, J.G., et al., *Systemic hypoxia alters gene expression levels of structural proteins and growth factors in knee joint cartilage.* Biochem Biophys Res Commun, 2005. **330**(2): p. 386-94.

385. Gunja, N.J. and K.A. Athanasiou, *Additive and synergistic effects of bFGF and hypoxia on leporine meniscus cell-seeded PLLA scaffolds.* J Tissue Eng Regen Med, 2010. **4**(2): p. 115-22.

386. Almarza, A.J. and K.A. Athanasiou, *Evaluation of three growth factors in combinations of two for temporomandibular joint disc tissue engineering.* Arch Oral Biol, 2006. **51**(3): p. 215-21.

387. Falanga, V., et al., *Hypoxia upregulates the synthesis of TGF-beta 1 by human dermal fibroblasts.* J Invest Dermatol, 1991. **97**(4): p. 634-7.

388. Martin, I., et al., *Enhanced cartilage tissue engineering by sequential exposure of chondrocytes to FGF-2 during 2D expansion and BMP-2 during 3D cultivation.* J Cell Biochem, 2001. **83**(1): p. 121-8.

389. Hoben, G.M., V.P. Willard, and K.A. Athanasiou, *Fibrochondrogenesis of hESCs: growth factor combinations and cocultures.* Stem Cells Dev, 2009. **18**(2): p. 283-92.

390. Kalpakci, K.N., E.J. Kim, and K.A. Athanasiou, *Assessment of growth factor treatment on fibrochondrocyte and chondrocyte co-cultures for TMJ fibrocartilage engineering.* Acta Biomater, 2011. **7**(4): p. 1710-8.

391. Solorio, L.D., et al., *Chondrogenic differentiation of human mesenchymal stem cell aggregates via controlled release of TGF-beta1 from incorporated polymer microspheres.* J Biomed Mater Res A, 2010. **92**(3): p. 1139-44.

392. Martinez-Ferrer, M., et al., *Dermal transforming growth factor-beta responsiveness mediates wound contraction and epithelial closure.* Am J Pathol, 2010. **176**(1): p. 98-107.

393. Lijnen, P., et al., *Transforming growth factor-beta 1 promotes contraction of collagen gel by cardiac fibroblasts through their differentiation into myofibroblasts.* Methods Find Exp Clin Pharmacol, 2003. **25**(2): p. 79-86.

394. Grinnell, F. and C.H. Ho, *Transforming growth factor beta stimulates fibroblast-collagen matrix contraction by different mechanisms in mechanically loaded and unloaded matrices.* Exp Cell Res, 2002. **273**(2): p. 248-55.

395. Tateshita, T., I. Ono, and F. Kaneko, *Effects of collagen matrix containing transforming growth factor (TGF)-beta(1) on wound contraction.* Journal of Dermatological Science, 2001. **27**(2): p. 104-13.

396. Montesano, R. and L. Orci, *Transforming growth factor beta stimulates collagen-matrix contraction by fibroblasts: implications for wound healing.* Proc Natl Acad Sci U S A, 1988. **85**(13): p. 4894-7.

397. Joannides, A., et al., *Efficient generation of neural precursors from adult human skin: astrocytes promote neurogenesis from skin-derived stem cells.* Lancet, 2004. **364**(9429): p. 172-8.

398. Riekstina, U., et al., *Characterization of human skin-derived mesenchymal stem cell proliferation rate in different growth conditions.* Cytotechnology, 2008. **58**(3): p. 153-162.

399. Shih, D.T., et al., *Isolation and characterization of neurogenic mesenchymal stem cells in human scalp tissue.* Stem Cells, 2005. **23**(7): p. 1012-20.

400. Katz, A.J., et al., *Emerging approaches to the tissue engineering of fat.* Clin Plast Surg, 1999. **26**(4): p. 587-603, viii.

401. Lindsey, W.H., *Osseous tissue engineering with gene therapy for facial bone reconstruction.* Laryngoscope, 2001. **111**(7): p. 1128-36.

402. Morgan, S.M., et al., *Formation of a human-derived fat tissue layer in P(DL)LGA hollow fibre scaffolds for adipocyte tissue engineering.* Biomaterials, 2009. **30**(10): p. 1910-7.

403. Sun, J.J. and X.S. Li, *A study on reconstruction of ossicular chain by an in situ bone tissue engineering technique.* Acta Otolaryngol, 2009. **129**(5): p. 507-11.

404. Yoshikawa, T. and H. Ohgushi, *Autogenous cultured bone graft--bone reconstruction using tissue engineering approach.* Ann Chir Gynaecol, 1999. **88**(3): p. 186-92.